Pharmakologische Beeinflussung des vaskulären Remodelings nach Angioplastie

Kumulative Habilitationsschrift
zur Erlangung des akademischen Grades
eines habilitierten Doktors der Medizin (Dr. med. habil.)
für das Fachgebiet Innere Medizin

vorgelegt
der Medizinischen Fakultät
der Martin-Luther-Universität Halle-Wittenberg

von
Dr. med. Jochen Dutzmann

Gutachter:

Prof. Dr. rer. nat. Sabine Steffens, München

Prof. Dr. med. Harald Langer, Mannheim

Datum der fakultätsöffentlichen Vorlesung: 28.04.2025

Datum der fakultätsöffentlichen Verteidigung: 13.05.2025

Referat

Neuartige Pharmaka sowie solche, die in nicht-kardiovaskulären Indikationsbereichen angewendet werden, können erwünschte oder unerwünschte (Neben-)Wirkungen auf das kardiovaskuläre System und insbesondere auf kardiovaskuläre Remodeling-Prozesse haben, wie sie zum Beispiel als Folge einer Angioplastie auftreten können.

In der vorliegenden Arbeit werden die vaskulären Effekte von fünf Pharmaka in humanen Endothel- und Glattmuskelzellen *in vitro* und im Mausmodell der endovaskulären Verletzung und Dilatation der Femoralarterie *in vivo* untersucht und die Einflüsse auf die Signaltransduktion vaskulärer Zellen ebenso wie auf die Pathophysiologie kardiovaskulärer Remodeling-Prozesse dargestellt.

Die systemische Therapie mit dem SGLT2-Inhibitor Empagliflozin, der zu den prognostisch relevanten Säulen der medikamentösen Herzinsuffizienz-Therapie gehört, sowie die systemische Therapie mit dem neuen nicht-steroidalen Mineralokortikoidrezeptorantagonist Finerenon, der insbesondere bei Patienten mit chronischer Niereninsuffizienz und Diabetes mellitus zur Therapie der Herzinsuffizienz empfohlen wird, beeinflussten nicht nur die Endothelzellfunktion und Glattmuskelzellproliferation, sondern verminderten im Tiermodell auch das negative vaskuläre Remodeling nach endovaskulärer Verletzung. Daneben entfalteten Pharmaka, die zurzeit klinische Anwendung in nicht nicht-kardiovaskulären Indikationsbereichen finden, wie Sirolimus, das zur antiinflammatorischen Therapie nach Organtransplantation eingesetzt wird, sowie GDC-0449 oder (+)-JQ1, die in der antiproliferativen Therapie verschiedener onkologischer Erkrankungen verwendet werden, ihre antiinflammatorische und antiproliferative Kapazität auch im Rahmen vaskulärer Remodeling-Prozesse. Besonders die Erforschung von GDC-0449 erweiterte das umfassendere Verständnis pathophysiologischer Zusammenhänge vaskulärer Remodeling-Prozesse: GDC-0449 zeigte eine selektive antiproliferative und antiinflammatorische Beeinflussung adventitieller Fibroblasten ohne vaskuläre Endothel- oder Glattmuskelzellen zu beeinflussen und unterstreicht somit den erheblichen Einfluss der Adventitia auf das vaskuläre Remodeling.

Zusammenfassend erweitert die vorliegende experimentelle Untersuchung einerseits das grundlegende Verständnis der Pathophysiologie vaskulärer Remodeling-Prozesse und sensibilisiert andererseits für die möglichen vaskulären (Neben-)Wirkungen von Pharmaka, die abseits vaskulärer Indikationen eingesetzt werden.

Dutzmann, Jochen. Pharmakologische Beeinflussung des vaskulären Remodelings nach Angioplastie, Halle (Saale), Martin-Luther-Universität Halle-Wittenberg, Medizinische Fakultät, Habilitation, 105 Seiten, 2024

Inhaltsverzeichnis

Abkürzungsverzeichnis

ACE	angiotensin converting enzymes
$ApoE^{-/-}$	Apolipoprotein E-defizienten
ARNI	Angiotensin-Rezeptor-Neprilysin-Inhibitoren
BET	Bromodomain and extra-terminal
BMS	Bare-metal stents
CCL	CC-chemokine ligand
CDK	Cyklin-abhängige Kinase
DAPT	Duale antithrombozytäre Therapie
DES	Drug-eluting stents
ECM	Extrazelluläre Matrix
FGF	Fibroblast growth factor
FOXO1	Forkhead-Box-Protein O1
ICAM	Intercellular adhesion molecule
IGF	Insulin-like growth factor
IL	Interleukin
ISR	In-Stent-Restenose
KHK	Koronare Herzerkrankung
Mac-1	Macrophage-1 antigen
MR	Mineralokortikoid-Rezeptor
MRA	Mineralokortikoid-Rezeptor-Antagonisten
mTOR	mechanistic target of rapamycin
NF-κB	Nuclear factor κB
pAVK	Peripher-arterieller Verschlusskrankheit
PCI	Perkutane Koronarintervention
PDGF-BB	Platelet-derived growth factor
RNA	Ribonukleinsäure
Sca-1	Stem cell antigen-1
SGLT2	Natrium-Glucose-Co-Transporter 2
Shh	Sonic hedgehog
SMO	Smoothened
TGF-β	Transforming growth factor beta
VCAM	Vascular cell adhesion molecule
VEGF	Vascular endothelial growth factor

1 Einleitung und Stand der Forschung

1.1 Das klinische Problem der Restenose nach Angioplastie

Die unverändert hohe Inzidenz und Mortalität ischämischer Herzkreislauferkrankungen unterstreichen die enorme klinische Bedeutung von Angioplastien und Stent-Implantation als wesentliche therapeutische Säule bei Patienten mit koronarer Herzerkrankung (KHK) oder peripher-arterieller Verschlusskrankheit (pAVK).[1] Trotz bedeutsamer technologischer Fortschritte hinsichtlich des Designs und der Beschichtung von Stents in den vergangenen Jahren schmälern In-Stent-Restenosen (ISR) insbesondere bei Patienten mit Diabetes mellitus den Erfolg dieser Therapie.[2,3]

Angioplastien führen zu einer mechanischen Verletzung des Endothels und der gesamten Gefäßwand, gefolgt von einer inflammatorischen Heilungsreaktion. ISR entstehen, wenn diese Reaktion über den physiologischen Heilungsprozess hinausgeht, durch eine überschießende Proliferation und Migration glatter Gefäßmuskelzellen mit konsekutiver Neointimabildung.[4,5] Mit der Einführung von Drug-eluting stents (DES), die antiproliferative Wirkstoffe wie Everolimus, Sirolimus oder Zotarolimus freisetzen, konnte die Rate erneuter Revaskularisierungen im Vergleich zu Bare-metal stents (BMS), also reinen Metallstents erheblich reduziert werden.[6] Da die antiproliferative Wirkung der genannten Substanzen zellunspezifisch ist, wird auch die Reendothelialisierung der implantierten Stents beeinträchtigt und bedingt ein erhöhtes Risiko für In-Stent-Thrombosen.[7] Zwar konnte dieses Risiko durch eine verlängerte duale antithrombozytäre Therapie (DAPT) deutlich reduziert werden, diese wiederum ist jedoch mit einem deutlich erhöhten Blutungsrisiko assoziiert.[8] Trotz zuletzt weiterer Verbesserung der Stentdesigns mit dünneren Stentstreben, verbesserter Polymerbeschichtungen und dem Einsatz biokompatibler Materialien zeigen aktuelle Vergleichsstudien zwischen DES und koronaren Bypass-Operationen ein weiterhin häufiges Auftreten von ISR auch in Patienten, die mit DES versorgt wurden.[9,10]

Zur besseren Kontrolle des klinischen Problems der ISR ist einerseits ein besseres Verständnis der zugrundeliegenden Pathophysiologie essenziell, so dass auf dieser Basis neue Therapieansätze entwickelt werden können. Andererseits ist die Untersuchung von vaskulären (Neben-)Wirkungen von Pharmaka wichtig, die bisher abseits vaskulärer Indikationen eingesetzt werden.

1.2 Pathophysiologie der Neointimabildung

Als ISR wird eine mehr als 75%ige Verengung des Gefäßquerschnitts innerhalb eines Stents durch neointimales Gewebe bestehend aus Glattmuskelzellen und Proteoglykan-

Kollagen-Matrix bezeichnet.[11] Der zeitliche Verlauf der Reendothelialisierung und der Neointima-Entstehung unterscheiden sich zwischen unterschiedlichen Tierspezies und menschlichen Iliakal- und Koronararterien: Während im Tiermodell das maximale Neointima-Wachstum etwa 28 Tage nach Angioplastie erreicht wird, zeigt es sich im Menschen nach 6-12 Monaten (**Abbildung 1**).[12]

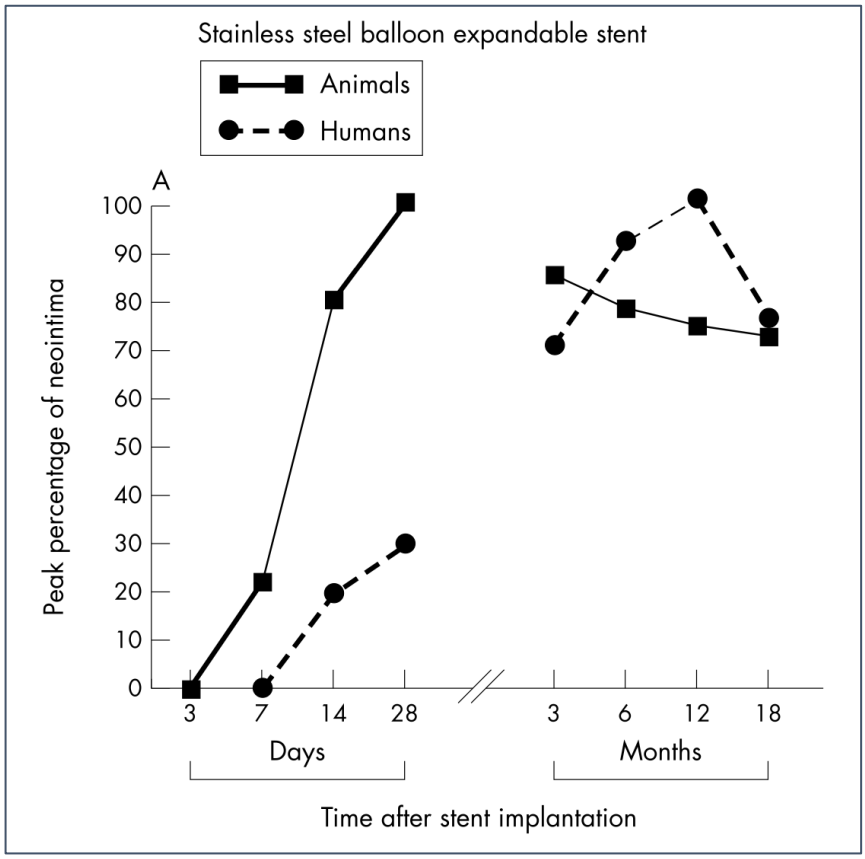

Abbildung 1 Zeitliche Beziehung des maximalen neointimalen Wachstums bei Tieren und Menschen nach Platzierung eines BMS. Die morphometrischen Analysen stammen hauptsächlich von Schweine- und menschlichen Koronarstents. Bei Tieren wird das maximale Neointima-Wachstum nach 28 Tagen beobachtet, im Vergleich zu 6–12 Monaten bei Menschen. (Mit freundlicher Genehmigung aus Virmani et al.[12])

Die zelluläre Signalantwort unmittelbar nach mechanischer endovaskulärer Verletzung durch eine Angioplastie wird bisher in drei aufeinander folgende Phasen eingeteilt: eine frühe Phase, die durch Thrombozyten-Aktivierung und Inflammation charakterisiert ist, gefolgt von einer intermediären Phase der Bildung von Granulationsgewebe, die im Wesentlichen durch die Migration und Proliferation von Glattmuskelzellen charakterisiert ist, sowie eine späte Phase des Gewebeumbaus.[13]

1.2.1 Die frühe inflammatorische Phase

In der frühen Phase nach Angioplastie führt die teilweise bis komplette Zerstörung der intimalen Endothelzellen zur Thrombozyten-Aktivierung und -Aggregation, zur Infiltration zirkulierender Immunzellen und der Freisetzung von Zytokinen und Wachstumsfaktoren.[14–16] Dabei binden thrombozytäre Glykoproteine (GP) Ib/V/IX an den

von-Willebrand-Faktor der subendothelialen Basalmembran und thrombozytäre GP VI an Kollagen und schütten Adenosindiphosphat, Thrombin und Thromboxan A2 aus, wodurch es zu einer weiteren Thrombozytenadhäsion und Fibrinbindung über GP IIb/IIIa kommt.[17] An der Oberfläche von aktivierten Thrombozyten und aktivierten Endothelzellen wird das Adhäsionsmolekül P-Selectin exprimiert, über das es zu *Rolling* von Leukozyten und schließlich unter anderem über das β_2-Integrin *macrophage-1 antigen* (Mac-1; CD11b/CD18) oder thrombozytären oder endothelialen Rezeptoren wie dem *intercellular adhesion molecule* (ICAM)-*1* und -*2* oder dem *vascular cell adhesion molecule* (VCAM)-*1* zur festen Leukozyten-Adhäsion kommt.[18,19] Die Adhäsion von Leukozyten wird über zahlreiche spezifische Chemokine wie *CC-chemokine ligand-2* (CCL2; *monocyte chemotactic protein*/MCP-1), *CC-chemokine ligand-5* (CCL5; RANTES) und *CXC-Motiv-Chemokin-12* (CXCL12; *stromal cell derived-factor*/SDF-α) orchestriert.[20,21] Letzteres ist mitunter entscheidend für die Adhäsion von *stem cell antigen-1* $(Sca\text{-}1)^+$ und $CD34^+$ zirkulierenden hämatopoetischen Progenitorzellen.[20] Nachdem die Differenzierung dieser zirkulierenden Progenitorzellen in Endothel- und Glattmuskelzellen und somit ein signifikanter zellulärer Beitrag zur neointimalen Läsion lange kritisch diskutiert wurde, konnte unsere Arbeitsgruppe zeigen, dass zirkulierende Progenitorzellen während der frühen inflammatorischen Phase zwar in die neointimale Läsion einwandern, jedoch nicht in Glattmuskelzellen differenzieren.[22,23] Seither mehren sich Arbeiten, die eine Beteiligung nicht zirkulierender, wohl aber residenter adventitieller Progenitorzellen hypothetisieren.[24,25] Der Einfluss adventitieller Zellen auf das vaskuläre Remodeling nach Angioplastie ist Gegenstand der hier vorgelegten Arbeit.

Der frühe inflammatorische Prozess nach Angioplastie-bedingter Endothelverletzung ist entscheidend für die Initiierung und Progression der Glattmuskel-Proliferation und der Neointima-Formation. Die Anzahl adhärierender $CD115^+$ Monozyten korrelierte im Tierexperiment ebenso wie die Anzahl infiltrierender $CD14^+$ Makrophagen mit der Größe der entstehenden neointimalen Formation. Auch in histopathologischen Präparaten aus humanen Koronararterien konnte ein starker Zusammenhang zwischen früher chronischer Inflammation und neointimalem Wachstum gezeigt werden.[26] Neben Monozyten und Makrophagen wurde daneben Neutrophilen ein entscheidender Einfluss auf Glattmuskelzellen zugesprochen.[27]

Auf die Endothelverletzung folgt die Formation einer dünnen Thrombusschicht, die (unter DAPT und Heparin-Therapie) Gefäß- und Stentoberfläche bedeckt. Während diese Thrombusschicht zu Granulationsgewebe umgebaut wird und eine Neointima bildet, wird sie innerhalb weniger Wochen komplett von Endothelzellen bedeckt, die von den Wundrändern aus einwachsen („Reendothelialisierung“).[28] Während tierexperimentell

eine beschleunigte Reendothelialisierung durch endotheliale Progenitorzellen gezeigt werden konnte, die die konsekutive Inflammation und Neointima-Formation vermindert, ließ sich diese Beobachtung in klinischen Studien nicht bestätigen.[12]

1.2.2 Die intermediäre Phase der Bildung von Granulationsgewebe

Im Wesentlichen stimuliert durch die Ausschüttung von *vascular endothelial growth factor* (VEGF) migrieren und proliferieren Endothelzellen von beiden Enden der enodvaskulären Gefäßverletzung aus über die verletzten Bereiche der Gefäßwand. Gleichzeitig wird die durch Thrombozytenadhäsion entstandene Thrombusschicht durch Glattmuskelzellen und Makrophagen ersetzt, die Granulationsgewebe bilden. Die eingewanderten Makrophagen phagozytieren Zelltrümmer und produzieren – ebenso wie Endothelzellen und Thrombozyten – Wachstumsfaktoren, Chemokine und Zytokine, wie zum Beispiel *fibroblast growth factor* (FGF), *insulin-like growth factor* (IGF), *transforming growth factor beta* (TGF-β) und vor allem auch *platelet-derived growth factor-BB* (PDGF-BB).[29] Diese wiederum stimulieren die Transition glatter Muskelzellen von einem kontraktilen zu einem synthetischen Phänotyp – charakterisiert durch eine verminderte Expression kontraktiler Proteine wie zum Beispiel *smooth muscle-myosin heavy chain* (SM-MHC) – sowie ihre Proliferation und Migration.[11]

Bisher unveröffentlichte Arbeiten unserer Arbeitsgruppe legen eine frühe durch $CD45^+$ Leukozyten induzierte und der Proliferation medialer Glattmuskelzellen vorausgehende Proliferation adventitieller Zellen nahe, die anschließend durch die Produktion von Chemokinen wie Interleukin (IL)-6 die Bildung der neointimalen Läsion durch die Migration medialer Glattmuskelzellen stimulieren (Abbildung 2). Die exakte Beteiligung adventitieller Zellen an vaskulären Remodeling-Prozessen ist jedoch bisher ungeklärt und wird in der vorgelegten Arbeit untersucht.

Bezeichnend für die intermediäre Phase des vaskulären Remodelings nach Angioplastie ist der Eintritt medialer vaskulärer Glattmuskelzellen in den Zellzyklus. Diese Zellen, die sich normalerweise in der nicht-proliferativen G_0-Phase befinden, werden durch den oben dargestellten Einfluss zahlreicher Chemokine aktiviert, verändern ihren Phänotyp und treten reguliert durch verschiedene Cykline und Cyklin-abhängige Kinasen (CDK) in den Zellzyklus mit G_1-, S-, G_2- und M-Phase ein, resultierend in ihrer übermäßigen Proliferation.[28,30]

1.2.3 Die späte Phase des Gewebeumbaus

Kennzeichnend für die späte Phase des Gewebeumbaus ist eine Reduktion des Gefäßdurchmessers mit Stenosierung des Gefäßes durch die Ausbildung einer Neointima, das sogenannte „negative Remodeling“.[4] Charakteristisch ist neben der

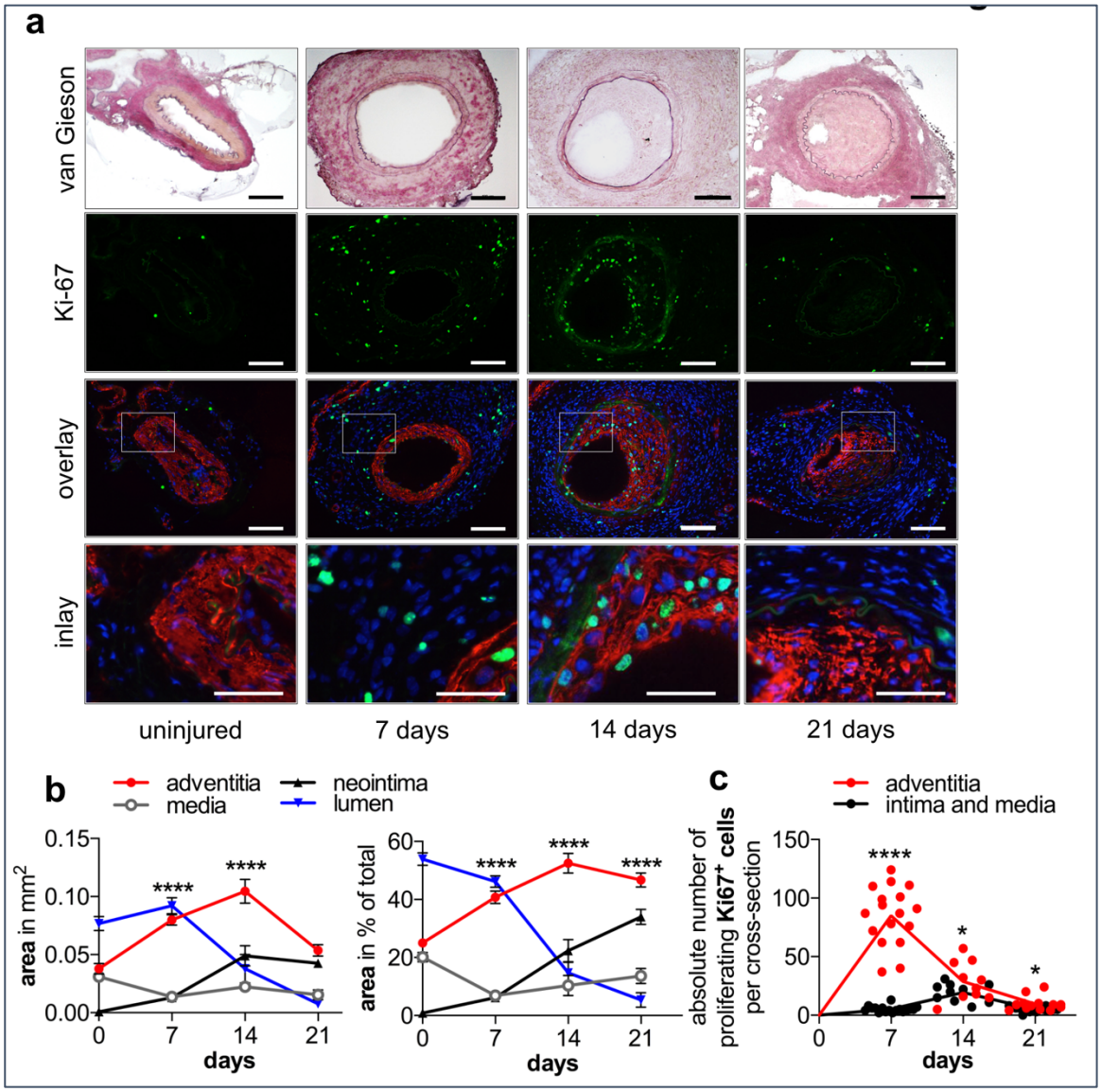

Abbildung 2 Proliferation und Wachstum der Adventitia gehen der medialen Proliferation und Bildung der Neointima nach endovaskulärer Verletzung voraus. Gezeigt sind repräsentative van Gieson-gefärbte und in der Immunfluoreszenz gegen den Proliferationsmarker Ki-67 gefärbte Bilder von nativen sowie verletzten murinen Femoralarterien zu unterschiedlichen Zeitpunkten (a). Die Dicke der Adventitia wurde planimetrisch in van Gieson-Bildern bestimmt (b, ***P<0.0001 verglichen zu 0 Tagen). Proliferierende Ki-67⁺ Zellen finden sich vorwiegend in der Adventitia 7 Tage nach endovaskulärer Verletzung (c, *P<0.05, ****P<0.0001 verglichen mit der Zahl proliferierender Zellen in Intima und Media).

Funktionsänderung glatter Gefäßmuskelzellen eine begleitende Veränderung der extrazellulären Matrix (ECM).[31,32] Die während der intermediären Phase bestehende ECM aus Plasmaproteinen wie Fibrin, Fibrinogen und Fibronectin, die Makrophagen und Glattmuskelzellen ein gutes Adhäsions- und Proliferationsgerüst bietet, wird durch Matrix-Metalloproteinasen verdaut und durch eine längerfristige ECM aus Kollagen Typ I und III ersetzt. In dieser ECM differenzieren Glattmuskelzellen und gehen in einen nicht-proliferativen Status über.[32]

1.3 Pharmakotherapeutische Ansätze zur Beeinflussung vaskulärer Remodeling-Prozesse

Erste pathophysiologische Konzepte zur Prävention der ISR wurden bereits vor Entwicklung der ersten Stents in der Ära der reinen Ballonangioplastie entwickelt. Damals wurden insbesondere Thrombozyten und die plasmatische Blutgerinnung als entscheidend für die Proliferation vaskulärer Glattmuskelzellen angesehen und daher zunächst die orale Therapie mit zahlreichen antithrombozytären und antithrombotischen Substanzen untersucht. Das Versagen all dieser Therapieansätze in klinischen Studien stimulierte die grundlagenwissenschaftliche pathophysiologische Aufarbeitung der ISR nach endovaskulärer Gefäßverletzung wie sie bei der Angioplastie entsteht. Als grundlegende Mechanismen wurde einerseits der „elastische Recoil" der Gefäße identifiziert, was zum breiten klinischen Einsatz von BMS Anfang der 1990er Jahre führte. Der Preis für die Prävention des „elastischen Recoils" durch Koronarstents war jedoch eine ausgedehntere ISR-Entwicklung durch die in Kapitel 1.2 dargestellten Mechanismen. Die Identifikation des Zellzyklus als finaler Signalweg für die Entstehung intimaler Hyperplasie legte die pharmakologische Verwendung von Zellzyklus-Regulatoren zur Prävention der Neointimabildung nahe. Das bessere Verständnis des Stellenwertes der Proliferation und Migration vaskulärer Glattmuskelzellen resultierte um die Jahrtausendwende in der Verwendung von DES, deren Stentstreben mit zytotoxischen oder zytostatischen Substanzen beschichtet werden, die über Polymere freigesetzt werden. Die Beschichtungen von DES mit dem zytotoxischen Actinomycin D, das mittels eines permanenten Polymers freigesetzt wurde, dessen Verbleib in der Gefäßwand wiederum proinflammatorisch wirkte, sowie mit hochdosiertem Paclitaxel versagten jedoch in klinischen Studien und führten aufgrund toxischer Effekte zu höheren ISR-Raten.[33,34] Dagegen zeigten immunsuppressive Substanzen wie Sirolimus und seine Analoga (insbesondere Everolimus und Zotarolimus) sowie niedrigdosiertes Paclitaxel vielversprechendere Ergebnisse (Abbildung 3).[35,36]

Die molekulare Zielstruktur von Sirolimus, auch Rapamycin genannt, ist das *mechanistic target of rapamycin* (mTOR), das unter anderem über die Verhinderung der Degradation des CDK-Inhibitors $p27^{kip1}$ die Proliferation und Migration vaskulärer Glattmuskelzellen reguliert.[37] Darüber hinaus wirkt Sirolimus allerdings zellunspezifisch über die Deaktivierung des p70 S6-Kinase-Signalwegs auch auf den Zellzyklus-Progress von Endothelzellen und führt so zu einer verzögerten Reendothelialisierung.[38] Da die verzögerte Reendothelialisierung nach wie vor eine verlängerte DAPT erforderlich macht, besteht ein weiterhin hoher Forschungsbedarf für ein besseres Verständnis der Pathophysiologie, für eine Verbesserung der verwendeten Wirkstoffe sowie für innovative Stentdesigns. So ist die Verwendung von DES-Beschichtungen mit

zellspezifischen Wirkstoffen erstrebenswert, die die Proliferation von vaskulären Glattmuskelzellen hemmen, während jene von vaskulären Endothelzellen verbessert wird. Daneben besteht ein Bedarf an Stentdesigns mit sehr dünnen oder komplett abbaubaren Polymeren ohne die Verwendung von Metallstreben (sogenannte „Scaffolds“), um eine persistierende Inflammation zu vermeiden.

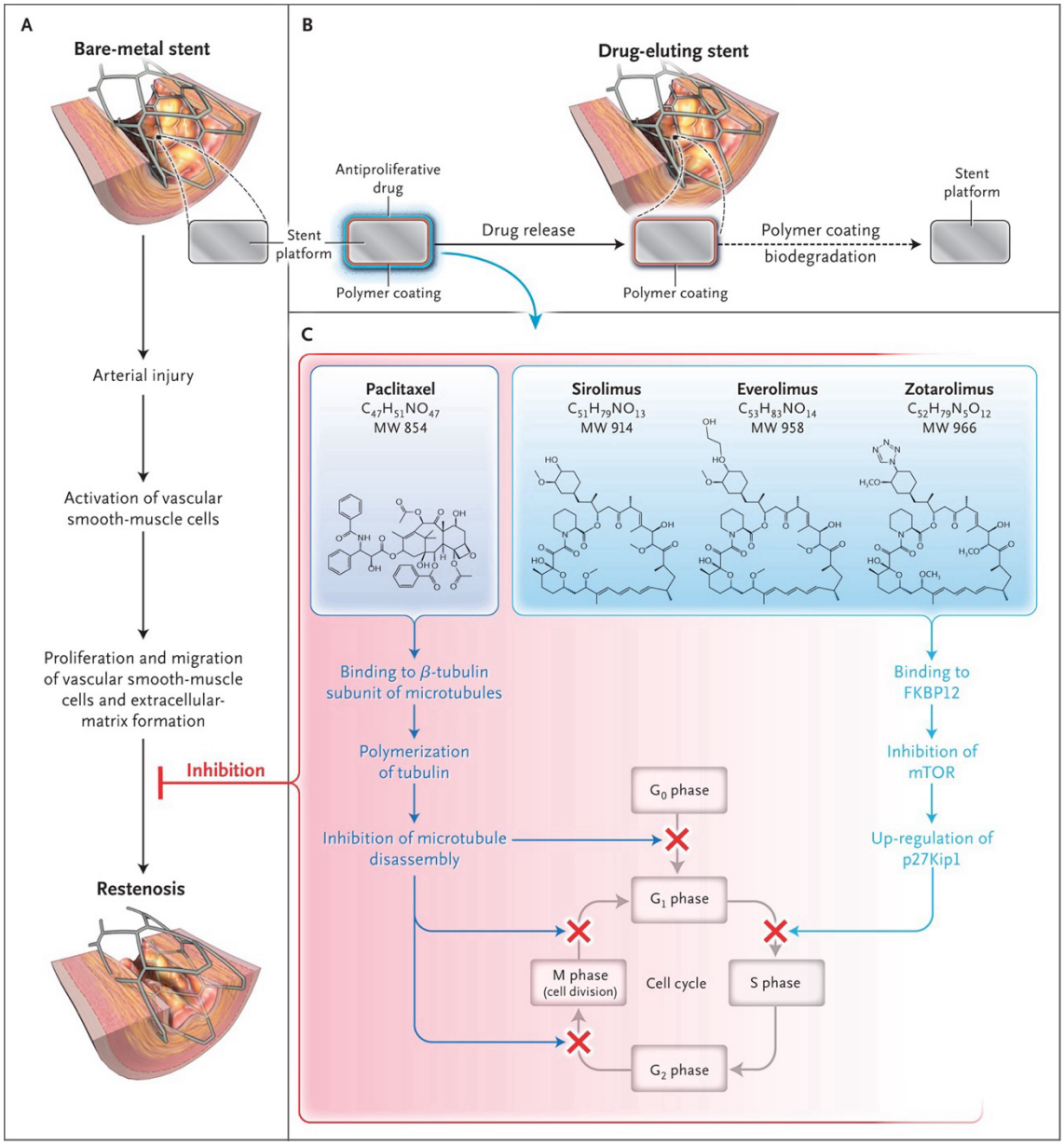

Abbildung 3 Komponenten und Wirkungsmechanismen von BMS (A) und DES (B). DES bestehen aus drei Komponenten: einer metallischen Plattform, einer Polymerbeschichtung als Arzneimittelträger und zur kontrollierten Arzneimittelfreisetzung sowie einem antiproliferativen Wirkstoff. Der antiproliferative Wirkstoff wird im Laufe der Zeit freigesetzt, während die Stent-Plattform und die dauerhafte Polymerbeschichtung in der Koronararterie verbleiben. In (C) sind die für DES verwendeten antiproliferativen Wirkstoffe und ihr Wirkmechanismus dargestellt. Sirolimus, Everolimus und Zotarolimus hemmen mTOR und führen zu einer Hochregulierung von $p27^{Kip1}$. Dies blockiert die Proliferation der Glattmuskelzellen in der G_1-Phase des Zellzyklus. Im Gegensatz dazu bindet Paclitaxel an die β-Tubulin-Untereinheit von Mikrotubuli und stoppt so die Zellreplikation in den G_0-, G_1- und M-Phase des Zellzyklus der Glattmuskelzellen. MW: Molekulargewicht. (Mit freundlicher Genehmigung aus Stefanini et Homes[3], Copyright Massachusetts Medical Society).

Schon bevor Sirolimus-Derivate als Wirkstoffbeschichtungen von DES eingesetzt wurden, wurden sie aufgrund ihrer antiinflammatorischen und antiproliferativen Eigenschaften in der onkologischen Therapie und Transplantationsmedizin genutzt.[39] Der Blick auf onkologische Therapiestrategien war für die Entwicklung anti-proliferativer Therapien im koronarvaskulären Bereich stets beispielhaft und mag es – insbesondere hinsichtlich sogenannter „targeted therapies", die zielgerichtet bestimmte (Tumor-)Zellen beeinflussen, ohne gesunde Zellen zu betreffen – auch weiterhin sein.

1.4 Pharmakotherapie der Herzinsuffizienz und Implikationen für vaskuläre Remodeling-Prozesse

Die weltweit häufigste Ursache einer Herzinsuffizienz ist die ischämische Herzkrankheit.[40] Die stete Verbesserung der Herzinfarktversorgung und insbesondere die Fortschritte in der Koronarrevaskularisation in den letzten Jahren führten zwar zu einer Reduktion der herzinfarktbedingten Mortalität, gleichzeitig jedoch auch zu einer vermehrten Inzidenz herzinfarktbedingter Herzinsuffizienzen.[41] Die pharmakologische Therapie bildet eine der wesentlichen Säulen in der Behandlung der Herzinsuffizienz. Wegen der vorwiegenden kardiovaskulären Ätiologie der Herzinsuffizienz sind die vaskulären Effekte der entsprechenden Wirkstoffe von zentraler Bedeutung.

Die Entwicklung moderner Herzinsuffizienztherapien begann in den späten 1980ern und erreichte mit der sogenannten „pharmakologischen Ära" in den 1990ern ihren Höhepunkt. Das grundlegende pharmakologische Therapieprinzip stellte neurohumoralen Intervention mit der Tripletherapie aus Betablocker, Inhibitoren des *angiotensin converting enzymes* (ACE) und Antagonisten des Mineralokortikoid-Rezeptors (MRA) dar. Nach der „Device-Ära" in den 2000er Jahren, in der implantierbare Kardioverter-Defibrillatoren und kardiale Resynchronisationssysteme Einzug in die Leitlinien hielten, erlebte in der letzten Dekade das pharmakologische Management der Herzinsuffizienz eine „Renaissance": Zur Hemmung des Renin-Angiotensin-Aldosteron-Systems wurde ein Neprilysin-Inhibitor ergänzt und die neue Medikamentenklasse der Angiotensin-Rezeptor-Neprilysin-Inhibitoren (ARNI) geschaffen.[42] Daneben wurde in kardiovaskulären Sicherheitsendpunktstudien, die durch die FDA für antidiabetische Wirkstoffe gefordert sind, für Hemmstoffe des renalen Natrium-Glucose-Co-Transporters 2 (SGLT2) überraschend ein kardioprotektiver Effekt beobachtet, der sich in kontrollierten Folgestudien für Patienten mit Herzinsuffizienz mit und ohne Diabetes bestätigen ließ.[42,43] Neben Betablockern, ACE-Hemmern/ARNIs und MRAs fanden SGLT2-Inhibitoren so als „vierte Säule" Einzug in die pharmakologische Therapie der Herzinsuffizienz. Neben der Einführung neuer Wirkstoffgruppen gab es mit der Entwicklung nicht-steroidaler MRAs außerdem eine Weiterentwicklung bestehender

Wirkstoffgruppen mit dem Ziel zur Reduktion von Nebenwirkungen.[44] Finerenon als bisher einziges zugelassenes Präparat dieser Wirkstoffgruppe wird seither für den Einsatz bei Patienten mit Herzinsuffizienz, Diabetes mellitus Typ 2 und chronischer Niereninsuffizienz in den Leitlinien der Europäischen Gesellschaft für Kardiologie empfohlen.[45]

Für ARNIs konnte inzwischen zumindest ein proliferationshemmender Effekt auf vaskuläre Glattmuskelzellen gezeigt werden.[46] Die Untersuchung der vaskulären Effekte von Empagliflozin als Vertreter der SGLT2-Inhibitoren sowie von Finerenon ist Gegenstand der vorliegenden Arbeit.

2 Hypothesen und Ziele

Neuartige und in nicht-kardiovaskulären Indikationsbereichen angewandte Pharmaka können erwünschte oder unerwünschte (Neben-)Wirkungen auf das kardiovaskuläre System und insbesondere auf kardiovaskuläre Remodeling-Prozesse haben.

1. In der vorliegenden Arbeit soll am Beispiel der systemischen Therapie von Organtransplantierten mit Sirolimus die Wirkung innerhalb dieses Indikationsbereichs auf kardiovaskuläre Remodeling-Prozesse untersucht werden.
2. Der nicht-steroidale MRA Finerenon und SGLT2-Inhibitoren wie Empagliflozin ergänzen seit Kurzem die prognostisch relevante medikamentöse Therapie der Herzinsuffizienz. Da ein wesentlicher Anteil der Herzinsuffizienzen vaskulär-ischämisch bedingt sind, sind die Wirkungen dieser Substanzen auf das kardiovaskuläre System von hoher Relevanz und sollen in der vorliegenden Arbeit beispielhaft untersucht werden.
3. Am Beispiel der gezielten onkologischen Therapien mit GDC-0449 (Vismodegib), das durch die EMA und die FDA zur Therapie des Basalzellkarzinoms zugelassen ist, sowie (+)-JQ1, das klinische Verwendung zur Therapie von Kopf-Hals-Tumoren findet, soll in der vorliegenden Arbeit die mögliche Erweiterung des Indikationsbereichs auf die gezielte Therapie kardiovaskulärer Remodeling-Prozesse untersucht werden.
4. Die Untersuchung der den oben beschriebenen Substanzeffekten zugrundeliegenden Signalkaskaden in humanen vaskulären Zellen *in vitro* sowie im Mausmodell nach endovaskulärer Verletzung *in vivo* sollen einen Beitrag zum pathophysiologischen Verständnis vaskulärer Remodeling-Prozesse liefern.

3 Originalarbeiten

Daniel JM*, Dutzmann J*, Brunsch H, Bauersachs J, Braun-Dullaeus R, Sedding DG, **"Systemic application of sirolimus prevents neointima formation not via a direct anti-proliferative effect but via its anti-inflammatory properties"**, Int J Cardiol (2017), pii: S0167-5273(17)31611-X. DOI: 10.1016/j.ijcard.2017.03.052

Dutzmann J, Koch A, Sonnenschein K, Haertlé M, Korte L, Thum T, Bauersachs J, Sedding DG*, Daniel JM*, **"Sonic Hedgehog-Dependent Activation of Adventitial Fibroblasts Promotes Neointima Formation"**, Cardiovasc Res (2017) 113(13):1653-1663, DOI: 10.1093/cvr/cvx158

Dutzmann J*, Musmann RJ*, Haertlé M, Daniel JM, Sonnenschein K, Schäfer A, Kolkhof P, Bauersachs J, Sedding DG, **"The novel mineralocorticoid receptor antagonist finerenone attenuates neointima formation after vascular injury"**, PLoS One (2017) 12(9):e0184888. DOI: 10.1371/journal.pone.0184888

Dutzmann J*, Haertlé M*, Daniel JM, Kloss F, Musmann RJ, Kalies K, Knöpp K, Pilowski C, Sirisko M, Sieweke JT, Bauersachs J, Sedding DG#, Gegel S#, **"BET bromodomain containing epigenetic reader proteins regulate vascular smooth muscle cell proliferation and neointima formation"**, Cardiovasc Res (2021) 117(3):850-862. DOI: 10.1093/cvr/cvaa121

Dutzmann J*, Bode LM*, Kalies K, Korte L, Kloss FJ, Sirisko M, Pilowski C, Koch S, Schenk H, Daniel JM, Bauersachs J, Sedding DG **"Empagliflozin prevents neointima formation by impairing smooth muscle cell proliferation and accelerating endothelial regeneration"**, Front Cardiovasc Med (2022), 9:956041. DOI: 10.3389/fcvm.2022.956041

3.1 Systemic application of sirolimus prevents neointima formation not via a direct anti-proliferative effect but via its anti-inflammatory properties

Die systemische Therapie mit Sirolimus, wie sie zum Beispiel zur Immunsuppression bei organtransplantierten Patientinnen und Patienten erfolgt, bewirkt eine deutliche Verminderung des Auftretens von ISR. Die zugrundeliegenden molekularen Mechanismen der Wirkung von Sirolimus auf den vaskulären Remodeling-Prozess waren jedoch bisher unbekannt und sollten in vorliegender Studie untersucht werden.

Hierzu erfolgte im Mausmodell die Induktion negativen vaskulären Remodelings durch Dilatation der Femoralarterie von C57BL/6-Mäusen. Die konsekutive Sirolimus-Therapie erfolgte mittels täglicher intraperitonealer Injektion (2mg/kg KGW/d). Nach 14 Tagen konnte eine Reduktion des Ki-67$^+$ Anteils und damit proliferierender neointimaler Zellen gezeigt werden, nach 28 Tagen zeigte sich außerdem eine Verminderung der neointimalen Fläche. Gleichzeitig zeigte sich eine beeinträchtigte Reendothelialisierungskapazität. Interessanterweise zeigte Sirolimus *in vitro* in Konzentrationen, die Serumkonzentration nach systemischer Applikation entsprechen, sowie das Serum von mit Sirolimus behandelten Mäusen keinen Effekt auf die Proliferation glatter Muskel- oder Endothelzellen. Im Gegensatz dazu zeigte sich nach Behandlung mit Sirolimus *in vitro* oder dem Serum von mit Sirolimus behandelten Mäusen eine verminderte Adhäsion von CD45$^+$ Leukozyten und aus dem Knochenmark stammender CD34$^+$ Progenitorzellen in Co-Kultur mit Endothelzellen. Diese Beobachtung konnte am ehesten auf eine verminderte Expression der endothelialen Adhäsionsmoleküle ICAM-1 und VCAM-1 zurückgeführt werden. *In vivo* reduzierte Sirolimus außerdem die Expression der Adhäsionsmoleküle ICAM-1 und VCAM-1 sowie die Rekrutierung MOMA-2$^+$ monozytärer Zellen in neointimalen Läsionen.

Die in dieser Arbeit gezeigten Daten stellen die zum damaligen Zeitpunkt gängige Annahme infrage, dass eine systemische Therapie mit Sirolimus unmittelbar die Proliferation von Glattmuskel- und Endothelzellen und dadurch vaskuläre Remodeling-Prozesse beeinflusst. Zur direkten Hemmung der Proliferation dieser Zellen scheinen deutlich höhere Sirolimus-Konzentrationen notwendig zu sein, als durch eine systemische Sirolimus-Therapie im Tiermodell erreicht werden. Jedoch verhindern die geringeren Sirolimus-Serumkonzentrationen bei systemischer Sirolimustherapie die Rekrutierung zirkulierender inflammatorischer Zellen an vaskulären Läsionen und reduzieren auf diese Art und Weise indirekt die Proliferation von Glattmuskel- und Endothelzellen. Die vaskulären Effekte bei systemischer Sirolimustherapie scheinen also auf eine Reduktion der inflammatorischen Antwort zurückzuführen sein.

Neben dem grundlagenwissenschaftlichen Beitrag zum Verständnis der Mechanismen des Einflusses systemischer Sirolimustherapien auf das vaskuläre Remodeling, legen die in dieser Arbeit veröffentlichten Daten für die klinische Anwendung eine Fortführung der dualen plättchenhemmenden Therapie nach PCI aufgrund der verzögerten Reendothelialisierung nahe.

International Journal of Cardiology 238 (2017) 79–91

Contents lists available at ScienceDirect

International Journal of Cardiology

journal homepage: www.elsevier.com/locate/ijcard

Systemic application of sirolimus prevents neointima formation not *via* a direct anti-proliferative effect but *via* its anti-inflammatory properties☆

Jan-Marcus Daniel [a,1,2], Jochen Dutzmann [a,1,2], Hannes Brunsch [a,2], Johann Bauersachs [a,3], Rüdiger Braun-Dullaeus [b,3], Daniel G. Sedding [a,*,2]

[a] Dept. of Cardiology and Angiology, Hannover Medical School, Hannover, Germany
[b] Dept. of Cardiology, Angiology and Pneumology, Otto-von-Guericke University Magdeburg, Magdeburg, Germany

ARTICLE INFO

Article history:
Received 10 August 2016
Received in revised form 6 January 2017
Accepted 12 March 2017
Available online 14 March 2017

Keywords:
Neointima formation
Sirolimus
Re-endothelialization
Inflammation
Smooth muscle cells
Progenitor cells

ABSTRACT

Background: Systemic treatment with sirolimus, as used for immunosuppression in transplant patients, results in markedly low rates of in-stent restenosis. Since the underlying mechanisms remain obscure, we aimed to determine the molecular and cellular effects of systemic sirolimus treatment on vascular remodeling processes.
Methods and results: Systemic sirolimus treatment significantly reduced smooth muscle cell (SMC) proliferation 14 days after wire-induced injury and neointima formation 28 days after injury in C57BL/6 mice, while simultaneously impairing re-endothelialization. Interestingly, *in vitro*, sirolimus had no direct effect on the proliferation of SMC or endothelial cells (EC) at serum concentrations observed after systemic application. In contrast, sirolimus reduced the adhesion of leukocytes ($CD45^+$) and bone marrow-derived progenitor cells ($CD34^+$) to activated EC by down-regulating the adhesion molecules ICAM-1 and VCAM-1. In addition, sirolimus treatment also significantly reduced the upregulation of ICAM-1 and VCAM-1 and the recruitment of monocytic cells ($MOMA\text{-}2^+$) in neointimal lesions *in vivo*.
Conclusion: Our findings show that systemic sirolimus treatment effectively prevents SMC and EC proliferation *in vivo* without directly affecting these cells. Instead, sirolimus prevents neointima formation and re-endothelialization by attenuating the inflammatory response after injury with secondary effects on SMC and EC proliferation. Thus, despite a similar net effect, the mechanisms of systemic sirolimus treatment are largely different from the local effects achieved after application of sirolimus-eluting stents.

1. Introduction

Vascular proliferative diseases comprise atherosclerosis, restenosis following percutaneous coronary intervention (PCI), venous bypass graft failure, and transplant vasculopathy [1]. The pathophysiology is characterized by endothelial dysfunction or endothelial injury in the case of PCI and stenting, an inflammatory response to the injured vessel segments and proliferation of vascular smooth muscle cells (SMC). Therapeutic strategies addressing the excessive formation of a neointimal lesion as the cause of restenosis have predominantly been based on inhibiting the proliferation and migration of resident SMC [2]. Drug-eluting stents (DES) have successfully been introduced into clinical practice, and sirolimus or its derivates are currently the most frequently used substances incorporated in DES. Because local sirolimus inhibits endothelial recovery, it is necessary to prolong dual antiplatelet therapy after deployment of a DES, compared with the duration of dual anti-platelet therapy after the implantation of a bare-metal-stent (BMS) [3]. Even though the use of DES has strongly reduced the rates of restenosis, a relevant number of patients, especially those

Abbreviations: α-SMA, α-smooth muscle actin; BMPC, bone marrow-derived progenitor cells; BMTx, bone marrow transplantation; CFSE, carboxyfluorescein succinimidyl ester; DES, drug-eluting stents; EC, endothelial cells; ICAM-1, intercellular adhesion molecule 1; mTOR, mammalian target of rapamycin; PCI, percutaneous coronary intervention; PDGF-BB, platelet-derived growth factor-BB; Sca-1, stem cell antigen 1; SMC, smooth muscle cells; SM-like cells, smooth muscle-like cells; VCAM-1, vascular cell adhesion protein 1; VEGF, vascular endothelial growth factor.

☆ **Acknowledgement of grant support**: This study was supported by a German Research Foundation (Cluster of excellence REBIRTH) grant to DS and JB.

* Corresponding author at: Vascular Remodeling and Regeneration Group, Dept. of Cardiology and Angiology, Hannover Medical School, Carl-Neuberg-Str. 1, D-30625 Hannover, Germany.
E-mail address: sedding.daniel@mh-hannover.de (D.G. Sedding).

[1] These authors contributed equally to the manuscript.
[2] This author takes responsibility for all aspects of the reliability and freedom from bias of the data presented and their discussed interpretation.
[3] This author supervised the design of the study and added important content to the manuscript.

http://dx.doi.org/10.1016/j.ijcard.2017.03.052

with diabetes mellitus or after treatment of vessels with small diameters, still develop a relevant narrowing of the treated lesions, requiring repeated revascularization [4,5]. To selectively and efficiently optimize current treatment strategies it is therefore important to better understand the pathophysiology of neointima formation with its different aspects of the inflammatory response to injury, SMC proliferation and re-endothelialization.

The cellular and molecular mechanisms by which sirolimus exerts its clinical effect are incompletely understood. Sirolimus can directly prevent the proliferation of activated resident medial SMC after injury. More precisely, sirolimus induces cell cycle arrest in the late G1 phase by binding the cytosolic immunophilin FK506-binding protein 12 (FKBP12) and inhibiting the mammalian target of rapamycin (mTOR). The degradation of the cyclin-dependent kinase inhibitor p27kip is thereby prevented, resulting in cell cycle arrest in the G1 phase and preventing the proliferation and migration of SMC [6]. However, a recent study has proposed that SMC express only minimal levels of FKBP12, so that very high local concentrations of sirolimus are necessary to achieve a direct anti-proliferative effect on vascular SMC and endothelial cells (EC) [7]. Since the inhibition of the inflammatory response to injury has become a recent focus in preventing neointima formation, the effect of sirolimus on other cell types is an intriguing question. In a mouse model of wire-induced injury, locally applied sirolimus, mimicking the release of sirolimus from a DES, was found to reduce bone marrow-derived progenitor cell (BMPC) accumulation and SMC proliferation within the lesion, resulting in diminished neointima formation. In this model, the local application of sirolimus also retarded the process of re-endothelialization [8].

Previous studies have suggested that a substantial number of BMPC accumulating in the neointimal lesion differentiate into "smooth muscle-like cells" (SM-like cells) and account for the neointimal cellular mass [9,10]. Even though a significant differentiation of BMPC into genuine SMC in the process of neointima formation was challenged by our group and others, the paracrine effects of leukocytes and other BM-derived circulating cells within the neointima are certainly pivotal for the activation of local cells and subsequent lesion development [11,12]. The markers of circulating cells exerting a high plasticity are still a matter of debate, but the most commonly used markers are among others stem cell antigen (Sca)-1 in mice and CD34 in humans [13]. It has been shown that grafted Sca-1$^+$ cells home into the intima of inflamed arteries and cause enhanced inflammation and neointima formation [14]. In contrast, circulating Sca-1$^+$ cell levels also correlate with endothelial recovery, so that these cells may play a dual role in restenosis by promoting both re-endothelialization and neointimal SMC proliferation [15]. In a previous clinical observation, angioplasty and stenting were shown to induce the expression of adhesion molecules on monocytic cells, and in-stent-restenosis was independently correlated with the upregulation of the leukocyte integrin Mac-1 [16]. Known ligands of Mac-1 are the intercellular adhesion molecule-1 (ICAM-1) and vascular cell adhesion molecule-1 (VCAM-1) and blocking of ICAM-1 or VCAM-1 has been reported to prevent the accumulation of monocytic cells as well as the recruitment of BMPC [17]. All these data indicate that targeting the inflammatory response to injury represents an important approach in preventing clinical restenosis.

Sirolimus is an immunosuppressant drug that is widely used in patients following kidney or heart transplantation [18,19]. In contrast to tacrolimus, sirolimus is not a calcineurin inhibitor but it has similar actions of suppressing the immune system. Of note, the main advantage of sirolimus compared with calcineurin inhibitors is its low nephrotoxicity [18]. In the clinical setting, systemic application of sirolimus (2 mg/day for 30 days, without a loading dose) has also shown efficacy for the prevention of in-stent restenosis with minor adverse events [20]. The mechanism underlying this inhibition, however, is not clear. Interestingly, a strong and significant reduction in in-stent-restenosis following PCI and BMS application was also seen in renal transplant patients receiving other immunosuppressive agents [21]. In the current study, we thus aimed to further evaluate the differential anti-inflammatory and anti-proliferative effects of sirolimus on vascular cells, and to dissect the mechanisms, which are responsible for the inhibition of neointima formation following systemic application of sirolimus.

Our data show that systemic sirolimus treatment effectively reduces SMC proliferation and neointima formation. However, serum levels achieved after systemic application of sirolimus were not sufficient to directly affect SMC or EC proliferation *in vitro*. Consistently, dose-finding experiments revealed that high concentrations of sirolimus were necessary to directly prevent SMC or EC proliferation, which probably can only be achieved by local drug application directly into the tissue, as with the use of DES. In contrast, EC activation and adhesion molecule expression (ICAM-1 and VCAM-1), as well as subsequent leukocyte adhesion, is prevented by serum levels achieved after systemic application of sirolimus *in vitro*. In accordance with these results, we found a significantly reduced recruitment and accumulation of circulating BM-derived cells to injured vessel segments after systemic treatment with sirolimus. Subsequently, the proliferation of local SMC, as well as endothelial regeneration and re-endothelialization, were significantly impaired. These data provide evidence that – despite a similar net effect of local or systemic sirolimus application on neointima formation – completely different molecular and cellular mechanisms are responsible for this effect. Moreover, our data further underscore the pivotal role of the early inflammatory response for later activation and proliferation of local SMC as well as for EC regeneration and neointima formation.

2. Methods

2.1. Animals

All procedures involving experimental animals were approved by the institutional committee for animal research of Giessen University (GI 20/10 Nr. 40/2002) and complied with the directive 2010/63/EU of the European Parliament. All animals received humane care according to the institution's guidelines. All experiments were performed on at least 8-week-old adult male C57BL/6 mice purchased from Charles River (Sulzfeld, Germany). Enhanced green fluorescence protein (eGFP)-transgenic mice on a C57BL/6 mouse background (*C57BL/6-Tg(CAG-EGFP)1Osb/J*) were purchased from The Jackson Laboratory (Bar Harbor, ME, USA). Sample sizes for *in vivo* experiments were 5–10 for each group depending on the difference between means of interest. Calculation of sample sizes was performed by the Institute of Biometrics of the Hannover Medical School (No. 14.0082) and animals were randomly assigned to any group.

2.2. Irradiation and bone marrow transplantation (BMTx)

C57BL/6 mice were irradiated with a dose of 9.5 Gy and BMTx was performed on the same day with ~5×10^6 cells derived from eGFP-transgenic littermates (eGFP$^+$-BM) by tail vein injection as previously described [11]. Enrofloxacin (Baytril®, Bayer, Leverkusen, Germany) was administered to the drinking water for 2 weeks after BMTx. At 12 weeks after transplantation, flow cytometry analysis (FACS Scan, Becton Dickinson, Franklin Lakes, NJ, USA) of blood samples was performed to monitor the success of BMTx (eGFP$^+$-cells per total mononuclear cells). In addition, we analyzed peripheral blood samples for leukocyte subpopulations and compared the proportion of leukocyte subpopulations between transplanted and non-transplanted mice by flow cytometry.

2.3. Wire-induced injury of the femoral artery

The dilation of the left femoral artery was performed as described previously [11]. In brief, male C57BL/6 mice were anaesthetized using 100 mg ketamine hydrochloride/kg body weight (Anesketin, Albrecht, Aulendorf, Germany) and 16 mg xylazine hydrochloride/kg body

weight (Rompun® 2%, Bayer, Leverkusen, Germany). The femoral artery was dilated using a straight spring wire (0.38 mm in diameter; Cook, Bloomington, IN, USA) that was inserted approximately 10 mm towards the iliac artery. Post-interventional analgesic therapy was performed by intraperitoneal (i.p.) administration of 0.1 mg buprenorphine/kg body weight/day for 3 days. Blood was drawn from the right ventricle and the vessels were harvested at the indicated time points. The arteries were fixed in 4% paraformaldehyde (PFA) and embedded in Tissue Tek OCT embedding medium (Sakura Finetek Europe B. V., Zoeterwoude, The Netherlands). All arteries were snap-frozen and stored at −80 °C until sectioning.

2.4. Administration of sirolimus

Sirolimus was purchased from Sigma-Aldrich (Munich, Germany) and dissolved in 0.2% sodium carboxymethylcellulose, 0.25% polysorbate-80 in water. Sirolimus was administered by daily i.p. injection until harvesting of the vessels at a dosage of 2 mg/kg body weight/day. The dose of sirolimus was based on the literature with respect to its use as an immunosuppressant in mice [22,23]. This dose results in serum levels comparable to sirolimus serum levels in transplant patients [24]. The vehicle used in control groups was the solvent for sirolimus.

2.5. Morphometry

The dilated part of the femoral artery was excised, embedded in Tissue-Tek O.C.T. (VWR, Hannover, Germany), snap frozen and cut into 6-μm serial sections. 3 cross-sections each at 750 μm intervals over a length of at least 4.5 mm throughout the excised artery segment were stained with van Gieson staining. For morphometric analyses, ImageJ 1.48 software (National Institutes of Health, Bethesda, MD, USA) was used to measure the external elastic lamina, internal elastic lamina, and lumen circumference, as well as medial and neointimal area. The intima-to-media (I/M-ratio) was calculated from neointimal area divided by medial area. Luminal stenosis was calculated as percent stenosis = [1 − (AL/AN)] × 100 (AL = luminal area, and AN = area of the normal artery defined as the area surrounded by internal elastic lamina).

2.6. Immunohistochemistry

Femoral artery cross-sections were incubated with antibodies recognizing α-smooth muscle actin (α-SMA, Sigma-Aldrich), calponin (Abcam, Cambridge, UK), Ki-67 (Abcam), von Willebrand factor (vWF, Dako, Glostup, Denmark), monocyte + macrophage antibody (MOMA)-2 (Serotec, Oxford, UK), Sca-1/Ly-6A/E (R&D Systems, Minneapolis, MN, USA), ICAM-1 and VCAM-1 (Santa Cruz Biotechnology, Dallas, TX, USA), and CD34 (BD Pharmingen, Franklin Lakes, NJ, USA). Ensuing incubations were carried out with Cy5- or Cy3-coupled secondary antibodies (Molecular Probes, Eugene, OR, USA) and counterstained with nuclear 4.6-diamidino-2-phenylindole (DAPI) (Linares, Wertheim, Germany). Monoclonal antibodies to α-SMA were labeled directly with Cy3. For negative controls, the primary antibody was substituted by an appropriate species- and isotype-matched control antibody (Santa Cruz Biotechnology). Function-blocking mouse anti-human ICAM-1 (cloneP2A4) and VCAM-1 (clone P1B8) antibodies were obtained from Chemicon International (Hempshire, UK). Semi-quantitative analysis of immunohistochemistry was performed using a visual scale ranging from 1 to 4, indicating very low staining for 1 and very strong staining for 4.

2.7. Microscopy

Tissue samples were analyzed using bright field or immunofluorescence microscopy (DMRB, Leica, Wetzlar, Germany) equipped with appropriate filter blocks. For deconvolution analysis of *z*-axis image stacks, a piezo stage scanner (PI, Karlsruhe, Germany) was used together with three-dimensional image processing software (Autoquant Deblur 9.3; Media Cybernetics, Rockville, MD, USA). In addition, confocal microscopy was performed on a subset of slides (Eclipse TE2000-E, Nikon, Tokyo, Japan).

2.8. Assessment of re-endothelialization

To measure the re-endothelialized area, wild-type animals were perfused *in vivo* with Evans blue dye (Sigma-Aldrich) 0, 7 and 14 days after injury, as described previously [25]. Briefly, 50 μL of 5% Evans blue diluted with saline were injected into the tail vein 10 min before the animals were sacrificed, followed by fixation *via* perfusion with 4% paraformaldehyde (PFA) for 5 min. Blood, saline, and fixative were removed through an incision in the right atrium. Pictures of *en face* prepared injured arteries were taken and re-endothelialization was assessed. The re-endothelialized area was calculated as difference between the non-stained and blue-stained area of the injured vessel segment by computer-assisted morphometric analysis (ImageJ 1.48 software) and presented as percentage of re-endothelialization.

2.9. Cell culture, in vitro assays and western blotting

Human coronary artery SMC, human coronary artery EC as well as $CD34^+$ cells and $CD45^+$ cells derived from G-CSF-mobilized peripheral blood cells by immunomagnetic separation were all purchased from Cambrex (Verviers, Belgium). Vascular cells between passages 3 and 6 were used for all experiments and cells were cultured in optimized growth medium (Cambrex) according to the supplier's protocols. Serum from mice treated with sirolimus or vehicle control for 14 days was obtained 2 h after the last i.p. injection of sirolimus. Platelet-derived growth factor (PDGF)-BB and vascular endothelial growth factor (VEGF) were purchased from Sigma-Aldrich. Quantification of cell proliferation was assessed using a BrdU-based Cell Proliferation ELISA assay according to the manufacturer's protocol (Cat. 11 647 229 001, Roche Applied Science, Mannheim, Germany). $CD34^+$ cells and $CD45^+$ cells were used for the adhesion assay on activated human coronary artery EC. Activation of EC was performed by adding TNF-α (10 ng/mL, Sigma-Aldrich) for 8 h in the presence or absence of sirolimus in the concentrations indicated or in the presence or absence of blocking antibodies against ICAM-1 or VCAM-1. $CD34^+$ cells and $CD45^+$ cells were labeled with carboxyfluorescein succinimidyl ester (CFSE, 5 μM), and identical cell numbers were placed onto culture dishes containing the activated EC. After 60 min of co-culture at 37 °C, non-adherent cells were removed by washing and adherent $CD45^+$ cells or $CD34^+$ cells were evaluated by counting labeled cells in three fields of view per condition. To analyze changes in protein expression, EC were cultured for 8 h in the absence or presence of TNF-α (10 ng/mL) and with or without sirolimus (1 ng/mL). Western Blotting was performed as previously described [26]. All *in vitro* experiments were performed at least in triplicates of independent experiments (n = 3–4 in each experiment).

2.10. Statistical analysis

Data were stored and analyzed on personal computers using Microsoft Excel 2010 (Microsoft Corporation, Redmond, WA, USA) and GraphPad Prism 6.01 (GraphPad Software Inc., La Jolla, CA, USA). The data are presented as the mean ± SD. The data were compared using analysis of variance (ANOVA), with Fisher's corrected *t*-test as the post-hoc analysis. Depending on the number of comparisons, ANOVA was followed by pair-wise multi-comparison using the Tukey method (comparison of 6 or more groups). $p < 0.05$ was considered statistically significant in all comparisons.

3. Results

3.1. Systemic sirolimus treatment prevents SMC proliferation and neointima formation

To assess SMC proliferation *in vivo*, we performed Ki-67 and α-SMA staining in cross-sections of neointimal lesions. Systemic sirolimus treatment with 2 mg/kg/day significantly prevented the proliferation of medial and neointimal SMC compared with the control group 14 days after injury (0.15 ± 0.01 *vs.* 0.08 ± 0.01, n = 5, $^{**}p = 0.002$, Fig. 1A + B).

Systemic sirolimus treatment (2 mg/kg/day) also significantly reduced neointima formation and luminal stenosis 28 days after wire-induced injury (intima/media ratio: 0.31 ± 0.18 *vs.* 1.01 ± 0.36, n = 5 for 28 days after injury, $^{***}p < 0.001$, Fig. 1C, D, and luminal stenosis 48.84 ± 20.43% *vs.* 16.44 ± 11.25%, n = 5, $^{**}p = 0.001$, Fig. 1E). Systemic sirolimus treatment using a reduced dose (1 mg/kg) resulted in a clear trend towards reducing neointima formation but just missed statistical significance (0.62 ± 0.14 *vs.* 0.90 ± 0.28, n = 5, $p = 0.08$, Supplemental Fig. 1).

3.2. Sirolimus retards re-endothelialization following vascular injury

Because the effects of sirolimus are not cell-type specific, we assessed the effect of systemic sirolimus treatment on endothelial

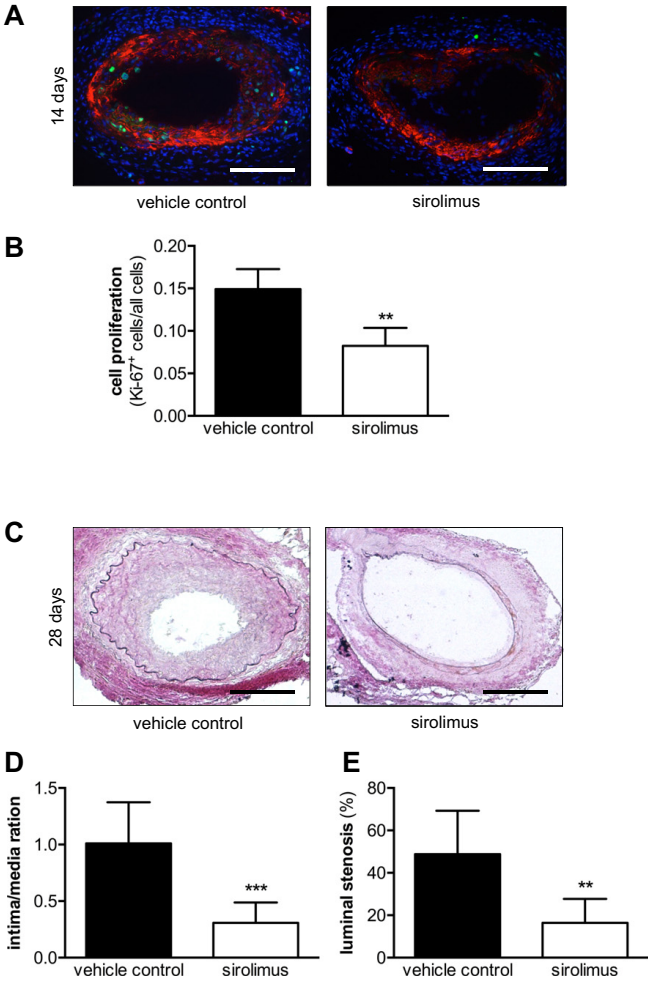

Fig. 1. Sirolimus prevents SMC proliferation and neointima formation after wire-induced injury. A, Representative cross-sections of mouse femoral arteries 14 days after injury treated with vehicle (n = 6 mice) or sirolimus (n = 5 mice) were stained for Ki-67 and α-SMA (scale bar: 100 μm). B, Proliferation of neointimal and medial cells was quantified by counting $Ki67^+$ cells at 14 days after vascular injury within the medial and neointimal layer (n = 5 per group, $^{**}p = 0.002$). C, Representative cross-sections of mouse femoral arteries 28 days after wire-induced injury treated with vehicle (n = 7 mice) or sirolimus (n = 9 mice) were stained for van Gieson (scale bar: 100 μm). D, Morphometric quantification of vehicle-treated (black bars) and sirolimus-treated (white bars) lesions was performed 28 days after injury. The intima-to-media (I/M-ratio) was calculated from the neointimal area divided by the medial area ($^{***}p < 0.001$). E, Luminal stenosis was calculated as percent stenosis = $[1 - (A_L/A_N)] \times 100$, A_L = luminal area, and A_N = area of the normal artery defined as the area surrounded by internal elastic lamina ($^{***}p = 0.001$).

recovery after vascular injury. *Re*-endothelialization of denuded femoral arteries was quantified by en face microscopy of harvested vessels following Evans blue-staining. Systemic daily sirolimus treatment significantly retarded re-endothelialization compared with that in control mice 14 days after vascular injury (54.6 ± 12.5 *vs.* 78.6 ± 7.8%, n = 4, $^{*}p = 0.017$, Fig. 2A, B). At 28 days after injury, the vessels of sirolimus-treated and control mice showed almost complete endothelial recovery (sirolimus: 96.5 ± 2.2%, control: 97.6 ± 1.7%, n = 4, $p = 0.461$, Fig. 2A, B). These data indicate that by continuous administration of sirolimus, re-endothelialization was retarded but completed after a longer time period.

3.3. Sirolimus inhibits the accumulation of all bone marrow-derived cells and monocytes within the neointima

To assess the contribution of all bone marrow-derived cells to the neointimal lesion, bone marrow transplantation (BMTx) of eGFP transgenic mice was performed into wild-type mice. The percentage of hematopoietic chimerism after irradiation and BMTx was assessed by flow cytometry of peripheral blood mononuclear cells 12 weeks after transplantation as previously described (88.43% ± 4.21, n = 6) [11]. At 12 weeks after BMTx, we performed dilation of the femoral artery. Following daily systemic treatment with sirolimus, we found a significant reduction in the relative number of $eGFP^+$ cells/all cells ($DAPI^+$) within the neointimal lesion compared with that in control vessels 14 and 28 days after injury (0.309 ± 0.294 *vs.* 0.090 ± 0.057 on day 14 and 0.411 ± 0.192 *vs.* 0.067 ± 0.093 on day 28, n = 10, $^{*}p = 0.043$ and $^{***}p < 0.001$; Fig. 3A, B). To further characterize the population of BM-derived ($eGFP^+$) cells following injury, tissue sections were analyzed for the expression of MOMA-2, a marker for monocytes/macrophages, within the neointimal and the medial layer. At 14 days after injury, sirolimus treatment resulted in a trend towards a reduced relative number of $MOMA\text{-}2^+eGFP^+$ cells/all $eGFP^+$ cells (0.079 ± 0.146 *vs.* 0.025 ± 0.056, n = 8, $p = 0.458$). At 28 days after injury, we detected a significant reduction in the relative number of $MOMA\text{-}2^+eGFP^+$ cells/all $eGFP^+$ cells in the neointima following systemic sirolimus treatment compared with that in control vessels (0.201 ± 0.098 *vs.* 0.062 ± 0.121, n = 8, $^{*}p = 0.040$, Fig. 3C, D). These results indicate that systemic sirolimus treatment in general prevents the accumulation of BM-derived circulating cells and monocytes after vascular injury.

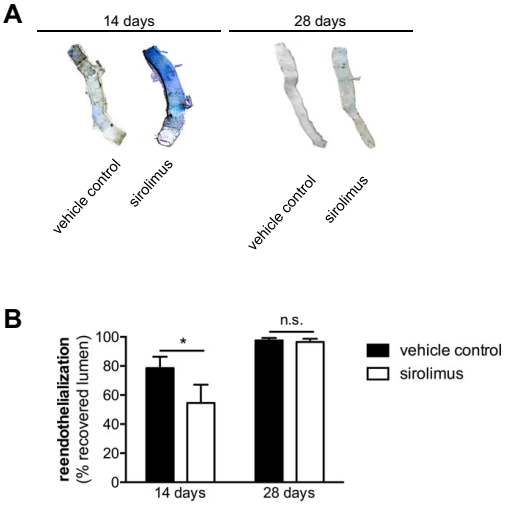

Fig. 2. Sirolimus impairs re-endothelialization after vascular injury. A, Representative images of mouse femoral arteries 14 days (left) and 28 days (right) after wire-induced injury treated with vehicle or sirolimus. Evans blue staining identifies segments of each artery that have not recovered functionally intact endothelium. B, Quantification of re-endothelialized area assessed by Evans blue dye staining of whole-mounted femoral arteries 14 days and 28 days after injury (n = 4, $^{*}p = 0.017$, n.s. = not significant ($p = 0{,}461$)).

3.4. Accumulation and differentiation of BMPC into bona fide vascular cell types is an extremely rare event

To assess the effect of systemic sirolimus treatment on the accumulation of BMPC within the lesions following vascular injury, we performed immunohistochemistry of mice after BMTx with $eGFP^+$ BM for Sca-1, calponin and vWF. In the sirolimus treated group as well as in the control group, we found only a few eGFP/Sca-1 double-positive cells 14 days after injury (< 0.5%, Fig. 4A). Moreover, only a few BM-derived cells expressed markers for differentiated SMC (calponin, Fig. 4B) or EC (vWF, Fig. 4C). The number of double-positive cells was very low (<0.1%) 28 days after injury in both groups; therefore, no significant differences could be detected. In contrast, a peripheral blood count after treatment with sirolimus did not show significant differences in leukocyte, erythrocyte, or platelet numbers following BMTx with $eGFP^+$ bone marrow (Supplemental Table 1).

3.5. Sirolimus prevents proliferation of SMC and EC in vitro only at high concentrations

Since neointima formation is dependent on the proliferation of SMC and is reciprocally correlated with EC proliferation, we assessed the direct effects of sirolimus on the proliferation of these vascular cell types *in vitro*. Importantly, sirolimus only inhibited the proliferation of SMC in response to growth medium at concentrations as high as 20 ng/mL; there were no significant effects at lower concentrations (n = 4, $^{**}p = 0.009$, Fig. 5A). Likewise, sirolimus only prevented proliferation of EC in a dose-dependent manner at high concentrations (n = 4, $^{*}p = 0.022$, $^{***}p < 0.001$, Fig. 5B). These data suggest that the anti-proliferative effect of systemic sirolimus treatment on SMC and EC may rather be an indirect effect, since systemic application of sirolimus does not result in serum concentrations as high as needed to directly prevent SMC and EC proliferation.

3.6. Sirolimus reduces expression of ICAM-1 and VCAM-1 in activated EC and prevents adhesion of BMPC and monocytes at low concentrations in vitro

Recruitment of BM-derived cells to the site of vascular injury is dependent on various cellular adhesion molecules. ICAM-1 and VCAM-1 are pivotal molecules in this process. Therefore, we quantified the effects of sirolimus on ICAM and VCAM expression in activated EC and performed cell adhesion experiments on activated EC using $CD45^+$ leukocytes and BMPC. Treatment with a low dose sirolimus (1 ng/mL) significantly reduced the expression of ICAM-1 and VCAM-1 in EC after activation with TNF-α, as detected by western blotting (n = 3, Fig. 6A). To address the direct effects of sirolimus on the adhesion of leukocytes and BMPC, human $CD45^+$ cells and purified $CD34^+$ cells were allowed to adhere to TNF-α-stimulated EC, and the effect of sirolimus and neutralizing antibodies to ICAM-1 and VCAM-1 on cell adhesion was assessed. Sirolimus dose-dependently attenuated the adhesion of leukocytes ($CD45^+$) to stimulated EC (sirolimus 20 nM: 32 ± 8, sirolimus 1 nM: 57 ± 10, control: 84 ± 22 cells/high power field, n = 4, $^{***}p < 0.001$, Fig. 6B). Moreover, we found a dose-dependent inhibition of sirolimus of the adhesion of $CD34^+$ cells to stimulated EC (sirolimus 20 nM: 13 ± 8, sirolimus 1 nM: 36 ± 12, control: 78 ± 16 cells/high power field, n = 4, $^{**}p = 0.003$, Fig. 6C). Preincubation of EC with neutralizing antibodies to ICAM-1 (40

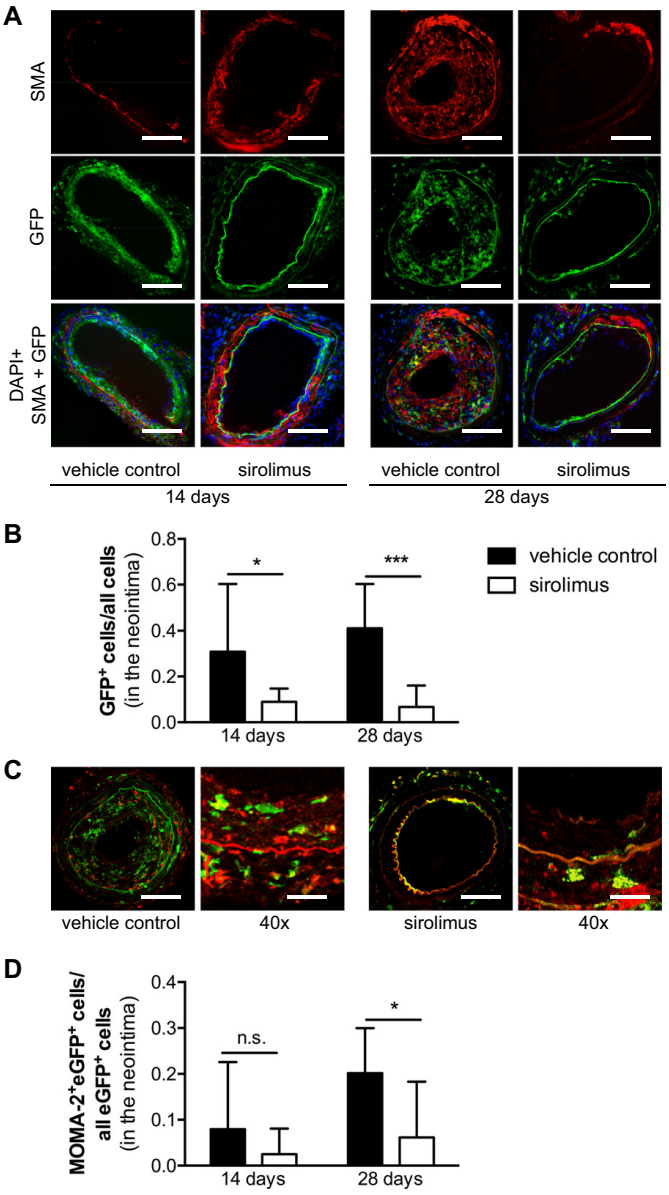

Fig. 3. Sirolimus prevents the accumulation of BM-derived cells in the neointima. A, Representative cross-sections of mouse femoral arteries 14 days and 28 days after injury treated with vehicle or sirolimus were stained for DAPI (blue) to localize nuclei and α-SMA (red). The eGFP signal represents the endogenous signal (green) without additional antibody staining, (scale bar: 100 μm). B, Cells of the neointima and media expressing both eGFP (green) and DAPI were correlated to the total cell count, and the relative number of $eGFP^+$ (BM-derived) cells in the neointima and media was quantified ($^*p = 0.043$, $^{***}p < 0.001$). C, Representative cross-sections of mouse femoral arteries 14 days and 28 days after injury treated with vehicle or sirolimus were stained for MOMA-2 (red) to localize monocytes/macrophages (scale bars: 100 μm and 25 μm (40×)). D, Cells of the neointima and media expressing both MOMA-2 (red) and eGFP (green) were correlated to the total cell count of all $eGFP^+$ cells and the relative number of monocytes/macrophages in the neointima and media was quantified ($^*p = 0.040$).

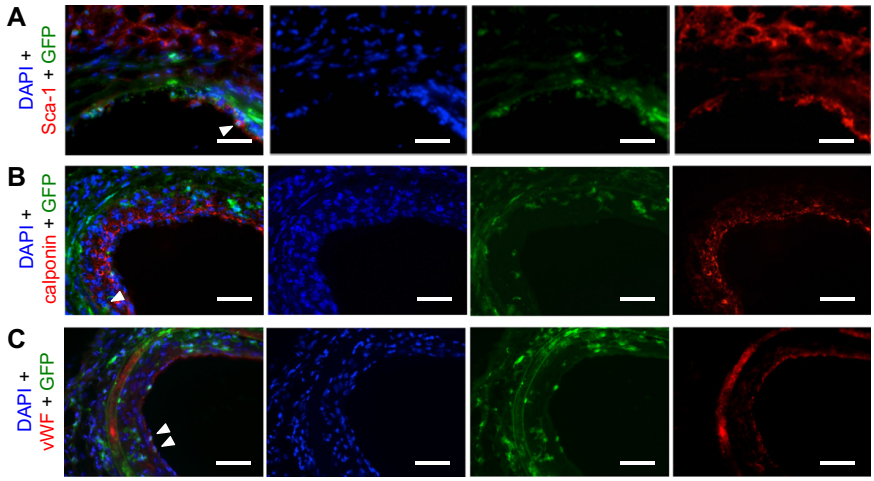

Fig. 4. Accumulation and differentiation of BMPC into *bona fide* vascular cell types is an extremely rare event. A, Representative cross-sections of mouse femoral arteries 14 days after injury treated with vehicle or sirolimus were stained for DAPI (blue) and Sca-1 (red) to identify BMPC. Cells of the neointima and media expressing both Sca-1 (red) and eGFP (green) indicate BMPC (arrowhead) (scale bar: 50 μm). B,C Representative cross-sections of mouse femoral arteries 28 days after injury treated with vehicle or sirolimus were stained for calponin (red) to detect BM-derived SMC, or vWF (red) to detect BM-derived EC (scale bars 50 μm).

μg/mL) or VCAM-1 (40 μg/mL) was effective in reducing adhesion of $CD45^+$ cell to activated EC (ICAM-1: 48 ± 11, VCAM-1: 41 ± 7, control IgG: 85 ± 13 cells/high power field, n = 4, $^{***}p < 0.001$, Fig. 6D). Interestingly, preincubation of EC with neutralizing antibodies indicated that only neutralizing antibodies to ICAM-1 but not to VCAM-1 significantly reduced $CD34^+$ cell adhesion (ICAM-1: 29 ± 6, VCAM-1: 57 ± 18, control IgG: 83 ± 13 cells/high power field, n = 4, $^{*}p = 0.022$, Fig. 6E). These data indicate that sirolimus directly prevents the expression of ICAM-1 and VCAM-1 and thus the adhesion of leukocytes and BMPC to the site of injury.

3.7. Sirolimus concentrations in mouse serum achieved after systemic application do not prevent the proliferation of SMC or EC but prevent the expression of ICAM-1 and VCAM-1 and the adhesion of leukocytes and BMPC in vitro

To determine whether serum levels of sirolimus in mice treated systemically with sirolimus can directly prevent vascular cell proliferation, sirolimus (2 mg/kg body weight, i.p.) or vehicle control was applied daily for 14 days and serum was isolated from treated mice 2 h after the last administration. SMC were incubated for 24 h with serum obtained from mice treated with sirolimus or with vehicle control in the presence or absence of PDGF-BB. Interestingly, incubation of SMC or EC with serum obtained from sirolimus treated mice did not affect SMC or EC proliferation, as determined by BrdU incorporation (n = 4, $p = 0.328$ w/o PDGF and $p = 0.998$ w/ PDGF in SMC and $p = 0.716$ w/o PDGF and $p = 0.796$ w/ PDGF in EC, Fig. 7A and B).

In contrast, incubation of EC with serum obtained from sirolimus-treated mice attenuated the adhesion of leukocytes ($CD45^+$) to stimulated EC (vehicle treated serum: 85.89 ± 12.76, sirolimus-treated serum: 46.00 ± 11.94 cells/high power field, n = 4, $^{***}p < 0.001$, Fig. 7C). Moreover, we found a significant inhibition of adhesion of $CD34^+$ cells to stimulated EC after incubation with serum obtained from sirolimus-treated mice as compared with EC incubated with serum from vehicle-treated mice (vehicle-treated serum: 36.89 ± 11.84, sirolimus-treated serum: 17.78 ± 3.99 cells/high power field, n = 4, $^{***}p < 0.001$, Fig. 7D).

3.8. Sirolimus prevents adhesion molecule expression after vascular injury

To assess the effects of systemic sirolimus treatment on the expression of ICAM-1 and VCAM-1 *in vivo*, we analyzed the expression of these cellular adhesion molecules following vascular injury. Treatment with sirolimus resulted in a significantly reduced expression of ICAM-1 and VCAM-1 14 days after vascular injury, indicating that this effect may contribute to the decreased accumulation of BM-derived cells within the developing neointima (ICAM-1: 0.8 ± 0.3 *vs.* 2.3 ± 0.4, n = 4, $^{*}p = 0.013$, VCAM-1: 1.2 ± 0.2 *vs.* 2.8 ± 0.3, n = 4, $^{**}p = 0.005$, Fig. 8A,B).

4. Discussion

Sirolimus and its derivates are currently widely used as anti-proliferative substances coated on DES. Systemic application of sirolimus is also effective in reducing in-stent-restenosis, but the mechanisms remain poorly understood [20]. Importantly, sirolimus is widely used as an immunosuppressive drug for the treatment of auto-immune diseases or after organ transplantation, especially following heart or kidney transplantation. These patients have a high risk of developing symptomatic coronary artery disease and often require PCI and/or coronary stent implantation. Therefore, we investigated the effects of systemic sirolimus application on neointima formation in a mouse model of vascular injury, and aimed to further elucidate the molecular and cellular mechanisms underlying the protective effect of sirolimus under these conditions. The mouse model used in this study is widely accepted for studies of post-angioplasty restenosis, because it closely resembles the angioplasty procedure that injures both endothelium and vessel wall [27]. Sirolimus was administered i.p. daily in a dose of 2 mg/kg body weight, which results in serum levels comparable so sirolimus serum levels in transplant patients [28,29]. Consistent with clinical observations, we found a significant reduction in neointima formation but, importantly, also in endothelial recovery after injury. Further, we demonstrated that the mechanisms of systemic sirolimus treatment are quite distinct from the effects of a local release of sirolimus from DES. Since a direct anti-proliferative effect in SMC and

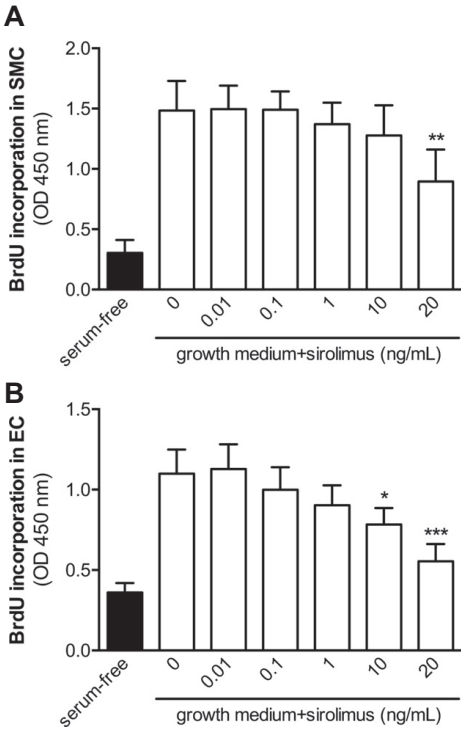

Fig. 5. Sirolimus only prevents proliferation of SMC and EC at high concentrations in a dose-dependent manner. A, SMC were grown in the presence or absence of growth medium and the indicated concentrations of sirolimus. Incorporation of BrdU was determined after 24 h (n = 4, $^{**}p = 0.009$). B, EC were grown in the presence or absence of growth medium and the indicated concentrations of sirolimus. Incorporation of BrdU was determined after 24 h (n = 4, $^{*}p = 0.022$, $^{***}p < 0.001$).

EC can only be observed after administration of high concentrations of sirolimus, as achieved by a local release into the vessel wall, the lower circulating drug levels after systemic sirolimus treatment exert anti-inflammatory properties, not direct anti-proliferative properties; thus, sirolimus only indirectly inhibits SMC and EC proliferation by preventing the inflammatory response and the release of growth factors and cytokines by the recruited leukocytes.

4.1. Mechanisms and cellular cross-talk during neointima formation

Vascular SMC from the medial layer are the predominant cell type within neointimal lesions. The inhibition of SMC proliferation and migration has thus been the primary therapeutic approach in recent years [13]. Other therapeutic strategies aim to attenuate the inflammatory response or to accelerate endothelial recovery following injury [2]. Importantly, inflammation and endothelial recovery are strongly related to each other, since leukocyte-derived growth factors and cytokines do not only stimulate the proliferation of SMC but also EC. On the other hand, stimulation of re-endothelialization has been shown to be effective in reducing the inflammatory response to injury, and also in directly preventing SMC proliferation, due to the release of nitric oxide in the course of neointimal lesion formation [25]. Moreover, inflammation and SMC proliferation are directly linked and a reduced inflammatory response results in reduced SMC proliferation and neointima formation [1].

4.2. BMPC in neointima formation

The design of the study using BMTx of $eGFP^+$ bone marrow cells enabled us to investigate the extent of the inflammatory response, as well as the accumulation and possible differentiation of circulating BMPC in the neointimal lesions. We therefore aimed to first determine the total number of cells recruited from the circulation, followed by a more detailed analysis of the cellular subtypes and their relative numbers after sirolimus treatment. Tracking all circulating and recruited cells from the circulation is mandatory for such an approach. Thus, we used a model of BMTx, in which -after the reconstitution of the transplanted BM- the vast majority of all circulating cells were eGFP-labeled (88.43% ± 4.21 $eGFP^+$, n = 6) and could be tracked over time [11]. Using specific antibodies for additional cell markers, we were able to differentially determine the numbers of resident *vs.* recruited cells expressing SMC or EC markers or markers of cells with high plasticity.

In accordance with prior reports, our data confirmed that circulating BMPC can temporarily accumulate within the lesion and express rather unspecific SMC marker genes, such as α-SMA. However, α-SMA is also expressed by monocytes/macrophages in a certain interim state; therefore, these cells do not necessarily represent differentiated genuine SMC [13]. Nonetheless, highly active and plastic BMPC recruited from the circulation may be important modulators of the local response to injury by the paracrine effects of these cells on the surrounding resident cells. These effects have predominantly been documented for the processes of angiogenesis and arteriogenesis with effects on EC, but also in atherosclerosis and neointima formation [30]. In accordance with our results, only a few BM-derived SM-like cells expressing SMA could be detected within atherosclerotic plaques in these studies. Nevertheless, using genetic mouse models, these cells were found to secrete various pro-inflammatory cytokines and mitogens, thereby promoting the proliferation of adjacent SMC and progression of the atherosclerotic lesion [31]. Since our *in vitro* data demonstrate that systemic application of sirolimus potently prevents not only the adhesion of inflammatory ($CD45^+$) cells but also of circulating BMPC ($CD34^+$), this combined action may contribute to the indirect anti-proliferative effect of sirolimus on local SMC and the prevention of neointima formation. However, further studies are required to precisely determine the relative importance of leukocytes *vs.* BMPC on the paracrine activation of resident cells.

4.3. Sirolimus attenuates the recruitment of circulating cells by down-regulation of the adhesion molecules ICAM-1 and VCAM-1

Our *in vitro* data showed that sirolimus has a direct inhibitory effect on the adhesion of leukocytes and BMPC to TNF-α-activated EC. Leukocyte recruitment is strongly dependent on the expression of both ICAM-1 and VCAM-1 in activated EC and inhibition of these molecules can effectively prevent the inflammatory response and vascular lesion formation [32]. We also showed that sirolimus prevents the up-regulation of these adhesion molecules in EC. In fact, a recent study confirmed that inhibition of the mTOR signaling complex mTORC2 by sirolimus can prevent the TNF-α-mediated induction of VCAM-1 in EC [33]. However, numerous other adhesion molecules are involved in the complex cascade of circulating cell recruitment, and may be influenced, as well. Thus, preventing the expression of ICAM-1 and VCAM-1 may represent only one aspect of the anti-adhesive properties of sirolimus, and other mechanisms very likely contribute to the potent *in vivo* effects observed in our study.

4.4. Systemic application of sirolimus only indirectly reduces SMC proliferation

The effect of sirolimus derived from DES on neointima formation is mainly explained by a local inhibition of the proliferation of resident

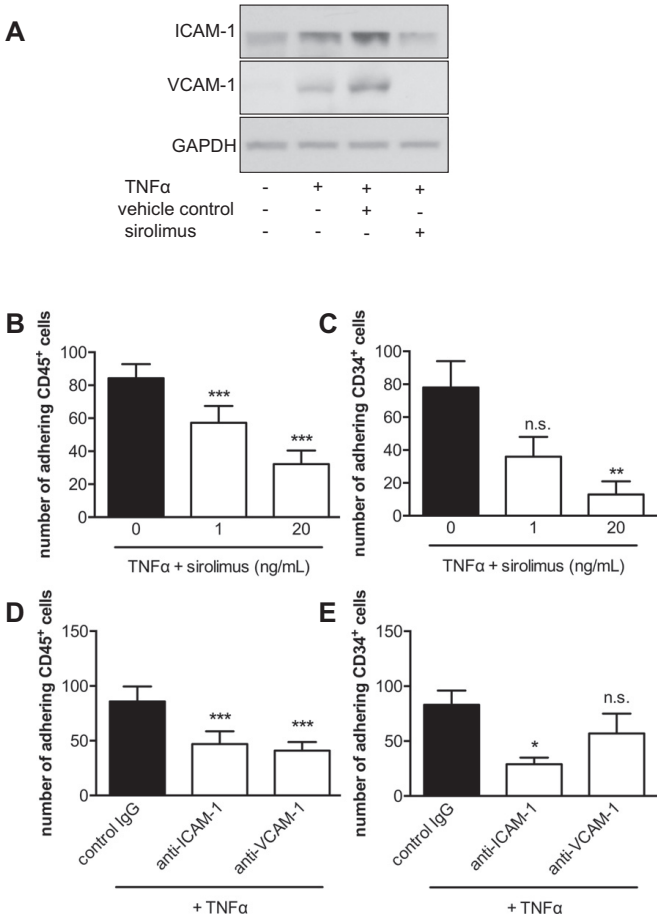

Fig. 6. Sirolimus prevents adhesion of leukocytes and BMPC to activated EC *in vitro* by down-regulation of ICAM-1 and VCAM-1. A, EC were cultured for 8 h in the absence or presence of TNFα and with sirolimus (1 ng/mL) or vehicle control. Expression of ICAM-1 or VCAM-1 was determined by Western Blotting in lysates from EC. Representative blots of three independent experiments are shown. B,C, EC were cultured in the absence or presence of TNFα and treated with sirolimus at the given concentrations or the control buffer. $CD45^+$ cells (B) or $CD34^+$ cells (C) were labeled with CFSE (5 μM) prior to co-culture in adhesion assays on EC. After 60 min of co-culture, nonadherent cells were removed by washing and adherent $CD45^+$ cells or $CD34^+$ cells were evaluated by counting labeled cells in three fields of view per condition (n = 4, ** $p = 0.003$, *** $p < 0.001$). D,E, The adhesion assay was performed under the same conditions, but instead of sirolimus treatment blocking antibodies against ICAM-1 (D) or VCAM-1 (E) were used, and adhering cells were quantified (n = 4, * $p = 0.022$, *** $p < 0.001$).

SMC and EC. Importantly, our data show that sirolimus only prevents SMC proliferation at relatively high concentrations of 20 ng/mL. This can be explained by the recent finding that vascular SMC only express low levels of FKBP12, which is the cytosolic target of sirolimus for inhibiting mTOR [7]. Accordingly, local tissue concentrations of sirolimus are high following the implantation of a DES and thus exert direct anti-proliferative effects. Despite the high local concentrations, the wide therapeutic range of sirolimus or its derivates explains the lack of toxic or apoptotic effects on cells of the vessel wall. Even though high local tissue concentrations are achieved, systemic concentration of sirolimus has not been reported to exceed concentrations of 4 ng/mL directly after DES implantation and is generally below detection levels at later time points [34]. In contrast, systemic application of sirolimus, *e.g.* following organ transplantation, is adapted to achieve serum concentrations of 4 to 12 ng/mL depending on the patient characteristics and the other drugs in the immunosuppressive regimen, and vascular tissue concentrations are not reported to exceed these serum concentration levels [35]. Therefore, only sirolimus derived from DES may have direct effects on SMC proliferation at concentrations as high as 20 ng/mL or more. In contrast, systemic application of sirolimus attenuates the recruitment of leukocytes and BMPC and thus indirectly attenuates SMC proliferation within the neointimal lesions, because SMC proliferation is largely triggered and driven by cytokines and growth factors released from infiltrating inflammatory cells after injury.

4.5. Systemic application of sirolimus prevents endothelial activation and attenuates re-endothelialization following injury

Endothelial recovery is a key aspect for the prevention or limitation of neointima formation. Since sirolimus released from DES retards endothelial recovery after PCI, dual anti-platelet therapy should be

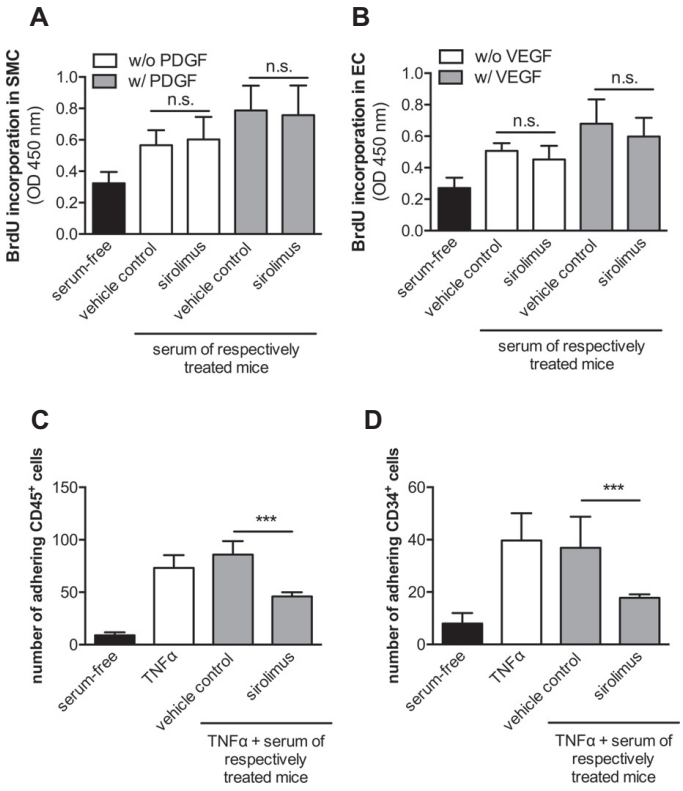

Fig. 7. Systemic concentration levels of sirolimus do not prevent SMC or EC proliferation but prevent adhesion of leukocytes and BMPC to activated EC *in vitro*. A, SMC were incubated for 24 h with serum obtained from mice treated with sirolimus (2 mg/kg body weight/day i.p.) or with vehicle control for 14 days in the presence or absence of PDGF-BB (10 ng/mL). Incorporation of BrdU was determined after 24 h ($n = 4$, n.s. = not significant ($p = 0.716$)). B, EC were incubated for 24 h with serum obtained from mice treated with sirolimus (2 mg/kg body weight/day i.p.) or with vehicle control for 14 days in the presence or absence of VEGF (20 ng/mL). Incorporation of BrdU was determined after 24 h ($n = 4$, n.s. = not significant ($p = 0796$)). C, EC were incubated with serum obtained from mice treated with sirolimus (2 mg/kg body weight/day i.p.) or with vehicle control in the presence or absence of TNFα. $CD45^+$ cells (C) or $CD34^+$ cells (D) were labeled with CFSE (5 μM) prior to co-culture in adhesion assays on EC. After 60 min of co-culture, nonadherent cells were removed by washing and adherent $CD45^+$ cells or $CD34^+$ cells were evaluated by counting labeled cells in three fields of view per condition ($n = 4$, $^{***}p < 0.001$, $^{***}p < 0.001$).

prolonged in order to prevent in-stent-thrombosis. We showed in our study that re-endothelialization is also impaired following systemic application of sirolimus after wire-induced injury in mice. According to our *in vitro* results, sirolimus only reduces proliferation of EC at higher concentrations of sirolimus, and serum from mice receiving systemic application of sirolimus did not prevent EC proliferation, so that a direct inhibitory effect of sirolimus on endothelial proliferation after systemic application of sirolimus at the concentrations used can be excluded. In contrast, serum isolated from mice after systemic sirolimus treatment attenuated the TNF-α-induced up-regulation of endothelial adhesion molecules, indicating that sirolimus exerts different effects on EC in a concentration-dependent manner.

It is well-established that endothelial recovery is very much dependent on the recruitment of leukocytes and BMPC. In accordance with these findings, a recent clinical trial demonstrated enhanced endothelial healing, when sirolimus-eluting DES were coated with CD34-recognizing antibodies on the luminal side, which captured and recruited circulating BMPC [30,36]. Our *in vitro* and *in vivo* data demonstrate that systemic treatment with sirolimus prevents the recruitment and the accumulation of leukocytes and BMPC. Therefore, the reduced re-endothelialization observed in our *in vivo* experiments after systemic sirolimus treatment is very likely due to a reduced expression of adhesion molecules and subsequently reduced recruitment of leukocytes and BMPC, which under normal conditions would support endothelial regeneration by the local secretion of growth factors and cytokines. However, BMPC levels are also positively correlated with restenosis, indicating that there is no specific effect of BMPC on re-endothelialization alone [15,37].

4.6. Effects of sirolimus on the function and differentiation of BMPC

In a previous report using a model of wire-induced injury in mice, the local application of sirolimus around the injured vessel segment resulted in a reduced accumulation and differentiation of BMPC into SM-like cells within neointimal lesions [8]. In accordance, our *in vitro* data show that serum of mice treated systemically with sirolimus also directly attenuated adhesion of $CD34^+$ BMPC to activated EC. However, even though our *in vivo* experiments using a systemic sirolimus application were designed to detect differences in the differentiation capacity of BMPC within neointimal lesions, the numbers of $eGFP^+$ cells expressing Sca-1 or vascular cell markers were very low and double-positive cells could only be observed occasionally, even in control animals.

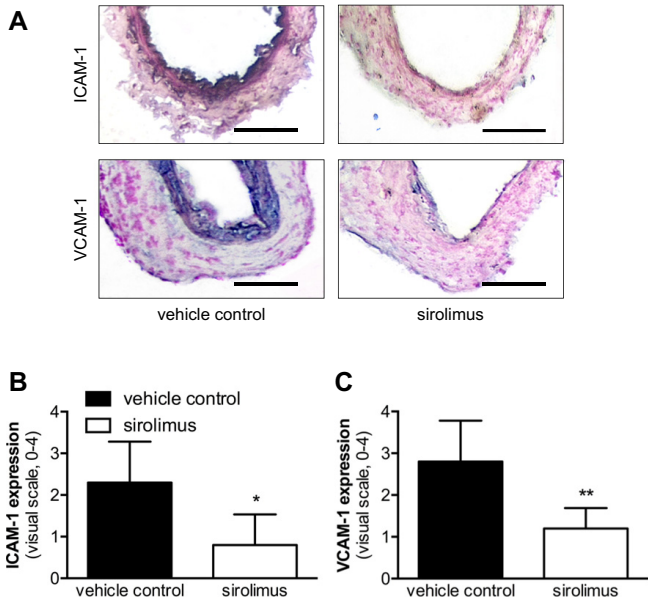

Fig. 8. Sirolimus prevents ICAM-1 and VCAM-1 adhesion molecule expression *in vivo*. A, Representative cross-sections of mouse femoral arteries 14 days after injury treated with vehicle or sirolimus (2 mg/kg body weight/day i.p.) were stained for ICAM-1 or VCAM-1 (scale bar: 50 μm). B, Quantification of ICAM-1 and VCAM-1 expression of mouse femoral arteries was performed using a visual scale ranging from 1 to 4 ($n = 4$, $^{*}p = 0.013$, $^{**}p = 0.005$).

Consequently, there was no statistical difference in the few $eGFP^{+}$ cells expressing SMC markers (calponin) or EC markers (vWF) between the sirolimus-treated group and the control group 14 or 28 days after injury.

The differing results in our study can be explained by the fact that novel, more specific labeling techniques and antibodies as well as 3D confocal laser scanning microscopy techniques were used that enable the identification of false positive results, as described previously by us and others [11,12].

Nevertheless, our *in vitro* findings on the inhibition of BMPC adhesion by sirolimus and the strongly reduced numbers of all BM-derived cells within the neointimal lesion also suggest that also BMPC recruitment may be reduced following treatment with sirolimus *in vivo*, even though our data 14 days and 28 days after injury do not provide clear evidence because of the low numbers of BMPC detected within neointimal lesions. Thus, the role of BMPC in the sirolimus-mediated effects remains largely elusive.

4.7. Clinical implications of basic research

Our data show that systemic application of sirolimus prevents post-angioplasty neointima formation and vessel narrowing by inhibiting the inflammatory response to injury and possibly the recruitment of BMPC to injured vessel segments. Importantly, systemic sirolimus treatment also impairs endothelial regeneration after angioplasty. This information is of particular importance for patients after organ transplantation, especially heart or kidney transplant recipients who are treated systemically with sirolimus, since these patients are at high risk of developing coronary artery disease and of receiving PCI. Under these conditions, systemic sirolimus treatment may support the effect of locally released sirolimus derivatives from DES to prevent restenosis of the dilated and stented vessel segments, which may beneficially influence the outcome of coronary interventions in these patients. On the other hand, our data indicate that re-endothelialization after coronary interventions may be severely impaired in patients receiving systemic sirolimus treatment. Thus, coronary interventions require a subsequent prolonged anti-platelet therapy because of the high thrombogenicity of non re-endothelialized vessel or stent segments. According to the data from this study, extreme caution should be paid to current approvals of new generation DES to reduce dual anti-platelet therapy time to 3 months only, since safety data for this approval have not been obtained in patients systemically treated with sirolimus or in organ transplant patients. The data from this study clearly indicate the need for further clinical trials to determine the optimal duration of anti-platelet therapy after coronary interventions in patients under systemic sirolimus treatment.

4.8. Study limitations

Despite the use of human cells in our *in vitro* experiments to best simulate the responses to sirolimus in human coronary arteries, the *in vivo* experiments of this study were performed in mice. Further studies in larger animals or in humans would be required to confirm these results.

Additionally, to determine the impact of systemic sirolimus treatment on the inflammatory response and the adhesion and recruitment of inflammatory cells, we aimed to also determine the effect on circulating BMPC. For this purpose, we decided to use a BMTx model. However, the number of BMPC expressing Sca-1 or vascular cell markers was found to be very low in neointimal lesions, so we could not detect a significant effect of systemic sirolimus treatment on BMPC recruitment or differentiation after injury. Even though these data are consistent with recent reports investigating the role of BMPC in atherosclerotic lesions [10,24], the initial BMTx may affect the number and functional capacity of circulating BMPC, so further studies in different animal models or humans are required to elucidate the impact of systemic sirolimus treatment on the function of BMPC during neointima formation. Due to the complex

and directly linked interplay of injury-induced inflammation and SMC proliferation, mechanistic data on the selective action of distinct sirolimus doses on either inflammation or SMC proliferation can only be obtained *ex vivo*. Even though it's very likely that these data reflect the processes *in vivo*, a direct proof has to be obtained.

5. Conclusions

The data presented in this manuscript challenge the current assumption that systemic treatment with sirolimus directly affects the proliferation of SMC or EC and thereby influences vascular lesion formation. Significantly higher concentrations than those usually achieved by systemic treatment seem necessary to directly prevent SMC or EC proliferation. Moreover, serum isolated from sirolimus-treated mice did not exert direct anti-proliferative properties on vascular cells *in vitro*. In contrast, sirolimus at (lower) concentrations usually achieved by systemic application potently prevented the recruitment of circulating inflammatory cells to the injured vessel segment. Therefore, the reduced proliferation of EC and SMC after systemic treatment with sirolimus is most likely an indirect effect of the reduced inflammatory response. These novel findings extend our understanding of the mechanisms responsible for the effects of systemic sirolimus treatment on vascular remodeling processes. Moreover, as a clinical implication, our data strongly suggest that dual anti-platelet therapy after PCI should be extended in patients receiving systemic sirolimus treatment because of delayed endothelial recovery.

Author contributions

Conception and design of the study: JMD, JD, HB, RBD, DGS. Acquisition of data: JMD, JD, HB, DGS. Analysis and interpretation of data: JMD, JD, HB, JB, RBD, DGS. Drafting the article or revising it critically for important intellectual content: JMD, JD, HB, JB, RBD, DGS. Final approval of the version to be submitted: JMD, JD, HB, JB, RBD, DGS.

Conflict of interest

The authors report no relationships that could be construed as a conflict of interest.

Funding

This work was supported by a German Research Foundation (Cluster of excellence REBIRTH) grant to DS and JB.

Acknowledgments

We thank Stefanie Wolfram and Mirja Sirisko for excellent technical assistance.

Appendix A. Supplementary data

Supplementary data to this article can be found online at http://dx.doi.org/10.1016/j.ijcard.2017.03.052.

References

[1] V.J. Dzau, R.C. Braun-Dullaeus, D.G. Sedding, Vascular proliferation and atherosclerosis: new perspectives and therapeutic strategies, Nat. Med. 8 (2002) 1249–1256.
[2] M.A. Costa, D.I. Simon, Molecular basis of restenosis and drug-eluting stents, Circulation 111 (2005) 2257–2273.
[3] E. Camenzind, W. Wijns, L. Mauri, V. Kurowski, K. Parikh, R. Gao, et al., Stent thrombosis and major clinical events at 3 years after zotarolimus-eluting or sirolimus-eluting coronary stent implantation: a randomised, multicentre, open-label, controlled trial, Lancet 380 (2012) 1396–1405.
[4] C. Stettler, S. Wandel, S. Allemann, A. Kastrati, M.C. Morice, A. Schomig, et al., Outcomes associated with drug-eluting and bare-metal stents: a collaborative network meta-analysis, Lancet 370 (2007) 937–948.
[5] G.W. Stone, A. Rizvi, W. Newman, K. Mastali, J.C. Wang, R. Caputo, et al., Everolimus-eluting versus paclitaxel-eluting stents in coronary artery disease, N. Engl. J. Med. 362 (2010) 1663–1674.
[6] K.A. Martin, E.M. Rzucidlo, B.L. Merenick, D.C. Fingar, D.J. Brown, R.J. Wagner, et al., The mTOR/p70 S6K1 pathway regulates vascular smooth muscle cell differentiation, American journal of physiology Cell physiology. 286 (2004) C507–C517.
[7] D. Zohlnhofer, C.A. Klein, T. Richter, R. Brandl, A. Murr, T. Nuhrenberg, et al., Gene expression profiling of human stent-induced neointima by cDNA array analysis of microscopic specimens retrieved by helix cutter atherectomy: detection of FK506-binding protein 12 upregulation, Circulation 103 (2001) 1396–1402.
[8] D. Fukuda, M. Sata, K. Tanaka, R. Nagai, Potent inhibitory effect of sirolimus on circulating vascular progenitor cells, Circulation 111 (2005) 926–931.
[9] M. Sata, A. Saiura, A. Kunisato, A. Tojo, S. Okada, T. Tokuhisa, et al., Hematopoietic stem cells differentiate into vascular cells that participate in the pathogenesis of atherosclerosis, Nat. Med. 8 (2002) 403–409.
[10] K. Tanaka, M. Sata, Y. Hirata, R. Nagai, Diverse contribution of bone marrow cells to neointimal hyperplasia after mechanical vascular injuries, Circ. Res. 93 (2003) 783–790.
[11] J.M. Daniel, W. Bielenberg, P. Stieger, S. Weinert, H. Tillmanns, D.G. Sedding, Time-course analysis on the differentiation of bone marrow-derived progenitor cells into smooth muscle cells during neointima formation, Arterioscler. Thromb. Vasc. Biol. 30 (2010) 1890–1896.
[12] H. Iwata, I. Manabe, K. Fujiu, T. Yamamoto, N. Takeda, K. Eguchi, et al., Bone marrow-derived cells contribute to vascular inflammation but do not differentiate into smooth muscle cell lineages, Circulation 122 (2010) 2048–2057.
[13] J.M. Daniel, D.G. Sedding, Circulating smooth muscle progenitor cells in arterial remodeling, J. Mol. Cell. Cardiol. 50 (2011) 273–279.
[14] X. Wang, M. Gao, S. Schouteden, A. Roebroek, K. Eggermont, P.P. van Veldhoven, et al., Hematopoietic stem/progenitor cells directly contribute to arteriosclerotic progression via integrin beta2, Stem Cells 33 (2015) 1230–1240.
[15] G.L. De Maria, I. Porto, F. Burzotta, M.F. Brancati, C. Trani, G. Pirozzolo, et al., Dual role of circulating endothelial progenitor cells in stent struts endothelialisation and neointimal regrowth: a substudy of the IN-PACT CORO trial, Cardiovascular revascularization medicine: including molecular interventions. 16 (2015) 20–26.
[16] T. Inoue, T. Uchida, I. Yaguchi, Y. Sakai, K. Takayanagi, S. Morooka, Stent-induced expression and activation of the leukocyte integrin Mac-1 is associated with neointimal thickening and restenosis, Circulation 107 (2003) 1757–1763.
[17] M. Deckert-Schluter, D. Schluter, H. Hof, O.D. Wiestler, H. Lassmann, Differential expression of ICAM-1, VCAM-1 and their ligands LFA-1, Mac-1, CD43, VLA-4, and MHC class II antigens in murine toxoplasma encephalitis: a light microscopic and ultrastructural immunohistochemical study, J. Neuropathol. Exp. Neurol. 53 (1994) 457–468.
[18] D.J. Moes, H.J. Guchelaar, J.W. de Fijter, Sirolimus and everolimus in kidney transplantation, Drug Discov. Today 20 (2015) 1243–1249.
[19] S. Guethoff, K. Stroeh, C. Grinninger, M.A. Koenig, E.C. Kleinert, A. Rieger, et al., De novo sirolimus with low-dose tacrolimus versus full-dose tacrolimus with mycophenolate mofetil after heart transplantation–8-year results, The Journal of Heart and Lung Transplantation: The Official Publication of the International Society for Heart Transplantation. 34 (2015) 634–642.
[20] S. Stojkovic, M. Ostojic, M. Nedeljkovic, G. Stankovic, B. Beleslin, V. Vukcevic, et al., Systemic rapamycin without loading dose for restenosis prevention after coronary bare metal stent implantation, Catheterization and Cardiovascular Interventions: Official Journal of the Society for Cardiac Angiography & Interventions. 75 (2010) 317–325.
[21] J.H. Jung, P.K. Min, J.Y. Kim, S. Park, E.Y. Choi, Y.G. Ko, et al., Systemic immunosuppressive therapy inhibits in-stent restenosis in patients with renal allograft, Catheterization and Cardiovascular Interventions: Official Journal of the Society for Cardiac Angiography & Interventions. 68 (2006) 567–573.
[22] B.R. Blazar, P.A. Taylor, D.C. Snover, S.N. Sehgal, D.A. Vallera, Murine recipients of fully mismatched donor marrow are protected from lethal graft-versus-host disease by the in vivo administration of rapamycin but develop an autoimmune-like syndrome, J. Immunol. 151 (1993) 5726–5741.
[23] H. Chen, S. Qi, D. Xu, J. Wu, P. Daloze, The immunosuppressive effect of rapamycin on mouse small bowel transplantation, Transplantation 61 (1996) 523–526.
[24] R.N. Saunders, M.S. Metcalfe, M.L. Nicholson, Rapamycin in transplantation: a review of the evidence, Kidney Int. 59 (2001) 3–16.
[25] J.M. Daniel, D. Penzkofer, R. Teske, J. Dutzmann, A. Koch, W. Bielenberg, et al., Inhibition of miR-92a improves re-endothelialization and prevents neointima formation following vascular injury, Cardiovasc. Res. 103 (2014) 564–572.
[26] J.M. Daniel, A. Prock, J. Dutzmann, K. Sonnenschein, T. Thum, J. Bauersachs, et al., Regulator of G-protein signaling 5 prevents smooth muscle cell proliferation and attenuates neointima formation, Arterioscler. Thromb. Vasc. Biol. 36 (2016) 317–327.
[27] T. Takayama, X. Shi, B. Wang, S. Franco, Y. Zhou, D. DiRenzo, et al., A murine model of arterial restenosis: technical aspects of femoral wire injury, Journal of visualized experiments: JoVE 10 (97) (2015).
[28] K. Bishu, O. Ogut, S. Kushwaha, S.F. Mohammed, T. Ohtani, X. Xu, et al., Anti-remodeling effects of rapamycin in experimental heart failure: dose response and interaction with angiotensin receptor blockade, PLoS One 8 (2013), e81325.
[29] T. Shioi, J.R. McMullen, O. Tarnavski, K. Converso, M.C. Sherwood, W.J. Manning, et al., Rapamycin attenuates load-induced cardiac hypertrophy in mice, Circulation 107 (2003) 1664–1670.
[30] G.P. Fadini, D. Losordo, S. Dimmeler, Critical reevaluation of endothelial progenitor cell phenotypes for therapeutic and diagnostic use, Circ. Res. 110 (2012) 624–637.
[31] H. Yu, V. Stoneman, M. Clarke, N. Figg, H.B. Xin, M. Kotlikoff, et al., Bone marrow-derived smooth muscle-like cells are infrequent in advanced primary atherosclerotic plaques but promote atherosclerosis, Arterioscler. Thromb. Vasc. Biol. 31 (2011) 1291–1299.

[32] D.G. Sedding, M. Trobs, F. Reich, G. Walker, L. Fink, W. Haberbosch, et al., 3-Deazaadenosine prevents smooth muscle cell proliferation and neointima formation by interfering with Ras signaling, Circ. Res. 104 (2009) 1192–1200.
[33] C. Wang, L. Qin, T.D. Manes, N.C. Kirkiles-Smith, G. Tellides, J.S. Pober, Rapamycin antagonizes TNF induction of VCAM-1 on endothelial cells by inhibiting mTORC2, J. Exp. Med. 211 (2014) 395–404.
[34] A.S. Thakkar, A.D. Abhyankar, S.I. Dani, D.N. Banker, P.I. Singh, S.A. Parmar, et al., Systemic exposure of sirolimus after coronary stent implantation in patients with de novo coronary lesions: Supralimus-Core® pharmacokinetic study, Indian Heart J. 64 (2012) 273–279.
[35] A.O. Gaber, B.D. Kahan, C. Van Buren, S.L. Schulman, J. Scarola, J.F. Neylan, Comparison of sirolimus plus tacrolimus versus sirolimus plus cyclosporine in high-risk renal allograft recipients: results from an open-label, randomized trial, Transplantation 86 (2008) 1187–1195.
[36] M. Haude, S.W. Lee, S.G. Worthley, S. Silber, S. Verheye, S. Erbs, et al., The REMEDEE trial: a randomized comparison of a combination sirolimus-eluting endothelial progenitor cell capture stent with a paclitaxel-eluting stent, JACC Cardiovascular interventions. 6 (2013) 334–343.
[37] A. Schober, R. Hoffmann, N. Opree, S. Knarren, E. Iofina, G. Hutschenreuter, et al., Peripheral CD34+ cells and the risk of in-stent restenosis in patients with coronary heart disease, Am. J. Cardiol. 96 (2005) 1116–1122.

3.2 Sonic hedgehog-dependent activation of adventitial fibroblasts promotes neointima formation

Vaskuläre Remodeling-Prozesse zeichnen sich durch beträchtliche funktionelle Veränderungen der Zellen in der gesamten Gefäßwand aus. Ein wesentliches pathophysiologisches Kennzeichen der Neointima-Bildung, z.B. im Rahmen einer ISR, ist die exzessive Proliferation glatter Gefäßmuskelzellen aus der Gefäßmedia. Im Rahmen der pathomechanistischen Aufarbeitung ist der Rolle der äußersten Gefäßschicht, der Adventitia, bisher verhältnismäßig wenig Aufmerksamkeit geschenkt worden. Sie galt lange lediglich als das Gefäß stützendes Bindegewebe mit untergeordneten (patho-)physiologischen Funktionen. Zuletzt wurden jedoch in der Adventitia mesenchymale Sca-1^+ Stammzellen beschrieben, die als vaskuläre Progenitorzellen dazu fähig zu sein scheinen, zumindest *in vitro* in glatte Gefäßmuskelzellen zu differenzieren. In diesem Prozess spielt der sogenannte *Sonic hedgehog* (Shh)-Signalweg eine entscheidende Rolle.

In der vorliegenden Arbeit sollte der Einfluss der Adventitia auf die Neointima-Bildung untersucht werden. Nach Dilatation der Femoralarterie von C57BL/6-Mäusen zeigte sich vor der Ausprägung einer Neointima immunhistochemisch eine hohe Proliferationsrate adventitieller Fibroblasten. Gleichzeitig zeigte sich eine gesteigerte Expression des Signalmoleküls Shh, von dem ein Einfluss auf die *In vitro*-Differenzierung mesenchymaler Stammzellen in glattmuskelartige Zellen gezeigt wurde, und des Moleküls *Smoothened* (SMO) aus dem gleichen Signalweg. *In vitro* stellte die kombinierte Stimulation von humanen aortalen adventitiellen Fibroblasten mit Shh und dem PDGF-BB einen deutlichen proproliferativen und promigratorischen Stimulus dar. PDGF-BB aktivierte in Fibroblasten die Proteinkinase und induzierte so die Translokation von SMO in die Plasmamembran, wo es von Shh aktiviert werden konnte. Das Kulturmedium auf diesem Wege aktivierter humaner adventitieller Fibroblasten enthielt hohe Konzentrationen der Interleukine 6 und 8 und stellte selbst wiederum einen deutlichen proproliferativen und promigratorischen Reiz auf glatte Gefäßmuskelzellen dar. Der spezifische SMO-Inhibitor GDC-0449 (Vismodegib), der durch die EMA und die FDA zur Therapie des Basalzellkarzinoms zugelassen ist, war dazu in der Lage, *in vitro* die Fibroblastenproliferation, Zytokinexpression und die daraus folgende parakrine Glattmuskelzellaktivierung zu verhindern. *In vivo* verminderte die SMO-Inhibition mit GDC-0449 signifikant die Proliferationsrate adventitieller Fibroblasten sowie der Neointima-Bildung nach Dilatation der Femoralarterien von C57BL/6-Mäusen.

Zusammenfassend unterstreichen die vorliegenden Daten die Bedeutung adventitieller Fibroblasten für die parakrine Aktivierung glatter Gefäßmuskelzellen und deren

anschließende Proliferation und Migration. Die Adventitia fungiert dabei als eine Art “Bioreaktor”, der die inflammatorische Kaskade aufrechterhält. Eine weiterführende Untersuchung der Adventitia könnte so nicht nur zum pathophysiologischen Verständnis vaskulärer Umbauprozesse beitragen, sondern auch postinterventionelle Therapiestrategien nach Angioplastie optimieren.

ESC European Society of Cardiology
Cardiovascular Research (2017) **113**, 1653–1663
doi:10.1093/cvr/cvx158

Sonic hedgehog-dependent activation of adventitial fibroblasts promotes neointima formation

Jochen Dutzmann[1], Alexander Koch[1], Simona Weisheit[1], Kristina Sonnenschein[1,2], Laura Korte[1], Marco Haertlé[1], Thomas Thum[2,3], Johann Bauersachs[1], Daniel G. Sedding[1†], and Jan-Marcus Daniel[1*†]

[1]Vascular Remodeling and Regeneration Group, Department of Cardiology and Angiology, Hannover Medical School, Carl-Neuberg-Str. 1, D-30625 Hannover, Germany; [2]Institute for Molecular and Translational Therapeutic Strategies (IMTTS), Hannover Medical School, Carl-Neuberg-Str. 1, D-30625 Hannover, Germany; and [3]National Heart and Lung Institute, Imperial College, Sydney St, Chelsea, London SW3 6NP, UK

Received 29 September 2016; revised 20 March 2017; editorial decision 4 August 2017; accepted 14 August 2017; online publish-ahead-of-print 16 August 2017

Time for primary review: 35 days

Aims Adventitial cells have been suggested to contribute to neointima formation, but the functional relevance and the responsible signalling pathways are largely unknown. Sonic hedgehog (Shh) is a regulator of vasculogenesis and promotes angiogenesis in the adult.

Methods and results Here we show that proliferation of vascular smooth muscle cells (SMC) after wire-induced injury in C57BL/6 mice is preceded by proliferation of adventitial fibroblasts. Simultaneously, the expression of Shh and its downstream signalling protein smoothened (SMO) were robustly increased within injured arteries. *In vitro*, combined stimulation with Shh and platelet-derived growth factor (PDGF)-BB strongly induced proliferation and migration of human adventitial fibroblasts. The supernatant of these activated fibroblasts contained high levels of interleukin-6 and -8 and strongly induced proliferation and migration of SMC. Inhibition of SMO selectively prevented fibroblast proliferation, cytokine release, and paracrine SMC activation. Mechanistically, we found that PDGF-BB activates protein kinase A in fibroblasts and thereby induces trafficking of SMO to the plasma membrane, where it can be activated by Shh. *In vivo*, SMO-inhibition significantly prevented the proliferation of adventitial fibroblasts and neointima formation following wire-induced injury.

Conclusions The initial activation of adventitial fibroblasts is essential for the subsequent proliferation of SMC and neointima formation. We identified SMO-dependent Shh signalling as a specific process for the activation of adventitial fibroblasts.

Keywords Neointima formation • Fibroblasts • Sonic Hedgehog • Smoothened

1. Introduction

Vascular remodelling processes are characterized by considerable functional changes of cells in the entire vessel wall. Excessive proliferation of resident smooth muscle cells (SMC) has been established as one of the pathophysiological hallmarks in the process of neointima formation.[1] For a detailed understanding of the underlying pathomechanisms, little attention has been drawn so far to the adventitia, which was mostly referred to as a connective tissue layer with minor (patho)-physiological functions. In adventitial niches, mesenchymal stem cells (MSC) expressing stem cell antigen (Sca)-1 represent vascular progenitor cells, which were shown to have the potential to differentiate into SMC-like cells *in vitro*, a process critically dependent on Sonic hedgehog (Shh) signalling.[2] Moreover, myofibroblasts have been suggested to accumulate in the adventitia following vascular injury, to subsequently proliferate, and to some extent migrate toward the lumen,[3] but the final contribution of these cells has been scarcely investigated so far. Interestingly, Shh has been implicated in the functional regulation of fibroblasts in different contexts, e.g. by promoting fibroblast migration.[4]

The Shh signal transduction cascade is crucial for the development of most tissues and organs as well as for vasculogenesis.[5] Binding of Shh to the transmembrane receptor patched-1 (PTCH1) interrupts the inhibitory effect of PTCH1 on the transmembrane protein smoothened (SMO), which results in activation of Gli transcription factors (Gli1-3).[6]

* Corresponding author. Tel: +49 511 532 5777; fax: +49 511 532 8194, E-mail: daniel.jan-marcus@mh-hannover.de

†These authors contributed equally to the study.

In addition to this so-called 'canonical' pathway, recent evidence points toward two distinct classes of 'non-canonical' Shh signalling, which are independent of Gli-mediated transcription. Type I requires Shh ligand binding and is mediated through PTCH1-interaction with molecules of other pathways (e.g. cyclin B1 and caspases) unrelated to SMO repression, whereas Type II is dependent on SMO signalling.[7] In addition to Shh ligand binding, several other factors are decisive for Shh-signalling activity. For instance, SMO accumulation in the plasma membrane has been shown to be associated with enhanced signalling activity.[8] Even though the detailed molecular function of SMO is not fully understood, the SMO-inhibitor GDC-0449 (Vismodegib) reveals promising results in the treatment of numerous proliferative diseases such as basal cell carcinoma and represents the first Shh pathway inhibitor that lately gained approval by the FDA as well as the European Medicine Agency.[9]

In this study, we investigated the impact of the adventitia on neointima formation and found that early activation of adventitial fibroblasts by SMO-dependent Shh signalling stimulated their proliferation and induced a robust expansion of the adventitial layer. These activated fibroblasts release pro-inflammatory cytokines and growth factors, thereby promoting the inflammatory response and the subsequent proliferation of SMC, which results in neointima formation. The specific SMO-inhibitor GDC-0449 selectively inhibited the activation of fibroblasts but not MSC or SMC. Mechanistically, we found that platelet-derived growth factor (PDGF)-BB cell-specifically induced the translocation of SMO to the plasma membrane in fibroblasts only and thus selectively rendered fibroblasts susceptible to SMO-dependent Shh inhibition. Importantly, perivascular application of GDC-0449 following wire-mediated vascular injury not only selectively prevented the proliferation and paracrine activation of adventitial fibroblasts but also significantly inhibited neointima formation and luminal stenosis.

2. Methods

For a detailed material and methods section, see Supplementary material online.

2.1 Cell culture

Human coronary artery smooth muscle cells, human coronary artery endothelial cells, and human aortic adventitial fibroblasts were purchased from Lonza (Cologne, Germany). $CD29^+$ $CD34^+$ $CD44^+$ $CD117^-$ $Sca1^+$ mouse mesenchymal stem cells were from LifeTechnologies (Carlsbad, CA, USA). $CD45^+$ cells were isolated from healthy human peripheral blood samples using the MACS MicroBeads technology (130-045-801, Miltenyi Biotec, Bergisch Gladbach, Germany). The investigation on human cells isolated from peripheral blood was approved by the local ethics board and conform to the Declaration of Helsinki.

2.2 Functional in vitro assays

Quantification of cell proliferation was assessed using a BrdU-based Cell Proliferation ELISA assay according to the manufacturer's protocol (Cat. 11 647 229 001, Roche Applied Science, Mannheim, Germany). Cell migration was determined in a fluorescence-blocking version of the Boyden chamber assay. PKA activity was assessed using a PKA Kinase Activity Assay Kit that is based on an ELISA according to the manufacturer's protocol (ab139435, Abcam, Cambridge, UK). Rho activity was measured using an Active Rho Detection Kit based on an immunoblot according to the manufacturer's protocol (8820, Cell Signaling, Danvers, MA, USA). For the evaluation of PKA and RhoA activity, stimulation of the cells was performed after 24 h of serum starvation and the activity was evaluated 15 min after stimulation for the ELISA-based PKA activity assay and 2 h after stimulation for the immunohistochemical detection of SMO at the plasma membrane as well as for the immunoblot-based detection of RhoA activity.

2.3 *In vitro* detection of cytokines and growth factors

For the evaluation of the supernatants of stimulated cells, MSC, fibroblasts, or leukocytes were incubated with test substances for 6 h after 24 h of serum-starvation. After the incubation, cells were washed three times with phosphate-buffered saline and incubated with serum-free medium for another 18 h. The supernatant was then collected and used as a test substance for further *in vitro* experiments. *In vitro* cytokine and growth factor release from adventitial fibroblasts was analysed by a human cytokine antibody array according to the manufacturer's instructions (ab133998, Abcam, Cambridge, UK) followed by densometric analysis (ImageJ 1.49v, National Institutes of Health, Bethesda, MD, USA).

2.4 Preparation of cellular lysates and immunoblot analysis

Protein extraction and semi-quantitative analysis of protein expression was measured by immunoblotting as previously described.[10] Immunoblotting of plasma membrane separations from whole cell lysates in the absence or presence of PDGF-BB was performed 2 h after stimulation using the Mem-PER Plus Membrane Protein Extraction Kit according to the manufacturer's protocol (Thermo Fisher Scientific, Waltham, MA, USA).

2.5 Quantitative real-time RT–PCR

Isolation of total RNA and synthesis of cDNA were performed using commercial kits (RNeasy Mini Kit, Qiagen, Hilden, Germany and High Capacity RNA-to-cDNA-Kit, Applied Biosystems, Foster City, CA, USA). Real-time PCR was performed on a Bio-Rad CFX96 Touch™ Real-Time PCR Detection System (Bio-Rad Laboratories, Hercules, CA, USA) using the iQ™ SYBR® Green Supermix (Bio-Rad Laboratories). Primer sequences, as well as a detailed description of primer validation, are shown in Supplementary material online, *Table S1*.

2.6 Animals and procedures

All procedures concerning animal experiments complied with the Directive 2010/63/EU of the European Parliament as well as with local ethical guidelines and had been approved by the Lower Saxony's institutional committee for animal research (Approval reference number 14/1472). All experiments were performed on at least 8-week-old adult male C57BL/6 mice purchased from Charles River (Sulzfeld, Germany). The electric de-endothelialization of the carotid artery and the wire-induced injury of the femoral artery were performed as previously described and as described in the Supplementary material online.[10,11] Mice were anaesthetized by a singular intraperitoneal injection of 100 mg/kg body weight ketamine hydrochloride (Anesketin, Albrecht, Aulendorf, Germany) and 16 mg/kg body weight xylazine (Rompun® 2%, Bayer Health Care AG, Leverkusen, Germany) diluted in 0.9% sodium chloride. Adequate anaesthesia was confirmed by the lack of a tail-pinch-induced pain reflex response. Immediately after injury, GDC-0449 (50 μM) or equal amounts of dimethyl sulphoxide (DMSO) as a control were locally applied in 100 μL of the thermosensitive Pluronic® F-127 gel (Sigma-Aldrich, St. Louis, MO) around the injured arteries. Post-interventional analgesic therapy was

performed by intraperitoneal (i.p.) administration of 0.1 mg buprenorphine/kg body weight/day for 3 d for all animal experiments. Mice were euthanized in a CO_2 chamber at the indicated time points.

2.7 Statistical analysis

Data were stored and analysed on personal computers using Microsoft Excel 2010 (Microsoft Corporation) and GraphPad Prism 6.01 (GraphPad Software Inc., La Jolla, CA, USA). Data among study groups were analysed using Mann–Whitney *U* test, Kruskal–Wallis H test followed by multiple comparisons using Dunn's method, or ordinary 1way ANOVA followed by pairwise multiple comparisons using the Tukey method depending on normality, the number of groups, and affecting factors. All data are represented as the mean ± standard error of the mean (SEM). A probability value <0.05 was considered statistically significant for all comparisons.

3. Results

3.1 Neointimal lesion formation is preceded by high adventitial proliferation rates

Following wire-induced vascular injury, a strong inflammatory response of $CD45^+$ cells to the adventitial layer and a significant increase in the adventitial cellular mass occur before the formation of a neointimal lesion.[12] Immunohistochemical detection of Ki-67 in arteries 7 d after injury revealed that cell proliferation starts mainly within the adventitial layer. The majority of proliferating cells were still localized within the adventitia 14 d after injury (57.08 ± 6.27% in the adventitia vs. 42.92 ± 6.27% in the intima and media, *Figure 1A–C*). Adventitial proliferation led to adventitial thickening in the course of neointima formation. At 7 d after injury, we performed co-staining of Ki-67 with CD45 as a pan-leukocyte marker, Sca-1 for the detection of MSC, or PDGF receptor-α, vimentin, and periostin as markers for fibroblasts, indicating that the large majority of the proliferating adventitial cells represents neither leukocytes nor MSC but can be referred to as fibroblasts (*Figure 1D* and *E*, see Supplementary material online, *Figure S1*).

3.2 Vascular expression of Shh, PTCH1, and SMO is increased following wire-induced injury

In response to vascular injury, the expression of Shh as well as its receptor PTCH1 and downstream target SMO was found to be increased compared with sham-operated arteries, as determined by immunoblotting 14 d after injury (see Supplementary material online, *Figure S2A*). Further immunohistochemical analysis revealed that in injured arteries, the enhanced Shh expression was predominantly located in the medial layer and the developing neointimal lesion, whereas increased PTCH1

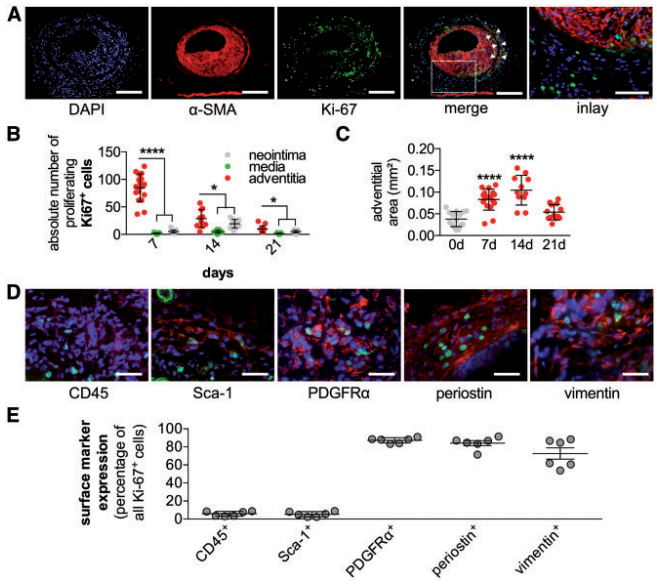

Figure 1 Predominantly adventitial cells proliferate following wire-induced vascular injury. (*A*) Representative neointimal lesion showing cell proliferation within the respective vascular layers as determined by immunohistochemical co-staining of Ki-67 (green) with α-smooth muscle actin (α-SMA, red), and DAPI (blue) 14 d after wire-induced injury of the murine femoral artery. (*B* and *C*) Quantification of Ki-67^+ proliferating cells as absolute numbers within the respective vascular layers and adventitial thickening 7, 14, and 21 d after injury. Data are presented as means ± SEM; $n = 13$ mice, more than 6 sections per mouse were analysed; $^*P < 0.05$, $^{****}P < 0.0001$ by 1way ANOVA followed by multiple comparisons using the Tukey method. (*D* and *E*) Co-staining of Ki-67 (green) with CD45, stem cell antigen-1 (Sca-1), platelet-derived growth factor receptor-α (PDGFR-α), periostin, and vimentin (all red) was performed 7 d after injury and proliferating cells were quantified. Data are presented as means ± SEM; $n = 6$ mice, more than 6 sections per mouse were analysed. Bars, 100 µm (*A*, DAPI, α-SMA, Ki-67, merge); 50 µm (*A*, inlay; *D*).

and SMO immunoreactivity was most prevalent within the medial and adventitial layer 14 d after injury. In contrast, we detected only a very low expression of PTCH1 and SMO in sham-operated vessels (see Supplementary material online, *Figure S2B*).

Co-staining of Shh with α-SMA clearly demonstrated high expression levels of Shh in neointimal SMC (see Supplementary material online, *Figure S2B*). *In vitro*, we detected strong expression levels of Shh in human CD45^{+} cells and in human coronary artery SMC under baseline conditions. Following stimulation with PDGF-BB, we found a strong upregulation of Shh within SMC but not leukocytes. Notably, PDGF-BB stimulation did also not change the baseline level of Shh protein expression in MSC compared with the respective serum-free controls nor did it induce detectable expression in human adventitial fibroblasts at all (see Supplementary material online, *Figure S2C–F*).

3.3 Inhibition of SMO prevents Shh- and PDGF-BB-induced proliferation and migration of fibroblasts

MSC, adventitial fibroblasts, and SMC were incubated with Shh (3.5 μg/mL) with or without PDGF-BB (30 ng/mL) in the presence or absence of the specific SMO inhibitor GDC-0449 (10 μM) to evaluate the functional impact of Shh pathway activation in vascular cells. The results from a modified Boyden chamber assay revealed a markedly enhanced migratory response to either Shh or combined Shh- and PDGF-BB-treatment in all cell types. Combined Shh- and PDGF-BB-treatment also significantly induced the proliferation of MSC, fibroblasts, and SMC as determined by BrdU incorporation. Importantly, GDC-0449 exclusively prevented fibroblast proliferation and migration induced by combined Shh- and PDGF-BB-treatment (2.798 ± 0.186-fold vs. 1.732 ± 0.131-fold increased proliferation and 3.261 ± 0.221-fold vs. 2.464 ± 0.158-fold increased migration compared with serum-free control in response to Shh- and PDGF-BB-treatment with or without GDC-0449, respectively, $n = 8$ and $n = 4$, $^{****}P < 0.001$ and $^{*}P < 0.05$). Treatment with GDC-0449 neither had an effect on proliferation nor migration in MSC, fibroblasts or SMC, when the respective cells were stimulated with Shh alone (*Figure 2A–D*). Following treatment of the respective vascular cell types with Shh and PDGF-BB, a genetic siRNA-mediated knockdown of SMO confirmed the inhibitory effect on proliferation and migration selectively in fibroblasts (see Supplementary material online, *Figure S3* and *Figure 2E* and *F*).

To investigate whether Shh can induce a SMC phenotype in fibroblasts, we analysed the expression of α-SMA as well as the more specific SMC marker genes calponin and smooth muscle myosin heavy chain. As determined by qPCR, these SMC marker genes remained unaffected in adventitial fibroblasts in response to treatment with Shh or combined treatment with Shh and PDGF-BB (see Supplementary material online, *Figure S4*).

3.4 Shh and PDGF-BB activation of fibroblasts trigger paracrine effects on SMC

Because neointima formation is dependent on the proliferation of medial SMC, we stimulated MSC, fibroblasts, or leukocytes with Shh or Shh and PDGF-BB for 6 h in the presence or absence of GDC-0449. The respective cell types were washed, incubated with serum-free medium for 18 h, and the collected supernatant was used for the induction of SMC proliferation and migration as well as a cytokine array. The supernatant of MSC stimulated with Shh increased the proliferation rates of SMC, and the supernatant of fibroblasts stimulated with Shh and PDGF-BB increased

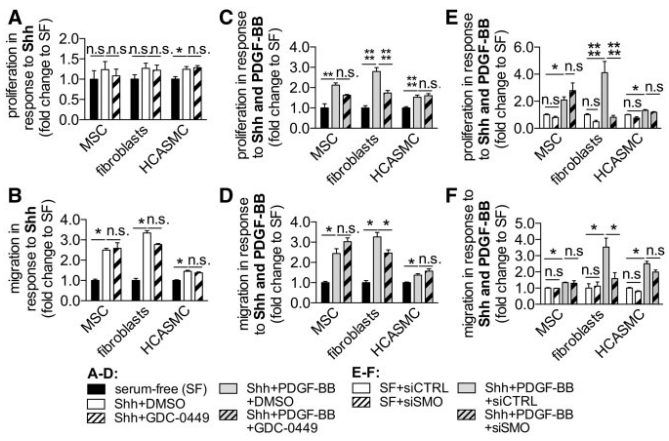

Figure 2 SMO inhibition selectively prevents Shh- and PDGF-BB-induced proliferation and migration of adventitial fibroblasts. (*A–D*) Sca-1^{+} murine mesenchymal stem cells (MSC), human aortic adventitial fibroblasts, and human coronary artery smooth muscle cells (HCASMC) were stimulated with either Shh (3.5 μg/mL) or Shh and PDGF-BB (30 ng/mL) in all respective experiments. Proliferation was assessed by a BrdU incorporation ELISA (*A* + *C*) and migration by a modified Boyden chamber assay (*B* + *D*) in the absence or presence of the SMO inhibitor GDC-0449 (10 μM), $n = 8$ independent experiments for BrdU and $n = 4$ for Boyden chamber assay. (*E* and *F*) MSC, fibroblasts or HCASMC were stimulated and proliferation and migration were assessed after SMO knockdown using siRNA (20 nM), $n = 8$ independent experiments for BrdU and $n = 4$ for Boyden chamber assay. $^{*}P < 0.05$, $^{**}P < 0.01$, $^{****}P < 0.0001$ by one-way ANOVA followed by multiple comparisons using the Tukey method for BrdU and Kruskal–Wallis H test followed by multiple comparisons using the Dunn's method for Boyden chamber assay. All data are presented as means ± SEM.

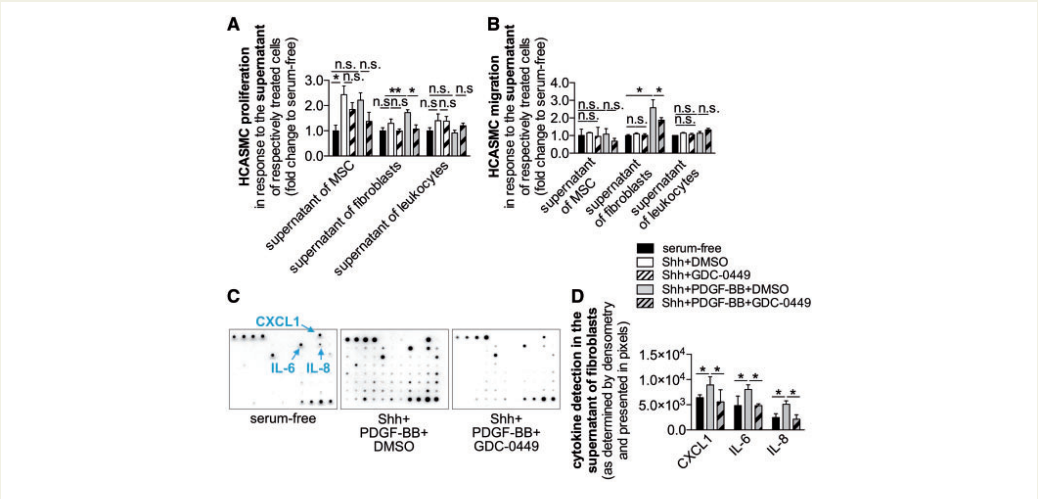

Figure 3 Shh and PDGF-BB activation of fibroblasts trigger paracrine effects on SMC. (*A* and *B*) Sca-1$^+$ murine mesenchymal stem cells (MSC), human aortic adventitial fibroblasts, and CD45$^+$ human leukocytes were stimulated with either Shh (3.5 μg/mL) or Shh and PDGF-BB (30 ng/mL) with or without the SMO inhibitor GDC-0449 (10 μM) followed by a 18-h-period of serum-free starvation. The supernatant of the respective cell types was used to stimulate HCASMC. Proliferation of the stimulated HCASMC was assessed by a BrdU incorporation ELISA (*A*) and migration by a modified Boyden chamber assay (*B*). Data are presented as means ± SEM, $n = 8$ independent experiments for BrdU; $^*P < 0.05$, $^{**}P < 0.01$, by one-way ANOVA followed by multiple comparisons using the Tukey method; $n = 4$ for Boyden chamber assays, $^*P < 0.05$, by Kruskal–Wallis *H* test followed by multiple comparisons using Dunn's method. (*C* and *D*) Human aortic adventitial fibroblasts were stimulated with Shh (3.5 μg/mL) and PDGF-BB (30 ng/mL) with or without the SMO inhibitor GDC-0449 (10 μM) followed by a period of serum-free starvation. Cytokine and growth factor appearance in the supernatant of the stimulated fibroblasts was determined by a cytokine antibody array (*C*) followed by densometric analysis with significant differences in CXCL1, IL-6, or IL-8 among other. Data are presented as means ± SEM; $n = 3$ independent experiments; $^*P < 0.05$ by Kruskal–Wallis *H* test followed by multiple comparisons using Dunn's method.

both proliferation and migration of SMC. The addition of GDC-0449 significantly reduced these effects only in fibroblasts (1.724 ± 0.109-fold vs. 1.069 ± 0.165-fold increased proliferation and 2.581 ± 0.451-fold vs. 1.880 ± 0.139-fold increased migration compared to serum-free control in response to Shh- and PDGF-BB-treatment with or without GDC-0449, respectively, $n = 8$ and $n = 4$, $^*P < 0.05$). In contrast, the supernatant of GDC-0449 treated MSC stimulated with Shh and PDGF-BB showed a trend toward reduced SMC proliferation, but this effect did not reach statistical significance. With respect to leukocytes, stimulation with Shh and PDGF-BB did not result in increased secretion of paracrine factors affecting SMC proliferation or migration (*Figure 3A* and *B*).

To identify SMO-dependent regulated cytokines apparent in the supernatant, we used the supernatant isolated from Shh and PDGF-BB stimulated fibroblasts from the same experiment mentioned above in a cytokine antibody array. We found a strong up-regulation of interleukin (IL)-6, IL-8 and the chemokine CXCL-1 in the supernatant of activated fibroblasts, which was attenuated by the addition of the SMO inhibitor GDC-0449 ($n = 3$, $^*P < 0.05$, *Figure 3C* and *D* and see Supplementary material online, *Table S2*).

3.5 PDGF-BB induces PKA-dependent SMO trafficking to the plasma membrane of fibroblasts

The SMO-inhibitor GDC-0449 exclusively prevents functional changes of fibroblasts induced by combined stimulation with Shh and PDGF-BB, so that we hypothesized that PDGF-BB might sensitize fibroblasts to Shh stimulation by altering the expression and/or the availability of SMO in the plasma membrane. Indeed, immunohistochemical evaluation and immunoblotting of plasma membrane separations from whole cell lysates revealed an increased translocation of SMO from the cytosol to the plasma membrane in adventitial fibroblasts 2 h after stimulation with PDGF-BB. In contrast, this effect was not observed in SMC or MSC following stimulation with PDGF-BB, as detected by immunohistochemical evaluation (*Figure 4A* and *B*). Thus, PDGF-BB-induced SMO translocation promotes Shh signalling selectively in fibroblasts and can be specifically inhibited by GDC-0449. The PDGF-BB-induced SMO trafficking to the plasma membrane of fibroblasts was dependent on PKA activity and could be prevented by the addition of KT5720, a specific PKA inhibitor (*Figure 4C*). In response to stimulation with PDGF-BB, PKA activity was strikingly enhanced in fibroblasts and also enhanced in SMC but not in MSC (*Figure 4D*). Consistent with this observation, we detected active PKA within the adventitial layer 14 d after vascular injury, as determined by staining for the catalytic gamma subunit of PKA (*Figure 4E*).

3.6 SMO-dependent fibroblast proliferation and migration is RhoA-dependent

To investigate the downstream Shh signalling in adventitial fibroblasts, we performed a qPCR-based pathway profiler analysis. Unexpectedly, we found a significant downregulation of the transcription factor Gli-dependent target genes PTCH1 and Gli1 itself (probably representing a

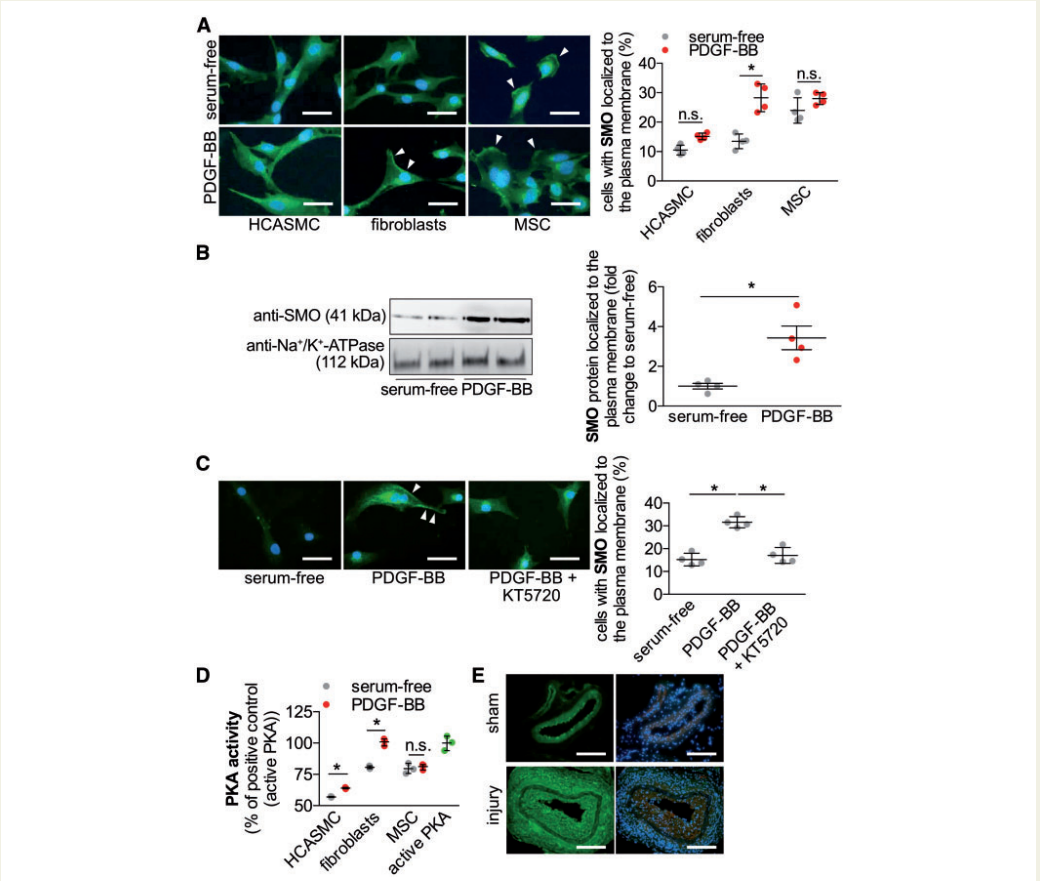

Figure 4 PDGF-BB induces PKA-dependent SMO trafficking to the plasma membrane of fibroblasts. (*A*) SMO localization to the plasma membrane in response to PDGF-BB (30 ng/mL) was assessed by immunofluorescence staining of SMO in human coronary artery smooth muscle cells (HCASMC), mesenchymal stem cells (MSC), and fibroblasts. The respective cell types with SMO located to the plasma membrane were quantified. Data are presented as means ± SEM; $n = 4$ independent experiments; $^{*}P < 0.05$ by Kruskal–Wallis *H* test. (*B*) SMO expression within plasma membrane separations from fibroblasts was analysed by immunoblotting in the presence or absence of PDGF-BB. The Na^{+}/K^{+}-ATPase served as a loading control. Data are presented as means ± SEM; $n = 4$ independent experiments; $^{*}P < 0.05$ by Mann Whitney *U* test. (*C*) PKA dependency was evaluated by immunofluorescence staining of SMO in human aortic adventitial fibroblasts with or without addition of the PKA-inhibitor KT5720 (0.1 μM). Data are presented as means ± SEM; $n = 4$ independent experiments; $^{***}P < 0.001$, $^{****}P < 0.0001$ by Kruskal–Wallis *H* test. (*D*) *In vitro* activity of PKA in response to PDGF-BB (30 ng/mL) was investigated in HCASMC, fibroblasts, and MSC using an ELISA-based PKA activity assay. Data are presented as means ± SEM; $n = 3$ independent experiments; $^{*}P < 0.05$, $^{***}P < 0.001$ by Kruskal–Wallis *H* test. (*E*) Representative immunofluorescence staining for the catalytic gamma subunit of PKA (active PKA, green) and co-staining with α-SMA (red) and DAPI (blue) in injured vs. sham-operated murine femoral arteries 14 d after the respective procedure ($n = 6$ mice; more than three sections per mouse were analysed). Bars, 100 μm.

positive feedback regulation) in response to 24 h of Shh and PDGF-BB treatment, which suggests that the signal transduction is not mediated via the canonical pathway but the non-canonical type II Shh-signalling pathway (*Figure 5A*). This finding was confirmed by qPCR of PTCH1 as a target of Gli1 at 4 h after stimulation with Shh and PDGF-BB (see Supplementary material online, *Figure S5*). Because we did not detect a significant up-regulation of other signal transducers of Shh, we focused on potential activators of the non-canonical type II pathway. Indeed, RhoA activity was significantly increased in fibroblasts in response to treatment with Shh and PDGF-BB, as determined by an immunoblot-based assay (*Figure 5B*). Moreover, immunohistochemical detection of active RhoA indicated a marked increase in RhoA activation following vascular injury and showed a predominant localization of active RhoA within the medial and adventitial layer (*Figure 5C*, see Supplementary

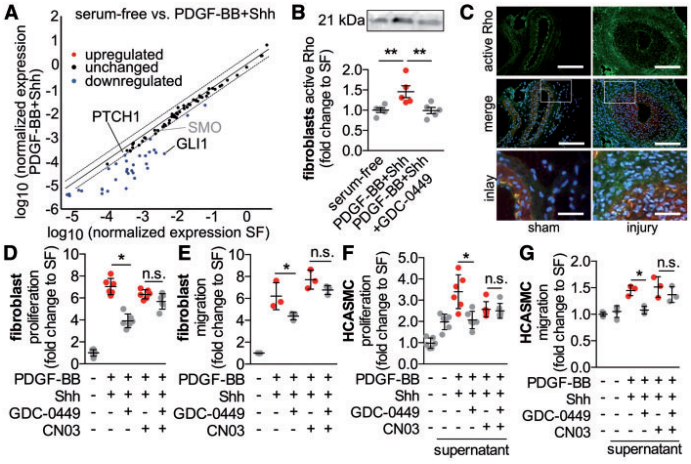

Figure 5 Shh and PDGF-BB treatment activate RhoA but attenuate the activity of Gli1. (*A*) Human aortic adventitial fibroblasts were stimulated with Shh (3.5 μg/mL) and PDGF-BB (30 ng/mL) in all respective experiments with or without the SMO inhibitor GDC-0449 (10 μM). A quantitative real-time PCR-based pathway profiler assay was performed to investigate the expression of Shh pathway genes. Continuous lines represent the median, broken lines the 95% confidence interval; $n = 3$ independent experiments; $P < 0.05$ by Kruskal–Wallis *H* test followed by multi comparisons using Dunn's method. (*B*) Fibroblasts were stimulated with or without the SMO inhibitor GDC-0449 (10 μM) and the *in vitro* activity of RhoA was measured by an immunoblot-based assay. Data are presented as means ± SEM; $n = 5$ independent experiments; $^{**}P < 0.01$ by one-way ANOVA followed by multiple comparisons using the Tukey method. (*C*) Representative immunofluorescence staining for active RhoA (green) and co-staining with α-SMA (red) and DAPI (blue) in injured vs. sham-operated murine femoral arteries 14 d after the respective procedure ($n = 6$ mice; more than three sections per mouse were analysed). (*D* and *E*) Fibroblasts were stimulated with or without the SMO inhibitor GDC-0449 (10 μM) and with or without the RhoA activator CN03 (1 μg/mL) for 24 h. Proliferation was assessed by a BrdU incorporation ELISA ($n = 6$ independent experiments) and migration by a modified Boyden chamber assay ($n = 3$ independent experiments). (*F* and *G*) Fibroblasts were stimulated with or without the SMO inhibitor GDC-0449 (10 μM) and with or without the RhoA activator CN03 (1 μg/mL) for 6 h and 18 h serum-starved. The respective supernatant was used to stimulate proliferation and migration of human coronary artery smooth muscle cells (HCASMC), as assessed by a BrdU incorporation ELISA ($n = 6$ independent experiments) and by a modified Boyden chamber assay ($n = 3$ independent experiments). Data are presented as means ± SEM; $^{*}P < 0.05$ by Kruskal–Wallis *H* test followed by multi comparisons using Dunn's method for all Boyden chamber assays. $^{*}P < 0.05$ by one-way ANOVA followed by multiple comparisons using the Tukey method for all BrdU incorporation ELISA. Bars, 100 μm (*C*, DAPI, α-SMA, active RhoA, merge); 50 μm (*C*, inlay).

material online, *Figure S6*). RhoA activation by the specific Rho activator CN03 rescued the inhibitory effect of GDC-0449 treatment on the proliferation, migration, and paracrine activity of fibroblasts activated with Shh and PDGF-BB, indicating that RhoA mediates these effects downstream of SMO (*Figure 5D–G*).

3.7 SMO inhibition selectively prevents adventitial cell proliferation and reduces neointima formation

The *in vivo* effects of fibroblast-selective SMO inhibition on neointimal lesion formation were evaluated after wire-induced injury of the mouse femoral artery and subsequent perivascular application of GDC-0449 in a thermosensitive self-degrading Pluronic® F-127 gel immediately after vascular injury. Here, we found a significant reduction in the total expanse of Ki-67^{+} proliferating cells following selective SMO inhibition compared with the vehicle-treated control 14 d after injury (17.00 ± 1.807% vs. 5.50 ± 1.176% Ki-67^{+} cells/all cells, $n = 6$, $^{***}P < 0.001$, *Figure 6A* and *B*). The analysis of the different vascular layers revealed that adventitial cells had a similar and significantly reduced proliferative response after GDC-0449 treatment (15.59 ± 0.684% vs. 8.652 ± 1.336%, adventitial Ki-67^{+} cells/total adventitial cells, $n = 6$, $^{**}P < 0.01$, *Figure 6C*). Although we found a clear trend towards an impaired proliferative response in the medial and neointimal layers, the data did not reach statistical significance 14 d after injury (*Figure 6D–E*).

Treatment with GDC-0449 strikingly reduced neointimal lesion formation 21 d after wire-induced injury (luminal stenosis 63.47 ± 10.35% vs. 18.09 ± 5.44%, $n = 6$, $^{**}P < 0.01$, *Figure 6F–H*). The medial area size was not affected by SMO inhibition, whereas the neointimal area was significantly reduced following treatment with GDC-0449 (*Figure 6I–K*). In addition, we detected no significant effect of GDC-0449 treatment on proliferation and migration of human coronary artery EC stimulated with Shh or Shh and PDGF-BB (*Figure 7A* and *B*). Notably, re-endothelialization following electrical endothelial injury of the murine carotid artery was not impaired by perivascular application of GDC-0449, as determined by Evan's blue staining and subsequent *en face* evaluation of the arteries 5 d after electric injury (*Figure 7C*). Furthermore, peripheral blood counts 21 d after injury did not indicate any significant

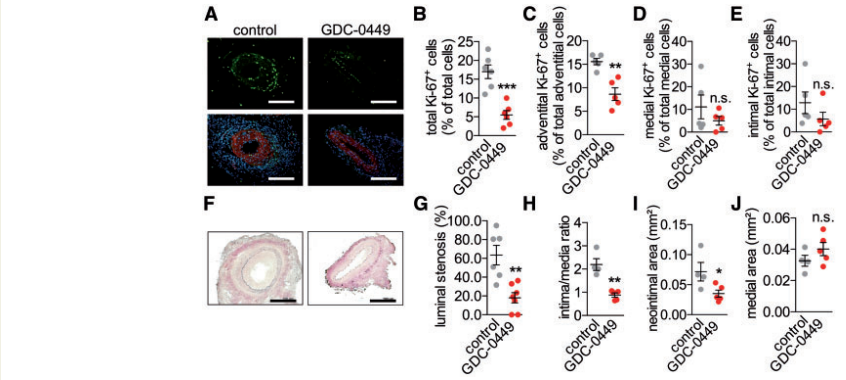

Figure 6 Local application of GDC-0449 prevents adventitial cell proliferation and neointima formation. (*A*) Wire-induced injury of the murine femoral artery was followed by perivascular application of a thermosensitive F-127 Pluronic gel containing GDC-0449 (50 μM) or vehicle. Representative immunofluorescence co-staining of Ki-67 (green) with α-smooth muscle actin (SMA, red), and DAPI (blue) 14 d after injury are shown. (*B–E*) Proliferation was quantified, and Ki-67$^+$ cells are presented as percentage of all DAPI$^+$ cells within all vascular layers (*B*), the adventitia (*C*), the media (*D*), and the neointma (*E*). (*F*) Following wire-induced injury and perivascular application of GDC-0449 (50 μM) or vehicle, van Gieson staining was performed for morphometric analysis 21 d after injury and representative images are shown. (*G–J*) Luminal stenosis (*G*), the intima/media ratio (*H*), the neointimal area (*I*), and the medial area (*J*) were analysed. Data are presented as means ± SEM; $n = 6$ mice for 14 d and $n = 6$ mice for 21 d; more than six sections per mouse were analysed $^*P < 0.05$, $^{**}P < 0.01$, $^{***}P < 0.001$ by unpaired *t*-test. Bars, 100 μm.

differences with regard to circulating leukocytes, erythrocytes, platelets, creatinine, or transaminases between the vehicle-treated mice and the GDC-0449-treated mice (see Supplementary material online, *Table S3*).

4. Discussion

Many aspects of vascular proliferative diseases remain poorly understood, including the activation of the cells of the adventitial layer after acute vascular injury, the underlying signalling mechanisms and the impact of the adventitia on SMC activation and neointima formation.[13] The data from this study demonstrate that PDGF-BB induces a PKA-dependent translocation of SMO to the plasma membrane of fibroblasts to facilitate Shh signalling. We found that the specific SMO inhibitor GDC-0449 selectively prevents the proliferation and migration of fibroblasts and furthermore impedes the secretion of cytokines from fibroblasts that induce the proliferation and migration of SMC *in vitro*. The Shh signal transduction pathway downstream of SMO is mainly mediated by activation of RhoA, and is referred to as non-canonical type II signalling. Importantly, inhibition of fibroblast activation by GDC-0449 strongly inhibited adventitial cell proliferation *in vivo* and the subsequent formation of a neointimal layer. Thus, our data highlight a currently underestimated impact of adventitial fibroblasts on neointima formation and link this mechanism to Shh-dependent signal transduction pathways via SMO and activation of RhoA.

In accordance with previous studies, we observed that the accumulation of inflammatory cells at very early time points after vascular injury was followed by adventitial thickening and adventitial cell proliferation with a large increase in absolute cell numbers.[12] As indicated by co-staining of the proliferation marker Ki-67 with CD45, Sca-1 or fibroblast markers, we found that most of the proliferating cells within the adventitia represent fibroblasts and neither leukocytes nor Sca-1$^+$ MSC. Although a reliable and specific marker for fibroblasts in immunohistochemistry does not exist, we conclude that the vast majority of these proliferating cells expressing PDGF receptor-α, vimentin, or periostin are fibroblasts. In fact, fibroblasts constitute the major cell fraction of adventitial cells and also show high proliferative rates in many other acute inflammatory diseases, including cardiac remodelling after myocardial infarction.[14] Shh has been crucially implicated in fibroblast activation and function.[4] Following wire-induced injury, we found an enhanced expression of Shh within the media and neointimal lesion, whereas PTCH1 and SMO were up-regulated within cells of the media and surrounding adventitial layer. Conclusively, our *in vitro* data suggest that Shh is produced by leukocytes, SMC and MSC but not by fibroblasts themselves, even though multiple bands on an immunoblot may be a concern for immunohistochemistry. Therefore, the initial Shh signalling is very likely mediated by early inflammatory cells, which are recruited to the vascular injury site (see Supplementary material online, *Figure S7*). In fact, it is known that Shh is up-regulated and released from inflammation-activated monocytes through activation of the NF-κB signalling pathway.[15] PDGF-BB is also upregulated in the process of neointima formation and we found that PDGF-BB was a strong inducer of Shh expression levels in SMC. With respect to the cross-talk between the neointima/media and the adventitia, we hypothesize that Shh derived from neointimal and medial cells may contribute to the proliferation of adventitial cells.

In response to Shh and PDGF-BB stimulation *in vitro*, fibroblasts and MSC exhibited increased proliferation and migration rates. Importantly, SMO inhibition with GDC-0449 as well as knock down of SMO using specific siRNAs selectively reduced the proliferation of fibroblasts, since there was no effect on MSC migration and also no significant reduction

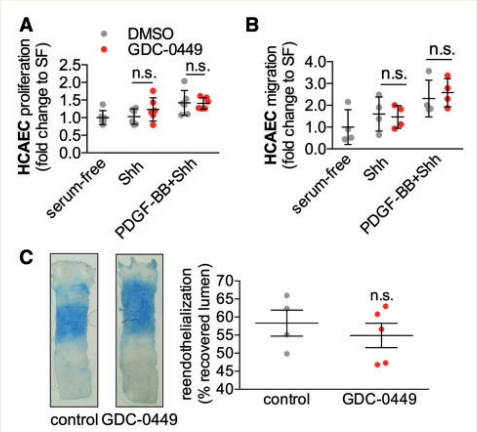

Figure 7 Local application of GDC-0449 does not influence re-endothelialization. (*A* and *B*) Human coronary endothelial cells (HCAEC) were stimulated with or without the SMO inhibitor GDC-0449 (10 μM). Proliferation was assessed by a BrdU incorporation ELISA and migration by a modified Boyden chamber assay, $n = 6$ independent experiments for BrdU and $n = 4$ independent experiments for Boyden chamber assay; P = n.s. by one-way ANOVA followed by multiple comparisons using the Tukey method (*A*) or Kruskal–Wallis *H* test followed by multiple comparisons using Dunn's method (*B*). Data are presented as means ± SEM. (*C*) Following electric perivascular injury of the carotid artery, re-endothelialization was assessed 5 d after injury by injection of Evan's Blue and *en face* analysis. Data are presented as means ± SEM; $n = 4$–5 mice; P = n.s. by unpaired *t*-test.

of MSC proliferation in the multi-variant analysis. Shh induced proliferation and migration of SMC, but in contrast to other studies using the less potent and less specific SMO inhibitor cyclopamine, we did not detect any significant effects of GDC-0449 on SMC proliferation and migration *in vitro*.[16,17] Moreover, neither GDC-0449 nor a siRNA-mediated knock down of SMO had a significant effect on SMC function after treatment with Shh/PDGF-BB. Thus, we conclude that the inhibitory effect of GDC-0449 on neointima formation is mainly derived from its strong and selective inhibitory effect on the activation of adventitial fibroblasts with secondary paracrine effects on SMC proliferation and migration.

Inflammatory cell-derived growth factors and cytokines have been related to direct activation of resident SMC. In addition, our data now show that the activation of adventitial fibroblasts is a further pathophysiological hallmark of the secretion of cytokines and the sustained inflammatory response contributing to SMC activation. Interestingly, we found that the supernatant isolated from Shh- and PDGF-BB-stimulated fibroblasts, but not leukocytes, induced both the proliferation and migration of SMC. Using the supernatant of activated fibroblasts from the same experiment, we also demonstrated that the stimulation of fibroblasts with Shh and PDGF-BB induces the secretion of IL-6, IL-8, and the chemokine CXCL1. IL-6 is known to drive the inflammatory response to vascular injury and has also been shown to directly induce SMC proliferation and migration.[18–20] IL-8 is a chemoattractant for neutrophils, monocytes and lymphocytes that is upregulated within neointimal lesions and induces SMC proliferation and migration.[21,22] The chemokine CXCL1 has neutrophil chemoattractant activity, triggers monocyte arrest on activated endothelium, and has also been linked to the process of neointima formation.[23,24]

Mechanistically, we found that PDGF-BB leads to activation of PKA and thereby translocation of SMO to the plasma membrane, an effect occurring selectively in fibroblasts. This result suggests that PDGF-BB selectively sensitizes fibroblasts to Shh signalling via SMO, which might explain the selective effect of the SMO-inhibitor GDC-0449 in inhibiting only the activation of fibroblasts in response to Shh and PDGF-BB. Next, we investigated the further downstream Shh signalling using a real-time qPCR-based profiler assay for Shh signalling. Surprisingly, we found a down-regulation of both Gli-1 and PTCH1, which are directly regulated by Gli-1 and thus also indicate activity of the canonical Shh-signalling pathway. In this context, active PKA can inhibit canonical Shh signalling by restraining the transcriptional activity of Gli-1.[25] Therefore, we hypothesized that there was an activation of an alternate pathway and found a strong increase in the activation of RhoA, which is a well-known activator of proliferation and migration in fibroblasts.[26,27] Interestingly, recent evidence demonstrated a subtle interplay between RhoA and PKA that governs protrusion–retraction cycles in migrating cells.[28] The detected enrichment in both RhoA and PKA activity described in this study may thus explain the enhanced cell proliferation and motility of adventitial fibroblasts.

Data on the contribution of fibroblasts to the neointimal cellular mass have been contradictory.[29,30] One reason might be the finding that in the developing neointimal lesion, myofibroblasts and de-differentiated SMC exert a very similar vascular cell phenotype.[3] Moreover, specific genetic markers of fibroblasts/myofibroblasts that would allow cell-tracking studies are lacking. The observations of high plasticity of different vascular cell types are also supported by recent evidence showing that in the developing atherosclerotic lesions in genetically modified apolipoprotein $E^{-/-}$ mice, >80% of SMC originate from different cell types including macrophages and MSC.[31] Thus, high cell plasticity and trans-differentiation of different cell types, including fibroblasts/myofibroblasts to SMC, seems to occur to a certain extent in the context of vascular proliferative diseases, especially in atherosclerosis.

In an attempt to determine a possible trans-differentiation from fibroblasts to neointimal SMC, we performed *in vitro*-experiments to track the expression of SMC marker genes after treating fibroblasts with Shh and PDGF-BB but detected no significant increase in any of the specific SMC marker genes. Conclusively, excellent work by Herring *et al.*[32] recently showed that following wire-induced injury in mice, the majority of the neointimal cellular mass is in fact derived from SMC of the medial layer. These data were acquired with a dual marker reporter system, and SMC were detected by tamoxifen-induced expression of GFP under the control of the smooth muscle myosin heavy chain promoter. While these results do not rule out a temporary contribution of adventitial fibroblasts to the cellular mass of the developing neointima, they do provide strong evidence that medial SMC are the major source of the definite neointimal cellular mass. Taken together, a direct contribution of a substantial portion of adventitial fibroblasts to the cellular mass of the neointima seems rather unlikely and the expanding adventitial fibroblast population might rather contribute indirectly via a paracrine activation of medial SMC.

Neointima formation is also dependent on endothelial recovery, so that we analysed the effects of Shh on EC function *in vitro* and endothelial recovery. We found no direct effect of Shh with or without application of GDC-0449 on endothelial function *in vitro* consistent with data from a landmark paper on Shh and angiogenesis by Pola *et al.*[33] We additionally

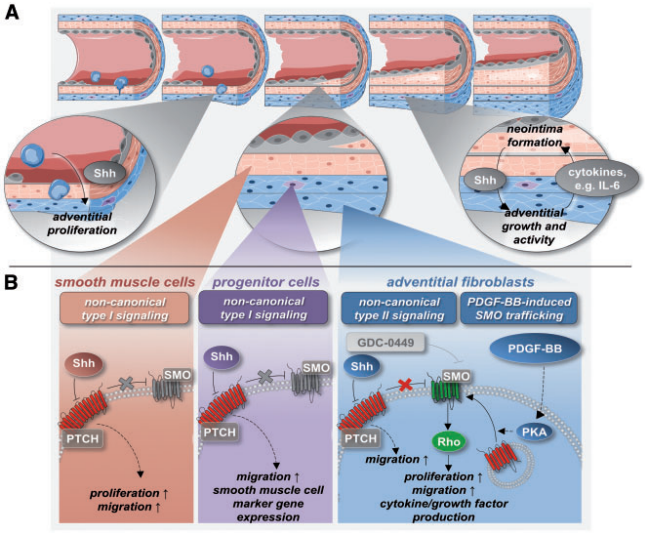

Figure 8 Shh-dependent activation of adventitial growth is critical for negative vascular remodelling. (*A*) Pathophysiological course of neointima formation focused on the initiating inflammatory reaction with subsequent adventitial thickening and formation of a 'bioreactor' with paracrine activity, which in turn accelerates neointimal lesion formation. (*B*) Cell-dependent activation of different Shh pathways. Shh induces cell proliferation and/or migration toward a SMO- and Gli-independent pathway (non-canonical type I signalling) in SMC and vascular progenitor cells, whereas fibroblast proliferation, migration, and cytokine release is induced toward a SMO-dependent and Gli-independent pathway (non-canonical type II signalling). Thus, SMO inhibition allows selective inhibition of fibroblast function.

showed that treatment with GDC-0449 does not have detrimental effects on endothelial regeneration 5 d after electric injury of the carotid artery.

In conclusion, our data highlight the so far underestimated role of adventitial fibroblasts in promoting paracrine effects on medial SMC and thus orchestrating the proliferative response to injury. The initial proliferation and expansion of the adventitial fibroblast population and the subsequent release of pro-inflammatory/pro-proliferative cytokines resembles an adventitial 'bioreactor' that further fuels the proliferation and migration of medial SMC and the neointimal narrowing following vascular injury (*Figure 8*). We found that this process is selectively mediated by Shh and PDGF-BB and that inhibition of SMO allows selective inhibition of fibroblasts leading to significant attenuation of neointima formation following vascular injury. Thus, we conclude that further deciphering the role of the adventitial layer will lead to a better understanding of vascular proliferative diseases and will help to optimize current treatment strategies.

Supplementary material

Supplementary material is available at *Cardiovascular Research* online.

Acknowledgements

We thank our colleagues for helpful discussions and especially Mirja Sirisko for excellent technical assistance.

Conflict of interest: none declared.

Funding

This work was supported by the Behring Roentgen Foundation (59-0033 to J.-M.D.); the Hannover Medical School (*Hochschulinterne Leistungsförderung*) (79330021 to J.-M.D.); and the German Research Foundation (Cluster of excellence REBIRTH to J.B., D.S., and J.-M.D.).

References

1. Dzau VJ, Braun-Dullaeus RC, Sedding DG. Vascular proliferation and atherosclerosis: new perspectives and therapeutic strategies. *Nat Med* 2002;**8**:1249–1256.
2. Passman JN, Dong XR, Wu SP, Maguire CT, Hogan KA, Bautch VL, Majesky MW. A sonic hedgehog signaling domain in the arterial adventitia supports resident Sca1+ smooth muscle progenitor cells. *Proc Natl Acad Sci USA* 2008;**105**:9349–9354.
3. Sartore S, Chiavegato A, Faggin E, Franch R, Puato M, Ausoni S, Pauletto P. Contribution of adventitial fibroblasts to neointima formation and vascular remodeling: from innocent bystander to active participant. *Circ Res* 2001;**89**:1111–1121.
4. Polizio AH, Chinchilla P, Chen X, Kim S, Manning DR, Riobo NA. Heterotrimeric Gi proteins link Hedgehog signaling to activation of Rho small GTPases to promote fibroblast migration. *J Biol Chem* 2011;**286**:19589–19596.
5. Byrd N, Grabel L. Hedgehog signaling in murine vasculogenesis and angiogenesis. *Trends Cardiovasc Med* 2004;**14**:308–313.
6. Rohatgi R, Scott MP. Patching the gaps in Hedgehog signalling. *Nat Cell Biol* 2007;**9**:1005–1009.
7. Jenkins D. Hedgehog signalling: emerging evidence for non-canonical pathways. *Cell Signal* 2009;**21**:1023–1034.
8. Milenkovic L, Scott MP. Not lost in space: trafficking in the hedgehog signaling pathway. *Sci Signal* 2010;**3**:pe14.

9. Sekulic A, Migden MR, Oro AE, Dirix L, Lewis KD, Hainsworth JD, Solomon JA, Yoo S, Arron ST, Friedlander PA, Marmur E, Rudin CM, Chang AL, Low JA, Mackey HM, Yauch RL, Graham RA, Reddy JC, Hauschild A. Efficacy and safety of vismodegib in advanced basal-cell carcinoma. *N Engl J Med* 2012;**366**:2171–2179.
10. Daniel JM, Dutzmann J, Bielenberg W, Widmer-Teske R, Gunduz D, Hamm CW, Sedding DG. Inhibition of STAT3 signaling prevents vascular smooth muscle cell proliferation and neointima formation. *Basic Res Cardiol* 2012;**107**:261.
11. Carmeliet P, Moons L, Stassen JM, De Mol M, Bouche A, van den Oord JJ, Kockx M, Collen D. Vascular wound healing and neointima formation induced by perivascular electric injury in mice. *Am J Pathol* 1997;**150**:761–776.
12. Daniel JM, Bielenberg W, Stieger P, Weinert S, Tillmanns H, Sedding DG. Time-course analysis on the differentiation of bone marrow-derived progenitor cells into smooth muscle cells during neointima formation. *Arterioscler Thromb Vasc Biol* 2010;**30**:1890–1896.
13. Havelka GE, Kibbe MR. The vascular adventitia: its role in the arterial injury response. *Vasc Endovascular Surg* 2011;**45**:381–390.
14. Tillmanns J, Hoffmann D, Habbaba Y, Schmitto JD, Sedding D, Fraccarollo D, Galuppo P, Bauersachs J. Fibroblast activation protein alpha expression identifies activated fibroblasts after myocardial infarction. *J Mol Cell Cardiol* 2015;**87**:194–203.
15. Yamasaki A, Kameda C, Xu R, Tanaka H, Tasaka T, Chikazawa N, Suzuki H, Morisaki T, Kubo M, Onishi H, Tanaka M, Katano M. Nuclear factor kappaB-activated monocytes contribute to pancreatic cancer progression through the production of Shh. *Cancer Immunol Immunother* 2010;**59**:675–686.
16. Morrow D, Cullen JP, Liu W, Guha S, Sweeney C, Birney YA, Collins N, Walls D, Redmond EM, Cahill PA. Sonic Hedgehog induces Notch target gene expression in vascular smooth muscle cells via VEGF-A. *Arterioscler Thromb Vasc Biol* 2009;**29**:1112–1118.
17. Li F, Duman-Scheel M, Yang D, Du W, Zhang J, Zhao C, Qin L, Xin S. Sonic hedgehog signaling induces vascular smooth muscle cell proliferation via induction of the G1 cyclin-retinoblastoma axis. *Arterioscler Thromb Vasc Biol* 2010;**30**:1787–1794.
18. Shoji M, Furuyama F, Yokota Y, Omori Y, Sato T, Tsunoda F, Iso Y, Koba S, Geshi E, Katagiri T, Suzuki H, Kobayashi Y. IL-6 mobilizes bone marrow-derived cells to the vascular wall, resulting in neointima formation via inflammatory effects. *JAT* 2014;**21**:304–312.
19. Klouche M, Bhakdi S, Hemmes M, Rose-John S. Novel path to activation of vascular smooth muscle cells: up-regulation of gp130 creates an autocrine activation loop by IL-6 and its soluble receptor. *J Immunol* 1999;**163**:4583–4589.
20. Chava KR, Karpurapu M, Wang D, Bhanoori M, Kundumani-Sridharan V, Zhang Q, Ichiki T, Glasgow WC, Rao GN. CREB-mediated IL-6 expression is required for 15(S)-hydroxyeicosatetraenoic acid-induced vascular smooth muscle cell migration. *Arterioscler Thromb Vasc Biol* 2009;**29**:809–815.
21. Wang YS, Wang HY, Liao YC, Tsai PC, Chen KC, Cheng HY, Lin RT, Juo SH. MicroRNA-195 regulates vascular smooth muscle cell phenotype and prevents neointimal formation. *Cardiovasc Res* 2012;**95**:517–526.
22. Yue TL, Wang X, Sung CP, Olson B, McKenna PJ, Gu JL, Feuerstein GZ. Interleukin-8. A mitogen and chemoattractant for vascular smooth muscle cells. *Circ Res* 1994;**75**:1–7.
23. Huo Y, Weber C, Forlow SB, Sperandio M, Thatte J, Mack M, Jung S, Littman DR, Ley K. The chemokine KC, but not monocyte chemoattractant protein-1, triggers monocyte arrest on early atherosclerotic endothelium. *J Clin Invest* 2001;**108**:1307–1314.
24. Furgeson SB, Simpson PA, Park I, Vanputten V, Horita H, Kontos CD, Nemenoff RA, Weiser-Evans MC. Inactivation of the tumour suppressor, PTEN, in smooth muscle promotes a pro-inflammatory phenotype and enhances neointima formation. *Cardiovasc Res* 2010;**86**:274–282.
25. Jiang J, Struhl G. Protein kinase A and hedgehog signaling in Drosophila limb development. *Cell* 1995;**80**:563–572.
26. Porter KE, Turner NA, O'Regan DJ, Balmforth AJ, Ball SG. Simvastatin reduces human atrial myofibroblast proliferation independently of cholesterol lowering via inhibition of RhoA. *Cardiovasc Res* 2004;**61**:745–755.
27. Jatho A, Hartmann S, Kittana N, Mügge F, Wuertz CM, Tiburcy M, Zimmermann WH, Katschinski DM, Lutz S, Gullberg D. RhoA ambivalently controls prominent myofibroblast characteritics by involving distinct signaling routes. *PLoS One* 2015;**10**:e0137519.
28. Tkachenko E, Sabouri-Ghomi M, Pertz O, Kim C, Gutierrez E, Machacek M, Groisman A, Danuser G, Ginsberg MH. Protein kinase A governs a RhoA-RhoGDI protrusion-retraction pacemaker in migrating cells. *Nat Cell Biol* 2011;**13**:660–667.
29. Li G, Chen SJ, Oparil S, Chen YF, Thompson JA. Direct *in vivo* evidence demonstrating neointimal migration of adventitial fibroblasts after balloon injury of rat carotid arteries. *Circulation* 2000;**101**:1362–1365.
30. De Leon H, Ollerenshaw JD, Griendling KK, Wilcox JN. Adventitial cells do not contribute to neointimal mass after balloon angioplasty of the rat common carotid artery. *Circulation* 2001;**104**:1591–1593.
31. Shankman LS, Gomez D, Cherepanova OA, Salmon M, Alencar GF, Haskins RM, Swiatlowska P, Newman AA, Greene ES, Straub AC, Isakson B, Randolph GJ, Owens GK. KLF4-dependent phenotypic modulation of smooth muscle cells has a key role in atherosclerotic plaque pathogenesis. *Nat Med* 2015;**21**:628–637.
32. Herring BP, Hoggatt AM, Burlak C, Offermanns S. Previously differentiated medial vascular smooth muscle cells contribute to neointima formation following vascular injury. *Vasc Cell* 2014;**6**:21.
33. Pola R, Ling LE, Silver M, Corbley MJ, Kearney M, Blake Pepinsky R, Shapiro R, Taylor FR, Baker DP, Asahara T, Isner JM. The morphogen Sonic hedgehog is an indirect angiogenic agent upregulating two families of angiogenic growth factors. *Nat Med* 2001;**7**:706–711.

3.3 The novel mineralocorticoid receptor antagonist finerenone attenuates neointima formation after vascular injury

Kardiovaskuläre Erkrankungen führen nicht selten zu einer Herzinsuffizienz mit reduzierter linksventrikulärer Funktion. Mineralokortikoidrezeptor-Antagonisten sind prognoseverbessernd bei dieser Erkrankung und werden daher regelhaft zu ihrer Therapie eingesetzt. Der Effekt von Mineralokortikoidrezeptor-Antagonisten auf vaskuläre Umbauprozesse ist daher von besonderem Interesse. Der zum Publikationszeitpunkt neue nicht-steroidale Minaeralokortikoidrezeptor-Antagonist Finerenon wurde als nebenwirkungsärmere und effizientere Alternative zu den damals herkömmlichen steroidalen Substanzen Spironolacton und Eplerenon entwickelt und war in klinischen Studien sicher und effizient in der Therapie der Herzinsuffizienz sowie der chronischen Niereninsuffizienz. In der vorliegenden Studie sollten die funktionellen Effekte von Finerenon auf vaskuläre Zellen *in vitro* sowie die Effekte auf vaskuläre Umbauprozesse nach endovaskulärer Verletzung *in vivo* untersucht werden.

In vitro zeigte sich eine dosisabhängige Reduktion der Inkorporation von Bromdesoxyuridin als Zeichen einer verminderten Proliferation glatter Gefäßmuskelzellen durch Finerenon. Ebenso zeigte sich eine verringerte Aktivität der Caspasen 3 und 7 als Hinweis auf eine Verhinderung der Aldosteron-induzierten Apoptose von Endothelzellen durch Finerenon. Die orale Applikation von Finerenon *in vivo* resultierte in einer verbesserten Reendothelialisierung drei Tage nach elektrischer Denudation der Arteria carotis von C57BL/6-Mäusen. Finerenon verminderte daneben die Proliferationsrate intimaler und medialer Zellen 10 Tage sowie die Bildung einer Neointima 21 Tage nach Femoralarteriendilatation in C57BL/6-Mäusen.

Zusammengefasst scheint Finerenon damit in der Wiederherstellung vaskulärer Integrität und der Vorbeugung negativer vaskulärer Umbauprozesse günstige Effekte auf das Gefäßsystem zu haben.

PLOS ONE

RESEARCH ARTICLE

The novel mineralocorticoid receptor antagonist finerenone attenuates neointima formation after vascular injury

Jochen Dutzmann[1☯], Robert-Jonathan Musmann[1☯], Marco Haertlé[1], Jan-Marcus Daniel[1], Kristina Sonnenschein[1], Andreas Schäfer[1], Peter Kolkhof[2], Johann Bauersachs[1], Daniel G. Sedding[1]*

1 Dept. of Cardiology and Angiology, Hannover Medical School, Hannover, Germany, **2** Global Drug Discovery, Cardiology Research, Bayer AG, Wuppertal, Germany

☯ These authors contributed equally to this work.
* sedding.daniel@mh-hannover.de

OPEN ACCESS

Citation: Dutzmann J, Musmann R-J, Haertlé M, Daniel J-M, Sonnenschein K, Schäfer A, et al. (2017) The novel mineralocorticoid receptor antagonist finerenone attenuates neointima formation after vascular injury. PLoS ONE 12(9): e0184888. https://doi.org/10.1371/journal.pone.0184888

Editor: Diego Alvarez de la Rosa, Universidad de la Laguna, SPAIN

Received: May 29, 2017

Accepted: September 3, 2017

Published: September 19, 2017

Data Availability Statement: All relevant data are within the paper and its Supporting Information files.

Funding: This study was supported by a fund from Bayer Pharma AG (Wuppertal, Germany) to DGS and JB. The funder provided support in the form of salaries for author PK, but did not have any additional role in the study design, data collection and analysis, decision to publish, or preparation of the manuscript. The specific roles of these authors

Abstract

Background

The novel nonsteroidal mineralocorticoid receptor (MR) antagonist finerenone holds promise to be safe and efficient in the treatment of patients with heart failure and/or chronic kidney disease. However, its effects on vascular function remain elusive.

Purpose

The aim of this study was to determine the functional effect of selective MR antagonism by finerenone in vascular cells *in vitro* and the effect on vascular remodeling following acute vascular injury *in vivo*.

Methods and results

In vitro, finerenone dose-dependently reduced aldosterone-induced smooth muscle cell (SMC) proliferation, as quantified by BrdU incorporation, and prevented aldosterone-induced endothelial cell (EC) apoptosis, as measured with a flow cytometry based caspase 3/7 activity assay.

In vivo, oral application of finerenone resulted in an accelerated re-endothelialization 3 days following electric injury of the murine carotid artery. Furthermore, finerenone treatment inhibited intimal and medial cell proliferation following wire-induced injury of the murine femoral artery 10 days following injury and attenuated neointimal lesion formation 21 days following injury.

Conclusion

Finerenone significantly reduces apoptosis of ECs and simultaneously attenuates SMC proliferation, resulting in accelerated endothelial healing and reduced neointima formation of the injured vessels. Thus, finerenone appears to provide favorable vascular effects through restoring vascular integrity and preventing adverse vascular remodeling.

are articulated in the 'author contributions' section. JD has received research support from the Hannover Medical School (Hochschulinterne Leistungsförderung, HiLF). KS has received a grant of the German Heart Foundation (Deutsche Herzstiftung). DGS and JB received research support from the German Research Foundation (Cluster of excellence REBIRTH).

Competing interests: The authors have read the journal's policy and have the following competing interests: PK is an employee of Bayer AG. This study was supported by a grant from Bayer Pharma AG to DGS and JB. JB and DS have received speaker fees and honoraria 348 from Bayer Pharma AG. This does not alter the authors' adherence to PLOS ONE policies on sharing data and materials.

Abbreviations: ACE, angiotensin-converting enzyme; ARTS, MinerAlocorticoid Receptor antagonist Tolerability Study; ARTS-HF, MinerAlocorticoid Receptor antagonist Tolerability Study-Heart Failure; BNP, brain natriuretic peptide; CKD, chronic kidney disease; EC, endothelial cell; MR, mineralocorticoid receptor; MRA, mineralocorticoid receptor antagonist; RAAS, renin-angiotensin-aldosterone system; SMC, smooth muscle cell.

Introduction

Whereas acute myocardial infarction incidence has decreased globally throughout the last two decades, the prevalence of ischemic heart failure and diabetes without or with kidney disease has steadily increased [1]. Direct deleterious effects of aldosterone and mineralocorticoid receptor (MR) activation occur in both the heart and kidneys [2]. MR blockade prevents some of these detrimental effects and markedly improves morbidity and mortality of patients with moderate to severe heart failure as evidenced by large randomized controlled clinical multi-center trials [3–6]. De Boer and colleagues showed that MRA use markedly increased over the last 20 years among patients with diabetic kidney disease, who are at high risk for vascular complications [7]. However, the available (steroidal) MR antagonists (MRAs) spironolactone, and its sole successor eplerenone, suffer from substantial drawbacks that limit their clinical use, e.g. hyperkalemia especially in patients with severe chronic kidney disease (CKD) [8]. A novel non-steroidal MRA, finerenone, has been developed in an effort to overcome these limitations by achieving high specificity for the MR as well as a balanced and equal tissue distribution between cardiac and renal tissues which is in contrast to steroidal MRAs. [9, 10]. The phase 2a MinerAlocorticoid Receptor antagonist Tolerability Study (ARTS) indeed confirmed a reduced risk for developing hyperkalemia in patients hospitalized for worsening chronic heart failure treated with finerenone compared with those treated with spironolactone despite comparable reduction of efficacy parameters like the brain natriuretic peptide (BNP), NT-proBNP, and albuminuria [11]. Moreover, in the phase 2b MinerAlocorticoid Receptor antagonist Tolerability Study-Heart Failure (ARTS-HF) the investigators found a lower incidence of the clinical composite endpoint (all-cause death, cardiovascular hospitalization or emergency presentation for worsening chronic heart failure) among patients treated with finerenone compared with eplerenone, even though the study was not powered for this observation [12].

Ischemic cardiomyopathy as a result of coronary artery disease is the leading cause for heart failure. Notably, overactivation of the MR has also been implicated in vascular remodeling processes following vascular injury in animal studies as well as in coronary artery disease and in-stent restenosis in clinical settings: Aldosterone has not only been shown to promote medial cell proliferation by direct effects on the smooth muscle cell (SMC)-MR, but to be an independent predictor for in-stent restenosis and mortality in patients with coronary artery disease [13–15]. In consequence, the effect of MRAs on vascular function and remodeling processes is of pivotal interest. Existing data on beneficial or detrimental vascular effects of spironolactone and eplerenone are inconsistent [16–18]. Based on the favorable vascular effects of MR knockout studies on the one hand [13], and the high specificity of finerenone for the MR and its unique tissue distribution profile in comparison to steroidal MRAs on the other hand, we aimed to assess the effects of finerenone on vascular remodeling processes.

Material and methods

Reagents

Aldosterone was purchased from Sigma-Aldrich (St. Louis, MO, USA). Finerenone was provided by Bayer Pharma AG (Wuppertal, Germany). For *in vitro*-studies, aldosterone or finerenone were dissolved in dimethylsulfoxide (DMSO, Cat. W387520, Sigma-Aldrich). For oral application in *in vivo*-studies, finerenone was dissolved in 40% macrogol (15)-hydroxystearate (Solutol®, Cat. 42966, Sigma-Aldrich) and 10% ethanol. *In vitro*, aldosterone was used at concentrations of 10 nM except for Fig 1A and 1C, where aldosterone was used at indicated concentrations.

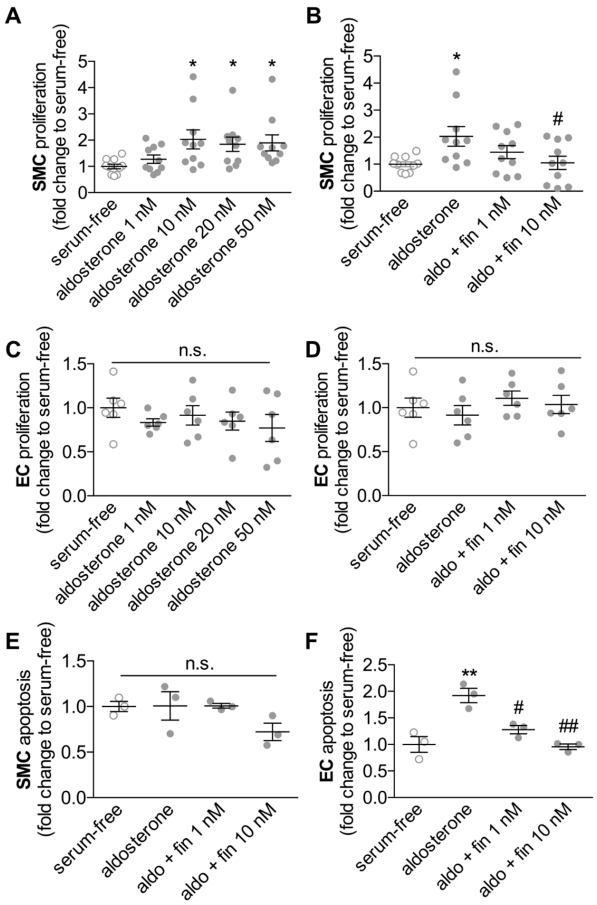

Fig 1. Functional effects of finerenone *in vitro*. Human smooth muscle cells (SMC) and human endothelial cells (EC) were incubated either with aldosterone alone or with aldosterone and different concentrations of finerenone, each dissolved in dimethylsulfoxide (DMSO, final concentration 0.1%) for 24 hours. A-D, Cell proliferation was determined by BrdU incorporation assays (n = 10 for SMCs/n = 6 for ECs, **P*<0.05 to serum-free, #*P*<0.05 to DMSO by ordinary 1way ANOVA followed by multiple comparisons using the Tukey method). E-F, Apoptosis was determined by flow-cytometry-based caspase 3/7 activity measurement (n = 3, ***P*<0.01 to serum-free, #*P*<0.05 and ##*P*<0.01 to DMSO by ordinary 1way ANOVA followed by multiple comparisons using the Tukey method, aldosterone 10 nM was used for B and D-F).

https://doi.org/10.1371/journal.pone.0184888.g001

Cell culture

Human coronary artery smooth muscle cells (SMC) and human umbilical vein endothelial cells (EC) were purchased from Lonza (Cologne, Germany). Cells between passages 2 and 4 were used for all experiments and cultured in optimized growth media according to the supplier's protocols.

Cells were incubated with aldosterone with or without finerenone for 24 hours after 24 hours of serum-starvation for the assessment of cell proliferation and apoptosis. Immediately prior to the addition of aldosterone, cells were preincubated with finerenone or vehicle for 30 minutes.

Functional in vitro assays

Quantification of cell proliferation was assessed by using a BrdU-based Cell Proliferation ELISA according to the manufacturer's protocol (Cat. 11 647 229 001, Roche Applied Science, Mannheim, Germany). Cell apoptosis was quantified by using a FLICA® 660 caspase 3/7 assay kit according to the manufacturer's protocol (Cat. 9152, ImmunoChemistry Technologies, Bloomington, MN, USA).

Vascular injury models

All procedures concerning animal experiments complied with the Directive 2010/63/EU of the European Parliament as well as with local ethical guidelines and had been approved by the Lower Saxony's institutional committee for animal research (LAVES). Adult male C57BL/6 mice were purchased from Charles River (Sulzfeld, Germany).

1.1.1. Mouse carotid artery model of reendothelialization. The electric deendothelialization of the carotid artery was performed as previously described [19]. Briefly, mice were anesthetized by a singular intraperitoneal injection of 100 mg/kg body weight ketamine hydrochloride (Anesketin, Albrecht, Aulendorf, Germany) and 16 mg/kg body weight xylazine (Rompun® 2%, Bayer Health Care AG, Leverkusen, Germany) diluted in 0.9% sodium chloride. Adequate anesthesia was confirmed by the lack of tail-pinch-induced pain reflex. The left common carotid artery was exposed through ventral middle line neck incision and injured with a bipolar microregulator (ICC50, ERBE-Elektromedizin GmbH, Tuebingen, Germany) below the carotid bifurcation. An electric current of 2 W was applied for the duration of 2 seconds to each millimeter of the carotid artery over a total length of 4 mm with the use of a size marker parallel to the artery. Immediately before surgery and then once daily, finerenone or vehicle was delivered as oral gavage. Three days after carotid injury, reendothelialization was evaluated by staining of the denuded area after injection of 50 μL of a 5% Evan's blue solution. Pictures of *en face* prepared injured arteries were taken and reendothelialization was assessed. The reendothelialized area was calculated as difference between the blue-stained area and the initially injured area by computer-assisted morphometric analysis (ImageJ 1.48 software, National Institutes of Health, Bethesda, MD, USA) and presented as percentage of reendothelialization.

1.1.2. Mouse femoral artery injury model of neointimal hyperplasia. The dilation of the femoral artery was performed as previously described [20, 21]. In brief, mice were anesthetized as described above. For the wire-induced injury model of the femoral artery, a straight spring wire (0.38 mm in diameter, Cook Medical Inc., Bloomington, IN, USA) was advanced through the profunda femoris artery for 1 cm into the femoral artery and left in place for 1 minute. After withdrawal, the profunda femoris artery was ligated and reperfusion of the dilated femoral artery was confirmed. Immediately before surgery and then once daily, finerenone or vehicle was delivered as oral gavage. At 21 days after dilation, mice were sacrificed, blood was drawn from the right ventricle, and perfusion with PBS or 4% para-formaldehyde (PFA, Carl Roth, Karlsruhe, Germany) in PBS was performed via the left ventricle. The femoral artery was carefully excised and postfixed in 4% PFA and embedded in Tissue-Tek OCT embedding medium (Sakura Finetek Europe B.V., Zoeterwoude, The Netherlands). Afterwards, the arteries were snap-frozen and stored at -80˚C until sectioning.

Morphometry

The whole femoral artery was cut in 6 μm serial sections and 6 cross-sections from regular intervals throughout the artery were stained with van Gieson staining (n = 6 mice per condition). For morphometric analyses, ImageJ 1.48 software was used to measure external elastic lamina, internal elastic lamina, and lumen circumference, as well as medial and neointimal area.

Immunofluorescence

Femoral artery cross sections or cell samples were incubated with antibodies recognizing α-SMA (C6198, Sigma-Aldrich) or Ki-67 (ab15580, Abcam plc). Ensuing incubations were carried out with Alexa 488-coupled secondary antibodies (LifeTechnologies) and counterstained with nuclear 4.6-diamidino-2-phenylindole (Immunoselect Antifading Mounting Medium DAPI, Dianova GmbH, Hamburg, Germany). Monoclonal antibodies to α-SMA were labelled directly with Cy3. Negative controls were conducted by substituting the primary antibody through an appropriate species- and isotype-matched control antibody (Santa Cruz Biotechnology).

Microscopy

Tissue samples were analyzed using bright-field and immunofluorescence microscopy (Eclipse TE2000-S, Nikon Instruments Europe B.V., Amstelveen, The Netherlands) equipped with appropriate filter blocks and image processing software (NIS Elements AR 4.20.01, Nikon Instruments Europe B.V.,).

Statistical analysis

Data were stored and analyzed on personal computers using Microsoft Excel 2010 (Microsoft Corporation) and GraphPad Prism 6.01 (GraphPad Software Inc., La Jolla, CA, USA). Data among study groups were analyzed by ordinary one-way ANOVA or 2way ANOVA followed by pair wise multi comparisons using the Tukey method depending on the number of groups and affecting factors. All data are represented as mean ± standard error of the mean (SEM). A probability value <0.05 was considered statistically significant for all comparisons.

Results

Finerenone prevents aldosterone-induced EC apoptosis and SMC proliferation in vitro

To investigate vascular cell function in response to aldosterone with or without finerenone *in vitro*, EC and SMC were incubated with different concentrations of aldosterone and finerenone. At 24 hours after stimulation, we detected significantly increased SMC proliferation rates following stimulation with 10 nM, 20 nM or 50 nM aldosterone as assessed by BrdU-incorporation assays. Whereas finerenone treatment at concentrations of 1 nM showed a clear trend towards reduced SMC proliferation rates, 10 nM finerenone sufficiently and significantly prevented aldosterone-induced SMC proliferation ($^{*}P<0.05$ to serum-free, $^{\#}P<0.05$ to DMSO, n = 6, Fig 1A and 1B). However, aldosterone did not affect EC proliferation *in vitro*, and there was also no effect of finerenone (Fig 1C and 1D).

In contrast, flow cytometry-based detection of FLICA®-labeled SMC revealed no aldosterone-dependent induction of SMC apoptosis (Fig 1E). In contrast, EC apoptosis was increased after stimulation with aldosterone *in vitro* but this effect could be prevented by the treatment

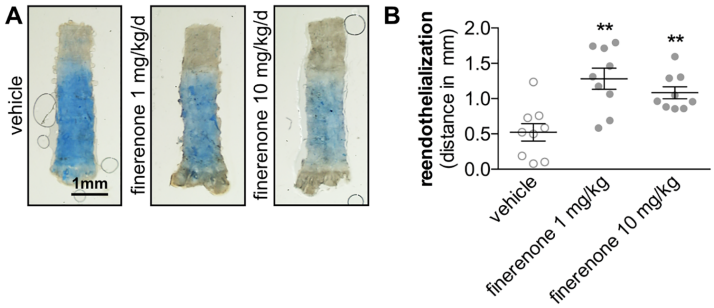

Fig 2. Finerenone promotes early endothelial recovery. Electrical denudation of the carotid artery was performed in 10 weeks old C57BL/6J mice. Finerenone or vehicle was daily delivered as oral gavage. A, Three days following injury, endothelial regeneration was evaluated by injection of a 5% Evan's blue solution and en face microscopy. B, The re-endothelialized distance was calculated by substraction of the deendothelialized distance from 4 mm (standardized denudated area, n = 9, $^{**}P<0.01$ by ordinary 1way ANOVA followed by multiple comparisons using the Tukey method).

https://doi.org/10.1371/journal.pone.0184888.g002

with finerenone even at low concentrations of 1 nM ($^{**}P<0.01$ to serum-free, $^{\#}P<0.05$ and $^{\#\#}P<0.01$ to DMSO, n = 6, Fig 1F).

Finerenone accelerates the re-endothelialization process following vascular injury

Early endothelial recovery was assessed by Evan's blue injection and en face microscopy 3 days after electric injury of the carotid artery in C57BL/6 mice. Daily oral application of finerenone (1 mg/kg/d or 10 mg/kg/d) markedly accelerated the re-endothelialization process at that time point compared with daily vehicle application (0.52 ± 0.12 mm re-endothelialization in vehicle-treated mice vs. 1.13 ± 0.16 mm in 1mg/kg/d finerenone-treated mice vs. 1.083 ± 0.086 mm in 10 mg/kg/d finerenone-treated mice, $^{**}P<0.01$ to vehicle, n = 8, Fig 2).

Finerenone reduces the recruitment of leukocytes and the inflammatory response following vascular injury

The number of accumulating leukocytes in vascular lesions was determined by immunohistochemical detection of the pan-leukocyte marker CD45 at 10 days following wire-induced injury of the murine femoral artery. Oral application of finerenone dose-dependently and significantly reduced the amount of leukocytes within both the intimal and the medial vascular layer (95.14 ± 5.07 in vehicle-treated mice vs. 66.33 ± 8.13 in 1 mg/kg/d finerenone-treated mice vs. 65.69 ± 4.26 in 10 mg/kg/d finerenone-treated mice, $^{*}P<0.05$, $^{**}P<0.01$, n = 6, Fig 3.

Finerenone attenuates smooth muscle cell proliferation and neointimal lesion formation following vascular injury

Intimal and medial cell proliferation was determined by immunohistochemical staining for the proliferation marker Ki-67 10 days following wire-induced injury of the murine femoral artery. Oral application of finerenone dose-dependently and significantly reduced the amount of proliferating Ki-67^{+} cells within both the intimal and the medial vascular layer (ratio of Ki-67^{+}/$DAPI^{+}$ cells 0.281 ± 0.032 in vehicle-treated mice vs. 0.127 ± 0.011 in 1 mg/kg/d

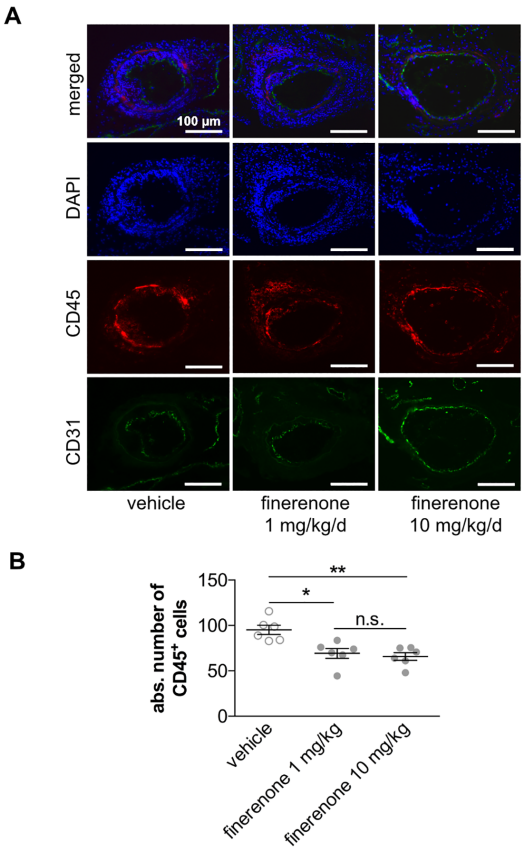

Fig 3. Finerenone reduces the intimal and medial leukocyte content. Wire-induced femoral artery dilation was performed in 10-week-old C57BL/6 mice. Finerenone or vehicle was daily delivered as oral gavage. A, Ten days after injury, leukocyte content was assessed by immunfluorescence staining for the pan-leukocyte marker CD45 (red). Co-immunostaining for CD31 (green) and staining of nuclei with DAPI (blue) was performed to assess the endothelial lining and the overall cell number for better morphological orientation and to allow quantification. B, The amount of leukocytes was determined as the total number of $CD45^+$ cells (n = 6, $*P<0.05$, $**P<0.01$ by ordinary 1way ANOVA followed by multiple comparisons using the Tukey method).

https://doi.org/10.1371/journal.pone.0184888.g003

finerenone-treated mice vs. 0.032 ± 0.002 in 10 mg/kg/d finerenone-treated mice, $^{**}P<0.01$, $^{***}P<0.001$, n = 6, Fig 4). Conclusively, formation of a neointimal lesion was significantly impaired in mice treated with 1 mg/kg/d finerenone 21 days after injury. This effect could be further augmented by application of 10 mg/kg/d finerenone (luminal stenosis 90.84 ± 0.922% in vehicle-treated mice vs. 57.02 ± 6.630% in 1 mg/kg/d finerenone-treated mice vs. 35.50 ± 6.340% in 10 mg/kg/d finerenone-treated mice, $^{*}P<0.05$, $^{**}P<0.01$, $^{****}P<0.0001$, n = 6, Fig 5).

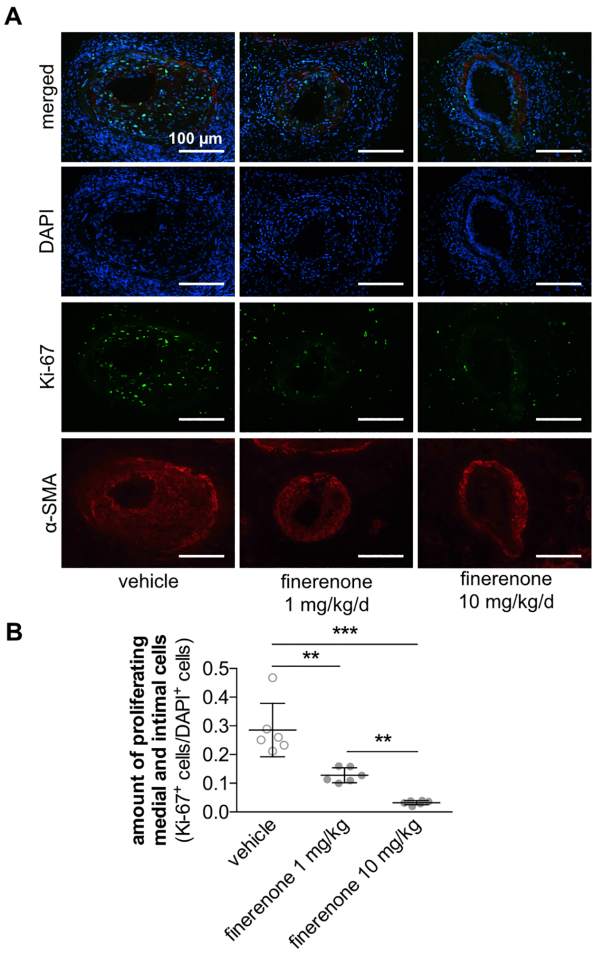

Fig 4. Finerenone prevents medial and intimal cell proliferation. Wire-induced femoral artery dilation was performed in 10-week-old C57BL/6 mice. Finerenone or vehicle was daily delivered as oral gavage. A, Ten days after injury, cell proliferation was assessed by immunfluorescence staining for DAPI (blue), α-smooth muscle actin (α-SMA, red), and Ki-67 (green). B, The amount of proliferating cells was determined as Ki-67$^+$ cells/DAPI$^+$ cells (n = 6, **P<0.01, ***P<0.001 by ordinary 1way ANOVA followed by multiple comparisons using the Tukey method).

https://doi.org/10.1371/journal.pone.0184888.g004

Peripheral blood samples 10 and 21 days after injury did not indicate any significant difference between the vehicle-treated group and the finerenone-treated group in regard to electrolyte metabolism, liver- or kidney function (Table 1). Most importantly, there was no increase in plasma potassium with the use of finerenone, in fact, there was rather a trend for a decrease in plasma potassium especially with the lower finerenone dose.

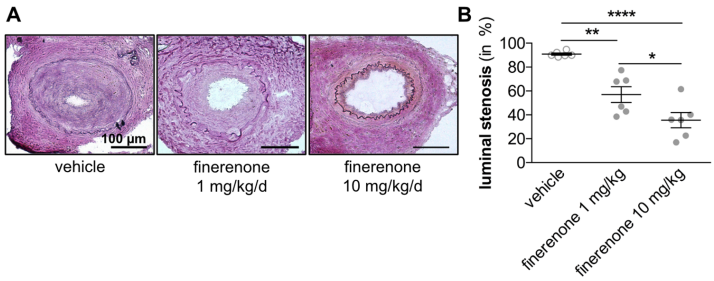

Fig 5. Finerenone attenuates neointima lesion formation. Wire-induced femoral artery dilation was performed in 10-week-old C57BL/6 mice. Finerenone or vehicle was daily delivered as oral gavage. A, 21 days after injury, neointimal lesion formation was assessed by van Gieson staining. B, Luminal stenosis was calculated as percent stenosis = [1 − (A_L/A_N)] × 100, A_L = luminal area, and A_N = area of the normal artery defined as the area surrounded by internal elastic lamina (n = 6, **P*<0.05, ***P*<0.01, *****P*<0.0001 by ordinary 1way ANOVA followed by multiple comparisons using the Tukey method).

https://doi.org/10.1371/journal.pone.0184888.g005

Discussion

Atherosclerotic vascular disease is the leading cause for heart failure. Thus, the impact of (novel) therapeutics for the treatment of heart failure on vascular remodeling processes is of fundamental interest. Inhibitors of the renin-angiotensin-aldosterone system (RAAS) have been shown to be not only cardio protective but in addition exhibit particular nephro protective effects in patients with diabetic kidney disease [5, 7]. Whereas certain evidence exists on favorable vascular effects of inhibitors of the angiotensin-converting enzyme (ACE) [23], findings on the influence of steroidal MRAs on vascular remodeling processes are inconsistent.

Here, we provide evidence that the highly specific novel non-steroidal MRA finerenone prevents aldosterone-induced SMC proliferation and EC apoptosis *in vitro*. *In vivo*, oral application of finerenone significantly accelerates the re-endothelialization process and thus limits leukocyte recruitment at the site of injury, and reduces the proliferation of SMC and neointimal lesion formation in mice.

Very recently, results from the ARTS-HF study verified beneficial effects of finerenone in the treatment of patients with chronic heart failure who also have diabetes mellitus and/or chronic kidney disease. In this high-risk population, finerenone exerted a good safety profile comparable with that of eplerenone but, in contrast, significantly reduced the composite end point of death from any cause, cardiovascular hospitalizations, or emergency presentations for worsening heart failure [12]. Moreover, the MR has been shown to be crucially involved in early myocardial healing processes after coronary artery ligation in mice [24], and treatment with finerenone resulted in improved left ventricular compliance as well as reduced interstitial

Table 1. Blood values in mice treated with vehicle or finerenone.

	ref. values [22]	vehicle	finerenone 1 mg/kg/d	*P* value	finerenone 10 mg/kg/d	*P* value
Potassium [mmol/l]	3.1–6.1	5.1±0	4.33±0.16	n.s.	4.6±0.2	n.s.
Sodium [mmol/l]	149–165	163±2	163.00±2.00	n.s.	164±0.00	n.s.
Chlorid [mmol/l]	n/a	104±2	107.33±1.11	n.s.	102±3	n.s.
creatinine [µmol/l]	28–11	8.5±2.5	6.67±0.44	n.s.	12±0.00	n.s.
Urea [mmol/l]	3.2–13.2	11.4±0.7	11.871.42	n.s.	10.65±0.65	n.s.

https://doi.org/10.1371/journal.pone.0184888.t001

fibrosis compared with control mice following myocardial infarction [25]. Our study now shows for the first time that finerenone may not only be beneficial in sufficiently treating heart failure or improving myocardial healing, but also in preventing vascular remodeling processes.

The underlying molecular signaling mechanisms responsible for the distinct effects of finerenone in vascular cells remain not well defined. However, the relative instability of the MR *in vitro*—as soon as vascular cells are removed from their native surrounding—has challenged previous attempts to further elucidate the underlying MR-dependent mechanisms [26]. Moreover, recent evidence for profound paracrine effects, which are dependent on intact MR-signaling, underlines the importance to study the impact of MRAs in intact organisms and tissues *in vivo* [27].

Mechanistically, well-conducted *in vivo* studies in animals with tissue-specific MR knockout indicated several possible underlying molecular processes: Vascular SMC-specific MR knockout decreased SMC proliferation and prevented pathological vascular remodeling in a wire-induced carotid injury model through a placental growth factor/type 1 vascular endothelial growth factor receptor pathway [13]. Notably, this conditional knockout also reduced oxidative stress in EC in a paracrine manner [25]. EC-specific MR knockout improved endothelial cell function in a mouse-model of western diet-induced endothelial dysfunction due to reduced oxidative stress and an increased anti-inflammatory polarization of macrophages [28]. Finally, selective deletion of the MR in myeloid cells has very recently been shown to limit macrophage accumulation and vascular inflammation following vascular injury through impaired nuclear factor-κB (NF-κB) signaling, thus preventing neointimal hyperplasia [29]. Given the distribution to the vascular space as well as well perfused organs and considering the MR selectivity of finerenone, finerenone-mediated vascular effects may predominantly involve these signaling pathways validated in genetically modified mouse models [25].

The high MR potency and selectivity combined with its physicochemical properties which lead to its unique tissue distribution profile may also be the reason for the clear and robust positive effect of finerenone on EC- and SMC function and neointima formation *in vivo* observed in this study [30]. In contrast, only inconsistent effects of spironolactone or eplerenone on vascular function were reported. Further studies will have to clarify the possibly distinct effects of the different classes of clinically available MRAs on vascular cell functions. Moreover, large animal studies or further clinical observations will be needed to confirm the positive effects of finerenone on vascular remodeling processes that were observed in this study.

Conclusions

The novel selective non-steroidal MRA finerenone promotes endothelial healing and inhibits neointimal lesion formation following vascular injury. Thus, in addition to its beneficial effects in heart failure therapy, finerenone might provide favorable vascular effects through restoring vascular integrity and preventing adverse vascular remodeling following percutaneous coronary interventions. This might be particularly important for the treatment of patients with ischemic cardiomyopathy due to coronary artery disease.

Supporting information

S1 File. ARRIVE guidelines checklist. A completed copy of the ARRIVE guidelines checklist, a document that aims to improve experimental reporting and reproducibility of animal studies for purposes of post-publication data analysis and reproducibility, is provided as supporting information.
(DOCX)

S2 File. Minimal data set. Raw data of all figures are provided as supporting information (Excel file).
(XLSX)

Acknowledgments

We thank our colleagues for helpful discussions and especially Mirja Sirisko for excellent technical assistance.

Author Contributions

Conceptualization: Jochen Dutzmann, Johann Bauersachs, Daniel G. Sedding.

Data curation: Jochen Dutzmann, Robert-Jonathan Musmann, Marco Haertlé, Kristina Sonnenschein.

Formal analysis: Jochen Dutzmann, Robert-Jonathan Musmann, Kristina Sonnenschein.

Funding acquisition: Johann Bauersachs, Daniel G. Sedding.

Investigation: Jochen Dutzmann, Daniel G. Sedding.

Methodology: Jochen Dutzmann, Jan-Marcus Daniel, Kristina Sonnenschein.

Project administration: Jochen Dutzmann, Daniel G. Sedding.

Resources: Peter Kolkhof, Johann Bauersachs.

Software: Johann Bauersachs, Daniel G. Sedding.

Supervision: Johann Bauersachs, Daniel G. Sedding.

Validation: Jochen Dutzmann, Robert-Jonathan Musmann, Jan-Marcus Daniel.

Visualization: Jochen Dutzmann.

Writing – original draft: Jochen Dutzmann.

Writing – review & editing: Jan-Marcus Daniel, Kristina Sonnenschein, Andreas Schäfer, Peter Kolkhof, Johann Bauersachs, Daniel G. Sedding.

References

1. Moran AE, Forouzanfar MH, Roth GA, Mensah GA, Ezzati M, Flaxman A, et al. The global burden of ischemic heart disease in 1990 and 2010: the Global Burden of Disease 2010 study. Circulation. 2014; 129(14):1493–501. https://doi.org/10.1161/CIRCULATIONAHA.113.004046 PMID: 24573351
2. Bauersachs J, Jaisser F, Toto R. Mineralocorticoid receptor activation and mineralocorticoid receptor antagonist treatment in cardiac and renal diseases. Hypertension. 2015; 65(2):257–63. https://doi.org/10.1161/HYPERTENSIONAHA.114.04488 PMID: 25368026.
3. Pitt B, Remme W, Zannad F, Neaton J, Martinez F, Roniker B, et al. Eplerenone, a selective aldosterone blocker, in patients with left ventricular dysfunction after myocardial infarction. N Engl J Med. 2003; 348(14):1309–21. https://doi.org/10.1056/NEJMoa030207 PMID: 12668699.
4. Montalescot G, Pitt B, Lopez de Sa E, Hamm CW, Flather M, Verheugt F, et al. Early eplerenone treatment in patients with acute ST-elevation myocardial infarction without heart failure: the Randomized Double-Blind Reminder Study. Eur Heart J. 2014; 35(34):2295–302. https://doi.org/10.1093/eurheartj/ehu164 PMID: 24780614.
5. Zwadlo C, Bauersachs J. Mineralocorticoid receptor antagonists for therapy of coronary artery disease and related complications. Curr Opin Pharmacol. 2013; 13(2):280–6. Epub 2013/01/22. https://doi.org/10.1016/j.coph.2012.12.007 PMID: 23333184.
6. Le HH, El-Khatib C, Mombled M, Guitarian F, Al-Gobari M, Fall M, et al. Impact of Aldosterone Antagonists on Sudden Cardiac Death Prevention in Heart Failure and Post-Myocardial Infarction Patients: A

Systematic Review and Meta-Analysis of Randomized Controlled Trials. PLoS One. 2016; 11(2): e0145958. https://doi.org/10.1371/journal.pone.0145958 PMID: 26891235

7. de Boer IH, Rue TC, Hall YN, Heagerty PJ, Weiss NS, Himmelfarb J. Temporal trends in the prevalence of diabetic kidney disease in the United States. JAMA. 2011; 305(24):2532–9. https://doi.org/10.1001/jama.2011.861 PMID: 21693741
8. Bauersachs J. The ARTS of third-generation mineralocorticoid receptor antagonists: achieving cardiovascular benefit with minimized renal side effects? Eur Heart J. 2013; 34(31):2426–8. https://doi.org/10.1093/eurheartj/eht235 PMID: 23824829.
9. Barfacker L, Kuhl A, Hillisch A, Grosser R, Figueroa-Perez S, Heckroth H, et al. Discovery of BAY 94–8862: a nonsteroidal antagonist of the mineralocorticoid receptor for the treatment of cardiorenal diseases. ChemMedChem. 2012; 7(8):1385–403. https://doi.org/10.1002/cmdc.201200081 PMID: 22791416.
10. Kolkhof P, Delbeck M, Kretschmer A, Steinke W, Hartmann E, Barfacker L, et al. Finerenone, a novel selective non-steroidal mineralocorticoid receptor antagonist protects from rat cardiorenal injury. J Cardiovasc Pharmacol. 2014. Epub 2014/03/14. https://doi.org/10.1097/FJC.0000000000000091 PMID: 24621652.
11. Pitt B, Kober L, Ponikowski P, Gheorghiade M, Filippatos G, Krum H, et al. Safety and tolerability of the novel non-steroidal mineralocorticoid receptor antagonist BAY 94–8862 in patients with chronic heart failure and mild or moderate chronic kidney disease: a randomized, double-blind trial. Eur Heart J. 2013; 34(31):2453–63. https://doi.org/10.1093/eurheartj/eht187 PMID: 23713082
12. Filippatos G, Anker SD, Bohm M, Gheorghiade M, Kober L, Krum H, et al. A randomized controlled study of finerenone vs. eplerenone in patients with worsening chronic heart failure and diabetes mellitus and/or chronic kidney disease. Eur Heart J. 2016; 37(27):2105–14. https://doi.org/10.1093/eurheartj/ehw132 PMID: 27130705
13. Pruthi D, McCurley A, Aronovitz M, Galayda C, Karumanchi SA, Jaffe IZ. Aldosterone promotes vascular remodeling by direct effects on smooth muscle cell mineralocorticoid receptors. Arterioscler Thromb Vasc Biol. 2014; 34(2):355–64. Epub 2013/12/07. https://doi.org/10.1161/ATVBAHA.113.302854 PMID: 24311380
14. Amano T, Matsubara T, Izawa H, Torigoe M, Yoshida T, Hamaguchi Y, et al. Impact of plasma aldosterone levels for prediction of in-stent restenosis. Am J Cardiol. 2006; 97(6):785–8. https://doi.org/10.1016/j.amjcard.2005.10.017 PMID: 16516576.
15. Ivanes F, Susen S, Mouquet F, Pigny P, Cuilleret F, Sautiere K, et al. Aldosterone, mortality, and acute ischaemic events in coronary artery disease patients outside the setting of acute myocardial infarction or heart failure. Eur Heart J. 2012; 33(2):191–202. https://doi.org/10.1093/eurheartj/ehr176 PMID: 21719456.
16. Wakabayashi K, Suzuki H, Sato T, Iso Y, Katagiri T, Takeyama Y. Eplerenone suppresses neointimal formation after coronary stent implantation in swine. Int J Cardiol. 2006; 107(2):260–6. Epub 2005/07/19. S0167-5273(05)00575-9 [pii] https://doi.org/10.1016/j.ijcard.2005.03.078 PMID: 16023229.
17. Kursaklioglu H, Iyisoy A, Amasyali B, Celik T, Ozturk C, Kose S, et al. Spironolactone does not prevent restenosis after coronary stenting in humans. Ann Acad Med Singapore. 2004; 33(6):769–74. PMID: 15608836.
18. Raz-Pasteur A, Gamliel-Lazarovich A, Coleman R, Keidar S. Eplerenone reduced lesion size in early but not advanced atherosclerosis in apolipoprotein E-deficient mice. J Cardiovasc Pharmacol. 2012; 60(6):508–12. https://doi.org/10.1097/FJC.0b013e31826f5535 PMID: 23232789.
19. Carmeliet P, Moons L, Stassen JM, De Mol M, Bouche A, van den Oord JJ, et al. Vascular wound healing and neointima formation induced by perivascular electric injury in mice. Am J Pathol. 1997; 150(2):761–76. Epub 1997/02/01. PMID: 9033288
20. Sata M, Maejima Y, Adachi F, Fukino K, Saiura A, Sugiura S, et al. A mouse model of vascular injury that induces rapid onset of medial cell apoptosis followed by reproducible neointimal hyperplasia. J Mol Cell Cardiol. 2000; 32(11):2097–104. Epub 2000/10/21. https://doi.org/10.1006/jmcc.2000.1238 PMID: 11040113.
21. Daniel JM, Dutzmann J, Bielenberg W, Widmer-Teske R, Gunduz D, Hamm CW, et al. Inhibition of STAT3 signaling prevents vascular smooth muscle cell proliferation and neointima formation. Basic Res Cardiol. 2012; 107(3):261. Epub 2012/03/16. https://doi.org/10.1007/s00395-012-0261-9 PMID: 22418922
22. Boehm O, Zur B, Koch A, Tran N, Freyenhagen R, Hartmann M, et al. Clinical chemistry reference database for Wistar rats and C57/BL6 mice. Biol Chem. 2007; 388(5):547–54. https://doi.org/10.1515/BC.2007.061 PMID: 17516851.

23. Powell JS, Clozel JP, Muller RK, Kuhn H, Hefti F, Hosang M, et al. Inhibitors of angiotensin-converting enzyme prevent myointimal proliferation after vascular injury. Science. 1989; 245(4914):186–8. PMID: 2526370.

24. Fraccarollo D, Berger S, Galuppo P, Kneitz S, Hein L, Schutz G, et al. Deletion of cardiomyocyte mineralocorticoid receptor ameliorates adverse remodeling after myocardial infarction. Circulation. 2011; 123 (4):400–8. https://doi.org/10.1161/CIRCULATIONAHA.110.983023 PMID: 21242479.

25. Gueret A, Harouki N, Favre J, Galmiche G, Nicol L, Henry JP, et al. Vascular Smooth Muscle Mineralocorticoid Receptor Contributes to Coronary and Left Ventricular Dysfunction After Myocardial Infarction. Hypertension. 2016; 67(4):717–23. https://doi.org/10.1161/HYPERTENSIONAHA.115.06709 PMID: 26902493.

26. Galigniana MD. Stability study on renal type I mineralocorticoid receptor. Life Sci. 1996; 59(7):511–21. PMID: 8761339.

27. Favre J, Gao J, Zhang AD, Remy-Jouet I, Ouvrard-Pascaud A, Dautreaux B, et al. Coronary endothelial dysfunction after cardiomyocyte-specific mineralocorticoid receptor overexpression. Am J Physiol Heart Circ Physiol. 2011; 300(6):H2035–43. https://doi.org/10.1152/ajpheart.00552.2010 PMID: 21441311.

28. Jia G, Habibi J, Aroor AR, Martinez-Lemus LA, DeMarco VG, Ramirez-Perez FI, et al. Endothelial Mineralocorticoid Receptor Mediates Diet-Induced Aortic Stiffness in Females. Circ Res. 2016; 118 (6):935–43. https://doi.org/10.1161/CIRCRESAHA.115.308269 PMID: 26879229

29. Sun JY, Li C, Shen ZX, Zhang WC, Ai TJ, Du LJ, et al. Mineralocorticoid Receptor Deficiency in Macrophages Inhibits Neointimal Hyperplasia and Suppresses Macrophage Inflammation Through SGK1-AP1/NF-kappabeta Pathways. Arterioscler Thromb Vasc Biol. 2016. https://doi.org/10.1161/ATVBAHA.115.307031 PMID: 26966277.

30. Kolkhof P, Nowack C, Eitner F. Nonsteroidal antagonists of the mineralocorticoid receptor. Curr Opin Nephrol Hypertens. 2015; 24(5):417–24. https://doi.org/10.1097/MNH.0000000000000147 PMID: 26083526

3.4 BET bromodomain-containing epigenetic reader proteins regulate vascular smooth muscle cell proliferation and neointima formation.

Epigenetische Mechanismen und ihre therapeutische Beeinflussung sind gegenwärtig in der Erforschung onkologischer und kardiovaskulärer Erkrankungen ebenso wie des Diabetes mellitus in den Fokus gerückt. Hierbei konnte insbesondere den epigenetischen BET (bromodomain and extra-terminal)-Ableseproteinen eine entscheidende Rolle zugeschrieben werden. Inwiefern diese Proteine auch an der Regulation vaskulärer Remodeling-Prozesse beteiligt sind und Gefäßzellen unmittelbar beeinflussen war Gegenstand der vorliegenden Arbeit. Untersucht wurden die Effekte von BET-Proteinen auf die Funktion humaner glatter Gefäßmuskelzellen *in vitro* sowie auf vaskuläre Umbauprozesse nach endovaskulärer Verletzung *in vivo*.

In vitro reduzierte die selektive Inhibition von BET-Proteinen durch das Molekül (+)-JQ1 dosis-abhängig die Proliferation und Migration glatter Gefäßmuskelzellen ohne apoptotische oder zelltoxische Einflüsse. Durchflusszytometrisch konnte ein Zellzyklusarrest in der G_0/G_1-Phase durch (+)-JQ1 nachgewiesen werden. Mittels Microarray- und Signalweganalysen konnte die transkriptionelle Regulation von Genen identifiziert werden, die durch das *Forkhead-Box-Protein O1* (FOXO1) transkriptionell reguliert werden. Die posttranskriptionelle durch sog. silencing (si)-Ribonukleinsäure (RNA) vermittelte Hemmung des am stärksten regulierten FOXO1-abhängigen Gens, *CDKN1A*, verminderte die antiproliferativen Effekte von (+)-JQ1. Mittels immunhistochemische Darstellung der Co-Lokalisation, Co-Immunopräzipitation sowie Promotor-Binding ELISA Assay-Daten konnten die direkte Bindung des BET-Proteins BRD4 an FOXO1 und die BRD4-abhängige Regulation der transaktivationellen Kapazität von FOXO1 bewiesen werden. *In vivo* verminderte die lokale perivaskuläre Applikation von (+)-JQ1 signfikant die Proliferation glatter Gefäßmuskelzellen und die Bildung einer neointimalen Läsion nach endovaskulärer Verletzung der Femoralarterie von C57BL/6-Mäusen.

Zusammenfassend konnte in der vorliegenden Arbeit gezeigt werden, dass die Inhibition des BET-Proteins BRD4 durch (+)-JQ1 die transaktivationelle Kapazität des Transkriptionsfaktors FOXO1 nach endovaskulärer Verletzung erhält. Durch die Expression des FOXO1-abhängigen Gens *CDKN1A* und die hiervon abhängige Induktion eines Zellzyklusarrests werden die Proliferation glatter Gefäßmuskelzellen und damit die Bildung einer neointimalen Läsion vermieden. BET-Ableseproteine könnten demzufolge als vielversprechende therapeutische Ziele zur Vermeidung postangioplastischer vaskulärer Remodelingprozesse dienen.

ESC European Society of Cardiology

Cardiovascular Research (2021) **117**, 850–862
doi:10.1093/cvr/cvaa121

BET bromodomain-containing epigenetic reader proteins regulate vascular smooth muscle cell proliferation and neointima formation

Jochen Dutzmann [1,2†], Marco Haertlé [2†], Jan-Marcus Daniel[1,2], Frederik Kloss [2], Robert-Jonathan Musmann[2], Katrin Kalies [1], Kai Knöpp [1,2], Claudia Pilowski[1], Mirja Sirisko[2], Jan-Thorben Sieweke [2], Johann Bauersachs[2], Daniel G. Sedding[1,2*†], and Simona Gegel[2†]

[1] Mid-Germany Heart Center, Division of Cardiology, Angiology, and Intensive Medical Care, University Hospital Halle, Martin-Luther-University Halle-Wittenberg, Ernst-Grube-Straße 40, 06120 Halle, Germany; and [2]Department of Cardiology and Angiology, Hannover Medical School, Carl-Neuberg-Str. 1, 30625 Hannover, Germany

Received 27 April 2019; revised 27 December 2019; editorial decision 22 March 2020; accepted 23 April 2020; online publish-ahead-of-print 30 April 2020

Time for primary review: 39 days

Aims Recent studies revealed that the bromodomain and extra-terminal (BET) epigenetic reader proteins resemble key regulators in the underlying pathophysiology of cancer, diabetes, or cardiovascular disease. However, whether they also regulate vascular remodelling processes by direct effects on vascular cells is unknown. In this study, we investigated the effects of the BET proteins on human smooth muscle cell (SMC) function *in vitro* and neointima formation in response to vascular injury *in vivo*.

Methods and results Selective inhibition of BETs by the small molecule (+)-JQ1 dose-dependently reduced proliferation and migration of SMCs without apoptotic or toxic effects. Flow cytometric analysis revealed a cell cycle arrest in the G0/G1 phase in the presence of (+)-JQ1. Microarray- and pathway analyses revealed a substantial transcriptional regulation of gene sets controlled by the Forkhead box O (FOXO1)1-transcription factor. Silencing of the most significantly regulated FOXO1-dependent gene, *CDKN1A*, abolished the antiproliferative effects. Immunohistochemical colocalization, co-immunoprecipitation, and promoter-binding ELISA assay data confirmed that the BET protein BRD4 directly binds to FOXO1 and regulates FOXO1 transactivational capacity. *In vivo*, local application of (+)-JQ1 significantly attenuated SMC proliferation and neointimal lesion formation following wire-induced injury of the femoral artery in C57BL/6 mice.

Conclusion Inhibition of the BET-containing protein BRD4 after vascular injury by (+)-JQ1 restores FOXO1 transactivational activity, subsequent *CDKN1A* expression, cell cycle arrest and thus prevents SMC proliferation *in vitro* and neointima formation *in vivo*. Inhibition of BET epigenetic reader proteins might thus represent a promising therapeutic strategy to prevent adverse vascular remodelling.

Keywords Bromodomains • Neointima formation • Smooth muscle cell proliferation • Restenosis • Epigenetics

1. Introduction

The process of neointima formation is common to various forms of vascular diseases such as atherosclerosis, in-stent restenosis, vein bypass graft failure, and transplant vasculopathy. The neointimal layer is formed by activated medial smooth muscle cells (SMCs) that proliferate and migrate into the intima in response to vascular injury.[1] A key component in SMC activation and vascular proliferative diseases progression is a disturbed epigenetic regulation and chromatin remodelling.[2,3]

Epigenetic modifications including DNA methylation and chromatin acetylation, which alter defined transcriptional cellular programmes, have extensively been studied during the last decades.[4] Covalent

* Corresponding author. Tel: +49 0 345 557 2623; fax: +49 0 345 557 2072, E-mail: daniel.sedding@uk-halle.de

† These authors contributed equally to the study.

epigenetic modifications of the nucleosome are recognized by so-called 'epigenetic readers', that facilitate chromatin remodelling, transcriptional initiation, and elongation.[5] One of them, the bromodomain motif, interacts with acetylated lysine-sidechains and is part of numerous chromatin-associated proteins.[6] In addition to the bromodomain motif, the bromodomain-containing proteins (BRD) 2, 3, and 4 as well as the bromodomain testis-specific protein (BRDT) contain an extra-terminal molecular interaction site and are thus classified as bromodomain and extra-terminal (BET) proteins.[7]

Available BET inhibitors competitively target the BRD proteins' binding site for acetylated histones and have recently been shown to exert favourable effects in the prevention and treatment of multiple diseases, for example cancer or diabetes.[8,9] To understand the role of BETs in the modulation of SMC function and to evaluate the impact of BET inhibition on vascular remodelling processes, we first studied the effects of the potent-selective BET inhibitors (+)-JQ1 and I-BET 151 in human coronary SMC *in vitro*. In response to bromodomain inhibition, we found a Forkhead box O (FOXO)1-dependent upregulation of *CDKN1A*, which, in agreement with previous reports, caused a cell cycle arrest in human SMCs.[10,11] Therefore, we further investigated the effect of BET inhibition *in vivo* on neointima formation following wire-induced injury of murine femoral arteries.

2. Material and methods

A detailed methods section is available as a Supplementary material online.

2.1 Cell culture

Human coronary artery SMCs and human coronary artery endothelial cells (ECs) were purchased from Lonza (Switzerland). Cells between passages 3 and 7 were used for all experiments. Cells were treated with the BET-specific bromodomain inhibitors (+)-JQ1 dissolved in DMSO (BPS Bioscience, USA) and I-BET 151 hydrochloride dissolved in DMSO (Tocris, USA) at indicated concentrations.

2.2 Cell proliferation and viability assay

Cell proliferation was determined by BrdU incorporation (Cell Proliferation ELISA Kit, Roche, Switzerland) and colorimetric measurement following manufacturer's instructions and as previously described.[12] Cell viability was determined by cleavage of WST-1 to formazan (Cell Proliferation Reagent WST-1, Roche) and colorimetric measurement following manufacturer's instructions and as previously described.[13] For siRNA-mediated knockdown, cells were transfected with siRNA as indicated before serum-starvation followed by growth medium (GM) stimulation (Provitro, Berlin, Germany). For inhibitor studies, indicated concentrations of (+)-JQ1 or I-BET 151 or an equal volume of vehicle control (DMSO; Carl Roth, Germany) were added to the GM.

2.3 Migration assay

Cell migration was assessed by a modified Boyden chamber assay as previously described.[14] Migration was determined 4 h after stimulation and incubation at a wavelength of 528 nm.

2.4 Cell cycle analysis

Cells were serum-starved for 16 h and treated with either (+)-JQ1, I-BET151, or DMSO at indicated concentrations for 24 h. Cell cycle was analysed using a flow cytometer at 605–635 nm and Cytometry List Mode Data Acquisition & Analysis Software (both: Gallios™, Beckman Coulter, USA).

2.5 Apoptosis assays

Apoptosis was determined by measurement of caspase 3 and 7 activity using the FLICA® 660 Caspase 3/7 Assay kit (ImmunoChemistry Technologies, LLC, USA) following manufacturer's instructions. Cells were treated with the respective inhibitors in basal medium (BM; Provitro, Berlin, Germany), 100 mM hydrogen peroxide (Carl Roth), or GM. Fluorescence signal was measured using a flow cytometer at 695/30 nm and Cytometry List Mode Data Acquisition & Analysis Software (both: Gallios™, Beckman Coulter).

2.6 siRNA-mediated gene knockdown

For siRNA-mediated knockdown of *BRD2*, *BRD3*, *BRD4*, *CDKN1A*, *GADD45A*, and *FOXO1*, cells were transfected with respective siRNAs (three unique 27mer siRNA duplexes; Origene, USA) according to manufacturer's instructions. Scrambled negative siRNA served as control.

2.7 RNA isolation and reverse transcription

Isolation of RNA from cells was performed using the RNeasy mini kit (Qiagen, Germany) according to the manufacturer's instructions. RNA from tissues was isolated after homogenization in 500 µL Trizol™ reagent (Invitrogen). The obtained RNA was reverse transcribed with the High-Capacity RNA-to-cDNA™ kit (Applied Biosystems, USA) according to manufacturer's instructions.

2.8 PCR and qRT–PCR

cDNA was amplified according to manufacturer's instructions with TaqDNA Polymerase, dNTP Set (both: Qiagen), and the respective primers in Mastercycler® reagent (Eppendorf, Germany). Subsequently, the cDNA was separated and visualized with the FlashGel™ System (Lonza).

Quantitative real-time PCR was performed using SYBR green® master mix with the respective primers and the CFX96 Touch™ Real Time PCR Detection System (both: Bio-Rad, USA). All analyses were performed in triplicate and either the DNA template or the reverse transcriptase was omitted for control reactions. Fold change expression levels were quantified and normalized to the geometric mean of at least two reference genes with the highest expression stability by use of the $2^{-\Delta\Delta Ct}$ relative quantification method.

Primer sequences and design are mentioned in the Supplementary material online.

2.9 Protein isolation and determination

Proteins of whole-cell lysates were isolated using RIPA buffer (cell signalling, USA) containing PMSF (Sigma-Aldrich) and EDTA-free protease inhibitor cocktail (Roche). For co-immunoprecipitation, proteins were previously cross-linked with dithiobis succinimidyl propionate (Thermo Fisher™, USA) according to manufacturer's instructions. Protein concentration was determined using the Protein Assay Dye Reagent Concentrate (Bio-Rad).

2.10 Immunoprecipitation

To analyse protein–protein association in FOXO1-transfected SMCs, we separated BRD4 protein complexes using an anti-BRD4 antibody (sc-48772, Santa Cruz, USA) and the Dynabeads™ Protein G

Immunoprecipitation Kit (Invitrogen) following manufacturer's instructions. Normal rabbit IgG (sc-2027, Santa Cruz) was used as control.

2.11 SDS-PAGE and western blotting

Protein isolates were denatured in Roti®-Load 1 buffer (Carl Roth), added to NuPAGE™ LDS sample buffer (Invitrogen), H_2O, and DTT (Sigma-Aldrich). Proteins were separated on 4–20% Mini-ProteanTGX precast gels (Bio-Rad) and transferred to the Immun-Blot® PVDF membrane (Bio-Rad).

Following primary antibodies were used:

BRD2 (sc-393720, Santa Cruz), BRD3 (SAB1412098, Sigma-Aldrich), BRD4 (ab128874, Abcam, UK), FOXO1 (14952, Cell Signalling, USA or ab52857, Abcam), and GAPDH (sc-32233, Santa Cruz).

2.12 Isolation of nuclear proteins and transcription factor activity

Nuclear proteins were obtained utilizing a commercial nuclear extraction kit (Abcam) following manufacturer's instructions. Activity of the transcription factor FOXO1 was analysed by means of the TransAM™ FKHR assay (Active Motif, USA) performed following the manufacturer's instructions.

2.13 Microarray analysis and sample preparation

RNA was isolated using the RNeasy mini kit (Qiagen) according to the manufacturer's instructions. RNA concentrations were measured using Nanodrop 2000c (Thermo Fisher, USA) and Agilent 2100 Bioanalyzer (Agilent Technologies, USA) according to the manufacturer's instructions.

Microarray analysis was conducted using the SurePrint G3 Human GE V2 8x60K Microarray Kit (Agilent Technologies, USA). Synthesis of Cy3-labelled cRNA was performed with the 'Quick Amp Labeling kit, one color' (Agilent Technologies) according to the manufacturer's recommendations. Slides were scanned on the Agilent Micro Array Scanner G2565CA (pixel resolution 3 µm, bit depth 20). Data extraction was performed with the 'Feature Extraction Software V10.7.3.1' using the extraction protocol file 'GE1_107_Sep09.xml'. Processed intensity values of the green channel ('gProcessedSignal' or 'gPS') were normalized by global linear scaling. gPS values of one sample were multiplied by an array-specific scaling factor and calculated by the following formula: normalized $gPS_{Array\ i} = gPS_{Array\ i} \times (1500/75\text{th Percentile}_{Array\ i})$.

Data were analysed with the Gene Set Enrichment Analysis (GSEA) software, whereas C5 gene ontology gene sets were obtained from MSigDB. A further gene set of 323 FoxO1-dependent genes was created based on a literature review (see Supplementary material online, *Table*).

Fold changes to the mean of basal medium probes were calculated and represented in graphs, using GraphPad Prism 7 (GraphPad Software Inc., USA).

Microarray data have been deposited in the GEO repository (GEO accession number: GSE138323).

2.14 Chromatin immunoprecipitation

About 2×10^7 cells were cultured in GM at a density of 13 500 cells/cm^2 and treated with (+)-JQ1 for 1 h. Cell samples were fixed, harvested, and lysed according to optimized manufacturer's instructions using the ChIP-IT™ Express Enzymatic Chromatin Immunoprecipitation Kit (Active Motif). Chromatin immunoprecipitation (ChIP) reactions were incubated overnight on an end-to-end rotator using 95 µL of isolated chromatin and either 2 µg of FOXO1 antibody (sc-374427, Santa Cruz) or of normal mouse IgG (sc-2025, Santa Cruz). Samples were washed, eluted, reverse cross-linked, and treated with Proteinase K according to manufacturer's instructions (Active Motif). DNA was analysed by qRT–PCR as described earlier. The FOXO1-binding motif GTAAACAA chosen for the analysis was selected using the ConTra v3 web server.[15]

2.15 Vascular injury models

All animal experiments have been performed according to Directive 2010/63/EU of the European Parliament as well as to local ethical guidelines. All procedures involving animals have been approved by the Lower Saxony's institutional committee for animal research (LAVES). Adult male C57BL/6 mice were purchased from Charles River (Germany).

2.16 Mouse femoral artery injury model of neointima formation

The dilatation of the femoral artery was performed as previously described.[14]

In brief, mice were anesthetized using a singular intraperitoneal injection of ketamine hydrochloride (100 mg/kg body weight; Anesketin, Albrecht, Germany) and xylazine (16 mg/kg body weight Rompun® 2%, Bayer Health Care AG, Germany). A straight spring wire (0.38 mm in diameter, Cook Medical, USA) was then inserted through the profunda femoris artery up to 1 cm into the femoral artery and left in place for 1 min to achieve an adequate wire-induced vessel injury. After removal of the wire, the profunda femoris artery was ligated (7-0 Prolene, Ethicon, USA) and perfusion of the dilated femoral artery was re-established. Immediately after dilatation, we covered the injured femoral artery with 50 µL of a 25% thermosensitive Pluronic® F-127 gel containing (+)-JQ1 (10 mM) or vehicle (DMSO).

Mice were sacrificed at 10 or 21 days by cervical dislocation. The femoral artery was carefully harvested and embedded in Tissue-Tek OCT embedding medium (Sakura Finetek Europe B.V., The Netherlands).

2.17 Mouse carotid artery model of re-endothelialization

Perivascular electric injury of the carotid artery was performed as previously described.[16] Mice were anesthetized as described earlier. After preparation of the left common carotid artery through ventral middle line neck incision, electric de-endothelialization was carried out with a bipolar microregulator (ICC50, ERBE-Elektromedizin GmbH, Germany) at a length of 5 mm below the carotid bifurcation (2 W for 2 s). The treated artery was subsequently coated with 50 µL of a 25% thermosensitive pluronic F-127 gel containing (+)-JQ1 (10 mM) or vehicle (DMSO). Five days after electric injury of the left carotid artery, mice were sacrificed by cervical dislocation and re-endothelialization was assessed following injection 50 µL 5% Evan's blue solution (Sigma-Aldrich) into the tail vein, careful dissection of the left carotid artery, and *en face* staining (Eclipse Ni-E microscope, Nikon, Japan). Re-endothelialization was calculated as difference between the length of the blue-stained area and the initially injured area, using computer-assisted morphometric analysis (ImageJ 1.48 software, National Institutes of Health, USA).

2.18 Morphometry

After harvesting, the dilated femoral arteries at the indicated time-points following injury, vessels were sliced in 6 µm serial sections and van Gieson staining (Carl Roth) was performed for six cross-sections from regular intervals throughout each artery.

ImageJ 1.48 software was used to calculate circumference of external elastic lamina, internal elastic lamina and lumen as well as medial and neointimal area.

2.19 Immunofluorescence

Samples were incubated with antibodies targeting α-SMA (C6198, Sigma-Aldrich), Ki-67 (ab15580, Abcam), BRD2 (sc-393720, Santa Cruz), BRD3 (SAB1412098, Sigma-Aldrich), BRD4 (ab128874, Abcam), or FOXO1 (ab52857, Abcam). After incubation with primary antibodies, samples were marked with Alexa 488- or 546-coupled secondary antibodies (Life Technologies) and counterstained with nuclear 4.6-diamidino-2-phenylindole (Immunoselect Antifading Mounting Medium DAPI, Dianova, Germany). For α-SMA staining, we used monoclonal antibodies which were labelled directly with Cy3. Matching species- and isotype control antibodies were used for negative controls (Santa Cruz). For bright-field and immunofluorescence microscopy an Eclipse NI-E microscope (Nikon Instruments Europe B.V., The Netherlands), adequate filter blocks and image processing software were used (NIS Elements AR 4.20.01, Nikon Instruments Europe B.V.).

2.20 Statistical analysis

All collected data were stored and analysed on personal and institutional computers which were equipped with Microsoft Excel 2010 (Microsoft Corporation), Microsoft Word 2010 (Microsoft Corporation), and GraphPad Prism 6.01 (GraphPad Software Inc., USA). For statistical analysis of data among study groups, we used unpaired *t*-test or one-way ANOVA followed by multiple comparisons correction with the Holm–Sidak method depending on the number of groups and comparisons. All results were reported as mean ± standard error of the mean (SEM). The probability value was set <0.05 to be considered statistically significant for all statistical analyses.

3. Results

3.1 BET proteins are expressed in SMCs, ECs, and the vascular wall

PCR and western-blot analysis revealed robust RNA expression levels of BET-containing proteins BRD2, BRD3, and BRD4 in SMCs as well as in ECs. On the protein level, the expression of BRD2, BRD3, and BRD4 was more pronounced in SMCs than in ECs, as determined by western blotting and immmunohistochemistry (*Figure 1A and B*). Whereas BRD2 and BRD3 revealed a perinuclear expression pattern, BRD4 appeared to be almost exclusively localized in the nucleus (*Figure 1C*, scale bar 5 µm). Consistently, immunofluorescence analysis of native murine femoral arteries showed a comparable cellular distribution of all three BETs *in vivo* with cytoplasmatic and perinuclear expression of BRD2 and BRD3 and a nuclear expression pattern of BRD4 (*Figure 1D*, scale bar 25 µm). In addition, we detected rather prominent BRD3 and BRD4 signals in SMC of the intimal and medial layer, and a weaker expression in the adventitia, whereas BRD2 was expressed in all vascular layers including the adventitial layer *in vivo*. Moreover, *in vivo*, BRD2, BRD3, and BRD4 seem to be expressed predominantly in SMC, since signals appeared to be much weaker in EC (*Figure 1D*).

3.2 BET inhibition induces G0/G1 cell cycle arrest and prevents SMC proliferation

To investigate the impact of BETs on vascular cell function *in vitro*, SMCs were incubated with the BET inhibitors (+)-JQ1 or I-BET 151. After 24 h, we detected a dose-dependent reduction of SMC proliferation in response to treatment with either (+)-JQ1 or I-BET 151 as assessed by

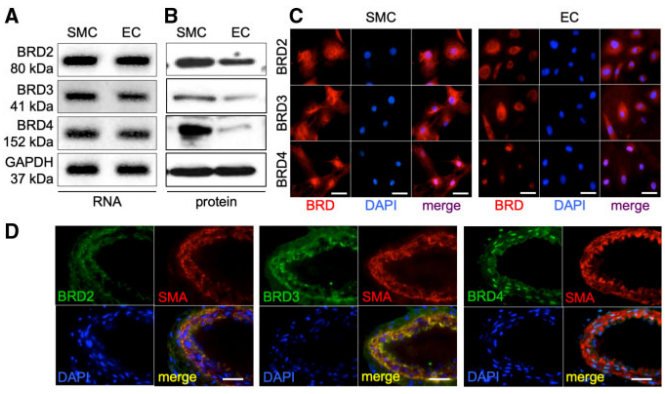

Figure 1 BET proteins are expressed in SMCs, ECs, and the vascular wall. PCR analysis (*A*) and western-blot analysis (*B*) verified the expression of the BET proteins BRD2, BRD3, and BRD4 in both human coronary artery SMCs and ECs ($n = 3$). Immunofluorescence staining revealed a perinuclear expression of BRD2 and BRD3 in SMCs and ECs and a nuclear localization of BRD4 in both cell types *in vitro* (*C*, $n = 3$, scale bar 5 µm) and in the murine vascular wall *in vivo* (*D*, $n = 6$, scale bar 25 µm).

BrdU-incorporation [GM+vehicle 100 ± 19.37% vs. GM + 1000 nM (+)-JQ1 14.75 ± 3.251% vs. GM + 1000 nM I-BET 151 3.059 ± 0.510%, ****$P < 0.0001$, *Figure 2A*]. Flow cytometry-based cell cycle analysis of propidium iodide-stained cells revealed BET-dependent G0/G1 arrest to the presence of (+)-JQ1 or I-BET 151 (*Figure 2B*). WST-1 conversion to formazan revealed a dose-dependent significant reduction of cellular metabolic activity in SMCs in response to (+)-JQ1, and a trend in the same direction in response to I-BET 151 [GM+vehicle 100 ± 7.691% vs. GM + 1000 nM (+)-JQ1 81.97 ± 5.452% vs. GM + 1000 nM I-BET 151 93.48 ± 11.76%, *$P < 0.05$, *Figure 2C*].

Beyond effects on proliferation and metabolic activity, GM-induced SMC migration was also dose-dependently attenuated in response to (+)-JQ1 or I-BET 151, as evaluated by a modified Boyden chamber assay [GM+vehicle 100 ± 8.51% vs. GM + 1000 nM (+)-JQ1 64.46 ± 5.609% vs. GM + 1000 nM I-BET 151 75.68 ± 11.42%, **$P < 0.01$, ****$P < 0.0001$, *Figure 2D*]. Additionally, immunofluorescence staining of the SMC marker proteins CALD1 and MYH11 verified a spindle-shaped SMC phenotype pointing out the prevention of a growth stimuli-induced phenotypic switch in response to BET inhibition. Conclusively, gene expression of these SMC marker genes was preserved in response to (+)-JQ1 as determined by qPCR analysis (*$P < 0.05$, **$P < 0.01$, $n = 6$, see Supplementary material online, *Figure S1*). We did not observe any change in SMC apoptosis rates in response to BET inhibition, neither with (+)-JQ1 nor with I-BET 151 [BM+vehicle 8.107 ± 3.632 $FLICA^+$ cells vs. BM + 1000 nM (+)-JQ1 7.783 ± 2.919 $FLICA^+$ cells vs. BM + 1000 nM I-BET 151 7.140 ± 0.5841 $FLICA^+$ cells, P = n.s., *Figure 2E*].

3.3 FOXO1-dependent genes are regulated in response to BET inhibition

To investigate the underlying mechanisms of the observed effects of BET inhibition on SMC function, we performed mRNA microarray expression analysis in SMC stimulated for 6 h with or without BET inhibition and non-proliferating SMC in basal medium. Due to the broader effects of (+)-JQ1 *in vitro* and the available data using structure-related substances *in vivo*, we focused on the use of the BET inhibitor (+)-JQ1 only.

Microarray analysis revealed a broad variety of regulated genes in response to stimulation with GM compared to SMCs cultured with basal medium, or SMCs cultured with GM and (+)-JQ1. GSEA revealed that BET inhibition predominantly alters the transcription of genes crucially involved in cell cycle regulation and thus proliferation (*Figure 3A and B*). A further analysis based on a literature-based compilation of FOXO1-controlled genes revealed that numerous genes out of the regulated gene sets are under transcriptional control of the transcription factor FOXO1 (red spots, *Figure 3C* and see Supplementary material online, *Table*). *Vice versa*, the majority of genes known to be regulated by FOXO1 was found to be regulated in response to (+)-JQ1 (**$P < 0.01$, FDR q-value 0.085, *Figure 3D* and see Supplementary material online, *Table*).

We further confirmed the upregulation of *CDKN1A*, one of the most significantly regulated FOXO1-dependent genes of the above-mentioned gene sets, by qPCR (*Figure 3E*). CDKN1A, a potent inhibitor of cell cycle-dependent kinases and responsible for the control of the G1-S checkpoint, and GADD45A, which is implicated in the control of cell cycle G2-M arrest, were confirmed to be significantly upregulated after treatment with (+)-JQ1 (*Figure 3E and F*). These effects of (+)-JQ1 could be prevented by siRNA-mediated silencing of FOXO1, thus approving a FOXO1-dependent expression of both genes. Moreover, siRNA-mediated silencing of *CDKN1A* but not of *GADD45A* partially reversed the antiproliferative effects of (+)-JQ1 (****$P < 0.0001$, $n = 6$, *Figure 3G*), indicating that the anti-proliferative effects of (+)-JQ1 are largely mediated by CDKN1A. ChIP and subsequent qPCR validated a direct interaction of the transcription factor FOXO1 and the genomic region of *CDKN1A* (*$P < 0.05$, $n = 3$, *Figure 3H*).

3.4 FOXO1 is expressed in SMCs and is crucial for (+)-JQ1-mediated inhibition of cell proliferation

Based on the pathway analysis and data obtained by GSEA, we identified the transcription factor FOXO1 as a potential key regulator of the (+)-JQ1-mediated differential mRNA expression. A further immunofluorescence analysis revealed a robust expression and nuclear localization of FOXO1 in quiescent SMCs *in vitro* and in native murine femoral arteries *in vivo* (*Figure 4A and B*). GM stimulation of SMC reduced the FOXO1 transcriptional activity, but this reduction was completely prevented after treatment with (+)-JQ1 [OD 450 nm, BM + vehicle 0.0679 ± 0.005 vs. GM + vehicle 0.0456 ± 0.002 vs. GM + 1000 nM (+)-JQ1 0.0649 ± 0.003, *P < 0.05, $n = 3$, *Figure 4C*]. Treatment with (+)-JQ1 did not alter FOXO1 protein expression in SMCs *in vitro*, as determined by western-blot analysis (*Figure 4D*). These data suggest that BET proteins are crucial for the GM-induced transactivational inactivation of FOXO1 and that there might exist a potential direct interaction of these proteins. To follow up on this hypothesis, we performed a siRNA-mediated knockdown of *FOXO1* in SMCs (*Figure 4E*). Following *FOXO1* knockdown, the inhibitory effect of (+)-JQ1 on SMC proliferation was indeed abolished, indicating that the anti-proliferative effect of BET inhibition is in fact largely dependent on the presence of FOXO1 [GM+vehicle 100 ± 26.46% vs. GM + 1000 nM (+)-JQ1+scrambled siRNA 32.05 ± 12.71% vs. GM + 1000 nM (+)-JQ1+FoxO1a siRNA 64.68 ± 10.69%, $n = 6$, *$P < 0.05$, *Figure 4F*].

3.5 Protein–protein interaction of FOXO1 and BRD4 is decisive for SMC proliferation

To identify the specific BRD proteins responsible for the observed effects on FOXO1 activity and SMC function, we assessed SMC proliferation following siRNA-mediated knockdown of each individual BRD protein (*Figure 5A*). Whereas depletion of BRD3 even augmented SMC proliferation, silencing of each, BRD2 and BRD4, effectively inhibited SMC proliferation, comparable to the effect of (+)-JQ1 [GM+vehicle 100 ± 8.063% vs. GM + 250 nM (+)-JQ1 55.71 ± 13.69% vs. GM+siBRD2 50.50 ± 7.068% vs. GM+siBRD3 247.069 ± 18.84% vs. GM+siBRD4 59.545 ± 9.672%, $n = 4$, ***$P < 0.001$, ****$P < 0.0001$ compared to GM+vehicle, *Figure 5B*]. Interestingly, the combined knockdown of all BRD proteins (BRD2, BRD3, and BRD4) also resulted in a significant reduction of SMC proliferation, comparable to the effects of (+)-JQ1 (53.53 ± 8.92%, $n = 4$, ****$P < 0.0001$ compared to GM+vehicle, *Figure 5B*). To follow up on a potential direct interaction, the localization of BRD proteins was assessed by immunohistochemistry. Whereas BRD2 and BRD3 were localized mainly in the cytoplasm, only BRD4 was found to be predominantly localized in the nucleus, as was FOXO1 (*Figure 5C*). Subsequent co-immunoprecipitation experiments confirmed a direct nuclear interaction of BRD4 and FOXO1 but not of other BRD proteins (*Figure 5D*).

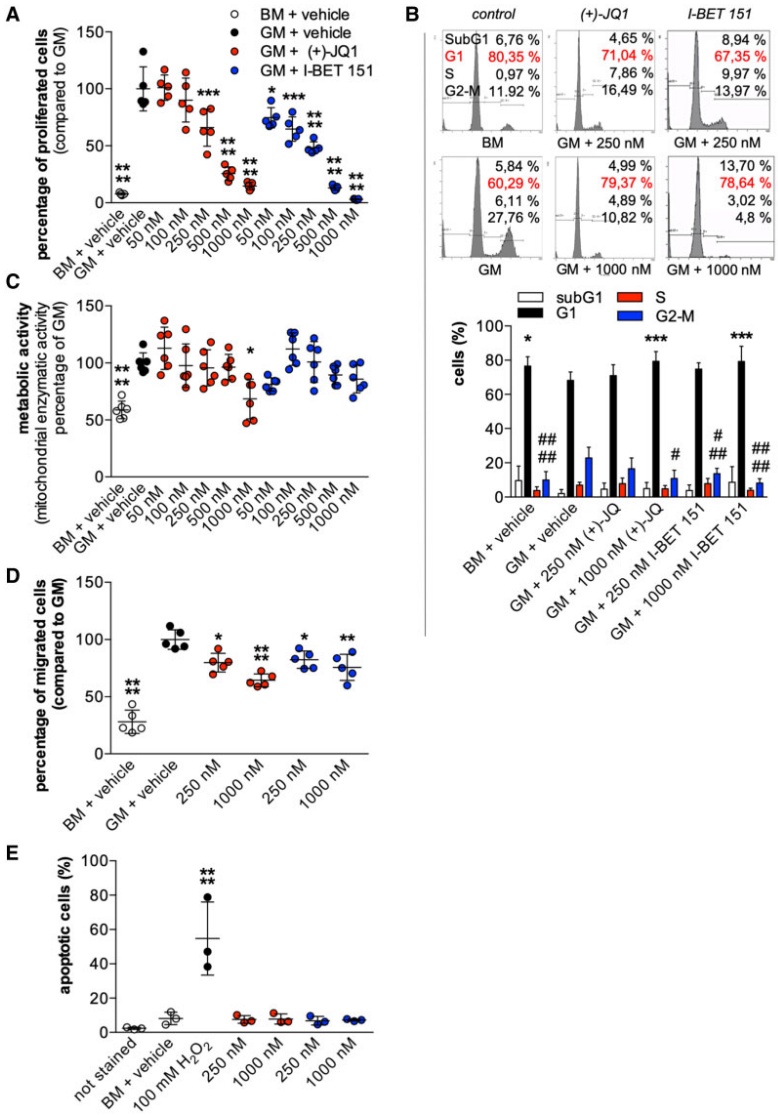

Figure 2 BET inhibition alters SMC function. BrdU incorporation as a surrogate for SMC proliferation in response to growth medium was prevented by BET inhibition (*A*, $n = 5$). Cell cycle analysis revealed a $G_{0/1}$ arrest in response to (+)-JQ1 or I-BET 151 (*B*, $n = 8$). Metabolic activity determined by WST-1 reduction to formazan (*C*, $n = 6$) and SMC migration as determined by a modified Boyden chamber assay (*D*, $n = 5$) revealed an inhibitory capacity of (+)-JQ1 on the metabolic activity of SMCs and of both inhibitors on SMC migration. Importantly, no effect on caspase 3/7 activity as a surrogate for SMC apoptosis was observed as determined by a flow cytometry-based FLICA assay (*E*, $n = 3$). $^{*/\#}P < 0.05$, $^{**}P < 0.01$, $^{***/\#\#\#}P < 0.001$, and $^{****/\#\#\#\#}P < 0.0001$ compared to GM + vehicle; one-way ANOVA followed by multiple comparisons correction with the Holm–Sidak method for all comparisons.

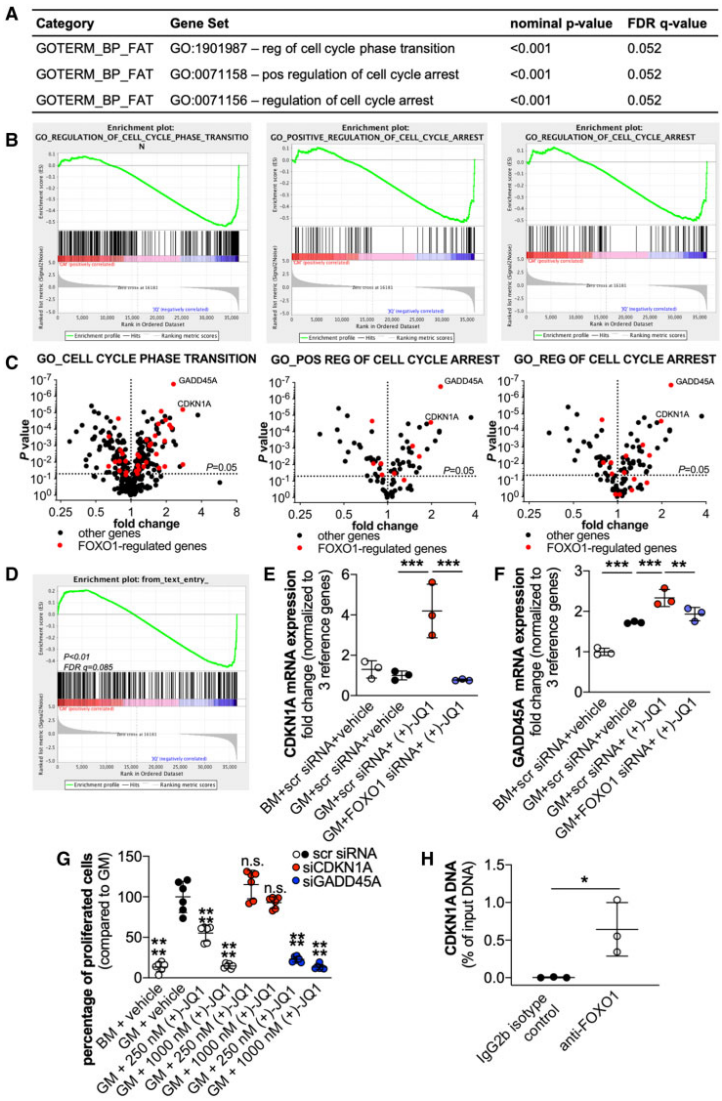

Figure 3 BET inhibition alters the expression of FOXO1-dependent genes for cell cycle control. Microarray- and subsequent gene set enrichment analyses was used to identify predominantly regulated gene sets in response to (+)-JQ1 treatment (*A*, $n = 3$). Enrichment plots visualized the regulation of the regulated gene sets (*B*, $n = 3$, $^{**}P < 0.01$, FDR < 25%, internal basal medium not shown). Volcano plots were chosen to present the gene regulation fold change of single genes of the in (*A*) and (*B*) mentioned gene sets and the level of significance of their regulation as well as an overlap with FOXO1-regulated genes [*C*, gene regulation in SMCs incubated with growth medium and (+)-JQ1 compared with SMCs incubated with growth medium and vehicle]. Enrichment plot of an analysis of FOXO1-dependent genes visualize their regulation in response to (+)-JQ1 (*D*, $^{**}P < 0.01$, FDR *q*-value 0.085). qPCR analysis validated the microarray results (*E* and *F*, $n = 3$, $^{**}P < 0.01$, $^{***}P < 0.001$; one-way ANOVA). BrdU incorporation analysis following siRNA-mediated depletion of *CDKN1A* (red) and *GADD45A* (blue) was used to investigate the impact of these genes on (+)-JQ1-mediated inhibition of SMC proliferation (*G*, $n = 6$, $^{****}P < 0.0001$; one-way ANOVA followed by multiple comparisons correction with the Holm–Sidak method). ChIP qPCR validated a direct interaction of FOXO1 and *CDKN1A* in response to (+)-JQ1 treatment for 30 min (*H*, $n = 3$, $^{*}P < 0.05$, paired *t*-test).

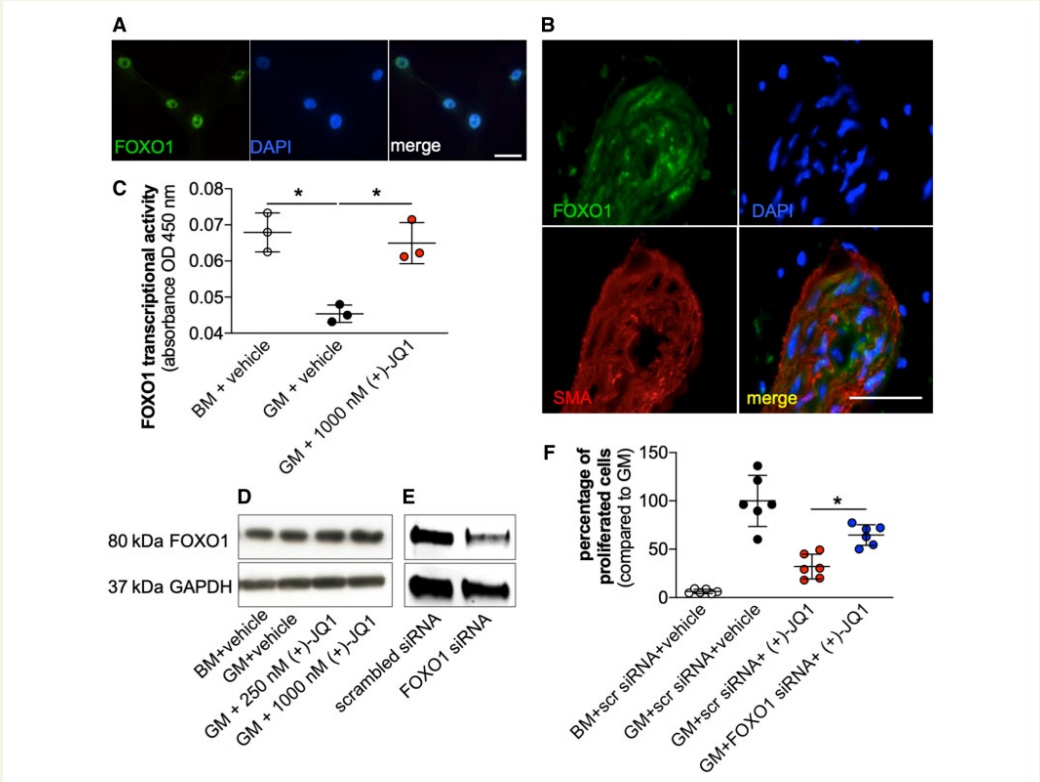

Figure 4 FOXO1 is expressed in SMCs and critical for bromodomain-mediated SMC proliferation. FOXO1 expression was investigated human coronary artery SMCs *in vitro* and in murine femoral arteries *in vivo* by immunofluorescence analysis (*A*, $n = 3$, scale bar 5 µm, and *B*, $n = 6$, scale bar 50 µm). The impact of (+)-JQ1 on the transcriptional activity of FOXO1 was evaluated using an ELISA-based promoter-binding analysis after (+)-JQ1 treatment for 1 h (*C*, $n = 3$, $^*P < 0.05$; one-way ANOVA). The impact of (+)-JQ1 on FOXO1 expression in SMCs was investigated by western-blot analysis after (+)-JQ1 treatment for 24 h (*D*, $n = 3$). Western-blot analysis was used to verify sufficient siRNA-mediated FOXO1 depletion following 24 h incubation (*E*). BrdU incorporation analysis was used to investigate the FOXO1-dependency of (+)-JQ1-mediated inhibition of SMC proliferation after incubation with siRNA for 24 h followed overnight treatment with (+)-JQ1 [*F*, 1000 nM (+)-JQ1, $n = 6$, $^*P < 0.05$; one-way ANOVA].

3.6 BET inhibition prevents SMC proliferation and neointima formation following vascular injury in mice

To determine the effect of (+)-JQ1-dependent Brd inhibition *in vivo*, we assessed intimal and medial SMC proliferation 10 days following wire-induced injury of the murine femoral artery of C57BL/6 mice. Local application of (+)-JQ1, released from a self-degrading thermosensitive Pluronic® F-127 gel which was applied around the injured vessel, significantly reduced the amount of proliferating (Ki-67$^+$) cells within both the intimal and the medial vascular layers [33.90 ± 5.478 Ki-67$^+$ neointimal cells in vehicle-treated mice vs. 0.80 ± 0.719 Ki-67$^+$ neointimal cells in (+)-JQ1-treated mice, $^{***}P < 0.001$, $n = 6$, *Figure 6A and B*]. Consistently, neointima formation was significantly reduced in mice treated with 10 mM (+)-JQ1 21 days after vascular injury [luminal stenosis 78.51 ± 2.119% in vehicle-treated mice vs. 22.04 ± 2.065% in (+)-JQ1-treated mice, $^{****}P < 0.0001$, $n = 6$, *Figure 6C–E*]. Importantly, (+)-JQ1 had no significant effect on the re-endothelialization of vessel segments following electric injury and denudation of mouse carotid arteries *in vivo* (P = n.s., $n = 4$, see Supplementary material online, *Figure SII*).

4. Discussion

With the recent advancements in the understanding of epigenetic processes, intensive research has been performed to decipher the impact of chromatin-modifying enzymes on cell signalling and thereby on the development and prevention of specific diseases. Although the majority of studies so far focused on manipulating epigenetic writers and erasers, that is histone acetyltransferases (HAT) and histone deacetylases, only recent studies also characterized the chromatin reading molecules like BETs. For this purpose, highly specific pharmacological BET inhibitors

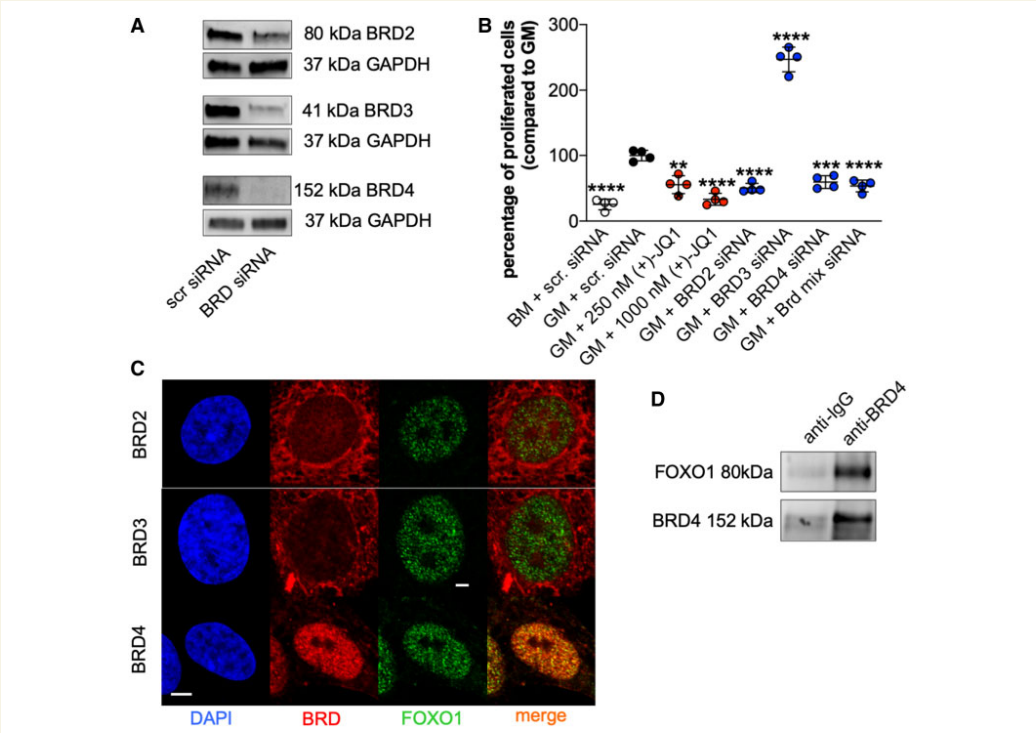

Figure 5 Brd4 directly interacts with FOXO1 and is decisive for SMC proliferation. siRNA-mediated depletion of Brd proteins was confirmed by western-blotting analysis ($n = 3$, *A*). SMC proliferation was evaluated by BrdU incorporation ELISA in the presence of different concentrations of (+)-JQ1 or siRNA of each single Brd protein as well as of siRNA of all Brd proteins (*B*, $n = 4$, ***$P < 0.001$, ****$P < 0.0001$; one-way ANOVA followed by multiple comparisons correction with the Holm–Sidak method). Co-localization of Brd proteins and FOXO1 was investigated by immunofluorescence analysis (*C*, $n = 3$, scale bar 5 μm). Direct interaction of BRD4 with FOXO1 was confirmed by immunoprecipitation of BRD4 or an isotype-matched IgG control antibody and incubation with a FOXO1 antibody (*D*, $n = 3$).

have been developed.[17] Whereas most basic science- and clinical studies focused on the therapeutic potential in oncology, only a few recent studies investigated the potential effects of BET inhibition in the context of cardiovascular diseases.

Initially, BET inhibition has been shown to suppress cardiomyocyte hypertrophy *in vitro* and pathologic cardiac remodelling *in vivo* in two basic science landmark studies.[18,19] The very recent Australian ASSURE (ApoA-1 Synthesis Stimulation and Intravascular Ultrasound for Coronary Atheroma Regression Evaluation; NCT01067820) trial provided clinical evidence for a reduced atherosclerotic plaque burden by the BET inhibitor apabetalone (RVX-208) as add-on therapy to high potency statins, hypothesizing that this effect was due to an additional BET-independent lipid-modifying effect, increasing HDL levels.[20]

In the present study, we show for the first time that specific BRD proteins are expressed in vascular cells and that BET inhibition plays a crucial role in SMC cell cycle regulation and proliferation *in vitro* and in neointimal lesion formation *in vivo*.

In our hands, solely BRD4 expression was restricted to the nucleus in SMCs, whereas BRD2 and BRD3 surprisingly showed a predominantly cytosolic, perinuclear expression. Fukazawa and Masumi[21] showed that BRD proteins own a common conserved 12-amino acid nuclear localization signal and are therefore suggested to be found in the nucleus. In line with their data, our data suggest that nuclear retention might differ between the single BRD proteins. After all, the detailed molecular mechanism of BET protein nuclear retention is not fully understood.

Although located outside the nucleus, siRNA-mediated silencing of BRD2 or BRD3 profoundly changed SMC proliferation. BRD proteins might thus exhibit mechanisms of action apart from their direct impact on transcription factor activity. Mitochondrial integrity and function have recently been implicated in the regulation of bromodomain inhibition and *vice versa*.[22–24] This relation has been at least in part attributed to altered expression of *MYC*. However, the respective publications lacked to show evidence for the hypothesized nuclear localization of BRD proteins as well as for a direct involvement of BRD proteins in the

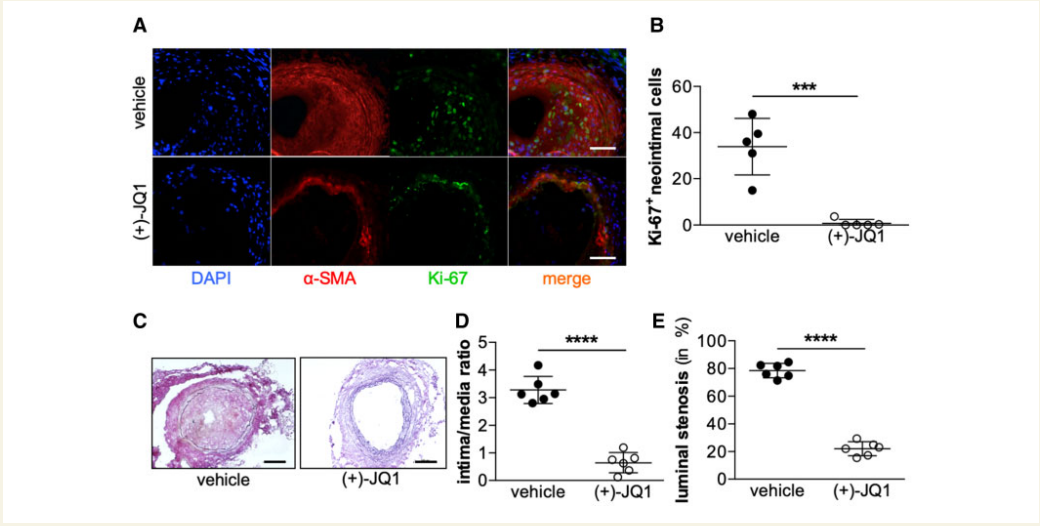

Figure 6 (+)-JQ1 inhibits SMC proliferation and prevents neointima formation in response to vascular injury. Immunofluorescence co-staining for Ki-67 (green), α-SMA (red), and DAPI (blue) of murine femoral artery cross-sections 10 days following wire-induced injury facilitated counting of neointimal proliferating cells (scale bar 50 µm, $n = 6$, $^{***}P < 0.001$, unpaired *t*-test; *A* and *B*). Morphometric analysis of van Gieson-stained sections 21 days following injury-enabled assessment of lumen reduction (scale bar 100 µm, $n = 6$, $^{****}P < 0.0001$, unpaired *t*-test; *C–E*).

transcriptional regulation of *MYC*. Hence, one could speculate about a cytosolic localization of BRD proteins as a prerequisite for a potential direct impact on mitochondrial and cellular function.

The here presented anti-proliferative effect of BET inhibition is consistent with previously published effects seen in epithelial cells, B-cells, and HeLa cells.[25,26] Whereas the inhibitory capacity of (+)-JQ1 on cellular metabolism could clearly be determined, the effect of I-BET151 did not reach statistical significance. In fact, there is no published systematic biophysical comparison of (+)-JQ1 and I-BET151 we could refer to. At least Baker *et al.*[27] determined higher IC_{50} values for I-BET151 compared to (+)-JQ1 in an assay comparable to ours in osteosarcoma cells in coherence with our results.

The maintenance of a contractile SMC phenotype in response to BET inhibition furthermore might implicate an improvement in atherosclerotic plaque stability. This might provide one rationale for the reported discrepancy between just moderate effects of apabetalone on plaque volume in the ASSURE study and a clear reduction in cardiovascular event rates in a pooled analysis.[28] Hence, our data clearly imply BET inhibition as a potential therapeutic approach to directly prevent adverse vascular remodelling processes independent of a lipid modulating effect.

In previous studies, rather unspecific BET bromodomain inhibitors were used. That is, apabetalone, which has been developed and clinically investigated as an ApoA1 modulator, initially not being aware of its BET bromodomain inhibiting effects, which were deciphered only later on.[29,30] However, in order to allow a rather selective targeting, and to dissect specific effects of BET inhibition from lipid-modifying effects as seen with apabetalone, the highly selective BET bromodomain inhibitors I-BET 151 and (+)-JQ1 were used in the current study.[31,32]

Mechanistically, microarray expression data, GSEA, and further pathway analyses revealed a predominant regulation of FOXO1-dependent genes in response to (+)-JQ1, of which *CDKN1A* was identified to be decisive for the observed anti-proliferative effects in our study. Besides *CDKN1A*, we found *GADD45A* to be robustly upregulated in response to (+)-JQ1. The transcriptional and post-transcriptional regulation of *GADD45A* is complex and orchestrated by numerous regulators including *MYC*.[33] *GADD45A* is even differentially regulated across different tumour cell lines.[34] It obtains pleiotropic effects *in vitro* including the ability to induce cell cycle arrest in the G2/M phase.[35] In contrast, (+)-JQ1 induced a cell cycle arrest in the G0/G1 but not the G2/M phase that was not rescued after silencing of *GADD45A*. Upregulation of *CDKN1A* in response to (+)-JQ1 might thus exceed the effect of *GADD45A* silencing and retain the cells in a quiescent state.

However, GADD45A might still have additional indirect anti-proliferative effects in the G0/G1 phase. First, GADD45A has been shown to regulate the phosphorylation and thus activation status of the signal transducer and activator of transcription 3 (STAT3), which we could implicate in SMC proliferation and the pathogenesis of neointima formation before.[14,36] Second, GADD45A and CDKN1A are hypothesized to interact with each other, even though the detailed interaction requires further investigation.[37]

Addition of (+)-JQ1 to GM indeed preserved the transcriptional capacity of FOXO1. Conclusive with the here investigated FOXO1-dependent transcription of *CDKN1A* in response to (+)-JQ1, siRNA-mediated silencing of FOXO1 partially reversed the (+)-JQ1-mediated effects on SMC proliferation. Notably, the level of BrdU incorporation still remained lower than that of vehicle control indicating alternative signalling pathways. The transcription factor activities of both interferon

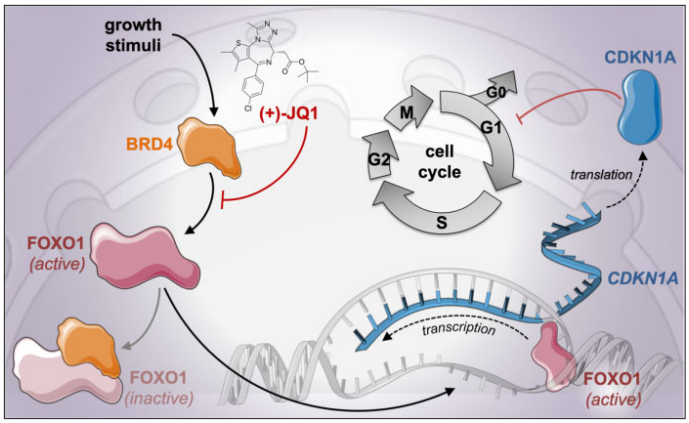

Figure 7 Mechanism of (+)-JQ1-induced cell cycle arrest in SMCs. (+)-JQ1 prevents growth stimuli-induced interaction between BRD4 and FOXO1 and thus maintains FOXO1 transactivational capacity. FOXO1 increases *CDKN1A* mRNA expression and G0/G1 cell cycle arrest.

regulatory factor 4 (IRF4) and Krüppel-like factor 5 (KLF5) have previously been shown to be depend on BRD4.[38,39] Both transcription factors have furthermore been implicated in the regulation of SMC proliferation *in vitro* and neointima formation *in vivo*.[40,41]

Indeed, we found a co-localization and direct interaction of FOXO1 and the BET bromodomain-containing protein BRD4 in the nucleus (*Figure 7*). FOXO1 acetylation by HAT decreases *CDKN1A* transcription, whereas BRD4 has an intrinsic HAT activity-located distal to the two bromodomains (BD1 and BD2) and an ET domain.[42,43] Therefore, FOXO1 acetylation by BRD4 seems to be conceivable at first sight.

(+)-JQ1, though, acts competitively at the BRD's binding site for acetylated histones located within BD1 and BD2. A direct interaction of FOXO1 with one of the two bromodomains seems hence more likely. Nagarajan *et al.*[44] reported histone-like motifs within the amino acid sequence of FOXO1, which were found to be acetylated in a curated mass spectrometry database. In contrast to BD1, BD2 is known not only to interact with acetylated lysines of histones but with those of other protein partners, too.[45,46] The histone-like motifs of FOXO1 and the BD2 domain of BRD4 could thus serve as direct interacting sites for each other.

Inhibition of BRD4 by (+)-JQ1 was found to enhance the transcriptional capacity of FOXO1, indicating that BRD4 functions as an endogenous inactivator of FOXO1. FOXO1 binds to condensed chromatin in a quiescent state, thereby recruiting other transcription factors to maintain transcriptional activity necessary for retaining physiological tissue homeostasis.[47] In response to mitogenic stimuli, FOXO1 is subjected to multiple modifications, including phosphorylation and acetylation. These modifications result in a modulation or inhibition of its transactivational capacity, a cytosolic translocation, and subsequent degradation.[48] Remarkably, current reports suggest that BET proteins can also be recruited to condensed chromatin, thereby orchestrating cell cycle regulation. DNA-binding affinity and transcriptional activity of FOXO1 is regulated by lysine acetylation and deacetylation on the one hand and protein–protein interaction on the other hand.[49]

Given the above findings, we postulate an additional mechanism regulating FOXO1 transactivational capacity, which may take part alternatively or in parallel to the previously well-described mechanisms: The epigenetic reader protein bromodomain-containing protein BRD4 represents an important regulator of FOXO1 function, contributing to FOXO1 inactivation under mitogenic and/or inflammatory stimulation.

FOXO1-induced gene transcription has been implicated in the development of numerous proliferative diseases, for example cancer, but also vascular diseases.[10,50] We previously found FOXO1-dependent gene transcription to be decisive for pulmonary artery SMCs proliferation in the pathogenesis of pulmonary artery hypertension.[10] In addition, FOXO1 function in vascular and inflammatory cells has also been implicated in atherosclerosis and venous bypass graft failure, but more importantly, also in neointima formation.[51–54] There, FOXO1 regulates CDKN1B in SMCs, which conclusively was regulated in our microarray analysis. CDKN1A and CDKN1B share a high structural and functional similarity as inhibitors of G1 cyclin-Cdk protein kinase activity.[55,56] Moreover, both are suggested to regulate each other's expression levels and to regulate different stages of G1 phase progression.[57,58] Thus, Foxo1-dependent regulation of neointima formation was shown to be dependent on both *CDKN1B* and *CDKN1A* expressions.

Importantly, (+)-JQ1 did not affect the endothelial recovery after denudation and thus does not impair vascular healing *in vivo*, most likely due to the low expression levels of Brd proteins in coronary artery ECs as compared to SMCs. However, others have shown a significant impact of (+)-JQ1 on the expression of endothelial adhesion molecules including ICAM-1, VCAM-1, and E-selectin *in vitro*. This results in an impairment of leucocyte recruitment *in vivo*, which might also result in reduced vascular inflammation and thus reduced SMC proliferation and neointima formation in our study.[59]

5. Conclusions

In conclusion, we present evidence that the BET bromodomain-containing protein BRD4 directly interacts with and modulates the activity of the transcription factor FOXO1. Following mitogenic stimulation, FOXO1 has to be inactivated to allow cell cycle entry and proliferation of SMC. BRD4 binding seems to be mandatory for FOXO1-inactivation, since BRD4 inhibition by (+)-JQ1 keeps FOXO1 in a transactivationally active state even under mitogenic stimulation. Due to the FOXO1-dependent continuous transactivation of CDKN1A, SMC remains in a quiescent phenotype, which prevents SMC proliferation and injury-induced neointima formation. The direct effects of BET inhibitors on SMC function provide a rationale for their therapeutic potential in preventing post-angioplasty restenosis and possibly also related vascular diseases like atherosclerosis.

Supplementary material

Supplementary material is available at *Cardiovascular Research* online.

Author's contributions

J.D., S.G., and D.G.S. planned the project and reviewed the data. J.D. and D.G.S. prepared the article. J.D., M.H., F.K., R.-J.M., and K.Kn. planned and performed the *in vivo* experiments. J.D., M.S., C.P., K.Ka., J.-T.S., and S.G. planned and performed the *in vitro* experiments. J.B. and J.-M.D. reviewed the data and corrected the article.

Acknowledgements

Microarray data used or referred to in this publication were generated by the Research Core Unit Genomics (RCUG) at Hannover Medical School. The authors thank Silke Pretzer for excellent technical assistance and all our colleagues for helpful discussions.

Conflict of interest: none declared.

Funding

This work was supported by the German Research Foundation, REBIRTH cluster of excellence; and an intramural grant of the Hannover Medical School to J.D. (HiLF, Hochschulinterne Leistungsförderung).

References

1. Dzau VJ, Braun-Dullaeus RC, Sedding DG. Vascular proliferation and atherosclerosis: new perspectives and therapeutic strategies. *Nat Med* 2002;**8**:1249–1256.
2. Alexander MR, Owens GK. Epigenetic control of smooth muscle cell differentiation and phenotypic switching in vascular development and disease. *Annu Rev Physiol* 2012;**74**:13–40.
3. Epstein FH, Gibbons GH, Dzau VJ. The emerging concept of vascular remodeling. *N Engl J Med* 1994;**330**:1431–1438.
4. Heerboth S, Lapinska K, Snyder N, Leary M, Rollinson S, Sarkar S. Use of epigenetic drugs in disease: an overview. *Genet Epigenet* 2014;**6**: 9–19.
5. Dawson MA, Kouzarides T, Huntly B. Targeting epigenetic readers in cancer. *N Engl J Med* 2012;**367**:647–657.
6. Tolani B, Gopalakrishnan R, Punj V, Matta H, Chaudhary PM. Targeting Myc in KSHV-associated primary effusion lymphoma with BET bromodomain inhibitors. *Oncogene* 2014;**33**:2928–2937.
7. Belkina AC, Denis GV. BET domain co-regulators in obesity, inflammation and cancer. *Nat Rev Cancer* 2012;**12**:465–477.
8. Amorim S, Stathis A, Gleeson M, Iyengar S, Magarotto V, Leleu X, Morschhauser F, Karlin L, Broussais F, Rezai K, Herait P, Kahatt C, Lokiec F, Salles G, Facon T, Palumbo A, Cunningham D, Zucca E, Thieblemont C. Bromodomain inhibitor OTX015 in patients with lymphoma or multiple myeloma: a dose-escalation, open-label, pharmacokinetic, phase 1 study. *Lancet Haematol* 2016;**3**:e196–e204.
9. Siebel AL, Trinh SK, Formosa MF, Mundra PA, Natoli AK, Reddy-Luthmoodoo M, Huynh K, Khan AA, Carey AL, Hall G, Van Cobelli C, Dalla-Man C, Otvos JD, Rye KA, Johansson J, Gordon A, Wong NCW, Sviridov D, Barter P, Duffy SJ, Meikle PJ, Kingwell BA. Effects of the BET-inhibitor, RVX-208 on the HDL lipidome and glucose metabolism in individuals with prediabetes: a randomized controlled trial. *Metabolism* 2016;**65**:904–914.
10. Savai R, Al-Tamari HM, Sedding D, Kojonazarov B, Muecke C, Teske R, Capecchi MR, Weissmann N, Grimminger F, Seeger W, Schermuly RT, Pullamsetti SS. Pro-proliferative and inflammatory signaling converge on FoxO1 transcription factor in pulmonary hypertension. *Nat Med* 2014;**20**:1289–1300.
11. Shi F, Li T, Liu Z, Qu K, Shi C, Li Y, Qin Q, Cheng L, Jin X, Yu T, Di W, Que J, Xia H, She J. FOXO1: another avenue for treating digestive malignancy? *Semin Cancer Biol* 2018;**50**:124–131.
12. Daniel J-M, Dutzmann J, Brunsch H, Bauersachs J, Braun-Dullaeus R, Sedding DG. Systemic application of sirolimus prevents neointima formation not via a direct anti-proliferative effect but via its anti-inflammatory properties. *Int J Cardiol* 2017;**238**: 79–91.
13. Dutzmann J, Koch A, Weisheit S, Sonnenschein K, Korte L, Haertlé M, Thum T, Bauersachs J, Sedding DG, Daniel J-M. Sonic hedgehog-dependent activation of adventitial fibroblasts promotes neointima formation. *Cardiovasc Res* 2017;**113**: 1653–1663.
14. Daniel J-M, Dutzmann J, Bielenberg W, Widmer-Teske R, Gündüz D, Hamm CW, Sedding DG. Inhibition of STAT3 signaling prevents vascular smooth muscle cell proliferation and neointima formation. *Basic Res Cardiol* 2012;**107**:261.
15. Kreft L, Soete A, Hulpiau P, Botzki A, Saeys Y, De Bleser P. ConTra v3: a tool to identify transcription factor binding sites across species, update 2017. *Nucleic Acids Res* 2017;**45**:W490–W494.
16. Carmeliet P, Moons L, Stassen JM, Mol M, De Bouché A, van den Oord JJ, Kockx M, Collen D. Vascular wound healing and neointima formation induced by perivascular electric injury in mice. *Am J Pathol* 1997;**150**:761–776.
17. Hewings DS, Rooney T, Jennings LE, Hay DA, Schofield CJ, Brennan PE, Knapp S, Conway SJ. Progress in the development and application of small molecule inhibitors of bromodomain–acetyl-lysine interactions. *J Med Chem* 2012;**55**:9393–9413.
18. Anand P, Brown JD, Lin CY, Qi J, Zhang R, Artero PC, Alaiti MA, Bullard J, Alazem K, Margulies KB, Cappola TP, Lemieux M, Plutzky J, Bradner JE, Haldar SM. BET bromodomains mediate transcriptional pause release in heart failure. *Cell* 2013;**154**:569–582.
19. Spiltoir JI, Stratton MS, Cavasin MA, Demos-Davies K, Reid BG, Qi J, Bradner JE, McKinsey TA. BET acetyl-lysine binding proteins control pathological cardiac hypertrophy. *J Mol Cell Cardiol* 2013;**63**:175–179.
20. Shishikura D, Kataoka Y, Honda S, Takata K, Kim SW, Andrews J, Psaltis PJ, Sweeney M, Kulikowski E, Johansson J, Wong NCW, Nicholls SJ. The effect of bromodomain and extra-terminal inhibitor apabetalone on attenuated coronary atherosclerotic plaque: insights from the ASSURE trial. *Am J Cardiovasc Drugs* 2019;**19**:49–57.
21. Fukazawa H, Masumi A. The conserved 12-amino acid stretch in the inter-bromodomain region of BET family proteins functions as a nuclear localization signal. *Biol Pharm Bull* 2012;**35**:2064–2068.
22. Lasorsa E, Smonksey M, Kirk JS, Rosario S, Hernandez-Ilizaliturri FJ, Ellis L. Mitochondrial protection impairs BET bromodomain inhibitor-mediated cell death and provides rationale for combination therapeutic strategies. *Cell Death Dis* 2015;**6**: e2014.
23. Ishida CT, Shu C, Halatsch M-E, Westhoff M-A, Altieri DC, Karpel-Massler G, Siegelin MD. Mitochondrial matrix chaperone and c-myc inhibition causes enhanced lethality in glioblastoma. *Oncotarget* 2017;**8**:37140–37153.
24. Piquereau J, Boet A, Péchoux C, Antigny F, Lambert M, Gressette M, Ranchoux B, Gambaryan N, Domergue V, Mumby S, Montani D, Adcock IM, Humbert M, Garnier A, Rucker-Martin C, Perros F. The BET bromodomain inhibitor I-BET-151 induces structural and functional alterations of the heart mitochondria in healthy male mice and rats. *Int J Mol Sci* 2019;**20**:1527.
25. Yang Z, He N, Zhou Q. Brd4 recruits P-TEFb to chromosomes at late mitosis to promote G1 gene expression and cell cycle progression. *Mol Cell Biol* 2008;**28**: 967–976.
26. Ottinger M, Christalla T, Nathan K, Brinkmann MM, Viejo-Borbolla A, Schulz TF. Kaposi's sarcoma-associated herpesvirus LANA-1 interacts with the short variant of BRD4 and releases cells from a BRD4- and BRD2/RING3-induced G1 cell cycle arrest. *J Virol* 2006;**80**:10772–10786.
27. Baker EK, Taylor S, Gupte A, Sharp PP, Walia M, Walsh NC, Zannettino AC, Chalk AM, Burns CJ, Walkley CR. BET inhibitors induce apoptosis through a MYC independent mechanism and synergise with CDK inhibitors to kill osteosarcoma cells. *Sci Rep* 2015;**5**:10120.
28. Nicholls SJ, Kausik •, Ray K, Johansson JO, Gordon A, Sweeney M, Halliday C, Kulikowski E, Wong N, Kim SW, Schwartz GG. Selective BET protein inhibition with apabetalone and cardiovascular events: a pooled analysis of trials in patients with coronary artery disease. *Am J Cardiovasc Drugs* 2018;**18**:109–115.
29. Picaud S, Wells C, Felletar I, Brotherton D, Martin S, Savitsky P, Diez-Dacal B, Philpott M, Bountra C, Lingard H, Fedorov O, Müller S, Brennan PE, Knapp S, Filippakopoulos P. RVX-208, an inhibitor of BET transcriptional regulators with selectivity for the second bromodomain. *Proc Natl Acad Sci U S A* 2013;**110**: 19754–19759.

30. McLure KG, Gesner EM, Tsujikawa L, Kharenko OA, Attwell S, Campeau E, Wasiak S, Stein A, White A, Fontano E, Suto RK, Wong NCW, Wagner GS, Hansen HC, Young PR. RVX-208, an inducer of ApoA-I in humans, is a BET bromodomain antagonist. *PLoS One* 2013;**8**:e83190.
31. Kempen HJ, Bellus D, Fedorov O, Nicklisch S, Filippakopoulos P, Picaud S, Knapp S. Lipid insights stimulation of hepatic apolipoprotein A-I production by novel thienotriazolodiazepines: roles of the classical benzodiazepine receptor, PAF receptor, and bromodomain binding. *Lipid Insights* 2013;**6**:47–54.
32. Ghosh GC, Bhadra R, Ghosh RK, Banerjee K, Gupta A. RVX 208: a novel BET protein inhibitor, role as an inducer of apo A-I/HDL and beyond. *Cardiovasc Ther* 2017;**35**:e12265.
33. Lal A, Gorospe M. Egad, more forms of gene regulation: the gadd45a story. *Cell Cycle* 2006;**5**:1422–1425.
34. Hollander MC, Fornace AJ. Genomic instability, centrosome amplification, cell cycle checkpoints and Gadd45a. *Oncogene* 2002;**21**:6228–6233.
35. Zhan Q, Antinore MJ, Wang XW, Carrier F, Smith ML, Harris CC, Fornace AJ. Association with Cdc2 and inhibition of Cdc2/Cyclin B1 kinase activity by the p53-regulated protein Gadd45. *Oncogene* 1999;**18**:2892–2900.
36. Yang F, Zhang W, Li D, Zhan Q. Gadd45a suppresses tumor angiogenesis via inhibition of the mTOR/STAT3 protein pathway. *J Biol Chem* 2013;**288**:6552–6560.
37. Zhao H, Jin S, Antinore MJ, Lung F-D, Fan F, Blanck P, Roller P, Fornace AJ, Zhan Q. The central region of Gadd45 is required for its interaction with p21/WAF1. *Exp Cell Res* 2000;**258**:92–100.
38. Chen C-H, Yang N, Zhang Y, Ding J, Zhang W, Liu R, Liu W, Chen C. Inhibition of super enhancer downregulates the expression of KLF5 in basal-like breast cancers. *Int J Biol Sci* 2019;**15**:1733–1742.
39. Gopalakrishnan R, Matta H, Tolani B, Triche T Jr, Chaudhary PM. Immunomodulatory drugs target IKZF1-IRF4-MYC axis in primary effusion lymphoma in a cereblon-dependent manner and display synergistic cytotoxicity with BRD4 inhibitors. *Oncogene* 2016;**35**:1797–1810.
40. Fujiu K, Manabe I, Ishihara A, Oishi Y, Iwata H, Nishimura G, Shindo T, Maemura K, Kagechika H, Shudo K, Nagai R. Synthetic retinoid Am80 suppresses smooth muscle phenotypic modulation and in-stent neointima formation by inhibiting KLF5. *Circ Res* 2005;**97**:1132–1141.
41. Cheng W-L, She Z-G, Qin J-J, Guo J-H, Gong F-H, Zhang P, Fang C, Tian S, Zhu X-Y, Gong J, Wang Z-H, Huang Z, Li H. Interferon regulatory factor 4 inhibits neointima formation by engaging Krüppel-like factor 4 signaling. *Circulation* 2017;**136**:1412–1433.
42. Chae Y-C, Kim K-B, Kang J-Y, Kim S-R, Jung H-S, Seo S-B. Inhibition of FoxO1 acetylation by INHAT subunit SET/TAF-Iβ induces p21 transcription. *FEBS Lett* 2014;**588**:2867–2873.
43. Devaiah BN, Case-Borden C, Gegonne A, Hsu CH, Chen Q, Meerzaman D, Dey A, Ozato K, Singer DS. BRD4 is a histone acetyltransferase that evicts nucleosomes from chromatin. *Nat Struct Mol Biol* 2016;**23**:540–548.
44. Nagarajan S, Bedi U, Budida A, Hamdan FH, Mishra VK, Najafova Z, Xie W, Alawi M, Indenbirken D, Knapp S, Chiang C-M, Grundhoff A, Kari V, Scheel CH, Wegwitz F, Johnsen SA. BRD4 promotes p63 and GRHL3 expression downstream of FOXO in mammary epithelial cells. *Nucleic Acids Res* 2017;**45**:3130–3145.
45. Huang B, Yang X-D, Zhou M-M, Ozato K, Chen L-F. Brd4 coactivates transcriptional activation of NF-B via specific binding to acetylated RelA. *Mol Cell Biol* 2009;**29**:1375–1387.
46. Jang MK, Mochizuki K, Zhou M, Jeong H-S, Brady JN, Ozato K. The bromodomain protein Brd4 is a positive regulatory component of P-TEFb and stimulates RNA polymerase II-dependent transcription. *Mol Cell* 2005;**19**:523–534.
47. Zaret KS, Carroll JS. Pioneer transcription factors: establishing competence for gene expression. *Genes Dev* 2011;**25**:2227–2241.
48. Wang Y, Zhou Y, Graves DT. FOXO transcription factors: their clinical significance and regulation. *Biomed Res Int* 2014;**2014**:1–13.
49. Daitoku H, Sakamaki J, Ichi, Fukamizu A. Regulation of FoxO transcription factors by acetylation and protein-protein interactions. *Biochim Biophys Acta Mol Cell Res* 2011;**1813**:1954–1960.
50. Kode A, Mosialou I, Manavalan SJ, Rathinam CV, Friedman RA, Teruya-Feldstein J, Bhagat G, Berman E, Kousteni S. FoxO1-dependent induction of acute myeloid leukemia by osteoblasts in mice. *Leukemia* 2016;**30**:1–13.
51. Mahajan S, Fender A, Meyer-Kirchrath J, Kurt M, Barth M, Sagban T, Fischer J, Schrör K, Hohlfeld T, Rauch BA. novel function of FoxO transcription factors in thrombin-stimulated vascular smooth muscle cell proliferation. *Thromb Haemost* 2012;**108**:148–158.
52. Tsuchiya K, Westerterp M, Murphy AJ, Subramanian V, Ferrante AW, Tall AR, Accili D. Expanded granulocyte/monocyte compartment in myeloid-specific triple FoxO knockout increases oxidative stress and accelerates atherosclerosis in mice. *Circ Res* 2013;**112**:992–1003.
53. Qiang L, Tsuchiya K, Kim-Muller J-Y, Lin HV, Welch C, Accili D. Increased atherosclerosis and endothelial dysfunction in mice bearing constitutively deacetylated alleles of Foxo1 gene. *J Biol Chem* 2012;**287**:13944–13951.
54. Abid MR, Yano K, Guo S, Patel VI, Shrikhande G, Spokes KC, Ferran C, Aird WC. Forkhead transcription factors inhibit vascular smooth muscle cell proliferation and neointimal hyperplasia. *J Biol Chem* 2005;**280**:29864–29873.
55. Toyoshima H, Hunter T. p27, a novel inhibitor of G1 cyclin-Cdk protein kinase activity, is related to p21. *Cell* 1994;**78**:67–74.
56. He G, Kuang J, Huang Z, Koomen J, Kobayashi R, Khokhar AR, Siddik ZH. Upregulation of p27 and its inhibition of CDK2/cyclin E activity following DNA damage by a novel platinum agent are dependent on the expression of p21. *Br J Cancer* 2006;**95**:1514–1524.
57. Orlando S, Gallastegui E, Besson A, Abril G, Aligú R, Pujol MJ, Bachs O. p27 Kip1 and p21 Cip1 collaborate in the regulation of transcription by recruiting cyclin-Cdk complexes on the promoters of target genes. *Nucleic Acids Res* 2015;**43**:6860–6873.
58. Kawamata S, Sakaida H, Hori T, Maeda M, Uchiyama T, Broxmeyer H, Katz A, Vainchenker W, Debili N. The upregulation of p27Kip1 by rapamycin results in G1 arrest in exponentially growing T-cell lines. *Blood* 1998;**91**:561–569.
59. Huang M, Zeng S, Zou Y, Shi M, Qiu Q, Xiao Y, Chen G, Yang X, Liang L, Xu H. The suppression of bromodomain and extra-terminal domain inhibits vascular inflammation by blocking NF-κB and MAPK activation. *Br J Pharmacol* 2017;**174**:101–115.

Translational perspective

Here, we demonstrate for the first time that the bromodomain and extra-terminal (BET) epigenetic reader proteins are important regulators of smooth muscle cell function. Currently available, highly specific inhibitors of these proteins like (+)-JQ1 potently prevent SMC proliferation after acute vascular injury, limiting neointima formation, and vessel re-occlusion following interventional treatment. Interfering with BET-function by using such inhibitors which are already in clinical use for the treatment of different diseases may represent an attractive and approach with high translational potential to support current interventional therapies by minimizing negative vascular remodelling processes.

3.5 Empaglifozin prevents neointima formation by impairing smooth muscle cell proliferation and accelerating endothelial regeneration.

SGLT2-Inhibitoren wurden initial als orale Antidiabetika entwickelt, zeigten jedoch bereits im Rahmen der von der FDA vorgeschriebenen Zulassungsstudien nicht nur eine kardiovaskuläre Unbedenklichkeit, sondern sogar vielversprechende kardioprotektive Effekte. In den Folgejahren entwickelten sich SGLT2-Inhibitoren zu einer der prognostisch relevanten Säulen medikamentöser Herzinsuffizienz-Therapie, unabhängig vom gleichzeitigen Vorliegen eines Diabetes mellitus. Die Effekte von SGLT2-Inhibitoren auf das Gefäßsystem waren zum Untersuchungs- und Publikationszeitpunkt der vorliegenden Arbeit unklar, waren jedoch insbesondere angesichts der häufig vaskulär-ischämischen Pathogenese einer Herzinsuffizienz unweigerlich von großer Bedeutung.

Zur Untersuchung von SGLT2-Inhibitoren auf das Gefäßsystem gelang zunächst der Nachweis von SGLT2 in humanen glatten Gefäßmuskel- und Endothelzellen ebenso wie in murinen Femoralarterien mittels Immunhistochemie- und Immunblotting-Verfahren. *In vitro* konnte durch die Behandlung mit dem SGLT2-Inhibitor Empagliflozin die Serum-induzierte Proliferationsantwort in humanen diabetischen und nicht-diabetischen Glattmuskelzellen dosisabhängig abgemildert werden. Gleichzeitig zeigte sich eine Zunahme der Zellzahl und Migrationskapazität humaner diabetischer, nicht aber diejenige humaner nicht-diabetischer Endothelzellen. Im Mausmodell der endovaskulären Verletzung der Femoralarterie resultierte die orale Applikation von Empagliflozin das Tierfutter in einer Reduktion der Anzahl proliferierender neointimaler Zellen und damit zur verminderten Bildung einer neointimalen Läsion nach endovaskulärer Verletzung. Vergleichbare Effekte konnten in Apolipoprotein E-defizienten ($ApoE^{-/-}$) Mäusen mit durch Streptozocin induziertem Diabetes mellitus nachgewiesen werden. Im Einklang mit den beschriebenen *In vitro*-Effekten auf Endothelzellen zeigte sich die Reendothelialisierung nach elektrischer Denudation der A. carotis und Behandlung mit Empagliflozin in C57BL/6-Mäusen nach drei Tagen nicht signifikant beeinflusst, während sie in diabetischen Mäusen signifikant verbessert war. Mittels RNA-Sequenzierung von mit Empagliflozin behandelten humanen glatten Gefäßmuskelzellen konnte eine deutliche transkriptionelle Regulation des für das vasoaktive Peptid Apelin codierenden Gens nachgewiesen werden. Rekombinantes Apelin zeigte *in vitro* die gleichen Effekte wie Empagliflozin.

Mit der vorliegenden Arbeit konnte somit erstmals der funktionelle Einfluss von Empagliflozin auf das Gefäßsystem gezeigt werden.

frontiers | Frontiers in Cardiovascular Medicine

TYPE Original Research
PUBLISHED 09 August 2022
DOI 10.3389/fcvm.2022.956041

OPEN ACCESS

EDITED BY
Dan Rudic,
Augusta University, United States

REVIEWED BY
Jian Xu,
University of Oklahoma Health Sciences Center, United States
Chun-Hsu Pan,
Taipei Medical University, Taiwan

*CORRESPONDENCE
Jochen Dutzmann
jochen.dutzmann@uk-halle.de

†These authors have contributed equally to this work

SPECIALTY SECTION
This article was submitted to Atherosclerosis and Vascular Medicine, a section of the journal Frontiers in Cardiovascular Medicine

RECEIVED 29 May 2022
ACCEPTED 25 July 2022
PUBLISHED 09 August 2022

CITATION
Dutzmann J, Bode LM, Kalies K, Korte L, Knöpp K, Kloss FJ, Sirisko M, Pilowski C, Koch S, Schenk H, Daniel J-M, Bauersachs J and Sedding DG (2022) Empagliflozin prevents neointima formation by impairing smooth muscle cell proliferation and accelerating endothelial regeneration. *Front. Cardiovasc. Med.* 9:956041. doi: 10.3389/fcvm.2022.956041

Empagliflozin prevents neointima formation by impairing smooth muscle cell proliferation and accelerating endothelial regeneration

Jochen Dutzmann [1*†], Lena Marie Bode[2†], Katrin Kalies[1], Laura Korte[2], Kai Knöpp[1], Frederik Julius Kloss[2], Mirja Sirisko[2], Claudia Pilowski[1], Susanne Koch[1], Heiko Schenk[3], Jan-Marcus Daniel[1,2], Johann Bauersachs[2] and Daniel G. Sedding [1]

[1]Mid-German Heart Center, Division of Cardiology, Angiology and Intensive Medical Care, University Hospital Halle, Martin-Luther-University Halle-Wittenberg, Halle (Saale), Germany, [2]Department of Cardiology and Angiology, Hannover Medical School, Hanover, Germany, [3]Department of Nephrology and Hypertension, Hannover Medical School, Hanover, Germany

Background: Empagliflozin, an inhibitor of the sodium glucose co-transporter 2 (SGLT2) and developed as an anti-diabetic agent exerts additional beneficial effects on heart failure outcomes. However, the effect of empagliflozin on vascular cell function and vascular remodeling processes remains largely elusive.

Methods/Results: Immunocytochemistry and immunoblotting revealed SGLT2 to be expressed in human smooth muscle (SMC) and endothelial cells (EC) as well as in murine femoral arteries. *In vitro*, empagliflozin reduced serum-induced proliferation and migration of human diabetic and non-diabetic SMCs in a dose-dependent manner. In contrast, empagliflozin significantly increased the cell count and migration capacity of human diabetic ECs, but not of human non-diabetic ECs. *In vivo*, application of empagliflozin resulted in a reduced number of proliferating neointimal cells in response to femoral artery wire-injury in C57BL/6J mice and prevented neointima formation. Comparable effects were observed in a streptozocin-induced diabetic model of apolipoprotein $E^{-/-}$ mice. Conclusive to the *in vitro*-results, re-endothelialization was not significantly affected in C57BL/6 mice, but improved in diabetic mice after treatment with empagliflozin assessed by Evan's Blue staining 3 days after electric denudation of the carotid artery. Ribonucleic acid (RNA) sequencing (RNA-seq) of human SMCs identified the vasoactive peptide apelin to be decisively regulated in response to empagliflozin treatment. Recombinant apelin mimicked the *in vitro*-effects of empagliflozin in ECs and SMCs.

Conclusion: Empagliflozin significantly reduces serum-induced proliferation and migration of SMCs *in vitro* and prevents neointima formation *in vivo*, while augmenting EC proliferation *in vitro* and re-endothelialization *in vivo* after vascular injury. These data document the functional impact of empagliflozin on vascular human SMCs and ECs and vascular remodeling in mice for the first time.

KEYWORDS

vascular remodeling, neointima formation, restenosis, SGLT2, diabetes

Introduction

Type 2 diabetes mellitus (T2DM) is a major risk factor for the development of in-stent restenosis after revascularization procedures in coronary artery disease. Despite the pioneering advance of using drug-eluting stents in revascularization therapy, in-stent-restenosis still occurs in approximately 1 out of 10 patients undergoing coronary artery stent implantation and patients with T2DM face a considerable higher risk of developing restenosis compared to patients with normoglycemic conditions according to the National Cardiovascular Data Registry database (1). Hallmarks of neointima formation are a disruption of endothelial integrity following revascularization and stent expansion in the vascular wall, accompanied by an inflammatory response, and consecutive stimulation of SMC proliferation and migration from the media toward the intimal layer (2, 3).

Sodium glucose co-transporter 2 (SGLT-2) inhibitors, gliflozins, initially FDA- and EMA-approved for the treatment of diabetes mellitus, have recently been recommended as first-line treatment for heart failure with reduced ejection fraction by several international cardiac societies (4–6). In fact, empagliflozin prevented hospitalizations for heart failure and cardiovascular death compared to placebo in T2DM patients with established coronary artery disease as shown in the EMPA-REG OUTCOME trial in 2015 (7). The ensuing EMPEROR-REDUCED and EMPEROR-PRESERVED trials confirmed these results regardless of the presence or absence of diabetes in 2020 and 2021 (8, 9). Intriguingly, the cardio-protective effects of empagliflozin were already seen at very early time points after randomization in both trials.

Not surprisingly, these results triggered a lively discussion on the pathophysiological and molecular mechanisms contributing to the beneficial effects on heart failure outcomes (10–13). SGLT-2 has not been detected in cardiomyocytes and the heart yet and sole normalization of blood glucose levels takes longer periods of time to exert cardiovascular benefits. Various reports suggested direct effects of SGLT-2 inhibition on vascular function (14). Yet, actual proof for any of these mechanisms is still lacking.

Here, we show direct and immediate effects on smooth muscle cell and endothelial cell proliferation and migration *in vitro* and neointimal lesion formation *in vivo*. These data suggest that direct vascular effects potentially contribute to the early cardio-protective effects of empagliflozin seen.

Materials and methods

Cell culture

Diabetic and non-diabetic human coronary artery smooth muscle cells (SMC) and human coronary artery endothelial cells (EC) were purchased from Lonza (Cologne, Germany). Cells between passages 3 and 6 were used for all experiments and cultured in optimized growth medium according to the supplier's protocols.

Functional *in vitro* assays

Total cell count was determined by cleavage of WST-1 to formazan (Cell Proliferation Reagent WST-1, Roche, Basel, Switzerland) and colorimetric measurement following manufacturer's instructions and as previously described (15). For siRNA-mediated knockdown cells were transfected with siRNA (4390843 and s12955, Ambion, Thermo Scientific, Rockford, IL, United States, and HuSR305853, OriGene Technologies, Rockville, MD, United States) according to the manufacturer's instructions and as indicated before serum-starvation followed by stimulation with 5% fetal calf serum (FCS). In brief, siRNAs were mixed with Opti-MEM® I medium (Thermo Scientific) and incubated with Lipofectamine® 2000 (Thermo Scientific) for 5 min. The mixture was added to the cells and incubated for 24 h. For inhibitor studies, indicated concentrations of empagliflozin were added to FCS. Recombinant full length apelin used has been the 77 amino acids preprotein, that is later processed to active apelin (ab152927, Abcam, Cambridge, United Kingdom).

Migration capacity was determined *via* a scratch-wound assay. The assay was performed in 24-well plates with cells seeded to confluence. After cell adherence to the well bottom a scratch wound was done with a pipette tip. Images were taken every 30 min over a period of 24 hwith a Cytation 1 (Biotek, Winooski, VT, United States). Scratch-area and cell-area were calculated with the Gen5 software (Biotek) for every image.

Apoptosis was determined by analysis of histone-associated deoxyribonucleic acid (DNA) fragments in the cytoplasm of apoptotic cells (REF 11544675001, Roche). Briefly, cells were seeded in a 96-well plate to confluence. Cells were incubated as indicated for 24 h, subsequently suspended in a sample solution, and added to the prepared microplate modules according to the manufacturer's instructions. Afterward, absorbance was measured using a colorimetric ELISA reader and apoptosis was assessed as specific enrichment of mono- and oligonucleosomes released into the cytoplasm according to the manufacturer's instructions.

Preparation of cellular lysates and immunoblot analysis

For cellular lysis, cells were washed twice in phosphate buffered saline and lysed in protein lysis buffer. Lysates were incubated on ice for 30 min and subsequently centrifuged at 4°C and 13000 rpm for 15 min. Protein concentration of the supernatant has been determined using a Bradford protein assay (Bio-Rad). After addition of sample buffer, dithiothreitol, and H_2O, the protein has been denatured at 95°C for 5 min. Protein mix was run on commercial precast 4–12% Bis-Tris gels (NuPAGE® SDS-PAGE Gel System, LifeTechnologies, Carlsbad, CA, United States) and transferred onto a nitrocellulose membrane by a commercial wet/tank blotting system (*Trans-Blot*®, Bio-Rad Laboratories, Hercules, CA, United States). After blocking with 5% milk, the blots were incubated with the primary antibody (anti-SGLT2, ab37296, Abcam or anti-GAPDH, sc-32233, Santa Cruz Biotechnology, Dallas, TX, United States) overnight at 4°C. The proteins were then detected by enhanced chemiluminescence (Pierce ECL Plus, Thermo Scientific) after labeling with a horseradish peroxidase-labeled secondary antibody according to the manufacturer's instructions (sc-2056, sc-2314, or sc-2004, Santa Cruz). Densitometric analysis was performed with ImageJ 1.49v.

Ribonucleic acid isolation, reverse transcription, and quantitative real-time polymerase chain reaction

Isolation of ribonucleic acid (RNA) from cells was performed using the RNeasy mini kit (Qiagen, Hilden, Germany) and obtained RNA was reverse transcribed with the High-Capacity RNA-to-cDNA™ kit (Applied Biosystems, Foster City, CA, United States) according to manufacturer's instructions and as previously described (16).

Quantitative real-time polymerase chain reaction (PCR) was performed using SYBR green® master mix with the respective primers and the CFX96 Touch™ Real Time PCR Detection System (both: Bio-Rad Laboratories) as previously described (16). All analyses were performed in triplicate and either the DNA template or the reverse transcriptase was omitted for control reactions. Fold change expression levels were quantified and normalized to the geometric mean of three reference genes with the highest expression stability by use of the $2^{-\Delta\Delta Ct}$ relative quantification method. Primer sequences were as follows: apelin (VHPS-447, Biomol, Hamburg, Germany), glyceraldehyde-3-phosphate dehydrogenase (GAPDH) fwd 5′-TGCACCACCAACTGCTTAGC-3′, rev 5′-GGCATGGACTGTGGTCATGAG-3′; F-box protein 7 (FBXO7) fwd 5′-GCTCGCACCTGAGGCAGTCC-3′, rev 5′-GTCTCTTCATCTCCAGTGAGGGG-3′; actin B fwd 5′-CCTCGCCTTTGCCGATCCG-3′, rev 5′-CGACGAGCGC GGCGATATCATC-3′.

Animals

All animal experiment procedures complied with the Directive 2010/63/EU of the European Parliament and local ethical guidelines. All procedures had been approved by the Lower Saxony's institutional committee for animal research (Niedersächsisches Landesamt für Verbraucherschutz und Lebensmittelsicherheit, approval reference number 16/2070) prior to the start of the experiments. All experiments were performed on at least 8-week-old adult male C57BL/6 mice purchased from Charles River (Sulzfeld, Germany). Sample size has been calculated by the Hannover Medical School Institute of Biometrics using nQuery Advisor 7.0. Investigators have been blinded at all stages of the experiments. Reporting in the manuscript follows the recommendations in the ARRIVE guidelines (17).

Apoe$^{TM1\,Unc}$ mice were treated with daily intraperitoneal injections of at least 50 mg kg^{-1} d^{-1} streptozotozin (Stz; 1.25 mg/200 µl citrate buffer) until serum glucose concentrations > 200 mg/dl, but for at least 5 days (18). Stz-treated mice with serum glucose > 200 mg/dl were classified as diabetic. Empagliflozin was added to mouse chow to deliver 10 mg kg^{-1} d^{-1} for 7 days (0.25 mg daily per animal estimating a mouse weight of 25–30 g and ingestion of 5 g rodent chow daily). Control mice got a standard diet. Serum and urine glucose measurement was performed to ensure the efficacy of Stz- and empagliflozin-treatment. In addition, body weight and serum cholesterol concentrations have been determined (**Supplementary Figure I**).

Vascular injury models

Mouse carotid artery model of re-endothelialization

Electric de-endothelialization of the carotid artery was performed at day 7 of empagliflozin treatment following previously described protocols (19). Mice were anesthetized using a singular intraperitoneal injection of ketamine hydrochloride (100 mg/kg body weight; Anesketin, Albrecht, Germany) and xylazine (16 mg/kg body weight Rompun® 2%, Bayer Health Care, Leverkusen, Germany). After preparation of the left common carotid artery through ventral middle line neck incision, electric de-endothelialization was carried out with a bipolar microregulator (ICC50, ERBE-Elektromedizin, Tübingen, Germany) at a length of 5 mm below the carotid bifurcation (2 W for 2 s). Three days after electrical injury of the left carotid artery, mice were anesthetized, 50 μl of 5% Evan's blue dye (Sigma-Aldrich, Darmstadt, Germany) was injected into the tail vein, and mice were sacrificed 5 min after Evan's blue dye injection by cervical dislocation and perfused with phosphate buffered saline. The left carotid artery was carefully dissected and reendothelialization was assessed by en face staining (Eclipse Ni-E microscope, Nikon, Japan). Re-endothelialization was calculated as the difference between the length of the blue-stained area and the initially injured area, using computer-assisted morphometric analysis (ImageJ 1.48 software, National Institutes of Health, United States).

Mouse femoral artery injury model of neointima formation

Wire-induced injury of the femoral artery was performed at day 7 of empagliflozin treatment as previously described (19). In brief, mice were anesthetized as described earlier. A straight spring wire (0.38 mm in diameter, Cook Medical, Bloomington, IN, United States) was then inserted through the profunda femoris artery up to 1 cm into the femoral artery and left in place for 1 min to achieve an adequate wire-induced vessel injury. After removal of the wire, the profunda femoris artery was ligated (7-0 Prolene, Ethicon, Johnson & Johnson, Norderstedt, Germany) and perfusion of the dilated femoral artery was re-established. Mice were sacrificed at 10 or 21 days by cervical dislocation. The femoral artery was carefully harvested and embedded in Tissue-Tek OCT compound medium (Sakura Finetek Europe B.V., Staufen im Breisgau, Germany). Then, the arteries were snap-frozen and stored at −80°C until sectioning.

Morphometry

After harvesting, the dilated femoral arteries at the indicated time-points following injury, vessels were sliced in 6 μm serial sections and Verhoeff–van Gieson staining (Carl Roth, Karlsruhe, Germany) was performed for six cross-sections from regular intervals throughout each artery. ImageJ 1.48 software was used to calculate circumference of external elastic lamina, internal elastic lamina and lumen as well as medial and neointimal area.

Immunofluorescence

Samples were incubated with antibodies targeting α-SMA (C6198, Sigma-Aldrich), Ki-67 (ab15580, Abcam), or SGLT-2 (ab37296, Abcam). After incubation with primary antibodies, samples were marked with Alexa 488- or 546-coupled secondary antibodies (Life Technologies, Carlsbad, CA, United States) and counterstained with nuclear 4.6-diamidino-2-phenylindole (Immunoselect Antifading Mounting Medium DAPI, Dianova, Germany). Matching species- and isotype control antibodies were used for negative controls (Santa Cruz). For bright-field and immunofluorescence microscopy an Eclipse NI-E microscope (Nikon Instruments Europe, Netherlands), adequate filter blocks and image processing software were used (NIS Elements AR 4.20.01, Nikon Instruments Europe).

Ribonucleic acid sequencing and analysis

Ribonucleic acid isolation

Ribonucleic acid was isolated as described above. RNA concentrations were measured using Nanodrop 2000c (Thermo Scientific) and Agilent 2100 Bioanalyzer (Agilent Technologies, Santa Clara, CA, United States) according to the manufacturer's instructions.

Ribonucleic acid sequencing library construction

Ribonucleic acid sequencing was conducted by Novogene (Novogene, Cambridge, United Kingdom). In brief, mRNA was enriched using oligo(dT) beads. The mRNA was then fragmented randomly in fragmentation buffer, followed by cDNA synthesis using random hexamers and reverse transcriptase. After first-strand synthesis, a custom second-strand synthesis buffer (Illumina, San Diego, CA, United States) was added with dNTPs, RNase H and Escherichia coli polymerase I to generate the second strand by nick-translation. The final cDNA library was ready after a round of purification, terminal repair, A-tailing, ligation of sequencing adapters, size selection and PCR enrichment. Library concentration was then quantified using a Qubit 2.0 fluorometer (Life Technologies) and diluted

to 1 ng/μl before checking insert size on an Agilent 2100 and quantifying to greater accuracy by quantitative PCR (qPCR) (library activity > 2 nM). Libraries were finally fed into HiSeq machines (Illumina) according to activities and expected data volume.

Ribonucleic acid sequencing processing

The original raw data was transformed to Sequenced Reads by base calling. Raw data was recorded in a FASTQ file, which contains sequence information (reads) and corresponding sequencing quality information. RNA-seq reads were then aligned to the Ensembl reference genome using the TopHat2 algorithm. Raw count data per gene was calculated using HTSeq software. The raw count matrix was then used by DESeq to quantify gene expression level as normalized counts. Transcripts with an adjusted $P < 0.05$ were considered differentially expressed. Data were analyzed with the Gene Set Enrichment Analysis (GSEA) software, whereas C5 gene ontology gene sets were obtained from MSigDB.

Ribonucleic acid-sequencing data have been deposited in the GEO repository (GEO accession number: GSE189538).

Statistical analysis

Data was stored and analyzed on personal computers using Microsoft Excel (Microsoft Corporation, Redmond, WA, United States) and GraphPad Prism 8 (GraphPad Software Inc., La Jolla, CA, United States). Study groups were compared using Mann–Whitney *U* test, Kruskal–Wallis *H* test followed by multiple comparisons using Dunn's method, or ordinary 1 way ANOVA followed by pairwise multiple comparisons using the Tukey method depending on normality, the number of groups, and affecting factors. The two one-sided test (TOST) procedure was used to test equivalence. All data are represented as the mean ± standard error of the mean (SEM). A probability value < 0.05 was considered statistically significant for all comparisons.

Results

Sodium glucose co-transporter 2 is expressed in smooth muscles, endothelial cells, and the vascular wall

Western-blot analysis revealed robust protein expression levels of SGLT-2 in human SMCs and ECs of non-diabetic as well as diabetic donors ($n = 3$, **Figures 1A,B**, full-length blots in **Supplementary Figure II**). However, SGLT-2 protein expression was substantially less compared to human embryonic kidney cells (data not shown). *In vivo*, immunofluorescence analysis of native murine femoral artery specimens confirmed vascular SGLT-2 expression using co-labeling of α-SMA ($n = 6$, **Figure 1C**, upper scale bar 100 μm, lower scale bar 25 μ m).

Empagliflozin improves vascular cell function *in vitro*

To investigate the impact of empagliflozin on vascular cell function *in vitro*, non-diabetic and diabetic coronary artery cells were incubated with empagliflozin. After 24 h, we detected a dose-dependent reduction of the number of non-diabetic as well as diabetic SMCs in response to treatment with empagliflozin as assessed by WST-1 cleavage to formazan (non-diabetic SMCs: FCS 5% 100 ± 2.178% vs. FCS 5% + 750 nM empagliflozin 71.859 ± 4.821%, $n = 3$, $^{*}P < 0.05$; diabetic SMCs: FCS 5% 100 ± 4.950% vs. FCS 5% + 750 nM empagliflozin 72.685 ± 7.016%, $n = 3$, $^{*}P < 0.05$; **Figure 2A**). Reduction in diabetic SMC count upon empagliflozin was potentially partially dependent on SGLT-2 expression, as SGLT-2 knockdown reduced the increase in total cell count as well upon FCS 5% (**Supplementary Figure III**). The effect was rather cytostatic than cytotoxic as empagliflozin did not induce apoptosis in a cell death detection assay based on the analysis of histone-associated DNA fragments (**Supplementary Figure IV**). In contrast, just the number of diabetic ECs increased in response to empagliflozin, while the number of non-diabetic ECs remained unaffected (non-diabetic ECs: serum-free 100 ± 3.57% vs. serum-free + 750 nM empagliflozin 106.737 ± 3.608%, $n = 3$, $P = 0.9997$; diabetic ECs: serum-free 100 ± 16.793% vs. serum-free + 750 nM empagliflozin 174.313 ± 26.914%, $n = 3$, $^{*}P < 0.05$; **Figure 2B**). Minimum required dosage of empagliflozin to significantly prevent the FCS-dependent increase in vascular cell count was determined at 750 nM in both SMCs and diabetic ECs, a dose that was used for all future *in vitro* experiments. Conclusive to the effects on vascular cell count, empagliflozin impaired the migrational capacity of non-diabetic and diabetic SMCs determined *via* a scratch-wound assay (cell coverage at 18 h compared to 0 h following stimulation; non-diabetic SMCs: serum-free 127.83 ± 3.51% vs. FCS 5% 166.91 ± 5.14% vs. FCS 5% + 750 nM empagliflozin 147.12 ± 5.197%, $n = 3$, $^{***}P < 0.001$, **Figure 2C**; diabetic SMCs: serum-free 112.45 ± 11.94% vs. FCS 5% 171.31 ± 2.23% vs. FCS 5% + 750 nM empagliflozin 155.01 ± 0.54%, $n = 3$, $^{*}P < 0.05$; **Figure 2D**). It furthermore improved the migrational capacity of diabetic, but not of non-diabetic ECs (cell coverage at 18 h following stimulation; non-diabetic ECs: serum-free 120.91 ± 4.48% vs. FCS 5% 142.33 ± 4.33% vs. serum-free + 750 nM empagliflozin 123.47 ± 3.41%, $n = 3$, $P = 0.2908$, **Figure 2E**; diabetic ECs: serum-free 104.59 ± 3.87% vs. FCS 5% 145.39 ± 4.08% vs. serum-free + 750 nM empagliflozin 130.45 ± 9.20%, $n = 3$, $^{****}P < 0.0001$; **Figure 2F**).

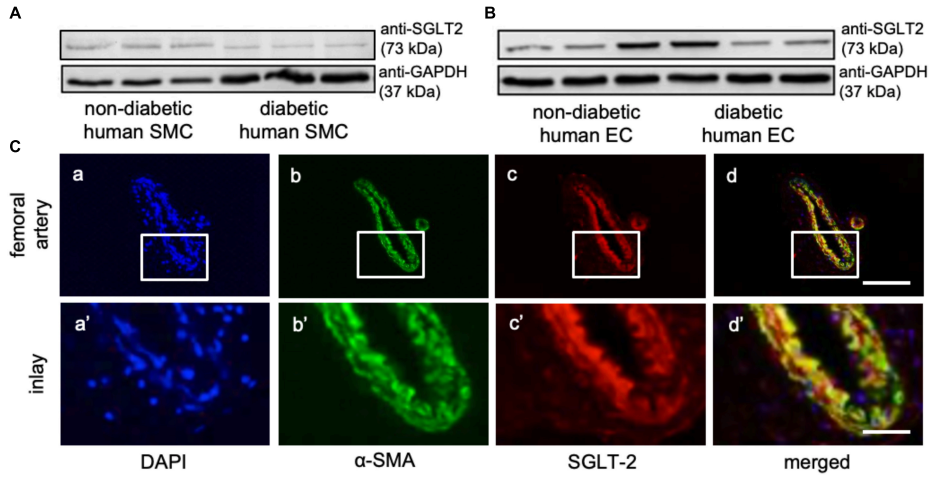

FIGURE 1
Sodium glucose co-transporter 2 (SGLT2) is expressed in human vascular cells and the murine femoral artery. **(A,B)** Western blot analysis for SGLT2 protein expression and glyceraldehyde-3-phosphate dehydrogenase (GAPDH) chosen as loading control in non-diabetic and diabetic human smooth muscle cells (SMCs, $n = 3$, **A**) and endothelial cells (ECs, $n = 3$, **B**). Full-length blots are presented in **Supplementary Figure II**. **(C)** Vascular SGLT2 expression in the native murine femoral artery as determined by immunohistochemical co-staining of α-smooth muscle actin (α-SMA, green) with SGLT-2 (red), and DAPI (blue; $n = 6$, upper scale bar 100 μm, lower scale bar 25 μm).

Empagliflozin accelerates re-endothelialization and prevents neointimal lesion formation *in vivo*

To study the *in vivo* effects of empagliflozin, we first determined the expanse of re-endothelialization 3 days following electrical de-endothelialization of the carotid artery in non-diabetic or diabetic C57BL/6 mice orally treated with empagliflozin or standard chow. In line with the observed effects *in vitro*, empagliflozin accelerates the re-endothelialization process in diabetic mice *in vivo*, but not in non-diabetic mice (non-re-endothelialized distance; non-diabetic mice: control 2.569 ± 0.105 mm vs. empagliflozin 2.298 ± 0.054 mm, $P = 0.24$; diabetic mice: control 3.088 ± 0.157 mm vs. empagliflozin 2.540 ± 0.094 mm, $n = 9$, $^{**}P < 0.01$, **Figures 3A,B**, scale bar 1 mm). Notably, re-endothelialization was significantly compromised in diabetic mice compared to non-diabetic mice ($P = 0.007$) and empagliflozin took the re-endothelialization capacity back to non-diabetic levels as assessed by TOST (pre-set equivalence margin $\delta = 0.30$ mm; 90% confidence interval for the difference between means (−0.22, 0.27), $P < 0.05$).

Oral treatment with empagliflozin impaired neointima formation 21 days after wire-induced injury of the murine femoral artery, conclusive to the aforementioned results in diabetic mice, but also in non-diabetic mice (neointima/media ratio; non-diabetic mice: control 4.79 ± 1.40 vs. empagliflozin 2.20 ± 0.42, $n = 9$, $^{***}P < 0.001$; diabetic mice: control 5.22 ± 1.35 vs. empagliflozin 2.71 ± 0.60, $n = 9$, $^{***}P < 0.001$, **Figures 3C,D**, scale bar 50 μm). Neointimal and medial cell proliferation was prevented by empagliflozin in both non-diabetic and diabetic mice, again in coherence with the effect of empagliflozin on SMC cell number *in vitro* (Ki-67^{+} cells/DAPI^{+} cells; non-diabetic mice: control 0.25 ± 0.0218% vs. empagliflozin 0.13 ± 0.0161, $n = 6$–7, $^{***}P < 0.001$; diabetic mice: control 0.16 ± 0.0256% vs. empagliflozin 0.07 ± 0.0122, $n = 8$, $^{*}P < 0.05$, **Figures 3E,F**, scale bar 50 μ m).

Empagliflozin increases apelin expression in smooth muscles and endothelial cells

In order to elucidate potential mechanisms of empagliflozin-mediated vascular effects, we performed differential RNA expression analysis on SMCs of diabetic donors by RNA-sequencing (**Supplementary Figure V**). Consistent with our earlier findings, gene set enrichment analysis revealed *"Negative Regulation of Vascular Smooth Muscle Cell Proliferation"* and *"Positive Regulation of Vascular Endothelial Cell Proliferation"* between the 20 most significantly regulated gene sets ($n = 3$, **Figures 4A,B**). Though, the last-mentioned was

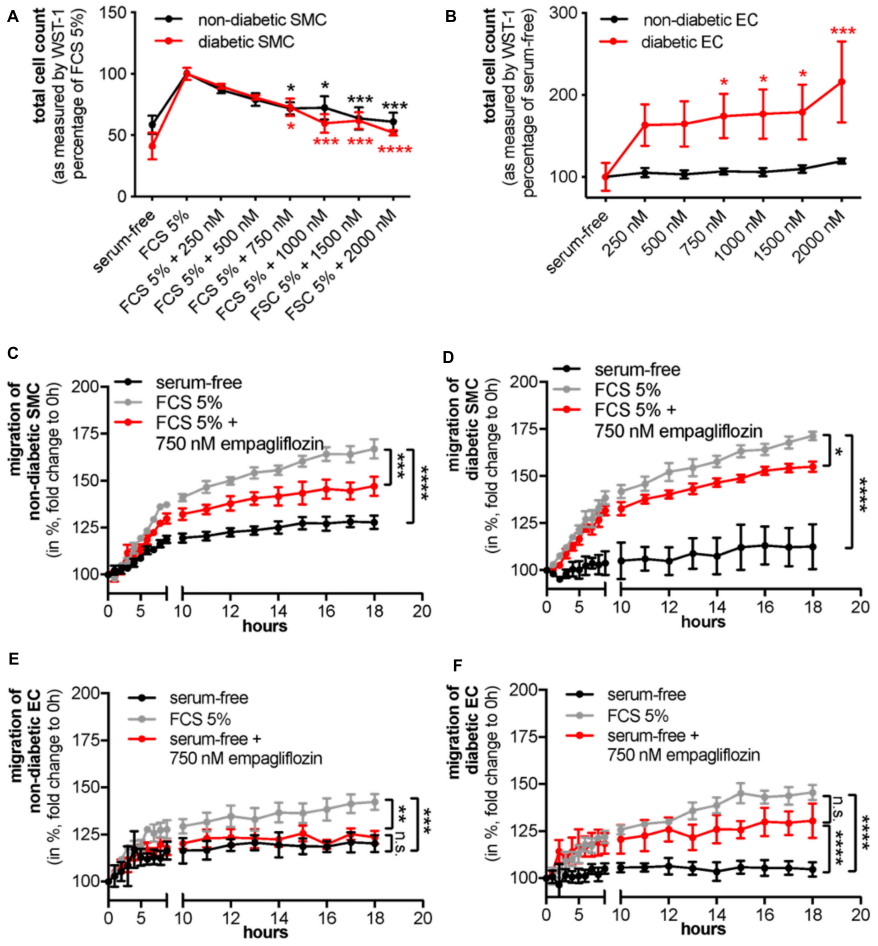

FIGURE 2
Empagliflozin improves diabetic endothelial cell (EC) function and prevents diabetic and non-diabetic smooth muscle cell (SMC) proliferation and migration. **(A,B)** Total cell count assessment of non-diabetic (black) and diabetic (red) SMCs **(A)** stimulated with 5% fetal calf serum (FCS) and indicated concentrations of empagliflozin and ECs with serum-free medium and indicated concentrations of empagliflozin **(B)** assessed by WST-1 cleavage to formazan at 24 h. **(C–F)** Determination of cell migration of non-diabetic **(C)** and diabetic **(D)** SMCs in serum free media (black), treated with 5% FCS (gray), and FCS 5% supplemented with 750 nM empagliflozin (red) as well as of non-diabetic **(E)** and diabetic ECs **(F)** in serum-free media (black), treated with 5% FCS (gray), and serum-free media supplemented with 750 nM empagliflozin (red) assessed by cell coverage at indicated time points in a scratch-wound assay (**A–F**: $n = 3$, *n.s.*, not significant, $^{*}P < 0.05$, $^{**}P < 0.01$, $^{***}P < 0.001$, $^{****}P < 0.0001$).

not significant after adjustment for the false discovery rate (FDR; FDR = 0.713). Notably, both gene sets overlapped by the vasoactive peptide apelin.

Quantitative real-time polymerase chain reaction validated significant upregulation of apelin in response to empagliflozin in both diabetic SMCs and diabetic ECs 24 h following stimulation ($n = 3$, Figures 4C,D). To investigate effects of apelin on vasculature, we treated diabetic human smooth muscle cells stimulated with FCS 5% and serum-starved endothelial cells with recombinant apelin. Apelin prevented the FCS-induced increase in SMC count whereas it augmented the number of ECs as assessed by WST-1 cleavage to formazan

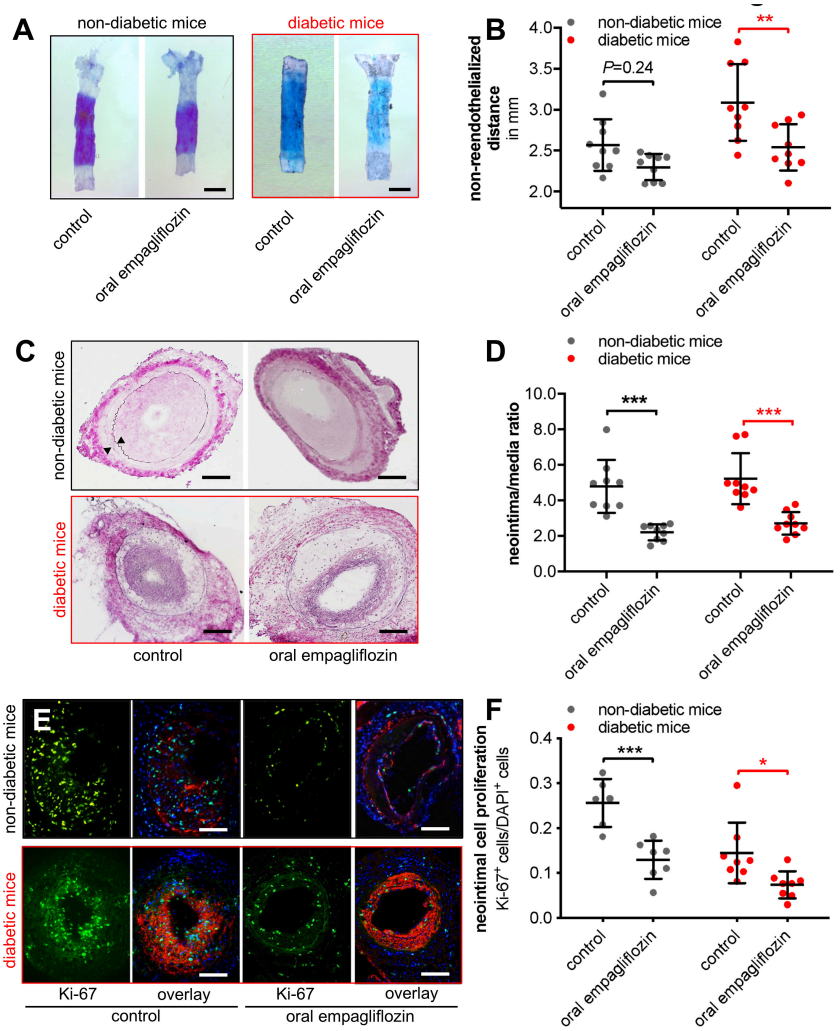

FIGURE 3
Empagliflozin improves vascular function in mice. **(A,B)** Evan's blue staining at 3 days after electrical injury of the murine carotid artery in non-diabetic and diabetic mice treated with empagliflozin or standard diet (**A**, scale bar 1 mm) and quantification of non-re-endothelialized distance (**B**, $n = 9$, $^{**}P < 0.01$). **(C,D)** Verhoeff–Van Gieson staining 21 days following wire-induced injury of non-diabetic and diabetic murine femoral arteries (**C**, scale bar 100 μm, arrowheads mark internal and external elastical laminae) and quantification of neointima/media ratio (**D**, $n = 9$, $^{***}P < 0.0001$). **(E,F)** Neointimal cell proliferation as determined by co-staining for Ki-67 (green), of α-smooth muscle actin (red), and DAPI (blue) at 10 days following wire-induced injury of non-diabetic and diabetic murine femoral arteries (**E**, scale bar 100 μm) and quantification (**F**, $n = 6–8$, $^{*}P < 0.05$, $^{***}P < 0.001$).

(diabetic SMCs: FCS 5% 100 ± 9.752% vs. FCS 5% + 600 nM apelin 83.29 ± 4.961%, $n = 3$, $^{*}P < 0.05$; diabetic ECs: serum-free 100 ± 4.811% vs. serum-free + 600 nM apelin 114.7 ± 6.733%, $n = 3$, $^{*}P < 0.05$, Figures 4E,F). SiRNA-mediated silencing of apelin in SMCs prove apelin-dependency of empagliflozin-mediated prevention of SMC proliferation,

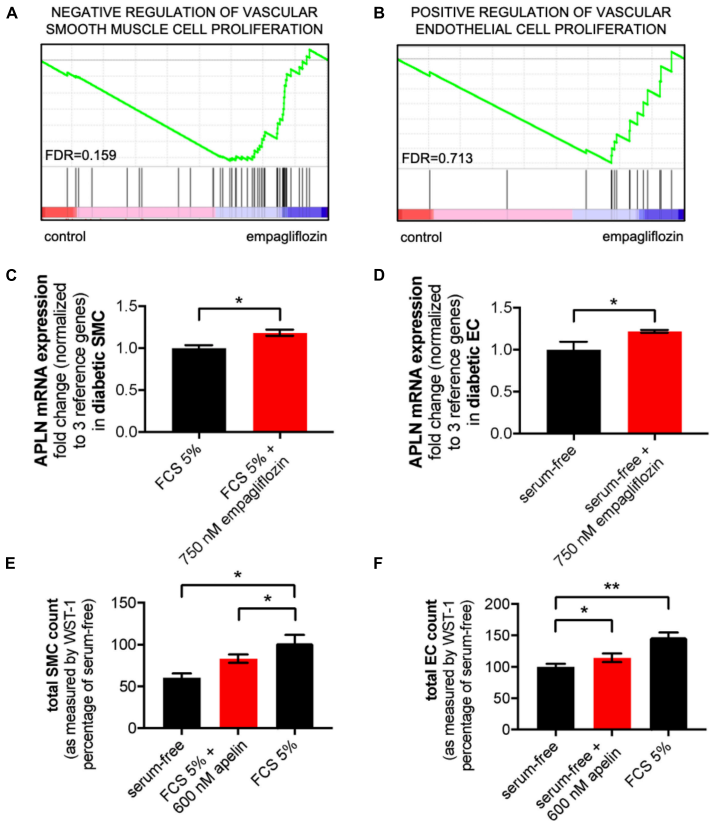

FIGURE 4
Apelin is upregulated by empagliflozin, prevents smooth muscle cell (SMC) proliferation and augments endothelial cell (EC) proliferation. **(A,B)** Two out of 20 most regulated gene sets from RNA-sequencing data of human diabetic coronary artery SMCs ($n = 3$). **(C,D)** Apelin mRNA expression as assessed by qRT-PCR in diabetic SMCs incubated with 5% fetal calf serum (FCS) with and without 750 nM empagliflozin (**C**, $n = 3$, $^*P < 0.05$) and in diabetic ECs incubated with serum-free medium with and without 750 nM empagliflozin (**D**, $n = 3$, $^*P < 0.05$). **(E,F)** Total cell count assessment of diabetic SMCs **(E)** stimulated with 5% FCS with or without 600 nM recombinant apelin and ECs with serum-free medium with or without 600 nM recombinant apelin **(F)** assessed by WST-1 cleavage to formazan at 24 h ($n = 3$, $^*P < 0.05$, $^{**}P < 0.01$).

but not empagliflozin-mediated prevention of SMC migration (**Supplementary Figure VI**).

Discussion

Sodium glucose co-transporter 2 inhibition initially developed to improve glycemic control in T2DM not only provides benefits in blood glucose lowering but also exerts cardiovascular advantages. For the first time, we present conclusive evidence that the SGLT2 inhibitor empagliflozin impairs smooth muscle cell proliferation and accelerates endothelial regeneration *in vitro* and prevents neointimal lesion formation and enhances re-endothelialization after vascular injury *in vivo*.

Our observations on the impact of empagliflozin on EC function and endothelial healing confirmed a significantly improved proliferation and migration capacity of diabetic ECs *in vitro* coherent with an accelerated, normalized re-endothelialization after electrical denudation of murine carotid arteries in a diabetic mouse model *in vivo*. However, the impact of empagliflozin on non-diabetic EC function did not reach statistical significance, neither *in vitro* nor *in vivo*. This might be the result of a comparable good cellular function of non-diabetic

ECs, so that empagliflozin treatment might not be able to further improve the re-endothelization capacity in these cells. In accordance with our findings, empagliflozin has repeatedly been shown to improve endothelial dysfunction and atherogenesis in diabetic rodents during the last few years (11, 14). We could confirm these empagliflozin-mediated effects on EC function in our mouse models for the investigation of neointimal lesion formation and could thus contextualize them with potential treatment strategies for the prevention of restenosis after percutaneous coronary intervention for the first time.

Importantly and in addition to the improvement of EC function, empagliflozin had opposing effects on diabetic as well as non-diabetic human coronary artery SMC function curbing hyperproliferation and hypermigration *in vitro* and preventing neointimal cell proliferation and neointimal lesion formation in response to wire-induced injury of the femoral artery *in vivo*. Conclusive with these results, two recently published studies provide evidence for a reactive oxygen species (ROS)-dependent anti-proliferative effect of empagliflozin on human aortic SMCs *in vitro*, even though seen at different concentrations of empagliflozin (20, 21). A recent Japanese study investigated the combined effects of empagliflozin and the dipeptidyl peptidase-4 (DPP-4) inhibitor linagliptin, another antidiabetic drug, on SMC function and neointima formation. The authors found comparable results with regard to the *in vitro* effects of SGLT2 inhibition on SMC cell count. Conversely to the here presented results, they reported an attenuated neointimal lesion formation in diabetic *db/db* mice following combined treatment with empagliflozin and linagliptin, but not following single treatment with empagliflozin or linagliptin. Remarkably, the guidewire used in this study for endovascular was considerably thinner than the one we have chosen (0.25 mm vs. 0.38 mm) resulting in an apparently smaller neointimal lesion size and thereby concealing the effects of empagliflozin on negative vascular remodeling (22).

Using RNA sequencing (RNA-seq) to decipher further mechanistic details, we identified the vasoactive peptide apelin to be upregulated in diabetic human coronary artery SMCs in response to empagliflozin treatment. Even though apelin did not count to the top regulated genes, it could be found in two of the most significantly regulated gene sets, which implicated apelin in both the negative regulation of SMC proliferation and the improvement of EC function. Apelin is widely expressed in various organs including heart and vasculature and is the endogenous ligand for the APJ receptor, which has been linked to the pathogenesis of cardiovascular diseases (23). The apelin-APJ pathway here appears to have opposing physiological roles to the renin-angiotensin system (24). In ECs, apelin has been shown to induce the release of nitric oxide (NO) and to promote cell proliferation and vascular healing (25–27). Importantly, apelin has also been shown to inhibit the proliferation and migration of murine aortic SMCs (28). As the effect of empagliflozin on SMCs, the apelin-dependent regulation of SMC function has been reported to be mediated through ROS. We could approve the empagliflozin-induced upregulation of apelin in diabetic SMCs as well as in diabetic ECs. Even although some contradictory results on the preventive effects of apelin on SMC proliferation and migration have been published, we could confirm the opposite effects on cell proliferation in diabetic SMCs and ECs treated with recombinant apelin (29–31). EC and SMC interaction has recently gained recognition in the pathogenesis of vascular remodeling processes and a likewise crosstalk through apelin seems to be plausible (32, 33). However, experimental clarification of this thesis goes beyond the scope of this study and might be subject of future studies.

The *in vivo* regulation and effect of apelin in rodent models of vascular remodeling is ambiguous: Global apelin knockout in mice has been shown to prevent neointimal lesion formation in non-diabetic mice (34). Carotid artery balloon injury increased vascular apelin and APJ mRNA expression in Wistar rats *vice versa*. Interestingly, pharmacological prevention of neointimal lesion formation by olmesartan further increased its expression in the same animals (35). In contrast, vascular apelin expression has been shown to be reduced in SMCs of spontaneously hypertensive rats compared to Wistar rats. However, exogenous apelin further increased SMC proliferation rates in this model (36). Finally, apelin prevents the angiotensin II-induced development of atherosclerotic lesions in apolipoprotein $E^{-/-}$ mice (37). All of the aforementioned results reflect the filigree regulation of apelin in vascular remodeling, even though most of the mentioned studies investigated whole vessel samples. Conditional knockout studies might be needed to finally clarify regulation and function of apelin in vascular disease. Even though we did not decipher the consecutive complex signaling cascade, we suppose the effects of empagliflozin on SMCs, ECs, and neointima formation to be at least in part apelin-dependent.

It has been discussed controversially, whether the impact of empagliflozin on cardiovascular outcomes is specifically dependent on myocardial or vascular SGLT2, SGLT2-independent, or the result of a concerted action and simultaneous modulation of multiple molecular and biochemical pathways (38). We here provide evidence for the existence of vascular SGLT2 in human EC and SMC and suppose a direct involvement of vascular SGLT2 rather than a systemic effect of empagliflozin based on the results of our *in vitro* experiments. Furthermore, siRNA-mediated silencing of SGLT2 impaired SMC proliferation and thereby underlined this assumption, even though we did not finally prove a SGLT2-dependency of empagliflozin-mediated vascular effects.

A recently published small open label, single-center, randomized, two-arm clinical trial provides translational insights and supports our here investigated hypothesis in a clinical setting (39). Hashikata and colleagues assigned 28 insufficiently controlled T2DM patients with coronary artery disease planned for DES stenting to receive empagliflozin

(n = 15, 19 lesions) or other glucose-lowering drugs (n = 13, 15 lesions). The primary endpoint, neointimal lesion size at 12 months after cardiovascular intervention assessed by optical coherence tomography (OCT), was significantly reduced in patients receiving empagliflozin compared with patients receiving other glucose-lowering drugs. Despite several limitations (e.g., small number of patients) and even though univariate regression analysis revealed associations of changes in blood pressure and neointimal lesion size indicating indirect effects, this study clearly underpins our hypothesis.

Conclusion

We here provide evidence that empagliflozin, recently established as a new standard therapy for heart failure with reduced ejection fraction, simultaneously prevents SMC proliferation and augments EC function finally resulting in improved vascular healing and impaired neointimal lesion formation following injury under non-diabetic, but also diabetic conditions. Even although we did not finally clarify the detailed mechanism, the observed effects might be dependent on vascular SGLT2 and involve the vasoactive peptide apelin. Empagliflozin might thus be promising for the prevention of vascular re-narrowing following percutaneous cardiovascular intervention, especially in diabetic patients at high risk for restenosis.

Data availability statement

The datasets presented in this study can be found in online repositories. The names of the repository/repositories and accession number(s) can be found below: https://www.ncbi.nlm.nih.gov/geo/, GSE189538.

Ethics statement

The animal study was reviewed and approved by Lower Saxony's Institutional Committee for Animal Research (Niedersächsisches Landesamt für Verbraucherschutz und Lebensmittelsicherheit, LAVES).

Author contributions

JD and LB conducted experiments, analyzed the data, and wrote the manuscript. KKa, LK, KKn, and FK conducted experiments, commented, and edited the manuscript. MS, CP, and SK conducted experiments and analyzed the data. HS, J-MD, and JB provided valuable suggestions and comments and edited the manuscript. DS supervised the study, interpreted the data, and wrote the manuscript. All authors contributed to the article and approved the submitted version.

Funding

This study was supported by the German Research Foundation (DFG), Cluster of Excellence REBIRTH.

Conflict of interest

The authors declare that the research was conducted in the absence of any commercial or financial relationships that could be construed as a potential conflict of interest.

Publisher's note

Supplementary material

The Supplementary Material for this article can be found online at: https://www.frontiersin.org/articles/10.3389/fcvm.2022.956041/full#supplementary-material

References

1. Shlofmitz E, Iantorno M, Waksman R. Restenosis of drug-eluting stents. *Circ Cardiovasc Interv.* (2019) 12:e007023. doi: 10.1161/circinterventions.118.007023

2. Daniel JM, Dutzmann J, Brunsch H, Bauersachs J, Braun-Dullaeus R, Sedding DG. Systemic application of sirolimus prevents neointima formation not *via* a direct anti-proliferative effect but *via* its anti-inflammatory properties. *Int J Cardiol.* (2017) 238:79–91. doi: 10.1016/j.ijcard.2017.03.052

3. Dzau VJ, Braun-Dullaeus RC, Sedding DG. Vascular proliferation and atherosclerosis: new perspectives and therapeutic strategies. *Nat Med.* (2002) 8:1249–56. doi: 10.1038/nm1102-1249

4. McDonagh TA, Metra M, Adamo M, Gardner RS, Baumbach A, Böhm M, et al. 2021 ESC guidelines for the diagnosis and treatment of acute and chronic heart failure. *Eur Heart J.* (2021) 42:3599–726. doi: 10.1093/eurheartj/ehab368

5. McDonald M, Virani S, Chan M, Ducharme A, Ezekowitz JA, Giannetti N, et al. CCS/CHFS heart failure guidelines update: defining a new pharmacologic standard of care for heart failure with reduced ejection fraction. *Can J Cardiol.* (2021) 37:531–46. doi: 10.1016/j.cjca.2021.01.017

6. Heidenreich PA, Bozkurt B, Aguilar D, Allen LA, Byun JJ, Colvin MM, et al. 2022 AHA/ACC/HFSA guideline for the management of heart failure: a report of the American college of cardiology/American heart association joint committee on clinical practice guidelines. *Circulation.* (2022) 145:e895–1032. doi: 10.1161/CIR.0000000000001063

7. Zinman B, Wanner C, Lachin JM, Fitchett D, Bluhmki E, Hantel S, et al. Empagliflozin, cardiovascular outcomes, and mortality in type 2 diabetes. *N Engl J Med.* (2015) 373:2117–28. doi: 10.1056/NEJMoa1504720

8. Packer M, Anker SD, Butler J, Filippatos G, Pocock SJ, Carson P, et al. Cardiovascular and renal outcomes with empagliflozin in heart failure. *N Engl J Med.* (2020) 383:1413–24. doi: 10.1056/NEJMoa2022190

9. Anker SD, Butler J, Filippatos G, Ferreira JP, Bocchi E, Böhm M, et al. Empagliflozin in heart failure with a preserved ejection fraction. *N Engl J Med.* (2021) 385:1451–61. doi: 10.1056/NEJMoa2107038

10. Butler J, Anker SD. The ethics of conducting clinical trials with sodium-glucose cotransporter-2 inhibitors in heart failure. *Circulation.* (2017) 136:1459–61. doi: 10.1161/CIRCULATIONAHA.117.029284

11. Butler J, Hamo CE, Filippatos G, Pocock SJ, Bernstein RA, Brueckmann M, et al. The potential role and rationale for treatment of heart failure with sodium-glucose co-transporter 2 inhibitors. *Eur J Heart Fail.* (2017) 19:1390–400. doi: 10.1002/ejhf.933

12. Fitchett DH, Udell JA, Inzucchi SE. Heart failure outcomes in clinical trials of glucose-lowering agents in patients with diabetes. *Eur J Heart Fail.* (2017) 19:43–53. doi: 10.1002/ejhf.633

13. Packer M, Anker SD, Butler J, Filippatos G, Zannad F. Effects of sodium-glucose cotransporter 2 inhibitors for the treatment of patients with heart failure. *JAMA Cardiol.* (2017) 2:1025. doi: 10.1001/jamacardio.2017.2275

14. Uthman L, Baartscheer A, Schumacher CA, Fiolet JWT, Kuschma MC, Hollmann MW, et al. Direct cardiac actions of sodium glucose cotransporter 2 inhibitors target pathogenic mechanisms underlying heart failure in diabetic patients. *Front Physiol.* (2018) 9:1575. doi: 10.3389/fphys.2018.01575

15. Dutzmann J, Koch A, Weisheit S, Sonnenschein K, Korte L, Haertlé M, et al. Sonic hedgehog-dependent activation of adventitial fibroblasts promotes neointima formation. *Cardiovasc Res.* (2017) 113:1653–63. doi: 10.1093/cvr/cvx158

16. Dutzmann J, Haertlé M, Daniel J-M, Kloss F, Musmann R-J, Kalies K, et al. BET bromodomain-containing epigenetic reader proteins regulate vascular smooth muscle cell proliferation and neointima formation. *Cardiovasc Res.* (2021) 117:850–862. doi: 10.1093/cvr/cvaa121

17. Kilkenny C, Browne WJ, Cuthill IC, Emerson M, Altman DG. Improving bioscience research reporting: the ARRIVE guidelines for reporting animal research. *PLoS Biol.* (2010) 8:e1000412. doi: 10.1371/journal.pbio.1000412

18. Furman BL. Streptozotocin-induced diabetic models in mice and rats. *Curr Protoc Pharmacol.* (2015) 70:5.47.1–20. doi: 10.1002/0471141755.ph0547s70

19. Dutzmann J, Musmann R-J, Haertlé M, Daniel J-M, Sonnenschein K, Schäfer A, et al. The novel mineralocorticoid receptor antagonist finerenone attenuates neointima formation after vascular injury. *PLoS One.* (2017) 12:e0184888. doi: 10.1371/journal.pone.0184888

20. Behnammanesh G, Durante GL, Khanna YP, Peyton KJ, Durante W. Canagliflozin inhibits vascular smooth muscle cell proliferation and migration: role of heme oxygenase-1. *Redox Biol.* (2020) 32:101527. doi: 10.1016/j.redox.2020.101527

21. Sukhanov S, Higashi Y, Yoshida T, Mummidi S, Aroor AR, Jeffrey Russell J, et al. The SGLT2 inhibitor empagliflozin attenuates interleukin-17A-induced human aortic smooth muscle cell proliferation and migration by targeting TRAF3IP2/ROS/NLRP3/Caspase-1-dependent IL-1β and IL-18 secretion. *Cell Signal.* (2021) 77:109825. doi: 10.1016/j.cellsig.2020.109825

22. Takahashi H, Nomiyama T, Terawaki Y, Horikawa T, Kawanami T, Hamaguchi Y, et al. Combined treatment with DPP-4 inhibitor linagliptin and SGLT2 inhibitor empagliflozin attenuates neointima formation after vascular injury in diabetic mice. *Biochem Biophys Rep.* (2019) 18:100640. doi: 10.1016/j.bbrep.2019.100640

23. Scimia MC, Hurtado C, Ray S, Metzler S, Wei K, Wang J, et al. APJ acts as a dual receptor in cardiac hypertrophy. *Nature.* (2012) 488:394–8. doi: 10.1038/nature11263

24. Ishida J, Hashimoto T, Hashimoto Y, Nishiwaki S, Iguchi T, Harada S, et al. Regulatory roles for APJ, a seven-transmembrane receptor related to angiotensin-type 1 receptor in blood pressure *in vivo*. *J Biol Chem.* (2004) 279:26274–9. doi: 10.1074/jbc.M404149200

25. Kasai A, Shintani N, Oda M, Kakuda M, Hashimoto H, Matsuda T, et al. Apelin is a novel angiogenic factor in retinal endothelial cells. *Biochem Biophys Res Commun.* (2004) 325:395–400. doi: 10.1016/j.bbrc.2004.10.042

26. Masoud AG, Lin J, Azad AK, Farhan MA, Fischer C, Zhu LF, et al. Apelin directs endothelial cell differentiation and vascular repair following immune-mediated injury. *J Clin Invest.* (2020) 130:94–107. doi: 10.1172/JCI128469

27. Tatemoto K, Takayama K, Zou MX, Kumaki I, Zhang W, Kumano K, et al. The novel peptide apelin lowers blood pressure *via* a nitric oxide-dependent mechanism. *Regul Pept.* (2001) 99:87–92. doi: 10.1016/s0167-0115(01)00236-1

28. Zhang P, Wang A-P, Yang H-P, Ai L, Zhang H-J, Wang Y-M, et al. Apelin-13 attenuates high glucose-induced calcification of MOVAS cells by regulating MAPKs and PI3K/AKT pathways and ROS-mediated signals. *Biomed Pharmacother.* (2020) 128:110271. doi: 10.1016/j.biopha.2020.110271

29. Wang C, Wen J, Zhou Y, Li L, Cui X, Wang J, et al. Apelin induces vascular smooth muscle cells migration *via* a PI3K/Akt/FoxO3a/MMP-2 pathway. *Int J Biochem Cell Biol.* (2015) 69:173–82. doi: 10.1016/j.biocel.2015.10.015

30. Liu Q-F, Yu H-W, You L, Liu M-X, Li K-Y, Tao G-Z. Apelin-13-induced proliferation and migration induced of rat vascular smooth muscle cells is mediated by the upregulation of Egr-1. *Biochem Biophys Res Commun.* (2013) 439:235–40. doi: 10.1016/j.bbrc.2013.08.051

31. Li F, Li L, Qin X, Pan W, Feng F, Chen F, et al. Apelin-induced vascular smooth muscle cell proliferation: the regulation of cyclin D1. *Front Biosci.* (2008) 13:3786–92. doi: 10.2741/2967

32. Balcells M, Martorell J, Olivé C, Santacana M, Chitalia V, Cardoso AA, et al. Smooth muscle cells orchestrate the endothelial cell response to flow and injury. *Circulation.* (2010) 121:2192–9. doi: 10.1161/CIRCULATIONAHA.109.877282

33. Dai Z, Zhu MM, Peng Y, Jin H, Machireddy N, Qian Z, et al. Endothelial and smooth muscle cell interaction *via* foxm1 signaling mediates vascular remodeling and pulmonary hypertension. *Am J Respir Crit Care Med.* (2018) 198:788–802. doi: 10.1164/rccm.201709-1835OC

34. Kojima Y, Kundu RK, Cox CM, Leeper NJ, Anderson JA, Chun HJ, et al. Upregulation of the apelin-APJ pathway promotes neointima formation in the carotid ligation model in mouse. *Cardiovasc Res.* (2010) 87:156–65. doi: 10.1093/cvr/cvq052

35. Li Y, Guo J, Yu H, Zhou J, Chu X, Hou B, et al. The effect of olmesartan on aortic intimal thickening after balloon injury through Apelin/APJ. *Cardiovasc Pathol.* (2020) 49:107230. doi: 10.1016/j.carpath.2020.107230

36. Xu T, Jia J, Xu N, Ye C, Zheng F, Yuan Y, et al. Apelin receptor upregulation in spontaneously hypertensive rat contributes to the enhanced vascular smooth muscle cell proliferation by activating autophagy. *Ann Transl Med.* (2021) 9:627. doi: 10.21037/atm-20-6891

37. Chun HJ, Ali ZA, Kojima Y, Kundu RK, Sheikh AY, Agrawal R, et al. Apelin signaling antagonizes Ang II effects in mouse models of atherosclerosis. *J Clin Invest.* (2008) 118:3343–54. doi: 10.1172/JCI34871

38. Vettor R, Inzucchi SE, Fioretto P. The cardiovascular benefits of empagliflozin: SGLT2-dependent and -independent effects. *Diabetologia.* (2017) 60:395–8. doi: 10.1007/s00125-016-4194-y

39. Hashikata T, Ikutomi M, Jimba T, Shindo A, Kakuda N, Katsushika S, et al. Empagliflozin attenuates neointimal hyperplasia after drug-eluting-stent implantation in patients with type 2 diabetes. *Heart Vessels.* (2020) 1:3. doi: 10.1007/s00380-020-01621-0

4 Diskussion

Die in dieser Habilitationsschrift zusammengefassten Arbeiten leisten einen wesentlichen Beitrag zum Verständnis kardiovaskulärer Remodeling-Prozesse nach Angioplastie und besonders zu Möglichkeiten ihrer pharmakologischen Beeinflussung. Insbesondere konnten die Effekte des SGLT2-Inhibitors Empagliflozin sowie des nicht-steroidalen MRA Finerenon, die beide in der Therapie der Herzinsuffizienz Anwendung finden, auf Endothel- und Glattmuskelzellen *in vitro* und im Mausmodell der endovaskulären Verletzung und Dilatation der Femoralarterie *in vivo* untersucht werden. Beide Substanzen erwiesen sich nicht nur als sicher, sondern beugten einer Neointimabildung nach Gefäßverletzung vor. Für die ebenfalls im Mausmodell untersuchte systemische Therapie mit dem mTOR-Inhibitor Sirolimus, der klinisch einerseits zur Prävention der ISR als Beschichtung von DES sowie andererseits als systemische Therapie nach Organtransplantationen Anwendung findet, konnte ebenfalls eine Beeinflussung des vaskulären Remodelings gezeigt werden, die allerdings über anti-inflammatorische und nicht über anti-proliferative Effekte vermittelt wurde. Die in der Onkologie verwendeten anti-proliferativen Substanzen Vismodegib (GDC-0449) und (+)-JQ1 verhinderten die Neointimabildung dagegen durch direkte antiproliferative Effekte auf vaskuläre Glattmuskelzellen, bemerkenswerterweise ohne die Reendothelialisierung der verletzten Gefäße zu beeinflussen. Die Verhinderung des negativen vaskulären Remodelings durch (+)-JQ1 über eine exklusive Beeinflussung adventitieller Fibroblasten unterstreicht die Bedeutung der äußersten Gefäßschicht und erweitert das pathophysiologische Verständnis der Neointimabildung grundlegend.

4.1 Effekte von Substanzen zur Therapie der Herzinsuffizienz auf die Neointimabildung

Da die ischämische Kardiomyopathie als Folge einer koronaren Herzerkrankung die häufigste Ursache für eine Herzinsuffizienz ist, sind die vaskulären Effekte von Substanzen in der Herzinsuffizienztherapie – insbesondere von Betablockern, ACE-Hemmern/ARNIs, MRAs und SGLT2-Hemmern, die als sogenannte „fantastic four“ die derzeitige Standardtherapie bei reduzierter linksventrikulärer Funktion sind – von zentralem Interesse.[40]

Für Substanzen aus der Medikamentenklasse der Betablocker konnte bereits um die Jahrtausendwende ein vaskuloprotektiver Effekt in experimentellen Studien nachgewiesen werden.[47–49] Obwohl in klinischen Studien keine Reduktion der Restenoserate nach Gefäßintervention nachgewiesen werden konnte, zeigte sich zumindest keine Aggravation des vaskulären Remodelings.[50–52] Für ACE-Hemmer zeigte sich ein ganz ähnliches Bild: Während im Tiermodell eine deutliche Reduktion der

Neointimabildung nachweisbar war, konnte in randomisierten kontrollierten klinischen Studien kein konklusiver Nachweis einer Reduktion der ISR nach Angioplastie erbracht werden.[53–56] Für Sacubitril/Valsartan als zurzeit einzigen Vertreter der ARNIs konnte zumindest *in vitro* ein antiproliferativer Effekt auf vaskuläre Glattmuskelzellen gezeigt werden.[46]

Die beiden MRAs Spironolacton und Eplerenon zeigen inkonsistente vaskuläre Effekte.[44] Spironolacton reduziert die Neointimabildung nach endovaskulärer Verletzung zwar im Klein-, nicht aber im Großtiermodell oder in klinischen Studien.[57–59] Eplerenon bewirkt dagegen eine Reduktion der Neointima sowohl im Klein- als auch im Großtiermodell. Klinische Studien zur Beeinflussung der ISR durch Eplerenon liegen nicht vor.[58,60]

In der vorliegenden Habilitationsschrift wird gezeigt, dass der hochspezifische neue nicht-steroidale MRA Finerenon die Aldosteron-induzierte Proliferation glatter Muskelzellen und der Apoptose von Endothelzellen *in vitro* verhindert. Die orale Applikation von Finerenon beschleunigte nach endovaskulärer Verletzung der murinen Femoralarterie den Reendothelialisierungsprozess, verminderte so die Rekrutierung von Leukozyten an der Verletzungsstelle und reduzierte letzten Endes die Proliferation vaskulärer Glattmuskelzellen und die Bildung einer Neointima. Darüber hinaus konnte eine Beteiligung des Mineralokortikoid-Rezeptors (MR) an myokardialen Heilungsprozessen nach Koronararterienligatur bei Mäusen und eine durch Behandlung mit Finerenon verbesserte linksventrikuläre Compliance sowie reduzierte interstitielle Fibrose nach Myokardinfarkt gezeigt werden.[61] Aktuelle multizentrische randomisierte kontrollierte klinische Studien zeigen eine Reduktion kardiovaskulärer Ereignisse durch Finerenon in Patienten mit und ohne chronische Herzinsuffizienz, die an Diabetes mellitus und/oder chronischer Nierenerkrankung leiden.[62–64] Zwar konnte die vorliegende Arbeit nicht zur mechanistischen Aufklärung der Finerenon-vermittelten vaskulären Effekte beitragen, allerdings deuten methodisch gut durchgeführte *In vivo*-Studien an Tieren mit gewebespezifischer MR-Deletion auf unterschiedliche zugrundeliegende molekulare Prozesse hin: Die vaskuläre glattmuskelzellspezifische MR-Deletion hatte auf diese Zellen einen über die *placental growth factor/VEGF receptor*-Signalkaskade vermittelten antiproliferativen Effekt und reduzierte durch parakrine Effekte den oxidativen Stress in Endothelzellen, was im Tiermodell nach einer endovaskulären Verletzung der Arterie carotis letztlich in einer Verminderung des negativen vaskulären Remodelings resultierte.[61,65] Auch die endothelzellspezifische Deletion des MR reduzierte den oxidativen Stress in Endothelzellen und beeinflusste die entzündungsspezifische Polarisation von Makrophagen.[66] Die selektive Deletion des MR in myeloiden Zellen verminderte die Makrophagen-Akkumulation und den vaskuläre

Entzündungsprozess nach endovaskulärer Verletzung durch Interferenz mit dem *nuclear factor-κB* (NF-κB)-Signalweg und begrenzte so die Neointimabildung.[67] Die vorgelegten Daten legen in Zusammenschau mit den Daten aus klinischen Studien einen protektiven vaskulären Effekt des neuen nicht-steroidalen MRAs Finerenon zumindest nahe, wenngleich konfirmatorische klinische Studien weiterhin nicht verfügbar sind.

Der kardioprotektive Wirkmechanismus von SGLT2-Hemmern in der Therapie der chronischen Herzinsuffizienz unabhängig von der linksventrikulären Funktion und unabhängig vom Vorhandensein eines Diabetes mellitus ist weiterhin nicht vollständig geklärt. Im Rahmen der Arbeiten zu der vorliegenden Habilitationsschrift konnte *in vitro* eine anti-proliferative Wirkung der Substanz Empagliflozin auf vaskuläre Glattmuskelzellen sowie im Tiermodell *in vivo* eine daraus resultierende verminderte Neointimabildung unabhängig vom Vorhandensein eines Diabetes mellitus nachgewiesen werden. Während die endotheliale Proliferations- und Migrationskapazität *in vitro* und Re-Endothelialisierung nach elektrischer Denudation der Arteria carotis im Mausmodell *in vivo* unter diabetischen Konditionen durch Empagliflozin-Therapie deutlich verbessert war, erreichten die endothelialen Funktionsänderungen unter nicht-diabetischen Konditionen weder *in vitro* noch *in vivo* statistische Signifikanz. Dies könnte das Ergebnis einer vergleichsweise guten zellulären Funktion nicht-diabetischer ECs sein, sodass die Behandlung mit Empagliflozin möglicherweise nicht in der Lage ist, die Re-Endothelialisierungskapazität in diesen Zellen weiter zu verbessern. Mittels RNA-Sequenzierung (RNA-seq) konnte durch Empagliflozin eine Regulation des vasoaktiven Proteins Apelin und eine Aktivierung des Apelin-APJ-Signalwegs, der eine entgegengesetzte physiologische Rolle zum Renin-Angiotensin-Aldosteron-System zu haben scheint, als möglicher Mechanismus identifiziert werden.

Die Effekte von SGLT2-Hemmern auf die Entwicklung einer ISR nach Angioplastie wurden kürzlich in einer sehr kleinen randomisierten Studie sowie in einer größeren Observationsstudie untersucht. Hashikata und Kollegen wiesen 28 unzureichend kontrollierten Patienten mit Diabetes mellitus und einer koronaren Herzkrankheit, die für eine Angioplastie mit der Implantation von DES geplant waren, entweder Empagliflozin (n=15) oder andere blutzuckersenkende Medikamente (n=13) zu. Der primäre Endpunkt, die Größe neointimaler Läsionen 12 Monate nach kardiovaskulärem Eingriff, die mittels optischer Kohärenztomographie bewertet wurde, war bei Patienten, die Empagliflozin erhielten, signifikant reduziert im Vergleich zu Patienten, die andere blutzuckersenkende Medikamente erhielten.[68] In einer italienischen Observationsstudie wurden bei 377 Patienten mit Diabetes mellitus nach akutem Myokardinfarkt über ein Jahr ISR-

bezogene harte kardiovaskuläre Endpunkte (kardialer Tod, erneuter Myokardinfarkt, Herzinsuffizienz) erfasst. Bei denjenigen 177 Patienten, die zum Infarktzeitpunkt eine bestehende Medikation mit SGLT2-Hemmern hatten, zeigten sich die ISR-bezogenen kardiovaskulären Endpunkte unabhängig von der Einstellung des Diabetes signifikant seltener und waren die Gefäßdiameter in der koronaren Computertomographie zum Follow-Up nach einem Jahr signifikant größer.[69]

Zusammenfassend können aus den dargestellten präklinischen Arbeiten und den diskutierten klinischen Arbeiten mindestens Hinweise auf eine vaskuläre Unbedenklichkeit der in der Verwendung als Herzinsuffizienztherapie neuen Substanzen Finerenon und Empagliflozin abgeleitet werden.

4.2 *Drug repurposing:* Direkte und indirekte Effekte von antiinflammatorischen und antiproliferativen Therapien auf die Neointimabildung

Die Praxis, bereits existierende Medikamente für die Behandlung von Krankheiten einzusetzen, für die sie ursprünglich nicht entwickelt wurden, bezeichnet man als *Drug repurposing*. Statt neue Medikamente von Grund auf zu entwickeln, wird bei der Wiederverwendung bereits vorhandener Medikamente ihr Potenzial für die Behandlung anderer Erkrankungen erforscht. Dieser Ansatz bietet den Vorteil, dass die Sicherheitsprofile und pharmakologischen Eigenschaften bereits bekannt sind, was den Entwicklungsprozess beschleunigen und die Kosten senken kann. SGLT2-Hemmer, die ursprünglich als orale Antidiabetika entwickelt worden waren, sind das derzeit prominenteste Beispiel für *Drug repurposing* in der Behandlung kardiovaskulärer Erkrankungen.[70]

Ein weiteres Beispiel, das in routinemäßiger klinischer Anwendung ist, ist die Beschichtung von DES mit dem antiproliferativ und antiinflammatorisch wirksamen Sirolimus. Sirolimus wurde zunächst und wird bis heute systemisch als immunsuppressive Medikation zur Behandlung von Autoimmunerkrankungen oder nach Organtransplantationen verwendet. Patienten mit diesen Erkrankungen haben im Vergleich zur Allgemeinbevölkerung ein per se höheres Risiko, eine symptomatische koronare Herzkrankheit zu entwickeln und benötigen oft eine PCI mit Stentimplantation. Im Rahmen der Arbeiten zur vorliegenden Habilitationsschrift wurde untersucht, wie eine (bei diesen Patienten ohnehin bestehende) systemische Sirolimus-Therapie vor negativem vaskulären Remodeling nach Angioplastie schützt. Zwar war bekannt, dass die systemische Applikation von Sirolimus zu einer verminderten Bildung von ISR führt, die detaillierten Mechanismen und möglichen klinischen Konsequenzen waren jedoch unklar.[71] Hier konnte gezeigt werden, dass die niedrigen zirkulierenden Serumspiegel nach systemischer Sirolimus-Behandlung anders als die hohen

Arzneimittelkonzentrationen, die bei lokaler Freisetzung erreicht werden, lediglich antiinflammatorische, aber keine direkte antiproliferative Wirkung auf die am vaskulären Heilungsprozess beteiligten Zellen ausüben. Die systemische Anwendung von Sirolimus verhindert so die Expression endothelialer Adhäsionsmoleküle und die Rekrutierung von Leukozyten einschließlich der konsekutiven Freisetzung von Wachstumsfaktoren und Zytokinen und hat so neben Effekten auf die Proliferation glatter Muskelzellen vor allem einen hemmenden Effekt auf die endotheliale Regeneration. Diese Daten unterstreichen die Notwendigkeit einer effektiven antithrombozytären Therapie nach Angioplastie, auch bei systemischer Therapie mit Sirolimus und mutmaßlich unabhängig von der DES-Beschichtung, auch bei DES neuerer Generationen, die mit anderen Substanzen beschichtet sind.

Die Notwendigkeit zellspezifischer antiproliferativer und antiinflammatorischer Therapien zur Prävention der ISR bei gleichzeitiger Beschleunigung der Reendothelialisierung legt auch weiterhin den Blick auf die Therapie onkologischer Krankheitsbilder mit der Idee des *Drug repurposings* nahe. Mit zunehmendem Verständnis epigenetischer Prozesse wurden im Bereich der onkologischen Forschung intensive Bemühungen unternommen, um den Einfluss chromatinmodifizierender Enzyme auf Mechanismen der zellulären Signaltransduktion und damit auf die Entwicklung und Prävention spezifischer maligner Erkrankungen zu entschlüsseln. In diesem Zusammenhang wurden hochspezifische pharmakologische Inhibitoren von BET-Ableseproteinen entwickelt und in klinischen Studien geprüft.[72,73] Im Rahmen der australischen BETonMACE-Studie wurde der BET-Inhibitor Apabetalon bereits bei kardiovaskulär erkrankten Patienten mit akutem Koronarsyndrom und Diabetes geprüft.[74] Zwar wurde der kombinierte primäre Endpunkt aus kardiovaskulärem Tod, nicht-tödlichem Myokardinfarkt und Schlaganfall nicht erreicht, in der parallel durchgeführten ASSURE-Studie zeigte sich im intravaskulären Ultraschall jedoch eine reduzierte atherosklerotische Plaquelast als Zeichen für einen positiven Effekt auf Umbauprozesse der Gefäßwand.[75] Mit den hochselektiven BET-Inhibitoren I-BET151 und (+)-JQ1 ließ sich der pathophysiologische Ansatz bestätigen: Während – mutmaßlich aufgrund einer geringen Expression von BET-Proteinen in koronararteriellen Endothel- im Vergleich zu koronararteriellen Glattmuskelzellen – die Reendothelialisierung durch BET-Inhibition nicht gestört wurde zeigte sich eine verminderte Glattmuskelzellproliferation und Neointimabildung. Die Bindung des BET-Protein BRD4 inaktiviert den Transkriptionsfaktor FOXO1, so dass (+)-JQ1 umgekehrt FOXO1 in einem aktiven Zustand hält, in dem es *CDKN1A* kontinuierlich transaktiviert und die vaskulären Glattmuskelzellen in einem ruhenden Phänotyp hält. Die so grundlagenwissenschaftlich gewonnenen pharmakologischen Erkenntnisse zeigen das therapeutische Potential der BET-Inhibition in der Prävention der ISR nach Angioplastie

sowie möglicherweise auch bei damit verbundenen vaskulären Erkrankungen wie der Atherosklerose auf.

4.3 Mechanismen in der Pathophysiologie der Neointimabildung

Nur ein Bruchteil der in Tierversuchen untersuchten Substanzen oder Therapiestrategien finden ihren Weg in die klinische Praxis, da die Struktur und Funktionsweise tierischer und menschlicher Organismen erhebliche Unterschiede aufweisen. Dennoch ist der hohe Stellenwert von Tierexperimenten zum besseren Verständnis der Pathophysiologie, auch im von *Drug repurposing*-Studien, unbestritten.[76] Im Rahmen der Arbeiten für die vorliegende Habilitationsschrift gelang eine nähere Charakterisierung der adventitiellen Proliferation in der frühen Phase der Bildung von Granulationsgewebe (vgl. Abschnitt 1.2.2) und eine Identifikation der proliferierenden Zellen überwiegend als Fibroblasten. Tatsächlich bilden Fibroblasten den Hauptzellanteil adventitieller Zellen und zeigen auch hohe Proliferationsraten bei vielen anderen akuten entzündlichen Erkrankungen, einschließlich der kardialen Remodellierung nach Myokardinfarkt.[77] Der Einsatz von Vismodegib (GDC-0449), das als Shh-Signalweg-Inhibitor für die Therapie des fortgeschrittenen oder metastasierten Basalzellkarzinoms zugelassen ist, führte zu einer spezifischen Verminderung der Proliferation und Migration adventitieller Fibroblasten sowie zu einer Verminderung der Sekretion von Zytokinen durch adventitielle Fibroblasten. Gleichzeitig blieben vaskuläre Glattmuskelzellen, Endothelzellen und insbesondere adventitielle Progenitorzellen unbeeinflusst. *In vivo* führte die Verminderung der adventitiellen Fibroblasten-Proliferation durch Vismodegib zu einer verminderten Neointimabildung und damit zum Beweis des hohen pathophysiologischen Stellenwertes adventitieller Fibroblasten im Rahmen der Neointimabildung. Mit einem Dual-Marker-Reporter-System gewonnene Daten zeigen, dass bei Mäusen nach drahtinduzierter Verletzung die Mehrheit der neointimalen Zellmasse tatsächlich von Glattmuskelzellen der Gefäßmedia stammt.[78] Ein direkter erheblicher Beitrag adventitieller Fibroblasten zur zellulären Masse der Neointima erscheint daher unwahrscheinlich. Die expandierende adventitielle Fibroblastenpopulation scheint eher einem adventitiellen „Bioreaktor“ gleichend indirekt über eine parakrine Aktivierung medialer Glattmuskelzellen zur Neointimabildung beizutragen. Im Rahmen einer bisher unveröffentlichten Nachfolgestudie unserer Arbeitsgruppe gelang uns methodisch durch die Entfernung sowie Transplantation der arteriellen Adventitia in der Maus eine substanzielle Untermauerung dieser Hypothese.

Der Einsatz von Vismodegib im Rahmen eines *Drug repurposing*-Ansatzes hat damit nicht nur erfolgreich eine Wirksamkeit im Tiermodell der Neointimabildung nach endovaskulärer Verletzung gezeigt, sondern viel grundlegendere Hinweise auf die

pathophysiologischen Grundlagen des negativen vaskulären Remodelings nach Angioplastie gegeben. Der konsequente Einbezug der arteriellen Adventitia bei der Entwicklung künftiger Strategien zur Therapie der ISR scheint damit zwingend notwendig.

5 Schlussfolgerungen

In der hier vorgelegten Arbeit wurde in humanen vaskulären Zellen *in vitro* und im Mausmodell der endovaskulären Verletzung und Dilatation der Femoralarterien *in vivo* für fünf pharmakologische Substanzen der Einfluss auf vaskuläre Remodeling-Prozesse, wie sie beispielsweise als Folge einer Angioplastie auftreten, mit unterschiedlichen Zielsetzungen untersucht. So konnte für den SGLT2-Inhibitor Empagliflozin ebenso wie für den nicht-steroidalen MRA Finerenon, die beide in der leitliniengerechten Therapie der Herzinsuffizienz Anwendung finden und deren vaskuläre Unbedenklichkeit daher besonders hohe Relevanz hat, gezeigt werden, dass unter experimentellen Bedingungen die Proliferation glatter Gefäßmuskelzellen gehemmt wurde, während Endothelzellen mindestens unbeeinflusst blieben, und der Bildung einer Neointima nach endovaskulärer Verletzung vorgebeugt werden konnte. Dies legt eine vaskuläre Unbedenklichkeit in der klinischen Anwendung zumindest nahe, was jedenfalls für SGLT2-Inhibitoren mit Hinweisen aus klinischen Studien untermauert wird.

Im Rahmen eines *Drug repurposing*-Ansatzes konnte zudem gezeigt werden, dass die systemische Therapie mit Sirolimus, wie sie zum Beispiel nach Organtransplantationen erfolgt, einer Neointimabildung vorwiegend durch antiinflammatorische Effekte vorbeugt. Durch die hochspezifische pharmakologische Inhibition von BET-Ableseproteinen, wie sie sonst zur Therapie einiger onkologischer Erkrankungen verwendet wird, gelang die spezifische Verminderung der Glattmuskelzellproliferation ohne die Reendothelialisierung zu verzögern und damit einen vielversprechenderen Ansatz zur Beschichtung von DES als die derzeit verwendeten Sirolimus-Derivate.

Besonders die Untersuchung von Vismodegib (GDC-0449) erweiterte das umfassendere Verständnis pathophysiologischer Zusammenhänge vaskulärer Remodeling-Prozesse und unterstreicht den erheblichen Einfluss der Adventitia auf das vaskuläre Remodeling.

6 Literaturverzeichnis

1 Roth GA, Abate D, Abate KH, *et al.* Global, regional, and national age-sex-specific mortality for 282 causes of death in 195 countries and territories, 1980-2017: a systematic analysis for the Global Burden of Disease Study 2017. *Lancet* 2018; **392**: 1736–88.

2 Taglieri N, Bruno AG, Ghetti G, *et al.* Target Lesion Failure With Current Drug-Eluting Stents: Evidence From a Comprehensive Network Meta-Analysis. *JACC Cardiovasc Interv* 2020; **13**: 2868–78.

3 Stefanini GG, Holmes DR. Drug-Eluting Coronary-Artery Stents. *New England Journal of Medicine* 2013; **368**: 254–65.

4 Costa MA, Simon DI. Molecular Basis of Restenosis and Drug-Eluting Stents. *Circulation* 2005; **111**: 2257–73.

5 Donisan T, Madanat L, Balanescu D V., Mertens A, Dixon S. Drug-Eluting Stent Restenosis: Modern Approach to a Classic Challenge. *Curr Cardiol Rev* 2023; **19**: 76–85.

6 Bønaa KH, Mannsverk J, Wiseth R, *et al.* Drug-Eluting or Bare-Metal Stents for Coronary Artery Disease. *New England Journal of Medicine* 2016; **375**: 1242–52.

7 Jensen LO, Maeng M, Kaltoft A, *et al.* Stent Thrombosis, Myocardial Infarction, and Death After Drug-Eluting and Bare-Metal Stent Coronary Interventions. *J Am Coll Cardiol* 2007; **50**: 463–70.

8 Pufulete M, Harris J, Pouwels K, *et al.* Real-world bleeding in patients with acute coronary syndrome (ACS) undergoing percutaneous coronary intervention (PCI) and prescribed different combinations of dual antiplatelet therapy (DAPT) in England: a population-based cohort study emulating a ‘target trial’. *Open Heart* 2022; **9**: e001999.

9 Park S-J, Ahn J-M, Kim Y-H, *et al.* Trial of Everolimus-Eluting Stents or Bypass Surgery for Coronary Disease. *New England Journal of Medicine* 2015; **372**: 1204–12.

10 Stone GW, Kappetein AP, Sabik JF, *et al.* Five-Year Outcomes after PCI or CABG for Left Main Coronary Disease. *New England Journal of Medicine* 2019; **381**: 1820–30.

11 Chaabane C, Otsuka F, Virmani R, Bochaton-Piallat M-L. Biological responses in stented arteries. *Cardiovasc Res* 2013; **99**: 353–63.

12 Virmani R, Kolodgie FD, Farb A, Lafont A. Drug eluting stents: are human and animal studies comparable? *Heart* 2003; **89**: 133–8.

13 Forrester JS, Fishbein M, Helfant R, Fagin J. A paradigm for restenosis based on cell biology: Clues for the development of new preventive therapies. *J Am Coll Cardiol* 1991; **17**: 758–69.

14 Welt FGP, Tso C, Edelman ER, *et al.* Leukocyte recruitment and expression of chemokines following different forms of vascular injury. *Vasc Med* 2003; **8**: 1–7.

15 Otsuka F, Finn A V, Yazdani SK, Nakano M, Kolodgie FD, Virmani R. The importance of the endothelium in atherothrombosis and coronary stenting. *Nat Rev Cardiol* 2012; **9**: 439–53.

16 Daniel J-M, Bielenberg W, Stieger P, Weinert S, Tillmanns H, Sedding DG. Time-course analysis on the differentiation of bone marrow-derived progenitor cells into smooth muscle cells during neointima formation. *Arterioscler Thromb Vasc Biol* 2010; **30**: 1890–6.

17 Furie B, Furie BC. Mechanisms of Thrombus Formation. *New England Journal of Medicine* 2008; **359**: 938–49.

18 McEver RP. Selectins: initiators of leucocyte adhesion and signalling at the vascular wall. *Cardiovasc Res* 2015; **107**: 331–9.

19 Weber C, Springer TA. Neutrophil accumulation on activated, surface-adherent platelets in flow is mediated by interaction of Mac-1 with fibrinogen bound to alphaIIbbeta3 and stimulated by platelet-activating factor. *J Clin Invest* 1997; **100**: 2085–93.

20 Massberg S, Konrad I, Schürzinger K, *et al.* Platelets secrete stromal cell–derived factor 1α and recruit bone marrow–derived progenitor cells to arterial thrombi in vivo. *J Exp Med* 2006; **203**: 1221–33.

21 Schober A. Chemokines in vascular dysfunction and remodeling. *Arterioscler Thromb Vasc Biol* 2008; **28**: 1950–9.

22 Sata M, Saiura A, Kunisato A, *et al.* Hematopoietic stem cells differentiate into vascular cells that participate in the pathogenesis of atherosclerosis. *Nat Med* 2002; **8**: 403–9.

23 Daniel J-M, Bielenberg W, Stieger P, Weinert S, Tillmanns H, Sedding DG. Time-course analysis on the differentiation of bone marrow-derived progenitor cells into smooth muscle cells during neointima formation. *Arterioscler Thromb Vasc Biol* 2010; **30**: 1890–6.

24 Grudzinska MK, Kurzejamska E, Hagemann N, *et al.* Monocyte chemoattractant protein 1-mediated migration of mesenchymal stem cells is a source of intimal hyperplasia. *Arterioscler Thromb Vasc Biol* 2013; **33**: 1271–9.

25 Chen Y, Wong MM, Campagnolo P, *et al.* Adventitial Stem Cells in Vein Grafts Display Multilineage Potential That Contributes to Neointimal Formation. *Arterioscler Thromb Vasc Biol* 2013; **33**: 1844–51.

26 Burke AP, Kolodgie FD, Farb A, Weber D, Virmani R. Morphological predictors of arterial remodeling in coronary atherosclerosis. *Circulation* 2002; **105**: 297–303.

27 Welt FG, Edelman ER, Simon DI, Rogers C. Neutrophil, not macrophage, infiltration precedes neointimal thickening in balloon-injured arteries. *Arterioscler Thromb Vasc Biol* 2000; **20**: 2553–8.

28 Grewe PH, Deneke T, Machraoui A, Barmeyer J, Müller K-M. Acute and chronic tissue response to coronary stent implantation: pathologic findings in human specimen. *J Am Coll Cardiol* 2000; **35**: 157–63.

29 Jawien A, Bowen-Pope DF, Lindner V, Schwartz SM, Clowes AW. Platelet-derived growth factor promotes smooth muscle migration and intimal thickening in a rat model of balloon angioplasty. *J Clin Invest* 1992; **89**: 507–11.

30 Nakazawa G, Otsuka F, Nakano M, *et al.* The Pathology of Neoatherosclerosis in Human Coronary Implants: Bare-Metal and Drug-Eluting Stents. *J Am Coll Cardiol* 2011; **57**: 1314–22.

31 Ross R. Atherosclerosis — An Inflammatory Disease. *New England Journal of Medicine* 1999; **340**: 115–26.

32 Galis ZS, Khatri JJ. Matrix Metalloproteinases in Vascular Remodeling and Atherogenesis. The Good, the Bad, and the Ugly. *Circ Res* 2002; **90**: 251–62.

33 Serruys PW, Ormiston JA, Sianos G, *et al.* Actinomycin-eluting stent for coronary revascularization: a randomized feasibility and safety study: the ACTION trial. *J Am Coll Cardiol* 2004; **44**: 1363–7.

34 Park D-W, Hong M-K, Mintz GS, *et al.* Two-year follow-up of the quantitative angiographic and volumetric intravascular ultrasound analysis after nonpolymeric paclitaxel-eluting stent implantation: late "catch-up" phenomenon from ASPECT Study. *J Am Coll Cardiol* 2006; **48**: 2432–9.

35 Taniwaki M, Stefanini GG, Silber S, *et al.* 4-Year Clinical Outcomes and Predictors of Repeat Revascularization in Patients Treated With New-Generation Drug-Eluting Stents: A Report From the RESOLUTE All-Comers Trial (A Randomized Comparison of a Zotarolimus-Eluting Stent With an Everolimus-Eluting Stent for Percutaneous Coronary Intervention). *J Am Coll Cardiol* 2014; **63**: 1617–25.

36 Valgimigli M, Tebaldi M, Borghesi M, *et al.* Two-Year Outcomes After First- or Second-Generation Drug-Eluting or Bare-Metal Stent Implantation in All-Comer Patients Undergoing Percutaneous Coronary Intervention: A Pre-Specified Analysis From the PRODIGY Study (PROlonging Dual Antiplatelet Treatment After Grading stent-induced Intimal hyperplasia studY). *JACC Cardiovasc Interv* 2014; **7**: 20–8.

37 Sun J, Marx SO, Chen H-J, Poon M, Marks AR, Rabbani LE. Role for p27 ^{Kip1} in Vascular Smooth Muscle Cell Migration. *Circulation* 2001; **103**: 2967–72.

38 Viñals F, Chambard JC, Pouysségur J. p70 S6 Kinase-mediated Protein Synthesis Is a Critical Step for Vascular Endothelial Cell Proliferation. *Journal of Biological Chemistry* 1999; **274**: 26776–82.

39 Gabardi S, Baroletti SA. Everolimus: a proliferation signal inhibitor with clinical applications in organ transplantation, oncology, and cardiology. *Pharmacotherapy* 2010; **30**: 1044–56.

40 Joseph P, Roy A, Lonn E, *et al.* Global Variations in Heart Failure Etiology, Management, and Outcomes. *JAMA* 2023; **329**: 1650–61.

41 Ezekowitz JA, Kaul P, Bakal JA, Armstrong PW, Welsh RC, McAlister FA. Declining In-Hospital Mortality and Increasing Heart Failure Incidence in Elderly Patients With First Myocardial Infarction. *J Am Coll Cardiol* 2009; **53**: 13–20.

42 Lam CSP, Docherty KF, Ho JE, McMurray JJ V., Myhre PL, Omland T. Recent successes in heart failure treatment. *Nat Med* 2023; **29**: 2424–37.

43 Zinman B, Wanner C, Lachin JM, *et al.* Empagliflozin, Cardiovascular Outcomes, and Mortality in Type 2 Diabetes. *New England Journal of Medicine* 2015; **373**: 2117–28.

44 Dutzmann J, Bauersachs J, Sedding DG. Evidence for the use of mineralocorticoid receptor antagonists in the treatment of coronary artery disease and post-angioplasty restenosis. *Vascul Pharmacol* 2018; **107**: 20–6.

45 McDonagh TA, Metra M, Adamo M, *et al.* 2023 Focused Update of the 2021 ESC Guidelines for the diagnosis and treatment of acute and chronic heart failure. *Eur Heart J* 2023; **44**: 3627–39.

46 Xu C, Zhang N, Yuan H, Wang L, Li Y. Sacubitril/valsartan inhibits the proliferation of vascular smooth muscle cells through notch signaling and ERK1/2 pathway. *BMC Cardiovasc Disord* 2024; **24**: 106.

47 Brehm BR, Wolf SC, Bertsch D, *et al.* Effects of nebivolol on proliferation and apoptosis of human coronary artery smooth muscle and endothelial cells. *Cardiovasc Res* 2001; **49**: 430–9.

48 Wolf SC, Sauter G, Preyer M, *et al.* Influence of nebivolol and metoprolol on inflammatory mediators in human coronary endothelial or smooth muscle cells. Effects on neointima formation after balloon denudation in carotid arteries of rats treated with nebivolol. *Cell Physiol Biochem* 2007; **19**: 129–36.

49 Feuerstein GZ, Ruffolo RR. Carvedilol, a novel vasodilating beta-blocker with the potential for cardiovascular organ protection. *Eur Heart J* 1996; **17 Suppl B**: 24–9.

50 Yndigegn T, Lindahl B, Mars K, *et al.* Beta-Blockers after Myocardial Infarction and Preserved Ejection Fraction. *New England Journal of Medicine* 2024; published online April 7. DOI:10.1056/NEJMoa2401479.

51 Zhang J, Zhang Q, Zhao K, Bian Y-J, Liu Y, Xue Y-T. Risk factors for in-stent restenosis after coronary stent implantation in patients with coronary artery disease: A retrospective observational study. *Medicine* 2022; **101**: e31707.

52 Serruys PW, Foley DP, Höfling B, *et al.* Carvedilol for prevention of restenosis after directional coronary atherectomy : final results of the European carvedilol atherectomy restenosis (EUROCARE) trial. *Circulation* 2000; **101**: 1512–8.

53 Desmet W, Vrolix M, De Scheerder I, Van Lierde J, Willems JL, Piessens J. Angiotensin-converting enzyme inhibition with fosinopril sodium in the prevention of restenosis after coronary angioplasty. *Circulation* 1994; **89**: 385–92.

54 Meurice T, Bauters C, Hermant X, *et al.* Effect of ACE inhibitors on angiographic restenosis after coronary stenting (PARIS): a randomised, double-blind, placebo-controlled trial. *Lancet* 2001; **357**: 1321–4.

55 Heeneman S, Sluimer JC, Daemen MJAP. Angiotensin-converting enzyme and vascular remodeling. *Circ Res* 2007; **101**: 441–54.

56 Powell JS, Clozel JP, Müller RK, *et al.* Inhibitors of angiotensin-converting enzyme prevent myointimal proliferation after vascular injury. *Science* 1989; **245**: 186–8.

57 Kursaklioglu H, Iyisoy A, Amasyali B, *et al.* Spironolactone Does Not Prevent Restenosis After Coronary Stenting in Humans. *Ann Acad Med Singap* 2004; **33**: 769–74.

58 Ward MR, Kanellakis P, Ramsey D, Funder J, Bobik A. Eplerenone Suppresses Constrictive Remodeling and Collagen Accumulation After Angioplasty in Porcine Coronary Arteries. *Circulation* 2001; **104**: 467–72.

59 Van Belle E, Bauters C, Wernert N, *et al.* Neointimal thickening after balloon denudation is enhanced by aldosterone and inhibited by spironolactone, and aldosterone antagonist. *Cardiovasc Res* 1995; **29**: 27–32.

60 Iqbal J, Macdonald LJ, Low L, *et al.* Contribution of Endogenous Glucocorticoids and Their Intravascular Metabolism by 11β-HSDs to Postangioplasty Neointimal Proliferation in Mice. *Endocrinology* 2012; **153**: 5896–905.

61 Gueret A, Harouki N, Favre J, *et al.* Vascular Smooth Muscle Mineralocorticoid Receptor Contributes to Coronary and Left Ventricular Dysfunction After Myocardial Infarction. *Hypertension* 2016; **67**: 717–23.

62 Filippatos G, Anker SD, Böhm M, *et al.* A randomized controlled study of finerenone vs. eplerenone in patients with worsening chronic heart failure and diabetes mellitus and/or chronic kidney disease. *Eur Heart J* 2016; **37**: 2105–14.

63 Pitt B, Filippatos G, Agarwal R, *et al.* Cardiovascular Events with Finerenone in Kidney Disease and Type 2 Diabetes. *N Engl J Med* 2021; **385**: 2252–63.

64 Agarwal R, Filippatos G, Pitt B, *et al.* Cardiovascular and kidney outcomes with finerenone in patients with type 2 diabetes and chronic kidney disease: the FIDELITY pooled analysis. *Eur Heart J* 2022; **43**: 474–84.

65 Pruthi D, McCurley A, Aronovitz M, Galayda C, Karumanchi SA, Jaffe IZ. Aldosterone promotes vascular remodeling by direct effects on smooth muscle cell mineralocorticoid receptors. *Arterioscler Thromb Vasc Biol* 2014; **34**: 355–64.

66 Jia G, Habibi J, Aroor AR, *et al.* Endothelial Mineralocorticoid Receptor Mediates Diet-Induced Aortic Stiffness in Females. *Circ Res* 2016; **118**: 935–43.

67 Sun J-Y, Li C, Shen Z-X, *et al.* Mineralocorticoid Receptor Deficiency in Macrophages Inhibits Neointimal Hyperplasia and Suppresses Macrophage Inflammation Through SGK1-AP1/NF-κB Pathways. *Arterioscler Thromb Vasc Biol* 2016; **36**: 874–85.

68 Hashikata T, Ikutomi M, Jimba T, *et al.* Empagliflozin attenuates neointimal hyperplasia after drug-eluting-stent implantation in patients with type 2 diabetes. *Heart Vessels* 2020; **1**: 3.

69 Marfella R, Sardu C, D'Onofrio N, *et al.* SGLT-2 inhibitors and in-stent restenosis-related events after acute myocardial infarction: an observational study in patients with type 2 diabetes. *BMC Med* 2023; **21**: 71.

70 Abdelsayed M, Kort EJ, Jovinge S, Mercola M. Repurposing drugs to treat cardiovascular disease in the era of precision medicine. *Nat Rev Cardiol* 2022; **19**: 751–64.

71 Stojkovic S, Ostojic M, Nedeljkovic M, *et al.* Systemic rapamycin without loading dose for restenosis prevention after coronary bare metal stent implantation. *Catheter Cardiovasc Interv* 2010; **75**: 317–25.

72 Hewings DS, Rooney TPC, Jennings LE, *et al.* Progress in the Development and Application of Small Molecule Inhibitors of Bromodomain–Acetyl-lysine Interactions. *J Med Chem* 2012; **55**: 9393–413.

73 Stathis A, Bertoni F. BET Proteins as Targets for Anticancer Treatment. *Cancer Discov* 2018; **8**: 24–36.

74 Ray KK, Nicholls SJ, Buhr KA, *et al.* Effect of Apabetalone Added to Standard Therapy on Major Adverse Cardiovascular Events in Patients With Recent Acute Coronary Syndrome and Type 2 Diabetes: A Randomized Clinical Trial. *JAMA* 2020; **323**: 1565–73.

75 Shishikura D, Kataoka Y, Honda S, *et al.* The Effect of Bromodomain and Extra-Terminal Inhibitor Apabetalone on Attenuated Coronary Atherosclerotic Plaque:

Insights from the ASSURE Trial. *American Journal of Cardiovascular Drugs* 2019; **19**: 49–57.

76 Libby P, Ridker PM, Hansson GK. Progress and challenges in translating the biology of atherosclerosis. *Nature* 2011; **473**: 317–25.

77 Tillmanns J, Hoffmann D, Habbaba Y, *et al.* Fibroblast activation protein alpha expression identifies activated fibroblasts after myocardial infarction. *J Mol Cell Cardiol* 2015; **87**: 194–203.

78 Herring BP, Hoggatt AM, Burlak C, Offermanns S. Previously differentiated medial vascular smooth muscle cells contribute to neointima formation following vascular injury. *Vasc Cell* 2014; **6**: 21.

7 Thesen

1. Vaskuläre Remodeling-Prozesse können auf vielfältige und unterschiedliche Art und Weise pharmakologisch beeinflusst werden. Die Untersuchung von Pharmaka aus anderen kardiovaskulären und nicht-kardiovaskulären Indikationsbereichen trägt dabei zum grundsätzlichen pathophysiologischen Verständnis und insbesondere zum Verständnis der Funktion, Zell-Zell-Interaktionen und Signaltransduktion vaskulärer Zellen bei.
2. Die systemische Therapie mit Sirolimus wie sie beispielsweise nach Organtransplantationen erfolgt vermindert die Proliferation von Endothel- und glatten Muskelzellen und beeinflusst vaskuläre Remodeling-Prozesse als indirekte Folge einer reduzierten Rekrutierung zirkulierender inflammatorischer Zellen an das verletzten Gefäßsegment.
3. Die systemische Therapie mit dem neuen nicht-steroidalen Mineralokortikoidrezeptorantagonist Finerenon, der insbesondere bei Patienten mit chronischer Niereninsuffizienz und Diabetes mellitus zur Therapie der Herzinsuffizienz empfohlen wird, fördert im Tiermodell die endotheliale Heilung und vermindert die Bildung einer neointimalen Läsion durch eine Verminderung der Invasion inflammatorischer Zellen, von Endothelzell-Apoptose sowie von Glattmuskelzellproliferation.
4. Die systemische Therapie mit dem SGLT2-Inhibitor Empagliflozin, das zu den prognostisch relevanten Säulen der medikamentösen Herzinsuffizienz-Therapie gehört, fördert im Tiermodell die endotheliale Heilung in Tieren mit Diabetes und vermindert die Bildung einer neointimalen Läsion unabhängig vom Vorliegen eines Diabetes mellitus infolge einer verminderten Glattmuskelzellproliferation und verbesserten Endothelzellenfunktion.
5. Die lokale Therapie mit dem selektiven SMO-Inhibitor GDC-0449 (Vismodegib), das zur Therapie des Basalzellkarzinoms zugelassen ist, vermindert im Tiermodell die Bildung einer neointimalen Läsion nach endovaskulärer Verletzung durch eine selektive Verminderung von Proliferation und Migration adventitieller Fibroblasten und verdeutlicht so die pathophysiologische Bedeutung der Adventitia bei vaskulären Remodeling-Prozessen.
6. Die lokale Therapie mit (+)-JQ1, einem klinisch für die Therapie von Kopf-Hals-Tumoren verwendeten Inhibitor des BET-Proteins BRD4, vermindert die Proliferation glatter Gefäßmuskelzellen durch die Förderung einer vom Transkriptionsfaktor FOXO1-abhängigen Transaktivierung des Zellzyklusproteins CDK-Inhibitor 1 und verhindert so die Bildung einer neointimalen Läsion nach endovaskulärer Verletzung im Tiermodell.

8 Selbstständigkeitserklärung

Hiermit erkläre ich, Jochen Dutzmann, dass ich diese Habilitationsschrift selbstständig verfasst und keine anderen als die angegebenen Quellen und Hilfsmittel benutzt habe.

9 Erklärung über frühere Habilitationsversuche

Hiermit erkläre ich, dass an keiner anderen Fakultät oder Universität ein Habilitationsverfahren anhängig ist. Bislang gab es keine etwaigen früheren Habilitationsverfahren oder abgelehnte Habilitationsgesuche an anderen Universitäten.

10 Lebenslauf

[Aus Datenschutzgründen entfernt]

[Aus Datenschutzgründen entfernt]

[Aus Datenschutzgründen entfernt]

[Aus Datenschutzgründen entfernt]

[Aus Datenschutzgründen entfernt]

11 Danksagung

[Aus Datenschutzgründen entfernt]

[Aus Datenschutzgründen entfernt]